UNIVERSITY OF NOTTINGHAM

DEPARTMENT OF CIVIL ENGINEERING

REFLECTION CRACKING IN ASPHALT OVERLAYS

by

Michael Andrew Caltabiano B.E.

Thesis submitted to the University of Nottingham for the degree of Master of Philosophy.

MARCH 1990

CHAPTER 1

INTRODUCTION

1.1 WHAT IS REFLECTION CRACKING?

Reflection cracking is the propagation of a previously defined crack through subsequent layers of a pavement. The predefined crack or discontinuity is most commonly due to the effects of temperature and shrinkage on a lower cement treated pavement layer or preformed cracks in portland cement concrete (PCC) pavements.

A distinction is made in this work between cracking due to the above-mentioned factors and cracking due to pavement failures such as block cracking or alligator cracking. These types of pavement cracks require remedial treatments of a structural nature.Figure 1.1 shows a typical cross-section of a cracked cement treated base pavement with cracking generally appearing every 5-7 metres along the length of the roadway (Williams (58)).

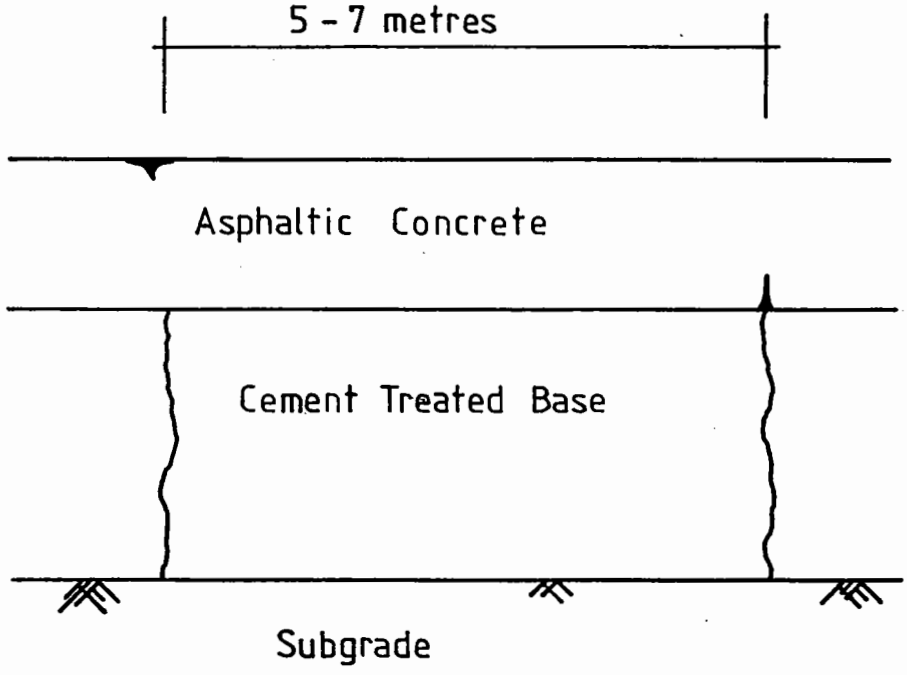

Figure 1.1 Typical Cross Section of Cement Treated Base Pavement

Plate 1.1 illustrates cracking in a PCC pavement that has been sealed with a modified binder. Some spalling of concrete at the crack edge is also visible.

DECLARATION

All work described in this thesis is of the author's own work and has not been submitted in any form for another degree or diploma at any University or other institution of tertiary education. Information derived from the published or unpublished work of others has been acknowledged in the text and a reference list is given.

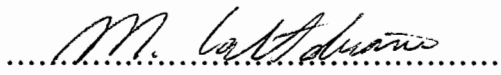

Author: M A Caltabiano

30th March 1990

ABSTRACT

Reflection cracking through asphaltic overlays has plagued road maintenance authorities world-wide since the early 1930's. This phenomenon has, over the last sixty years, been the subject of many field trials, laboratory testing, and computational studies for the development of prediction models. Despite this extensive research the complex nature in which existing pavements interact with an asphaltic concrete overlay has ensured that a single universal solution to the problem is not yet available.

The aim of the research described in this thesis was to evaluate under controlled laboratory conditions the relative effectiveness of various treatments to prevent reflection cracking. Earlier research in this field at the University of Nottingham allowed a three-fold testing program to be undertaken using the existing facilities, with modifications. The development of a beam test facility that could adequately model both thermal and traffic induced stresses in an overlay was the focus of the testing program. Other test facilities used were the shear box test to evaluate interface and frictional conditions for various interlayer treatments and the slab testing facility used to evaluate crack growth through asphaltic concrete overlays under the action of a moving wheel.

Experimentation was carried out on three treatments commonly used by road maintenance authorities to inhibit reflection cracking, that also have a history of field trial evaluation. These treatments were a) Polymer Modified Binder asphaltic concrete, b) Geotextile, non-woven and needle punched, and c) Geogrid of the polypropylene type.

All treatments delayed the propagation of cracking to different extents with the best results obtained for the two interlayer treatments. The beam test facility proved to be a most reliable and consistent method for determination of relative effectiveness of these

treatments. Particular attention was paid to the representation of field conditions wherever possible during the development of this device.

The shear box test results showed that there was a reduction in shear strength with the incorporation of an interlayer treatment. This reduction however was not considered to be significant under real pavement conditions. The interface evaluation of the materials used in beam and slab tests showed that these were a good approximation of the asphaltic concrete overlay bond to lower pavement layers.

The equipment developed has the capability of testing all current treatments on the commercial market aimed at preventing reflection cracking through overlays and is able to provide a relative indication of field performance.

ACKNOWLEDGEMENTS

The author is grateful to Professor S F Brown who as Head of Department made available his laboratories and facilities and provided guidance for the duration of this work.

The author is indebted to the Commissioner of the Main Roads Department, Queensland, Mr A McLennan and Dr R Gordon for providing the opportunity and continued support of the work conducted at Nottingham University.

The author gratefully acknowledges the advice and assistance of Dr J M Brunton who supervised this thesis. Thanks are also due to Mr K Cooper, Chief Experimental Officer and Mr B Brodrick, Senior Experimental Officer, who together with the assistance of Mr A Leyko and many other technicians contributed to the success of this work.

The continuous support from my wife, Andrea, however distant, was a source of constant encouragement throughout this work.

Finally the author would like to thank Ms J Adams and Ms S Gillespie for typing this manuscript.

TABLE OF CONTENTS

LIST OF FIGURES

CHAPTER 4

CHAPTER 5

LIST OF TABLES

LIST OF PLATES

CHAPTER 1

CHAPTER 3

CHAPTER 4

CHAPTER 7

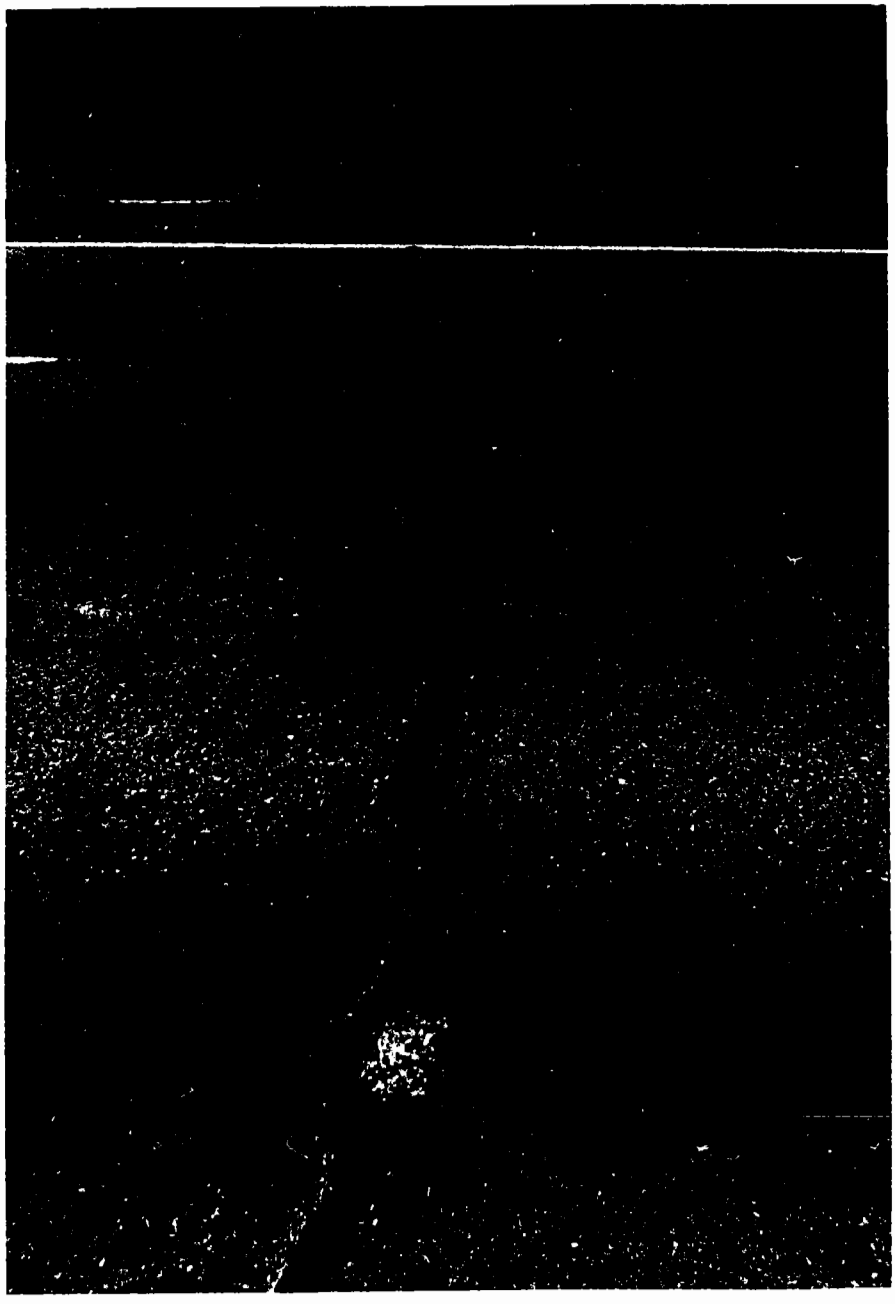

Plate 1.1 Cracking in a Portland Cement Concrete Pavement That Has Been Sealed With Modified Binder

1.2 EFFECTS OF REFLECTION CRACKING ON PAVEMENT STRUCTURES

Once reflection cracking propagates the full depth of the overlay the pavement becomes susceptible to the effects of water infiltration. These effects are wide ranging and can lead to the structural failure of the pavement. Some of the effects of water infiltration are listed below:-

(i) In cement treated base pavements a leaching of fines caused by the pumping of water in reflection cracks causes a loss of strength in the individual layers.

(ii) Wetting up of the subgrade reduces its elastic modulus causing excessive tensile strain in the upper pavement layers.

(iii) In colder climates water trapped in pavement cracks can undergo a freeze-thaw cycle, effectively widening cracks and leading to rapid pavement deterioration.

While water infiltration into the pavement is the dominant mode of distress after the onset of reflection cracking other factors also contribute to the degradation process.

(a) Oxidation of the asphaltic concrete open to the atmosphere makes the layer more susceptible to further cracking.

(b) A loss of rideability often occurs as crack edges deteriorate.

(c) When maintenance authorities seal pavement cracks with modified binders a loss in the aesthetic appeal of the roadway results.

All these factors ultimately lead to the premature failure of the pavement. In an economic environment which sees the costs associated with road construction ever increasing, the need to ensure that the design life of a pavement is reached, is of paramount importance. Non structural cracking such as reflection cracking does not in itself reduce the life of the pavement but the associated environmental factors acting on a roadway lead to its premature failure.

1.3 LABORATORY TESTING TO PREDICT RELATIVE EFFECTIVENESS OF TREATMENTS TO PREVENT REFLECTION CRACKING

The need to prevent reflection cracking has become a world-wide quest with many materials manufacturers claiming to have a product that can perform this task. These materials vary in quality and type from interlayer treatments of wire mesh to geotextiles with a mass in grams per square metre of less than 100, to a list of additives including several types of polymers and crumbed tyre rubber.

With a large range of materials on the market that claim to prevent reflection cracking there exists a need to develop a simple laboratory test that can make determinations of the individual materials ability to prevent the propagation of cracking through an asphaltic layer .

This work aims to develop a testing facility that will reflect the relative field performance of materials that claim to prevent reflection cracking. The advantage of an apparatus that can compare the performance of different treatments under the same test conditions is that it will provide a reliable and cost effective way of testing and reduce the number of field trials carried out to verify material performance. It is hoped through the continued use of the test facility developed, that a greater understanding of the relative performance of various interlayer treatments will be obtained.

A series of tests were conducted using predominantly existing laboratory facilities including a beam testing facility to which significant modifications were made to allow combined traffic and thermal loads to be applied to test specimens.

Chapter 2 presents an historical overview of the reflection cracking phenomenon, specifically, field trials undertaken, modelling of the problem and a review of the laboratory work conducted.

Chapters 3 to 7 deal with the test equipment development, experimental work completed and results obtained, followed in Chapters 8 and 9 by conclusions and recommendations for further work.

CHAPTER 2

REFLECTION CRACKING PHENOMENON

2.1 HISTORY OF REFLECTION CRACKING

Reflection cracking was first recognized as a major concern to road builders in 1932 (Von Quintus et al (1)) when at the annual meeting of the Highway Research Board, USA, it was highlighted as one of the principal forms of distress in resurfaced pavements.

One of the first recorded uses of an interlayer treatment in an asphaltic concrete overlay was reported by Maurer and Malasheski (2) to have been in the early 1930's. Woven cotton was placed between layers of asphaltic concrete,

"to strengthen the road surface and soften the ride". (Beckham and Mills (3)).

From these early beginnings to the mid 1950's there was very little recorded work associated with the reflection cracking problem, apart from a continuation of isolated field trials.

During the 1950's in the United States the reflection cracking problem again reached the forefront of Highway Engineers maintenance considerations as many major resurfacing projects over portland cement concrete (PCC) roads experienced premature failures. These failures were directly attributed to cracking in the surface of the overlay above a pre-existing joint in the lower pavement layers. (Luther et al (4), Rust (5)).

2.2 PRINCIPLES OF REFLECTION CRACKING

2.2.1 Introduction

As a result of these premature failures occurring on such a large scale, an examination of the factors associated with reflection cracking was initiated. This impetus for further

investigation was not confined to the United States but was also evident in the United Kingdom, South Africa and parts of Europe.

Reflection cracking is best described as the appearance of cracks at the surface of an asphaltic concrete layer that mirror those in a lower pavement layer. Often there is a tendency to label cracking in asphaltic concrete layers, that appear due to a structural failure of the pavement as reflection cracks. In the context of this work the propagation of alligator or closely spaced block cracks from structural failures in the lower pavement layers to the pavement surface will not be considered. A complete structural evaluation should be completed prior to the undertaking of any remedial work for such cracking patterns.

The reflection cracking phenomenon is of great importance to Engineers as it often signals the onset of premature failure in an otherwise structurally sound pavement. It is in this light that a significant amount of time and money has been invested in the pursuit of a better understanding of the complex mechanisms that dictate cracking through asphaltic concrete overlays. Haas and Ponniah (6) reported recently in a Canadian study (1983) that reflection cracking is considered the most predominant existing pavement problem.

2.2.2 Factors Related To Cracking and Crack Growth

The development of reflection cracks in an asphaltic concrete overlay can be directly attributed to the increase in tensile stress within the overlay. This tensile stress is affected by one or more of the following factors:-

(a) Traffic loading.

(b) Curing of cement treated bases (C.T.B).

(c) Excessive temperature change.

(d) Moisture loss in the subgrade.

(e) Loss of volatiles in the surface of the overlay.

(f) Absorption of binder into the aggregate.

(g) Moisture absorption and loss as a result of absorptive aggregates.

(h) Settlement of the subgrade.

(i) Compaction of the pavement after construction.

(j) Differential swelling of the subgrade.

The result of these factors acting on the pavement structure is that a crack develops in the overlay and propagates through it, reflecting lower pavement discontinuities.

The crack displacement or propagation can follow one or more of the three fracture modes illustrated in Figure 2.1 depending on the loading configuration. The use of these modes of fracture are widely reported in the literature by Haas and Ponniah (6), Molenaar (7) and Sicard (8).

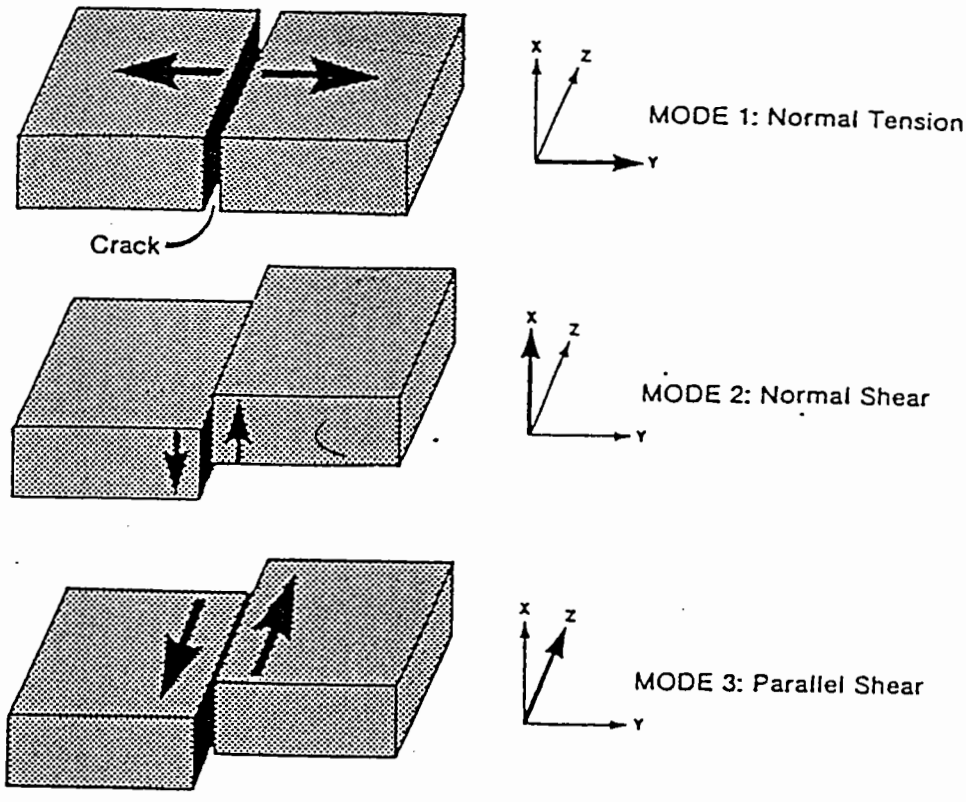

Figure 2.1 Three Modes of Fracture in Asphaltic Concrete Overlays

The actual fracture of the overlay occurs when the tensile strength is exceeded by the tensile stress due to combinations of the factors previously mentioned.

The progression of a crack through an asphaltic overlay was described in a visual manner by Goacolou and Marchand (9) as illustrated in Figure 2.2.

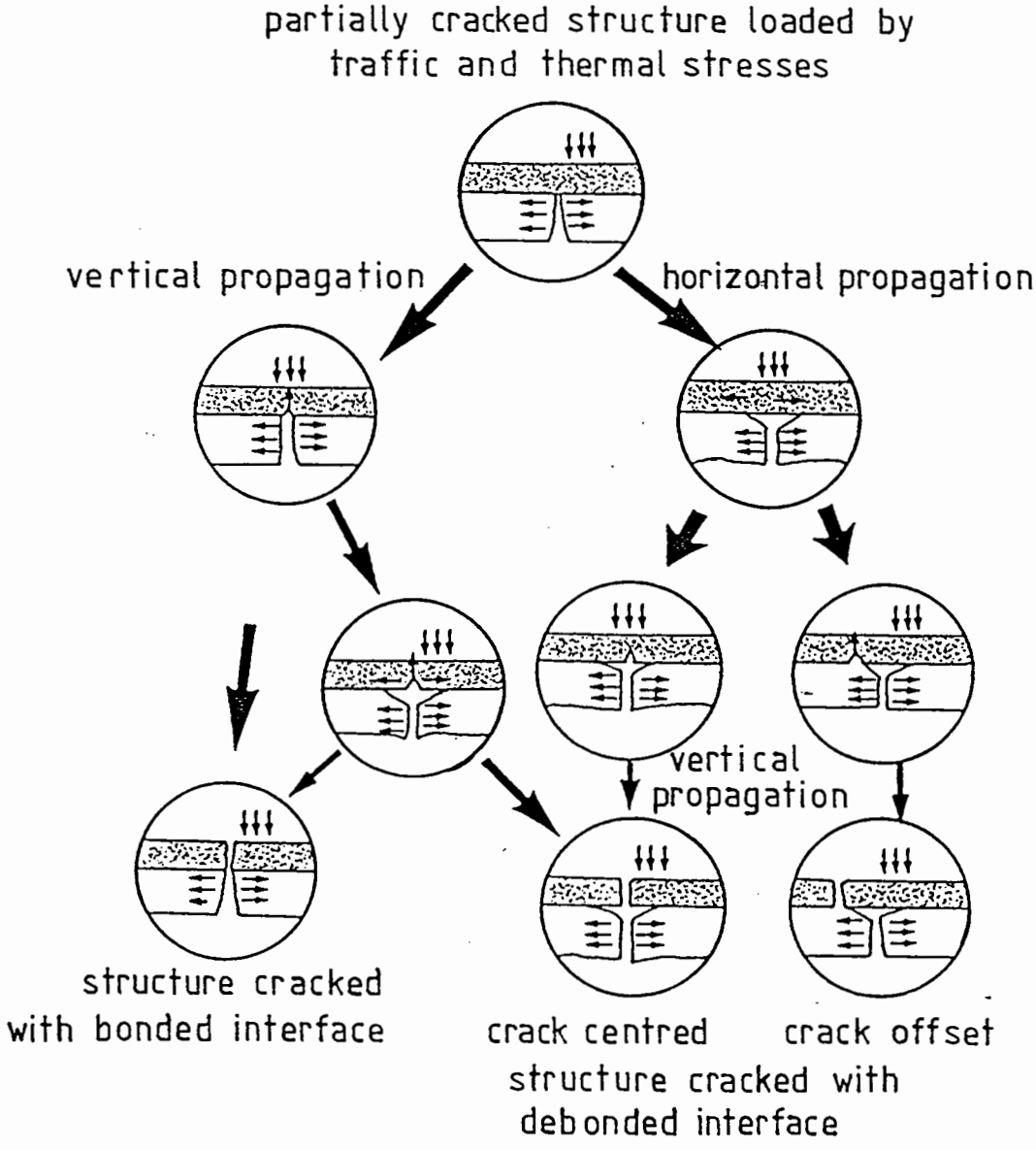

Figure 2.2 Crack Progression (after Goacolou and Marchand (9))

Marker (10) reported that the properties of a conventional overlay that resist the applied tensile stresses are:-

"(a) cohesion of the mix,

(b) thickness of the surfacing,

(c) stress relief due to pneumatic tyre traffic,

(d) adhesion/friction between the overlay and underlying base, and

(e) relative stiffness of the pavement structure under given conditions of environment and usage".

A diagrammatic representation of crack propagation in a plot of time against crack length by Colombier (11) is illustrated in Figure 2.3.

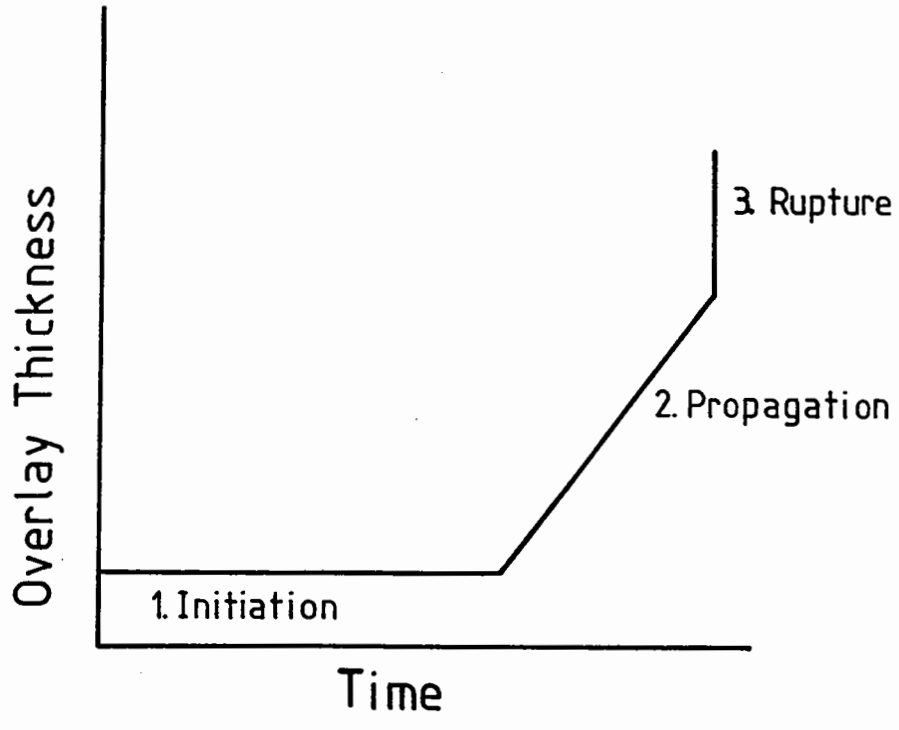

Figure 2.3 Diagrammatic Representation of Crack Propagation (after Colombier (11))

2.2.3 Overview of Treatments Used in the Prevention of Reflection Cracking

2.2.3.1 Introduction

Since the beginning of the 1930's when woven cotton was used as an interlayer treatment for asphaltic concrete overlays many different materials have been installed as part of site trials or used in laboratory testing programs. The mechanisms associated with each interlayer's performance in preventing the propagation of reflection cracks is generally not clearly expressed by the product manufacturers.

2.2.3.2 Range of Products Available

The extensive range of products on the market claiming to prevent reflection cracking are summarized in Table 2.1.

Only three methods of treatment were considered during the experiments conducted as part of this work. These were, geogrid (polypropylene), geotextile (non-woven, needle punched, polyester) and polymer modified binder (Styrene Butadine Styrene,SBS).

Table 2.1 Crack Inhibiting Products and the Constituent Materials

Products Available	Material Types
1. Fibre filaments	steel, polymer, glass.
2. Bond breakers at crack locations	sheetmetal, wax paper, aluminium foil, stone dust, sand.
3. Additives to the binder	Ethylene Vinyl Acetate (EVA), Styrene Butadine Styrene (SBS), Styrene Butadine Rubber (SBR), crumbed rubber, shredded car tyres.
4. Geotextiles	woven, non-woven, heat bonded, needle punched, polyester , polypropylene.
5. Geogrids	polypropylene (stiff), polyester (more flexible).
6. Wire mesh	heavy gauge, light gauge.
7. Interlayers	rubberized binder, polymer modified binder, bituminous seal, cushion courses.
8. Surface sealing	bituminous seal, rubberized/polymer modified seal, slurry seal.
9. Crack treatment	rubberized binder filler, strip treatments of type, geotextile, geogrid, interlayer.
10. Open graded asphaltic concrete	ordinary and modified binder, asphaltic concrete.
11. Upside down construction	crushed rock layer on top of C.T.B.

The three treatments selected for testing purposes in this work, as previously outlined, were chosen for the following reasons:-

(i) The treatments represent a wide range of those available from stiff grids to a modified binder asphaltic concrete.

(ii) The products are commonly available from manufacturers.

(iii) Development of a test apparatus to uniformly test this range of crack prevention methods should ensure that future trials using different treatments will be able to utilize the developed equipment.

(iv) Extensive field trials and laboratory work has been conducted using geogrids and geotextiles which have provided useful input to the development of test equipment for this project.

(v) With only three products a full testing program was able to be completed in the time allowed.

2.2.3.3 Methods of Prevention

With a vast range of proprietary products on the market the mechanisms associated with prevention of crack propagation have been summarized by Haas and Ponniah (6) and Rust (5) as the following.

(i) Low modulus interlayer.

The inclusion of a bituminous interlayer above the crack reduces the stress concentration at the crack front, by dissipation into the interlayer.

(ii) Tensile reinforcement.

The inclusion of a geotextile or geogrid has the same effect as steel in concrete. (Rust (5)). [Haas and Ponniah (6) report that it is difficult to quantify the mechanism by which these products control crack growth.]

(iii) Composite stress relieving interlayer.

The combination of mechanisms (i) and (ii) allows the low modulus interlayer to act as a stress attenuator with the reinforcement carrying the remaining stress.

The theories listed above do not explain the mechanisms associated with the inclusion of polymer modified binders in asphaltic concrete mixes.

2.3 DESIGN METHODS FOR CONVENTIONAL OVERLAYS

2.3.1 Introduction

Overlay design in general is based on a need to correct some pavement deficiency such as:-

(a) Structural inadequacy for the current traffic use.

(b) Structural inadequacy for future traffic requirements.

(c) The pavement has an inadequate level of serviceability, low skid resistance or poor rideability.

(d) Reflection cracking not accompanied by deformation or the pumping of fines.

The design of conventional overlays most commonly requires the determination of overlay depth through the use of deflection data (Rust (5)), however, three basic methods of overlay design are widely used.

(1) In-situ testing or laboratory testing of component materials to provide input for the structural redesign of pavements to meet new design requirements.

(2) Deflection measurements taken at the pavement surface usually by beam or falling weight deflectometer (FWD) devices, which give measurements of pavement response to an applied load.

(3) Analytical design using multi-layer elastic analysis.

2.3.2 Design Methods in Use

Deflection based methods are summarized by Rust (5) who reported on the Asphalt Institute Method (80), the State of California (CALTRANS) Procedure (81) and Transport and Road Research Laboratory (TRRL) method (82).

Gordon and Wyman (12) outlined the procedures for overlay design based on pavement surface deflection, which incorporate the following:-

"(a) relationships between pavement deflection level and performance expressed in terms of traffic usage

(b) relationships between reduction in deflection brought about by overlays of various thicknesses."

In the most part these relationships have been deduced from the results of full scale trials.

Analytical methods of overlay design evaluate asphaltic concrete layer stiffness properties from the input of deflection data and condition surveys, the Federal Highway Administration (FHWA) Procedure (83), and Shell Research Procedure (84) are examples of analytically based design procedures.

Brown et al (13) describes the procedure adopted for an analytical pavement design based on FWD data and a back-analysis procedure that enables insitu elastic stiffness to be obtained for each pavement layer.

None of these methods, however are applicable for tackling the reflection cracking problem. Some work has been conducted using an FWD device to test either side of a cracked PCC pavement. This testing was completed primarily to evaluate the structural adequacy of the joint in question. The Asphalt Institute method and the State of

California procedure set a minimum thickness for overlays over cracked pavements, however no technical basis for thickness is given.

2.4 DESIGN MODELS FOR REFLECTION CRACKING

2.4.1 Introduction

Current methods available for overlay design that consider reflection crack propagation are:-

(i) Fracture mechanics theory,

(ii) Finite element computer analysis,and

(iii) Mathematical - mechanical computational model.

The most widely used prediction methods are based on fracture mechanics theory and finite element analysis.

2.4.2 Design Models Developed

Jayawickrama et al (14) used a mechanistic-empirical model that incorporated fracture mechanics principles to design asphaltic concrete overlays over cracked pavements where the cracking was not a structural flaw. Fracture mechanics principles were used to develop a mechanistic model that predicted crack growth through asphalt overlays. This was then calibrated with actual pavement conditions to verify and produce a set of design equations that form the basis of a micro-computer program.

Crack growth through an asphaltic concrete layer is evaluated using a relationship between crack growth and number of load cycles, developed by Paris and Erdogan (15) as given in Equation 2.1.

$$\frac{dc}{dN} = A\,(\Delta K)^n \qquad (2.1)$$

Where c = crack length

N = number of cycles

A,n = overlay material constants

ΔK = stress intensity factor amplitude (K tearing, K shear, K thermal)

This equation can be integrated to give Nf, the number of cycles to failure as shown in Equation 2.2.

$$Nf = \int_0^h \frac{dc}{A(\Delta K)^n} \qquad (2.2)$$

where h = overlay thickness.

Equation 2.1 predicts the rate of crack propagation through an asphaltic concrete overlay due to environmental and traffic stresses imposed on the overlay. Figure 2.1, previously illustrated, defined the three modes of fracture due to these effects.

Two sets of laboratory experiments allowed determinations to be made of constants A and n. Beams of asphaltic concrete were loaded vertically (flexure) to simulate traffic stresses, then in a separate experiment beams were placed in horizontal tension to simulate thermal load effects. Crack growth rates were obtained and constants determined.

The stress intensity factor ΔK represents the combined effects of all three modes of fracture, thermal, shear and tearing. These factors can be expressed in terms as shown in Equations, 2.3, 2.4 and 2.5. Each ΔK is shown as a function of variables that can be evaluated or are known.

$$\Delta K_{thermal} = f_1 (E_o, h_0, S, \Delta T, c) \quad (2.3)$$

$$\Delta K_{shear} = f_2 (E_o, E_1, h_0, h_1, K_s, q, r, c) \quad (2.4)$$

$$\Delta K_{tearing} = f_3 (E_0, E_1, h_0, h_1, K_s, q, r, c) \quad (2.5)$$

where E_0 = stiffness of overlay

E_1 = stiffness of existing surface layer

h_0 = thickness of the overlay

h_1 = thickness of existing surface layer

c = crack length

S = average crack spacing

ΔT = 24 hour temperature drop

K_s = modulus of subgrade reaction

q = loading pressure

r = aggregate interlock ratio

These variables form the basis of input data required for the micro-computer program developed.

The mechanistic model was then put into a regression model where actual field data was introduced to produce design equations. The equations developed were then solved to give overlay life. Figure 2.4 illustrates a flow chart representing the process involved in the determination of overlay life.

The limitations of this type of program lie in the fact that it is partly based on United States site specific data. This reliance on in-situ data limits the use of the program to areas where similar environmental conditions exist.

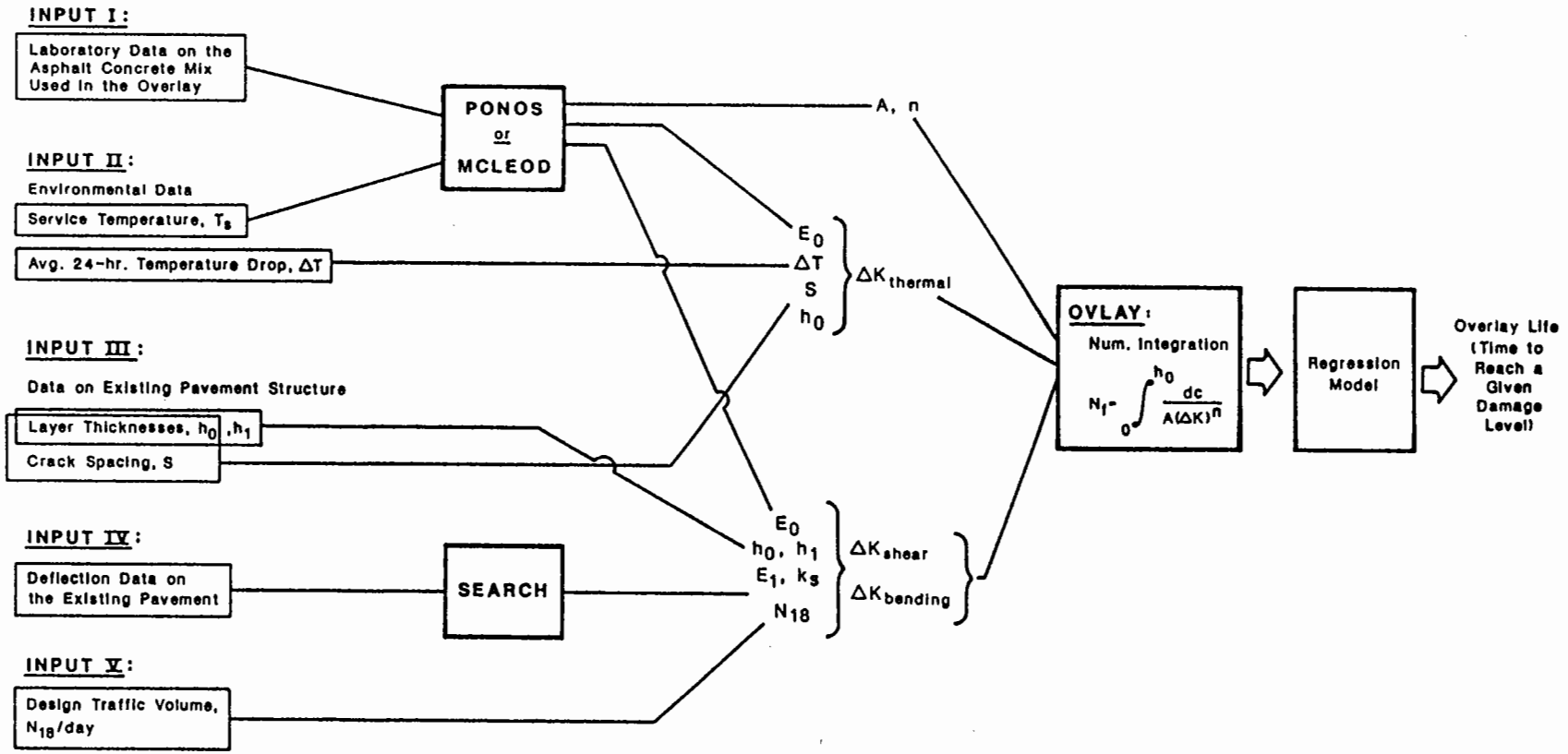

Figure 2.4 Flow Chart for the Design Program ODE (after Jayawickrama et al (14))

Finite element modelling procedures have been used by Van Gurp and Molenaar (16), and Clauwaert and Francken (17), Rust (5) also reports on a finite element procedure ANSR-I developed by Coetzee and Monismith (85).

Coetzee and Monismith used two dimensional finite element analysis to determine the stresses induced in an overlay for both traffic and thermal effects. This study analysed the influence of a rubberized binder interlayer or stress absorbing membrane interlayer (SAMI) placed between the underlying cracked surface and the subsequent overlay. Figures 2.5 and 2.6 illustrate the pavement configuration used and results obtained for a plot of crack tip stress against overlay thickness.

The procedure adopted by Coetzee and Monismith has the disadvantage of being limited by the use of only a single crack in the modelling process. This limitation necessarily means that modelling of slab behaviour is not possible. Nunn (18) described the warping of pre-cracked pavement base slabs under the action of thermal effects, where the temperature gradient from overlay surface to pavement base is of sufficient magnitude in combination with a hardening of the binder in the overlay surface to initiate surface cracking.

To ensure accurate modelling of the reflection cracking phenomenon the ability to consider slab effects would appear to be quite significant. Limitations in the modelling process for finite element programs, as discussed by Yandell and Curiskis (19) and Rust (5), reduce the usefulness of this technique.

Van Gurp and Molenaar (16) have developed a procedure to predict reflection crack growth in asphaltic concrete overlays. This procedure uses a linear elastic multi-layer program with modified input to allow determination of overlay design based on fatigue properties and crack propagation through the overlay. Fracture mechanics principles using Equation 2.1 from Paris and Erdogan (15) and finite element programs were used

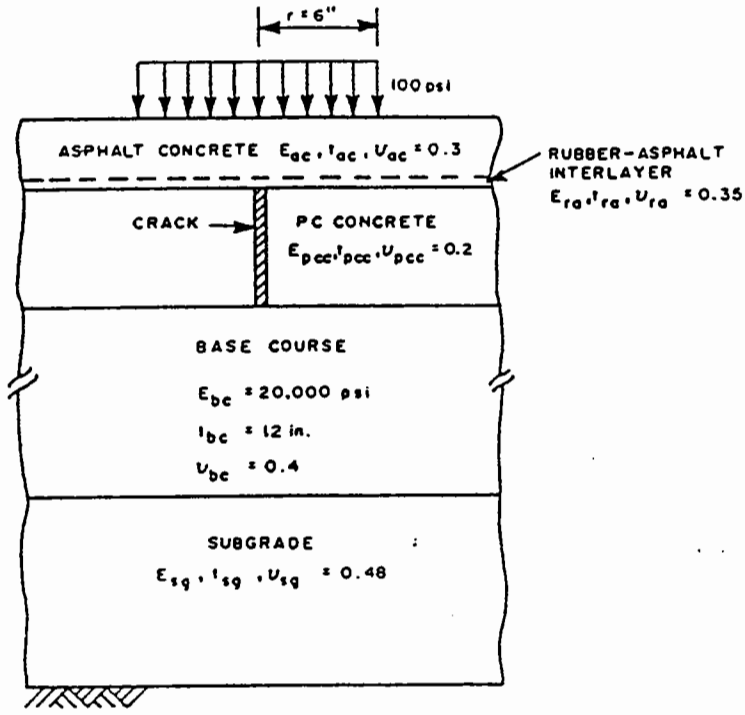

Figure 2.5 Schematic Representation of Pavement Structure Analysed by Coetzee and Monismith (after Rust (5))

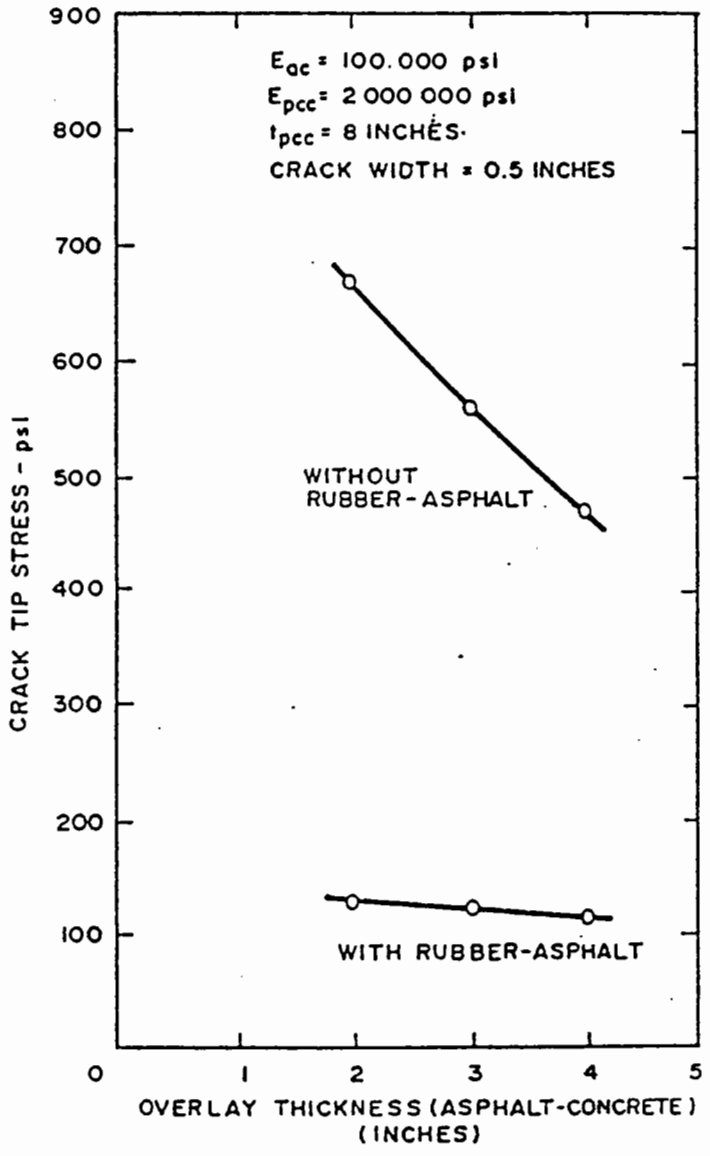

Figure 2.6 Effect of Asphalt Concrete Thickness on Crack Tip Stress by Coetzee and Monismith (after Rust (5))

to determine the number of load applications for full depth cracking to occur in the overlay. This information was then applied as a fatigue criterion in a linear elastic multi-layer program.

This simplified method takes no account of thermal effects and only traffic induced stresses were modelled. Van Gurp and Molenaar claim that the predominant mode for crack propagation is traffic induced loading. This would seem to contradict the findings of others (14), (18), (20) who report that the biggest movement and thus contribution to the reflection cracking problem in asphaltic overlays is derived from thermal movements.

Schmidt (21) uses a "mathematical mechanical computational" model to evaluate the progression of reflection cracks through an asphaltic concrete layer overlying a cement treated base. The model analyses the effects of traffic loading on the overlay. The asphaltic overlay is divided into a series of horizontal elements above the centre line of a pre-existing crack located in a cement treated base.

As loads are simulated on the surface of the overlay the maximum tensile stress occurs in the bottom element. When the bottom element cracks the maximum tensile stress conditions are applied to the second bottom element, whilst all other elements are accumulating non recoverable strains with each successive application of load. This damage associated with successive load applications is modelled by the Miner's Law principle. (Miner (22))

Miner's Law states that:

$$D = \sum_{i=1}^{j} \frac{n_i}{N_i} \qquad (2.6)$$

D = total cumulative damage, having a value of 1 at failure

j = number of strain levels

n_i = number of applications at level i

N_i = number of applications to cause failure at level i.

Repeated applications of load are applied until all elements have cracked. Figure 2.7 illustrates the progression of a crack through the elements.

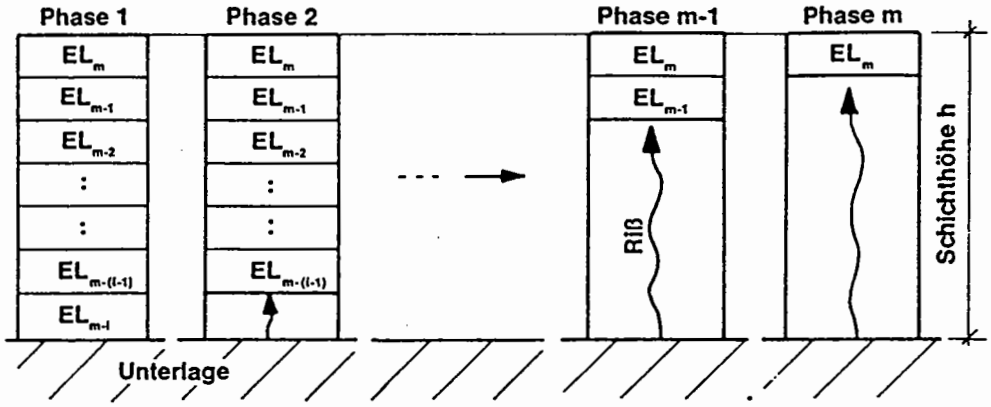

Figure 2.7 Schematic Diagram Showing an Asphaltic Layer Divided into Elements (after Schmidt (21))

This technique can be adapted for use in a finite element program with each elemental tensile stress compared to the fatigue strength of the asphaltic layer thus establishing the number of cycles to failure.

Schmidt states that the effects due to temperature change are minimal, due to the gradual nature in which they develop, thus allowing the asphaltic concrete time to display "relaxation behaviour". Schmidt concludes that the tensile stresses due to a change in temperature are very difficult to analyse and thus incorporation into a computational model is not yet possible.

2.5 FIELD TRIALS TO PREVENT/INHIBIT REFLECTION CRACKING

2.5.1 Introduction

Field trials to investigate the properties of interlayer materials or asphaltic concrete modifiers dates back to the 1930's. These trials were conducted to assess the relative merits of the following treatments (Von Quintus (1)).

(a) cushion courses

(b) stress or strain relieving interlayers

(c) increased overlay thickness.

Table 2.1 from Section 2.2.3.2 showed the current range of treatments available to aid in the rectification of cracked pavements. Rust (5) categorizes all reflection cracking treatments into four groups as outlined below:-

(1) Surface membranes or applications

(2) Overlays

(3) Composite systems with interlayers

(4) Other methods, recycling, heater scarification, rejuvenation.

The accurate evaluation of field trials is dependant on how carefully and detailed the initial pavement assessment is conducted. In reflection cracking trials, the nature of the problem dictates that the vast majority of trials will be conducted on pavements that have been in service for a number of years.

Many field trials have been completed neglecting to conduct a comprehensive condition survey, thus not clearly establishing the state of the road pavement prior to treatment. The results of such trials must be viewed in this light with no firm conclusions able to be drawn.

Other problems associated with field trials lie in the uniformity or otherwise of the existing pavements. Non-uniformity, if not recognized, can lead directly to inaccuracies in the results obtained from trial materials placed over substandard areas.

2.5.2 Geotextile Interlayer Trials

2.5.2.1 Introduction

The use of geotextiles as crack inhibiting interlayers in asphalt concrete construction is increasing each year. In 1988 the International Geotextile Society claimed that 600 million square metres of geotextile were used, throughout the world. In the United States alone 50 million square metres were used in the control of reflection cracking.

2.5.2.2 Successful Trials

Trials that have shown a positive effect in the retardation of reflection cracking in asphaltic overlays through the use of a geotextile have in general been well controlled.

A detailed field trial conducted by the Main Roads Department, Queensland, Australia ((23), (24), (25)), evaluated six treatments in an attempt to prevent reflection cracking from a cement treated base pavement. The six treatments, as shown below, including two different types of geotextile, were laid in 250-300 metre test Sections. Treatments

were placed in two ways (i) covering the entire test section (full width x length) or (ii) on a strip basis where only the existing cracks were treated.

(a) Polymer modified binder interlayers, full width and strip.

(b) Geogrid, full width and strip.

(c) Geotextiles, full width and strip.

(d) Polymer modified binder chip seals.

(e) Polymer modified asphaltic concrete.

(f) Adhesive backed strips, (rubber binders, geotextile on rubberized binder).

The general pavement configuration for this work was a 360mm cement treated base pavement placed in three layers on top of a subgrade CBR5. Subsequent to construction transverse cracking at regular intervals was observed with pumping of fines from the cracks during wet periods. Crack sealing was carried out using a polymer modified binder in an attempt to prevent pumping of fine material thus protecting the underlying layer from further deterioration.

The detailed survey conducted on the pavement prior to overlay used the following techniques:-

(i) visual rating including computer recorded defects,

(ii) video recording of condition prior to overlay,

(iii) deflection survey, and

(iv) excavation of test pits in the existing pavement in both cracked and uncracked pavement sections.

A consistent depth of 45mm of continuously graded asphaltic concrete was placed over all trial materials in November 1987. After fifteen months of service the geotextile treatment, although initially delaying the propagation of cracking, showed no improvement in the number of cracks recorded on the surface. The trial was however

considered a relative success as the geotextile membrane had stopped the pumping of fines.

Sadlier et al (26) confirm the good performance of the geotextile in the above-mentioned trial and outlined the following list of factors that affect geotextile performance.

(1) Type of geotextile.

(2) Asphaltic concrete type.

(3) Binder impregnation.

(4) Surface structure, evenness.

(5) Installation temperature.

(6) Construction method.

Dickson (27) completed several small trial sections in South Africa using a non-woven geotextile over different underlying pavement base conditions. Dickson concluded that there was some positive benefit in the use of a geotextile to delay the appearance of reflection cracks, but more importantly in preventing the pumping of fines.

Von Wijk and Vicelja (28) and Vicelja (29),(30) reported on 15 years of experience in the use of geotextiles under asphaltic concrete overlays. Trials using geotextiles that had been correctly installed were claimed to have prevented reflection cracking from appearing in the overlay surface. Vicelja stressed the importance of correct installation procedures and added to the list of factors affecting geotextile performance from Sadlier et al (26) with the following:-

(a) Appropriate tack coat rate for each individual fabric.

(b) Pavement surfaces must be prepared with no localized deficiencies or loose debris on the surface.

2.5.2.3 Unsuccessful Trials

Button (31) conducted an extensive series of trials in four different locations in the State of Texas (USA) over a three year period from 1979-1981. Within each area the pavement configuration was consistent, however over the four locations the pavement type varied from 75mm of asphaltic concrete on top of 375mm of flexible granular base to 100mm of asphaltic concrete on top of 300mm of flexible granular base covering 150mm of lime treated sub-base.

The aims set out in the study were as follows:-

"(1) to determine the types of distress if any, that fabrics can economically be used to correct,

(2) to ascertain fabric properties that will optimise field performance,

(3) to define satisfactory field installation procedures and,

(4) that realistic specification limits may be established."

Prior to the installation of these geotextiles no detailed condition survey was stated to have been carried out. Visual assessments of all areas indicated the presence of fatigue cracking, alligator cracking and rutting.

In some trial sections rectification of the worst affected areas took place. Overlay thickness for the four sections varied from 45mm to 31mm of continuously graded asphaltic concrete.

After nine years of monitoring Button concluded that :-

(a) No geotextile consistently showed signs of significant improvement in resistance to reflection cracking

(b) Thin overlays (less than 38mm) placed on geotextiles under high traffic volumes can result in premature failure of the overlay through slipping at the fabric interface or breakup of the overlay.

(c) Exposure of the geotextile to prolonged rainfall and traffic action after installation, prior to overlay, can adversely affect the adhesion of the geotextile to the pavement.

This study by Button, not surprisingly, found that geotextiles were ineffective in controlling cracking from pavement failures, namely alligator and fatigue cracks, with only a maximum of 45mm asphaltic overlay.

Maurer and Malasheskie (2) conducted a field trial using a range of geotextiles over the pavement configuration shown in Figure 2.8 with a thickness of overlay equal to 38 mm. The aim of this trial was to determine the cost effectiveness of geotextile interlayers when compared to a crack sealing operation that does not require an overlay.

Prior to the placement of any overlay material Maurer and Malasheskie conducted an extensive pavement evaluation by mapping surface cracks and conducting a structural survey using a Road Rater device. Based on this survey information the pavement area to be used as a trial was split into sections with equal distress levels. A high degree of control was exercised in the placement of both geotextile and overlay material. Checks on density of the asphaltic mix were conducted and checks were made to ensure that the geotextile was placed in accordance with the manufacturers specifications.

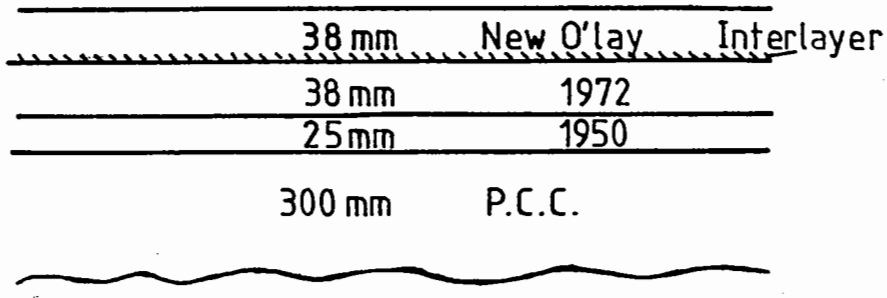

Figure 2.8 Cross Section of Pavement Configuration After Overlay (after Maurer and Malasheskie (2))

At the end of a continuous 44 month assessment program the rates of propagation for the range of geotextiles used were evaluated and compared with the control section. It was concluded that the alternative crack sealing treatment had a better cost benefit ratio in the life cycle cost predictions than the use of interlayers, relative to the initial construction costs. Thus none of the geotextiles used were considered cost effective.

Many field trials have been carried out using geotextiles with unfavorable conclusions drawn at the completion of a monitoring program. Johansson S.S (32) and Fukuoka (33) are typical of papers that claim unsuccessful trials in the use of geotextiles to prevent reflection cracking. However, in a vast majority of these cases, the pavements that were overlaid had failed in their ability to carry traffic loads with the required level of serviceability prior to the application of interlayer treatments.

2.5.2.4 Summary

In summary the use of geotextile interlayers in trial sections has been extensive and encompasses most countries of the world. The important points to come from the field trials in terms of overall performance and installation procedures are presented below.

(1) Geotextile effectiveness in the prevention of reflection cracking is based to some extent on the pavement type.

(2) Geotextiles do prevent the pumping of fines in the pavement structure.

(3) Tack coat rates must be appropriate for each fabric used.

(4) Pavement surface condition prior to fabric placement must be even and free from debris.

(5) A minimum overlay thickness of approximately 38mm is required to prevent slippage or pot-holing of the overlay.

(6) Subsequent to fabric placement and prior to overlay every effort must be made to keep it free from the effects of traffic and moisture.

(7) Good control is required on overlay placement and compaction.

2.5.3 Other Treatments Used in Field Trials

2.5.3.1 Geogrids

Atkinson and Gordon (34) presented the interim findings of the previously discussed Main Roads Department (MRD) trial ((23), (24), (25),) which incorporated the use of a polypropylene geogrid. All trial sections were covered with 45mm of asphaltic concrete.

The polypropylene geogrid posed many construction problems during installation, partly due to the inexperience of the construction crew with this form of interlayer treatment. As reported in the literature (24), (25), only one lane of the two lane trial could be accepted as placed satisfactorily. Unfortunately, no distinction is made in the results presented, to account for the problems experienced during this placement operation.

The fifteen month review of the trial showed that for the geogrid section, cracking had reflected from pre-existing cracks and new cracking in the surface was also recorded. Evidence of pumping from these cracks was also noted in the survey

Other trials completed with a polypropylene geogrid were conducted with overlay depths greater than 100mm over lean concrete sub-bases and PCC pavements (Oliver and Borroni (35), Gilchrist (36)). These trials have been in place on trunk roads in the United Kingdom for five years with no reports of surface cracking in two trials, and hairline cracking (less than 1mm) detected above the pre-existing concrete joints in another.

Oliver and Borroni (35) stress the importance of correct field installation of the grid to ensure that it works effectively and point to poor installation in recent failures of the grid in Queensland ((23), (24), (25)).

Kassner (37) referred to experience in Norway with the application of a polyester geogrid used to prevent the reflection of longitudinal cracking from a structurally deficient pavement. Figure 2.9 illustrates the surface cracking generated by poor construction practises over an existing roadway.

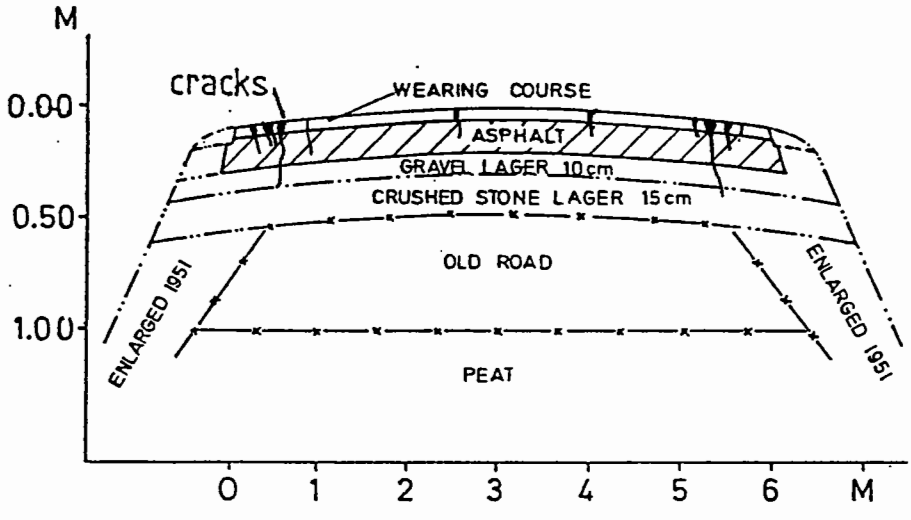

Figure 2.9 General Pavement Configuration Prior to Treatment (after Kassner (37))

Kassner states that fourteen years after the application of the grid in the transverse direction of the pavement and the application of an overlay of approximately 60mm depth no significant cracking occurred. Maintenance on the roadway has been determined by rutting rather than cracking. Unfortunately, no further technical details of this trial were reported, making it difficult to draw any firm conclusions.

It would appear that in the reported trials using geogrids significant retardation of reflection cracking is possible if a thickness of overlay greater than approximately 60mm is used.

2.5.3.2 Polymer Modified Binders

As part of the previously mentioned trial conducted by the Main Roads Department (23), (24), (25), a styrene butadine styrene (SBS) modified binder was used in a 45mm asphaltic concrete overlay over a cracked cement treated base pavement.

During the early monitoring conducted, the modified overlay had significantly delayed the appearance of reflection cracks. However, after the fifteen month review of the trial section, 90% of the number of cracks initially in the pavement had appeared on the surface of the overlay. Accompanying the crack appearance was the pumping of fines.

The use of polymer modified binder (EVA and SBS) in asphaltic concrete was tried by Walsh (38) on a 400 metre length of reinforced concrete pavement with a 70mm asphaltic concrete surfacing. The 70mm modified overlay also included a geotextile at the base of the overlay. After one years performance no cracking is reported to have appeared at the surface, however, no conclusion can be drawn as to the overlay effectiveness at this early stage.

There are very few reports on field trials using polymer modified binders available in the literature. The trials that have been reported indicate that there is some initial benefit in reduction of crack propagation but once cracks appear in the overlay surface, pumping of fines can occur.

2.5.3.3 Cement Treated Base Modifications

Schmidt (21) as part of previously described work developed a notching tool to induce temperature and shrinkage cracks at close spacings in the cement treated base or sub-base layers. This notching is intended to cause micro cracking at a known spacing along the pavement, thus reducing the magnitude of crack widths. The piece of equipment used to notch the 'green' cement treated pavement layer comprises a standard plate compacter with a 35mm steel wedge welded to the base.

Work carried out by Smith and Caltabiano (39) on cement treated base pavements, aimed to reduce the frequency and magnitude of cracking by modifying material specification limits. The properties of the base material that were modified together with alterations to the construction timing are described below:-

(i) The grading of the crushed rock untreated material was tightened on the percent passing 75μm sieve to give a range of 5-7%.

(ii) Plasticity Index (P.I) value was not to exceed 4.0.

(iii) Use of fly ash blend cement (25% fly ash 75% portland cement) in lieu of ordinary portland cement was required.

(iv) A maximum shrinkage for a cement treated beam made in accordance with MRD test Q207 was not to exceed 250 microstrain.

(v) The cement treated base pavement was to remain under a curing coat for 7 days (minimum).

(vi) A bituminous chip seal for trafficking purposes was to be provided.

(vii) The roadway was to be left under traffic for a minimum period of three months before placing an asphaltic concrete wearing course.

These measures when correctly employed increased the crack spacing from 7m to an average of 14m with an associated reduction in crack width. Unfortunately, the results obtained were not only dependent on the above measures but also on the competence of the construction crew. Poor quality controlled sections showed no increase in crack spacing and an indistinguishable reduction in crack widths.

2.5.4 Summary of Field Trials

In summary, the large number of field trials that have been conducted, especially since 1960 have been site specific to a large extent. A vast number of these trials have aimed to solve a particular problem in the pavement, as opposed to evaluation of relative performance based on the materials used in the overlay treatment.

A considerable percentage of trials have been conducted without taking full account of in-situ pavement conditions. This deficiency does not allow rational, objective judgements to be made regarding product performance.

All researchers have emphasized the importance of good field control of materials and processes such that clear trends can be established independent of these variables. Factors of particular significance that have been incorporated into the testing program completed as part of this work are listed below:-

(i) Control of mix properties and compaction standards is of paramount importance.

(ii) Installation procedures for geotextiles and geogrid must strictly follow the manufacturers specifications.

The general trends established in the field trials for individual interlayer treatments and modification of the overlay can be summarized as set out below.

(a)	Geotextile	- must have proper installation to be effective (30), (40),
		- can delay reflection cracking,
		- does stop pumping of fines.
(b)	Geogrids	- installation is vital to the success of the grid,(41),(35),
		- delay of reflection cracking is dependent on depth of overlay,
		- does not stop pumping of fines if cracking appears on the surface of the overlay.
(c)	Polymer	- placement procedure as for normal overlays,
	Modified Binder	- limited evidence of performance.

2.6 LABORATORY TEST WORK ON REFLECTION CRACKING

2.6.1 Introduction

The aim of conducting a program of laboratory testing is to evaluate materials and methods, in a controlled environment, that adequately models field conditions. By accurately modelling in-situ conditions the range of results obtained will have direct relevance and applicability to site performance. The data obtained can be used in a constructive manner ultimately contributing to the design process.

Haas and Ponniah (6) summarizes the experimental conditions that should be evaluated as part of a testing program investigating the reflection cracking problem. A list of these testing parameters can be given as follows:-

(i) Initial crack width opening, and maximum crack width.

(ii) Rate of temperature change.

(iii) Ambient temperature and number of temperature cycles.

(iv) Overlay thickness.

(v) Overlay stiffness as a function of temperature and rate of loading.

(vi) Traffic loads, speeds and number of cycles.

(vii) Combined thermal stress and traffic loading.

(viii) Type and location of crack reflection treatment.

(ix) Overlay mix type.

(x) Conditions of bond between overlay and crack reflection treatment and/or between the overlay and the underlying existing pavement.

Each of these parameters have been included in the testing program as part of this work.

2.6.2 Testing Incorporating Traffic Effects Only

Smith (42) reports that the earliest laboratory flexural testing of asphalt concrete beams was completed in 1972 by Draper and Gagle, who studied the effects of geotextile interlayers on flexural yield strength.

A laboratory study conducted by Yamaoka et al (43) endeavoured to compare differences between seven geotextiles in their ability to prevent the propagation of reflection cracking by the use of a flexural beam test device. Figure 2.10 shows the general test arrangement and dimensions of the beams used.

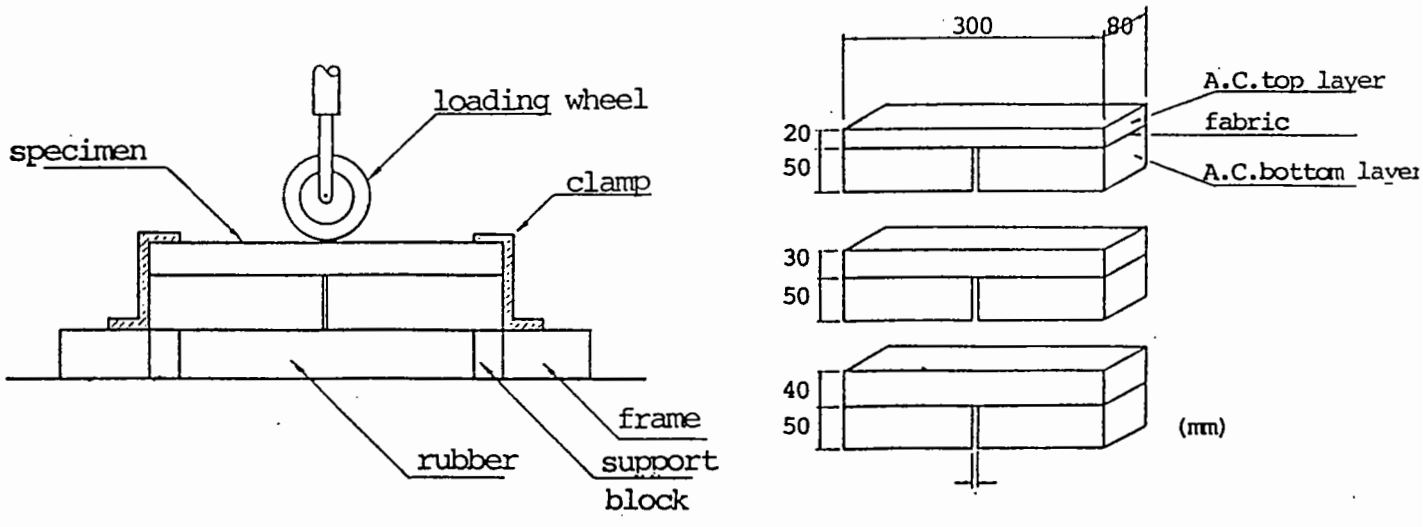

Figure 2.10 Experimental Set-Up for Beam Testing Device (after Yamaoka et al (43))

Beam testing was completed on three different overlay thicknesses 20mm, 30mm and 40mm with controls established for temperature, applied loading and speed of loading, and initial crack width.

Results from this testing program showed that fabric interlayer treated beams had greater lives when compared to control samples. Most results were obtained for the 30mm overlay thickness and showed a 1.7 to 4.2 increase in life over a control sample with no interlayer treatment.

No details of asphaltic mix type, maximum stone size, nor the compaction method or standard were given, therefore no comments can be made on the relevance of these factors to the results obtained. Previous field trials (30), (31) have, however, indicated the importance of not overlaying geotextiles with under 38mm of asphaltic concrete due to likely problems with slippage and the susceptibility to forming potholes in the overlay. Results documented for 20 and 30mm overlay depths would have limited field application.

Hughes (44) conducted an extensive program of laboratory testing as part of a study into the effects of polypropylene grids in pavements. Two pieces of test equipment were used in the evaluation of reflection cracking through asphaltic concrete overlays, these were a beam test facility and a slab test facility.

The beam testing facility consisted of a servo hydraulically controlled device that cycled 525mm long x 150mm wide x 100mm high continuously graded asphaltic concrete beams at 5 Hz between 1.3 kN and 8.3 kN in a sinusoidal pattern. This applied load was transferred to the specimen through a centrally located loading platen as shown in Figure 4.5, Section 4.0. Beams were manufactured by compacting the mix in a steel mould with a vibratory hammer and square foot attachment.

Results from beam testing showed that beams with a geogrid interlayer had greatly extended lives when compared to control beams. Hughes was able to consistently produce these results by exercising good control on test conditions and mix constituents.

The slab test facility allowed the tracking of a moving wheel over slabs of dimensions 1.22 metres long x 0.86 metres in width with varying thicknesses of 40mm to 100mm. The slabs were made in pairs using a continuously graded asphaltic material produced from an asphalt plant, placed on high quality timber boards and compacted using a single drum vibratory roller.

Results of this work showed that the inclusion of a grid inhibited crack propagation under the action of a moving wheel, confirming the results obtained from the beam testing facility.

Hughes experienced problems with debonding of the asphaltic concrete from the timber bases during the initial period of testing and was only able to complete three pairs of slabs, each pair of different thickness. However, as indicated, performance of the geogrid interlayer showed that it's inclusion had a beneficial effect on the life of the slabs tested.

2.6.3 Testing Incorporating Thermal Effects Only

Many investigators have carried out laboratory work on beam samples of asphaltic concrete to establish relationships between crack growth and number of thermal cycles. Haas and Ponniah (6) describes work carried out by Joseph et al which deals with low temperature reflection cracking. Clauwert and Francken (17) used a temperature controlled device to simulate thermal movements in pavements and hence record the propagation of reflection cracks above a predefined discontinuity.

Foulkes (20) conducted beam tests to model thermal movements of lower pavement layers due to 24 hour temperature variations. Crack growth was monitored by aluminium strips placed on the face of the beam. Dimensions of the beam were 1800 mm length x 125mm width x 125 height when compacted using a vibrating hammer. This sample was then trimmed down to a cross section of 100mm x 100mm. Initially the asphaltic concrete was fixed to the testing rig using an epoxy coating on steel plates. This method was later changed to emulsion covered concrete platens to better simulate field conditions.

The asphaltic mix used was a continuously graded mix with a nominal aggregate size ranging from 40 - 14mm, with a binder content of 4.2% and 3% air voids. From this testing Foulkes produced a load against fatigue life graph at different test temperatures.

Trimming sample cross sections down to 100mm x 100mm with a maximum aggregate size of 40mm may produce inherent weakness planes, and prejudice the results, however no indication of this occurrence was described by Foulkes.

2.6.4 Combined Thermal and Traffic Effects on a Single Specimen

There is no significant body of information on laboratory testing that combines the thermal and traffic loads induced in a pavement into one test. Vecoven (45) reported on limited work undertaken on beam tests in which a thermal load was applied by pulling the beam base plate apart at 50μm per min and was combined with a simulated traffic load applied vertically at 1 Hz (5km/hr effective traffic speed). Results were presented showing only one control test and one interlayer beam. No further comment can be made on this testing procedure due to the lack of presented information.

Smith (42) undertook a research program sponsored by FHWA to develop a simple laboratory test with the following aims:-

"(a) Analysis of the mechanisms by which reflection cracking occurs,

(b) Estimation of the benefits of using various interlayers,

(c) Definition of which interlayer properties correlate to crack retardation, and

(d) Avoidance of the extensive costs and delays that are associated with full-scale testing of inappropriate materials."

The beam testing facility used by Smith had the following set-up:-

(1) Sample size 300mm length x 75mm height x 75mm width.

(2) The loading configuration consisted of 4 loading "feet" that "walk" across the sample, simulating a moving wheel as illustrated in Figure 2.11.

(3) Rate of loading was 5 seconds/cycle.

(4) Room temperature 20°C - 23°C.

(5) Each loading foot produced a force large enough to give a maximum radius of curvature in the beam of 37.5 metres. This figure was chosen because at this radius, cracking would be expected in a 50mm thick asphaltic concrete pavement.

(6) Thermal loads were applied to the sample by tensioning the interlayer geotextile.

The full beam testing configuration used is illustrated in Figure 2.11.

The results obtained by Smith for flexural fatigue as illustrated in Figure 2.12, led to the following conclusions being drawn.

"(1) In closely controlled fatigue testing of asphaltic concrete specimens, the random error associated with aggregate position and orientation is sufficient to mask fabric related differences in fatigue life.

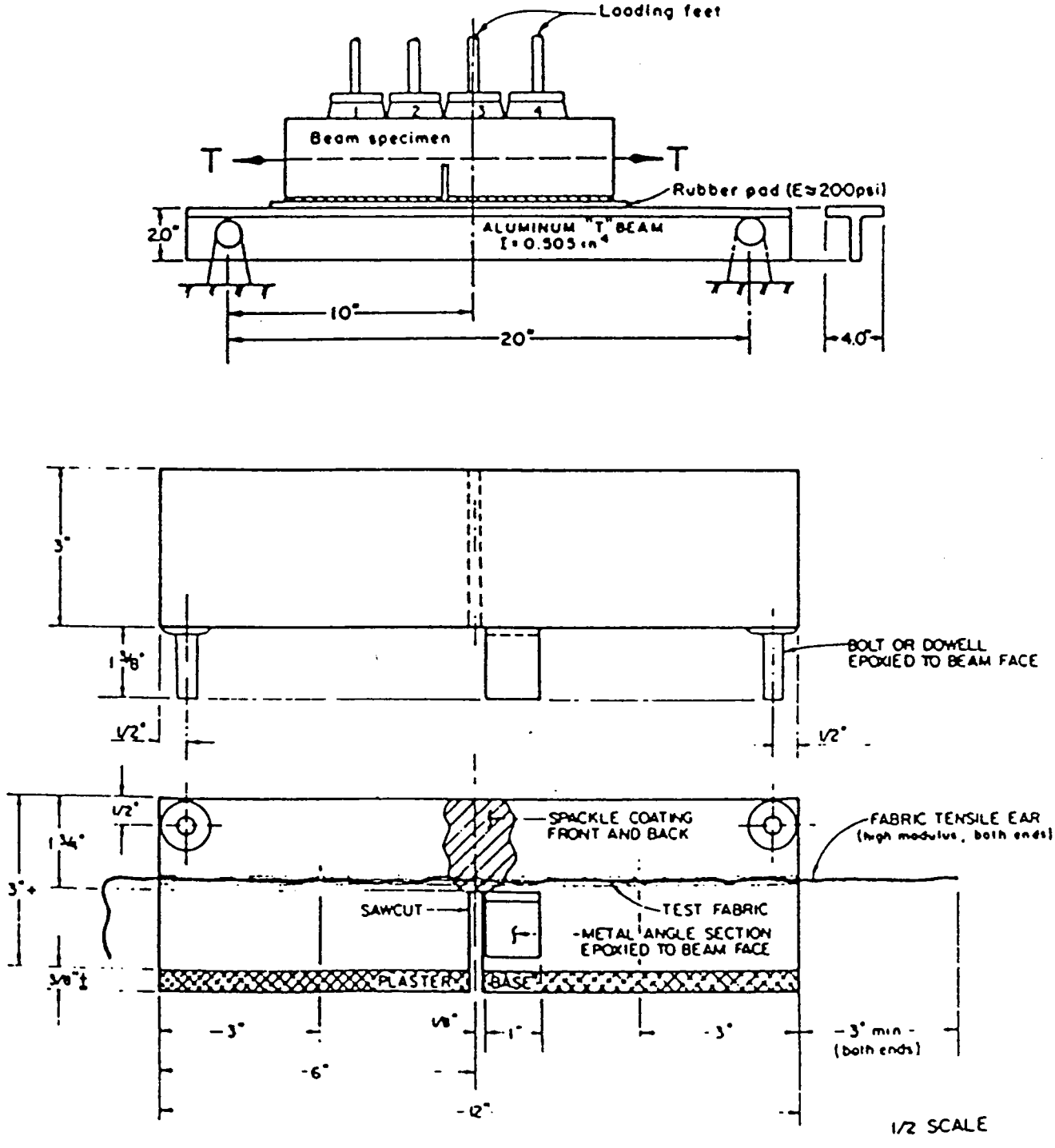

Figure 2.11 Testing Arrangement for Beam Specimens (after Smith (42))

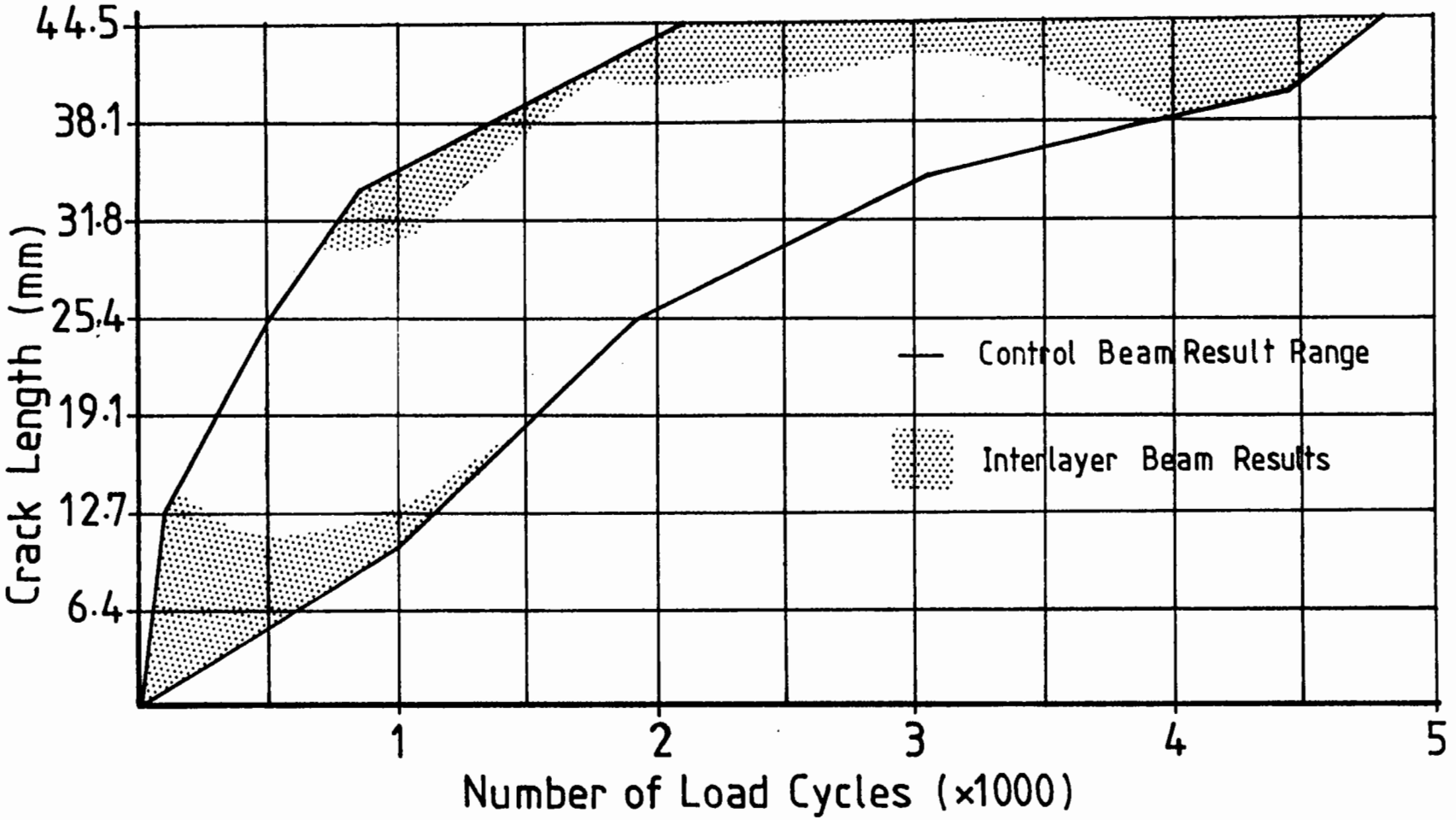

Figure 2·12 Average Crack Length vs. No. of Cycles (after Smith (42)).

(2) Paving fabrics do not appear to reduce the initial deflection of asphaltic concrete beams in laboratory testing. This suggests that a fabric interlayer is not a significant tensile reinforcing element in an asphaltic concrete pavement.

(3) Fatigue crack growth through the asphaltic concrete beam specimens did not appear to be delayed by fabric interlayers."

The results illustrated in Figure 2.12 would seem to indicate that either:-

(a) the method of testing, that is, slow vertical load cycling and an applied tensile load through the geotextile does not adequately model real pavement conditions, or

(b) the controls exerted on materials and processes used to manufacture the specimens was not of an adequate standard to give repeatable results.

2.6.5 Summary of Laboratory Testing

Laboratory testing that has been completed, has for the most part concentrated on the effects of traffic loading. Smith (42) who attempted to combine both traffic and thermal effects in a laboratory trial failed to obtain any meaningful results. The importance of establishing tight controls on all variables involved in the the testing process was stressed by Haas and Ponniah (6), and indeed should form the corner stone of any laboratory work.

There exists a need to develop test equipment that can adequately simulate the effects of both traffic and thermal influences in the pavement and asphaltic overlay. The test equipment and methods developed as part of this work have allowed a further understanding of the relative merits of interlayer performance to be gained and have hopefully started a movement toward testing these combined effects.

CHAPTER 3

INTERLAYERS AND ASPHALTIC MIXES

3.1 INTRODUCTION

Selection and appraisal of interlayers and asphaltic modifiers was based on material availability and a history of use in field trials. Material selection covered a range of interlayers from a stiff polypropylene grid to a geotextile and an asphaltic modifier. This wide range of products ensured that the test equipment would provide accurate and repeatable results for most types of materials used to prevent reflection cracking.

All interlayers and the asphaltic modifier chosen for testing have been used in field trials and are regularly used in practice for the control of reflection cracking. A data bank of information is available to form the basis for development work on a laboratory test facility.

The materials chosen for incorporation in this testing program are listed below:-

(a) Polypropylene geogrid.

(b) Polyester non-woven, needle punched geotextile.

(c) Polymer modified binder [Styrene Butadine Styrene (SBS)].

(d) Control mix, continuously graded, 20mm maximum stone size asphaltic concrete.

3.2 PROPERTIES OF THE INTERLAYERS AND MODIFIED MATERIALS

3.2.1 Polypropylene Geogrid

The geogrid dimensions and general configuration are illustrated in Figure 3.1. The grid was supplied in a 20 metre length by 4 metre width roll and was cut to the correct dimensions for testing purposes.

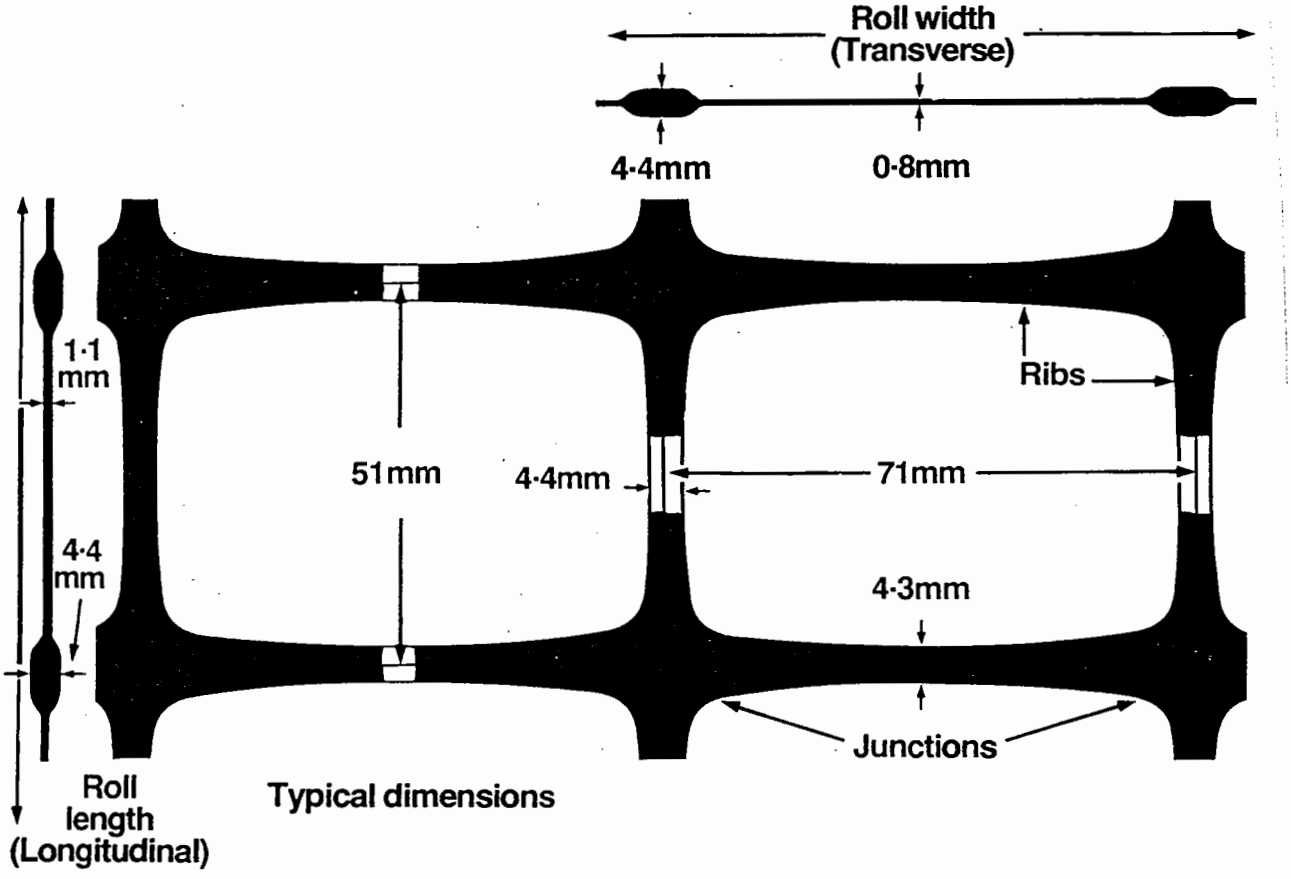

Figure 3.1 Geogrid Dimensions

The physical properties of the grid as supplied by the manufacturer are displayed in Table 3.1.

Table 3.1 Geogrid Properties

Direction	Tensile Strength kN/m	Peak Strain %
Transverse	18.0	10.0
Longitudinal	14.0	14.0

The weight of the material was 0.24 kg/m^2 and it had a softening point of 148°C when tested in accordance with BS 2782 Method of Testing Plastics.

Together with the supply of the grid the manufacturer provided installation instructions, which were followed during the course of laboratory work. The procedure for a site installation comprised the following steps:-

(i) Prepare a flat surface free from dust and vegetable matter.

(ii) Unroll the geogrid onto the desired pavement area.

(iii) Fix the leading edge of the grid to the pavement with fixing clips nailed into place.

(iv) Tension the grid using a tensioning bar which hooks into the geogrid across its full width and winch to a force of 300-500 kg, the maximum extension should be 250mm per 50 metre roll. This process ensures that all ripples are removed.

(v) Fix the free end of the grid in the same manner as previously described.

(vi) Apply a surface dressing to the grid of either:-

- bitumen spray and stone chippings or
- pad coat of asphaltic concrete, or
- slurry seal.

In the laboratory each step of the installation technique was followed with the exception of the tensioning process. The geogrid pieces were flattened out prior to use thus posing no curling problems in the testing moulds.

A bituminous seal with stone chippings was used as the fixation method. The spray rate of 100 pen bitumen used was 1.1 litres per square metre followed by an even covering of washed and heated 6mm nominal size chippings. Rolling of the chippings into the seal coat was completed using a 390mm length of steel pipe with a diameter of 100mm and a wall thickness of 12mm.

Plate 3.1 (a) and (b) show the bases used for beam testing with a gap spacer in place prior to the placement of the grid and application of the bituminous seal, followed by rolling of the chippings into the bituminous seal. A close up view of the finished application can be seen in Plate 3.2 (a).

3.2.2 Geotextile

The geotextile chosen was a polyester non-woven needle punched fabric with the following physical and mechanical properties.

(i) Weight 140 g/m^2.

(ii) Thickness 1.0mm.

(iii) Melting point 260°C.

(iv) Grab tensile test 680 N (DIN 53858 on sample 100mm x 200mm).

These material properties were selected as they conform to those recommended by Wright (46) (61) and are very similar to the fabrics used in the Main Roads Department of Queensland, Australia (MRD) field trials (23), (24), (25).

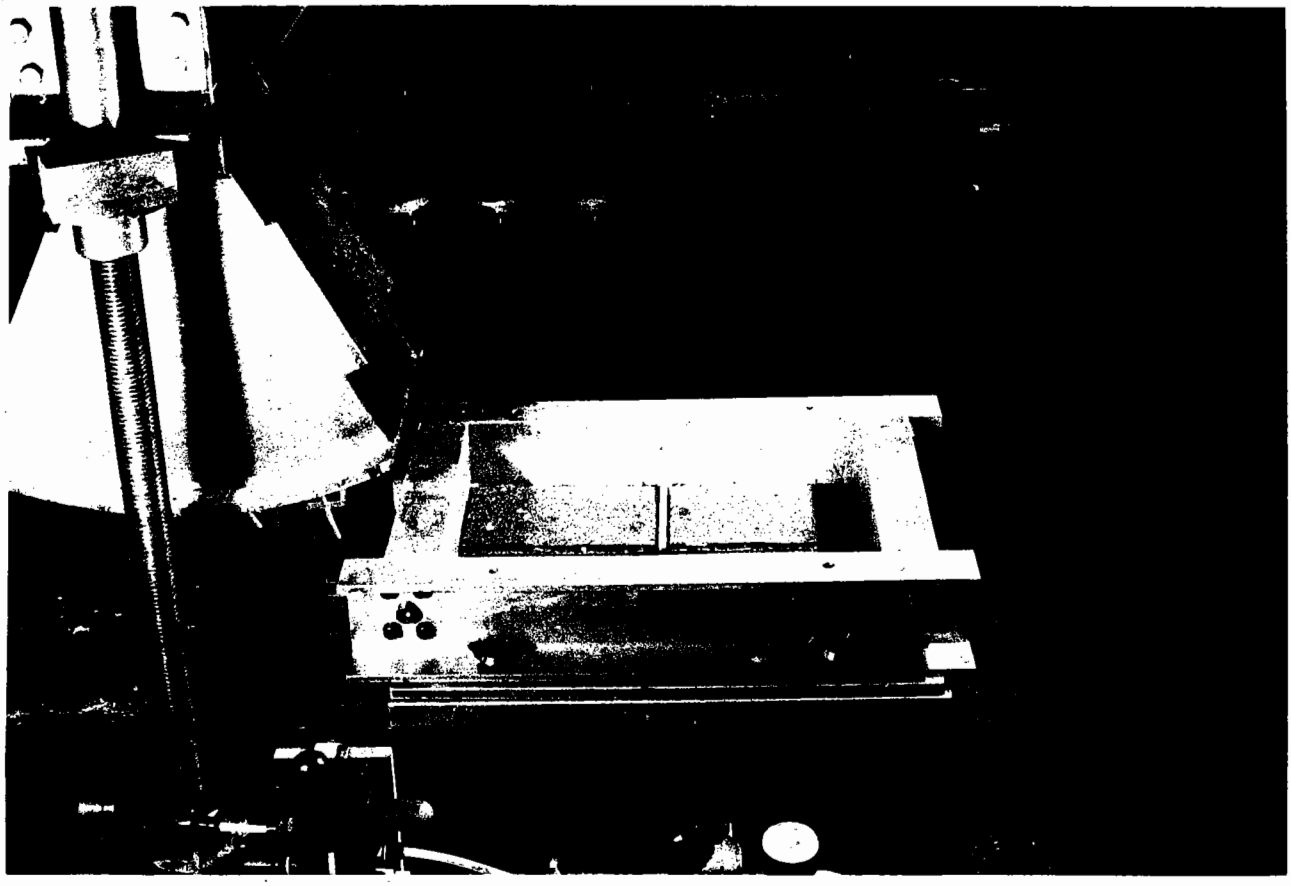

(a) Emery Paper Covered Bases With Gap Spacer

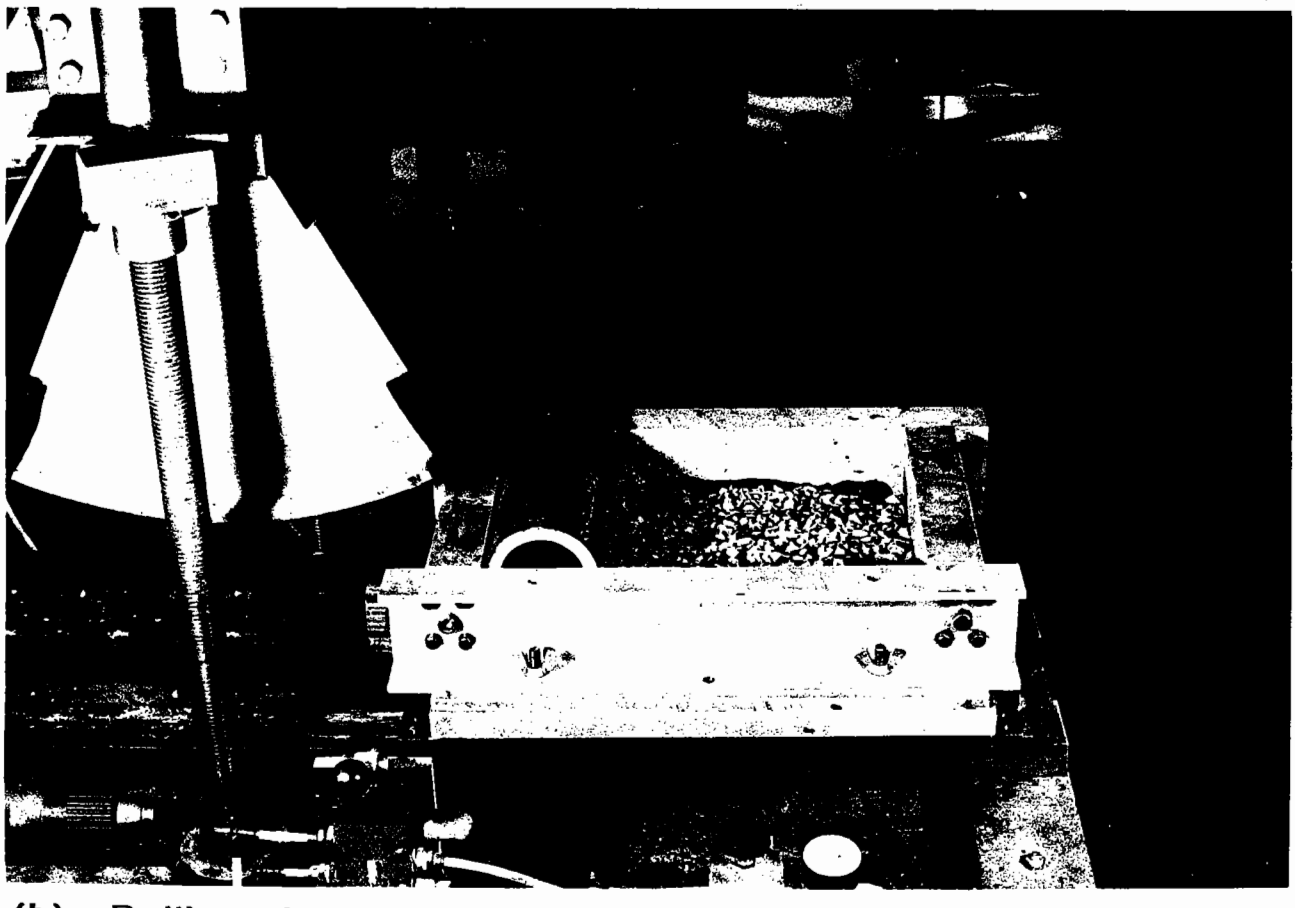

(b) Rolling of Chippings into the Bituminous Seal Fixing Method for Geogrid Interlayers

Plate 3.1 Interlayer Preparation for Beam Specimens in the Roller Compactor Mould

The procedure undertaken to place this fabric was recommended by the manufacturer and proven through field trials [Vicelja (30)] to produce the most consistent results and give the best performance from the geotextile. A bituminous seal using 100 pen binder was placed at a rate of 1.0 litres/m^2, the fabric was subsequently rolled onto the sprayed surface and the same roller used in the geogrid application was used to ensure that the binder invaded the geotextile.

Asphaltic concrete was placed directly on top of the fabric and compacted to the required density. No problems were experienced during this operation and no subsequent failures in test specimens were attributed to failure of the geotextile bond.

3.2.3 Asphaltic Modifier

The decision to use an asphaltic concrete modified with a polymer was made for two reasons, firstly a modified asphaltic concrete would provide a means of assessing the sensitivity of the test equipment and secondly a polymer modified binder has been used in recent field trials conducted in the UK (38) and Australia (23), (24), (25).

The Polymer used in the modified binder was a Styrene Butadine Styrene (SBS) which was supplied from the manufacturer pre-blended. The percentage of polymer by mass in the binder was stated to be 7.0% ± 1.0 with properties stated by the manufacturer as outlined in Table 3.2.

Table 3.2 Properties of Polymer Modified Binder

Test Description	Units	Value
Penetration at 25°C	0.1mm	90 ± 20*
Softening Point	℃	85 ± 10

* Tested and found to be 81.0.

As the product was pre-blended it was possible to incorporate it in the mixing process as for a standard binder. No difficulties were experienced during the mixing or compaction process as a result of the modified binder.

3.3 ASPHALTIC CONCRETE MIX CONSTITUENTS

3.3.1 Introduction

A continuously graded asphaltic concrete mix was used in all experimental facilities. The availability of mix gradings from the British Standards BS594 (86) and BS4987 (47) that could have been used were a hot rolled asphalt (a) wearing course, b) basecourse, c) modified basecourse or a continuously graded asphaltic concrete (dense bitumen macadam). Figure 3.2 illustrates the difference in these grading curves.

The choice of a continuously graded mix was made as this represents the current mixes used for overlays in most countries around the world.

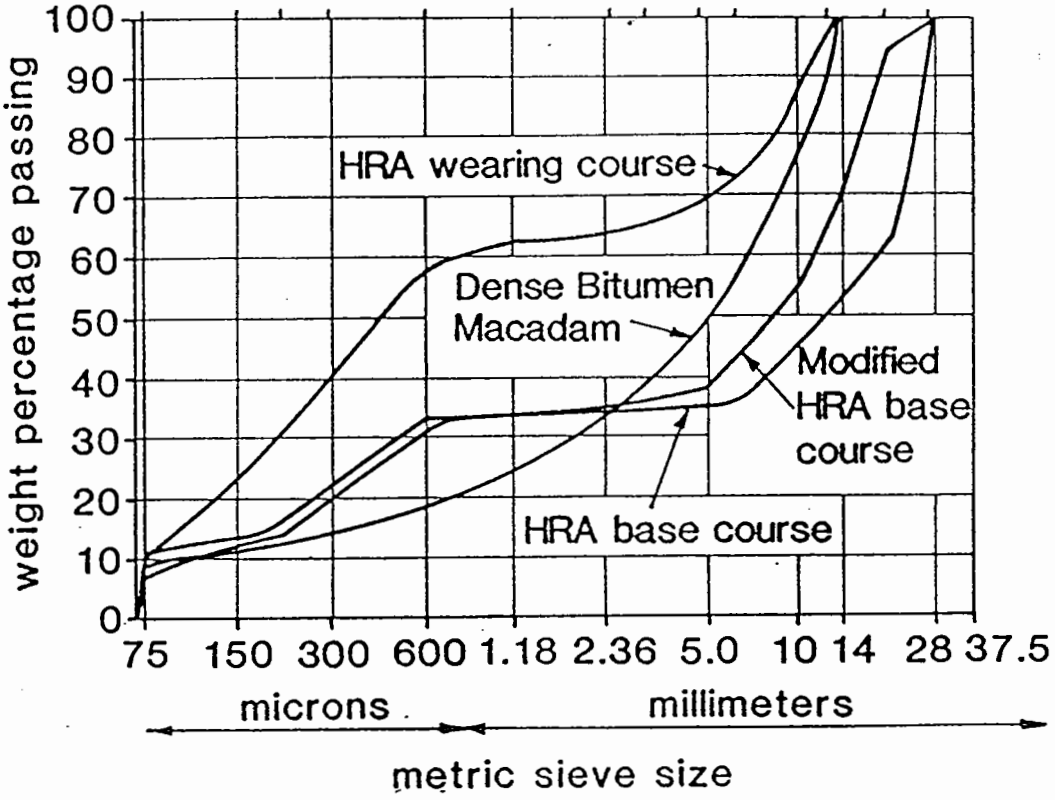

Figure 3.2 Aggregate Grading Curves from BS 4987 and BS 594

3.3.2 Binder Type

The standard binder used in all tests had a penetration at 25°C of 65 ± 5 and a softening point of 51 ± 0.5°C. This particular binder was chosen because it is directly comparable to a class 320 bitumen used in Australia for asphaltic concrete work. Shell International supplied the required conversion from class 320 to a penetration value of 65 at 25°C.

The consequence of selecting this penetration of binder was that blending of a 200 pen and blown bitumen was necessary on a regular basis to achieve the 65 pen required. Blending was completed in quantities of 10 to 15 kilograms as this proved to be the limit for successfully combining the two bitumen types with the mixing apparatus available. Penetration testing of both constituents was conducted before blending and the product was tested after blending.

3.3.3 Aggregate for Mixes

Aggregate used for all testing was supplied from the same quarry source. The rock type was a porphyritic andesite with a specific gravity equal to 2.81. The fine material used was from the same parent rock and had a specific gravity of 2.71.

Having decided that a continuously graded mix was to be produced the actual grading curve was based on the British Standard BS 4987 (47) 20mm maximum stone size dense bitumen macadam mix and Main Roads Department (MRD) (48) 20mm mix design for hot mixed asphalt paving. Both grading envelopes were plotted as shown in Figure 3.3 and a target grading chosen that approximates both specifications.

In Figure 3.3 only a single line with no bandwidths is indicated as the target grading. Material from each sieve size was individually weighed to ensure close agreement with the required grading curve. By choosing to produce an exact grading curve it was necessary to sieve all size fractions out of the supplied material before recombining. The total quantity of aggregate used for the testing program was 1850 kilograms.

3.4 MIX DESIGN

3.4.1 Introduction

The methods available for the design of the asphaltic mix were either BS 4987 (47) based on a recipe method or MRD specification form 11.09 (48) based on Marshall mix design procedures. As the grading chosen approximated both of these specifications, the Marshall mix design method was chosen, together with further requirements incorporated in MRD 11.09 as listed in Section 3.4.2.

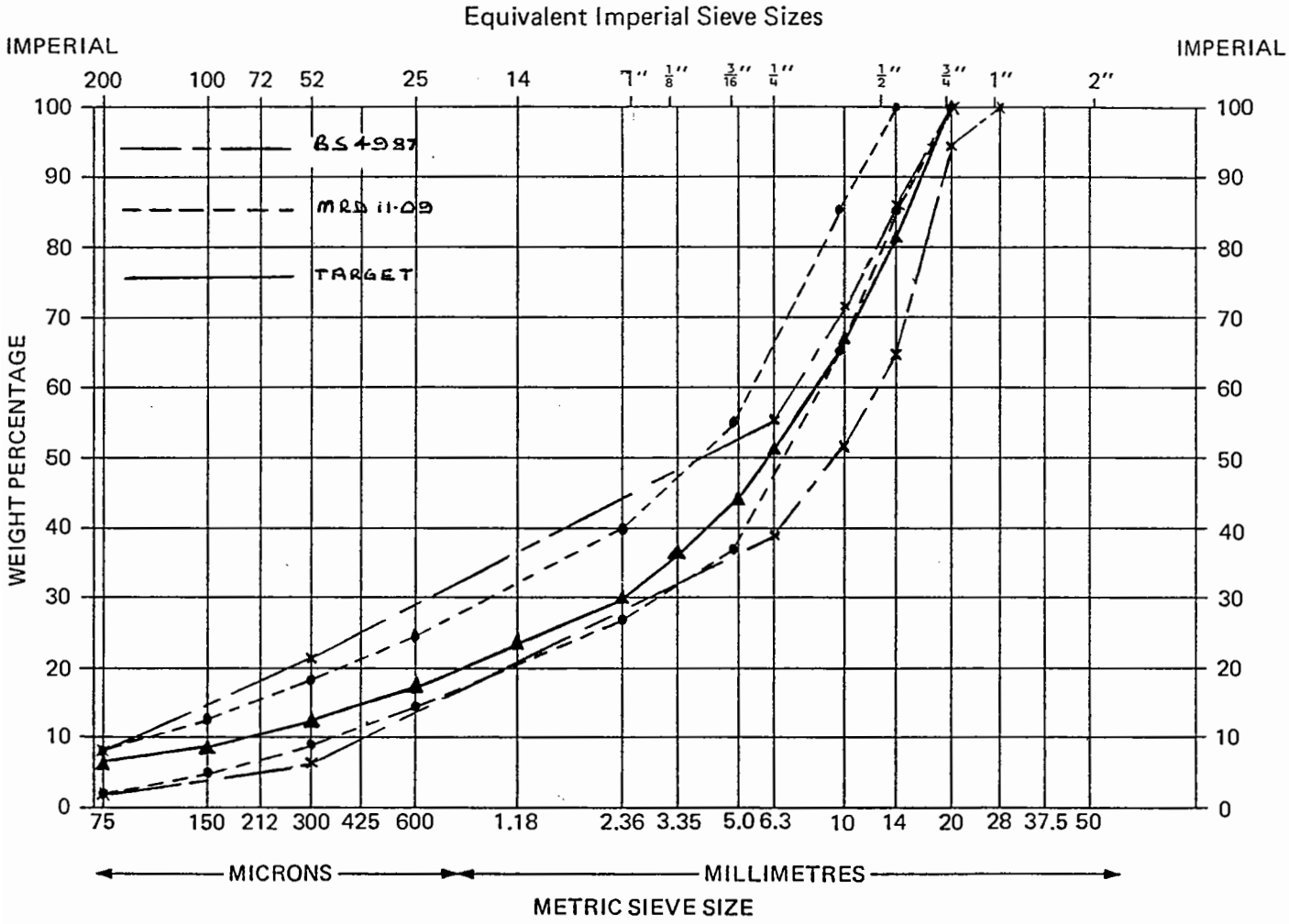

Figure 3.3 Target Grading used for all Asphaltic Concrete Mixes in the Testing Program

3.4.2 Mix Design Method

In specification 11.09 (48) the requirements for mix design are listed as follows:-

(a) Marshall mix design - 50 compaction blows on each face of the specimen.
- mix stability, 6 kN (min)
- flow of the mix 2mm (min)
- stiffness of the mix 2 kN/mm (min)

(b) Voids in mineral aggregate (VMA) - 20mm mix; 14% (min)

(c) Air voids in the compacted mix - 3% to 7%.

(d) Binder content -the amount required to satisfy (a),(b) and (c) above

The results of the Marshall test and verification procedure are shown in Table 3.3.

Table 3.3 Marshall Mix Design Results

	Marshall Stiffness kN/mm				
Test No.	Mould 1	Mould 2	Mould 3	Mould 4	Binder %
A	1.98	1.92	1.81	1.44	5.0
B	-	2.20	2.40	2.17	4.2
C	2.99	3.26	2.20	2.39	4.5

Density evaluation of Marshall pats was completed prior to the determination of stability and flow properties of the mix. The mean value of voids volume of those pats with 4.5% binder content by mass was 6.8%. Equation 3.1 shows how VMA is calculated.

$$VMA = Vv + Vb \quad (3.1)$$

where Vv = Volume of voids

Vb = Volume of binder

The volume of binder can be calculated by using Equation 3.2.

$$V_B = (100 - V_V) \quad \frac{\left(\frac{\%\ \text{Binder}}{\text{SG Binder}}\right)}{\left(\frac{\%\ \text{Agg.}}{\text{Spec. Grav. Agg}}\right) + \left(\frac{\%\ \text{Binder}}{\text{Spec. Grav. Binder}}\right)} \qquad (3.2)$$

The VMA for the mix was calculated to be 17.0. A binder content of 4.5% by mass was used for all testing as it satisfied the specification requirements. The Total Specific Gravity (TSG) of the mix was calculated using Equation 3.3 as shown below.

$$TSG = \frac{100}{\left(\frac{\%\ \text{Agg.}}{\text{Spec. Grav. Agg.}}\right) + \left(\frac{\%\ \text{Binder}}{\text{Spec. Grav. Binder}}\right)} \qquad (3.3)$$

A small computer spreadsheet was developed to calculate changes to the mass required on each sieve size to allow for variations in:-

(a) mould volume (shear box, beam testing, slab testing), and

(b) percentage of air voids.

A copy of this spreadsheet is illustrated in Figure 3.4.

The mixing procedure adopted for all samples was kept constant throughout the experimental program. Weighed aggregate was mixed in planet mixers with the maximum aggregate mass of 5.5 kilograms for each lot with the appropriate binder mass subsequently added. Mixing time was five minutes, ensuring a thoroughly blended product, which was then placed back in the ovens at 160°C to achieve a constant mix temperature for all lots. Plate 3.2 (b) shows the ovens and mixes used for the testing program. Consistency in the mixing process ensured that variations in results obtained from test procedures are independent of the raw products used or the asphaltic concrete mix.

MIX PROPORTIONS -CALCULATION CHART (input all variables)
DATE: 2 Mar 1990 (Vol.of 1/2 S/Box 0.00768 m3)
(Vol.of R/Comp.100mm0.0112m3)
VOL OF MOULD (m 3) .01120 (Vol.of R/Comp.75mm0.084m3)
PER AIR VOIDS(0.X) .06000
VOL OF MAT (m 3) .01053
T.S.G = 2.61 MASS OF SOLIDS(kg) 27.489

PER BINDER (0.X) .045 MASS 1.237
PER AGG (0.X) .955 MASS 26.252

NUMBER OF LOTS REQD. 5

MASS FOR EACH LOT (agg.) 5.250 kg
MASS FOR EACH LOT (binder) .247 kg

SIEVE SIZE (mm)	PERCENT RETAINED (%)	MASS RETAINED FOR MIX REQD.	CUMM. TOTAL
20	0	0	0
14	19	.998	.998
10	14	.735	1.733
6.30	16	.840	2.573
3.35	14	.735	3.308
2.36	7	.368	3.675
1.18	7	.368	4.043
600	6	.315	4.358
300	5	.263	4.620
150	3	.158	4.778
75	2	.105	4.883
DUST	7	.368	5.250
	TOTAL	5.250	5.250

Figure 3.4 Spreadsheet used to Evaluate Mix Quantities

Plate 3.2 (a) Completed Interlayer Treatment for the Geogrid

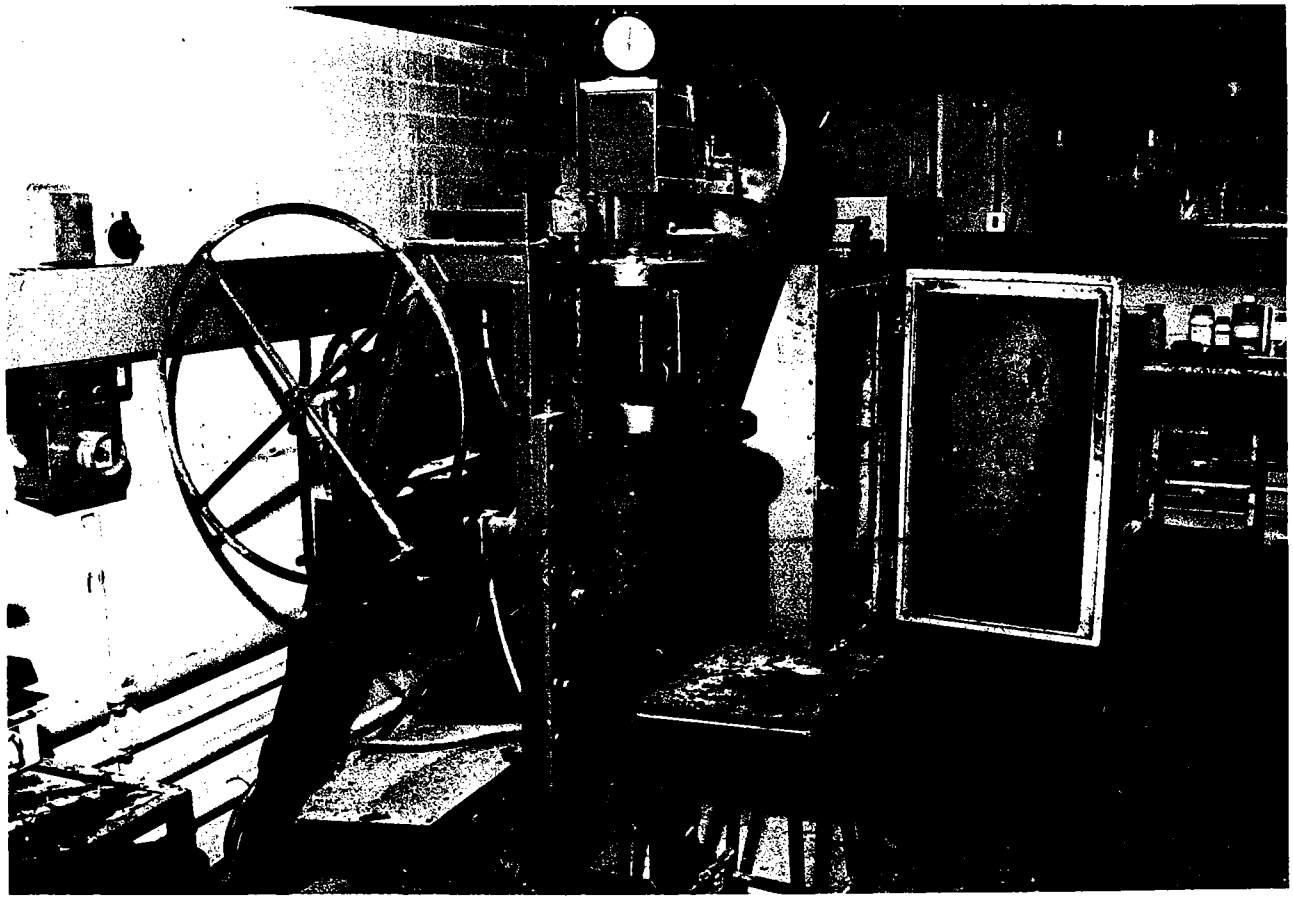

Plate 3.2 (b) Planet Mixer and Oven Used for all Asphaltic Concrete Mixing

CHAPTER 4

LABORATORY TEST FACILITIES

4.1 INTRODUCTION

A laboratory test program was conducted to evaluate the relative effectiveness of different treatments used to prevent reflection cracking in asphaltic concrete overlays. Three sets of laboratory test equipment were used to complete the research program which were the Shear Box, Beam Test Facility and Slab Test Facility.

Testing using this equipment has been conducted previously at Nottingham University by Hughes (44),(49), Brunton and Brown (50), Guo et al (54) and SWK Pavement Engineering (SWK(PE)) (51),(52),(53). The scope of testing in this work extends the use of these apparatus in both the method and purpose of use. Most development work has been completed on the beam testing facility to incorporate the effects of thermal and traffic loads in a single test specimen.

4.2 SHEAR BOX APPARATUS

4.2.1 Introduction

During the construction of a multilayer pavement structure the forming of interlayers between successive pavement layers is inevitable, as the compaction standard required to provide good mechanical properties can only be achieved in specified layer thicknesses. The maximum thickness is a function of material type and properties, together with current construction plant capabilities. Other factors that play an important role in the selection of layer thicknesses are tolerances on surface level, paver type and kerb tolerances.

Pavement design programs such as CIRCLY and BISTRO assume full bonding of successive pavement layers. Should some breakdown of this bond occur then the upper pavement layer becomes over-stressed causing the premature deterioration of the pavement structure. An example of this premature failure through debonding was reported by Kadar (55) in discussions on the use of the Accelerated Loading Facility (ALF) (66) in Queensland.

Kadar reported that a three layer cement treated base pavement was showing signs of distress due to debonding of the pavement layers after the infiltration of water, through reflection cracks and from the pavement shoulder on a one way cross-fall. As a result of layer debonding the traffic loads were not distributed to the lower pavement layers resulting in a closely spaced block cracking of the upper cement treated base layer.

In the case of interlayer treatments, construction techniques should be employed that prevent debonding occurring. Such treatments may include current slurrying of successive pavement layers in cement treated base construction. Reports of interlayers causing asphaltic overlay slippage have generally occurred where an excessive amount of tack coat has been applied [Vicelja (29)].

The shear box apparatus was used to make determinations of the shear strength along the interface of subsequent asphaltic layers. The interface conditions were varied to include the interlayer treatments used in this program of work.

4.2.2 Operation of the Shear Box

To evaluate the shear strength of each interlayer treatment used during the course of the experimental program, the shear box developed by Hughes (44) was used.

Hughes (44) reported that large shear boxes had been used in the past by Brady et al (67), Pike and Bishop (56) to examine unbound aggregates, and by Uzan et al (57) to test asphaltic specimens in a shear box of plan dimensions 150mm x 100mm.

As a result of the construction technique adopted by Hughes in his 320mm x 320mm plan dimension shear box, he reports that with front and rear faces intersecting the predetermined failure plane it is not possible to mobilize the full shearing strength simultaneously along the full length of this plane. This piece of test apparatus is not suited to the determination of the inter-relation between stresses and strains but to determine a peak shear stress at failure along a predetermined plane. This is precisely the context in which the apparatus has been used for the current series of tests.

The basic shear box apparatus and details of the baseplate and roller bearing carriage are illustrated in Figures 4.1, 4.2 and 4.3. Hughes determined the peak shear strength of the interface between two layers of asphaltic concrete, with and without the geogrid interlayer. The operation of the shear box is not too dissimilar to the familiar soil mechanics shear box test, except on a larger scale. To place and compact the two asphaltic concrete layers a timber mould was fitted onto the steel baseplate as illustrated in Plate 4.1.

Layers of 75mm thick asphaltic concrete were placed and compacted using a static load of 250 kN applied to the sample through a rigid steel plate for five minutes. This method of compaction achieved an average air voids content of 10.5% but does not represent typical compaction procedures followed on site.

Upon completion of the compaction process the timber mould is removed and four steel angles 75mm x 75mm that form part of the baseplate were butted against the bottom layer of the specimen. A top plate with saw tooth profile is placed on the second compacted layer, to which loading plates are connected to accommodate the horizontal actuator.

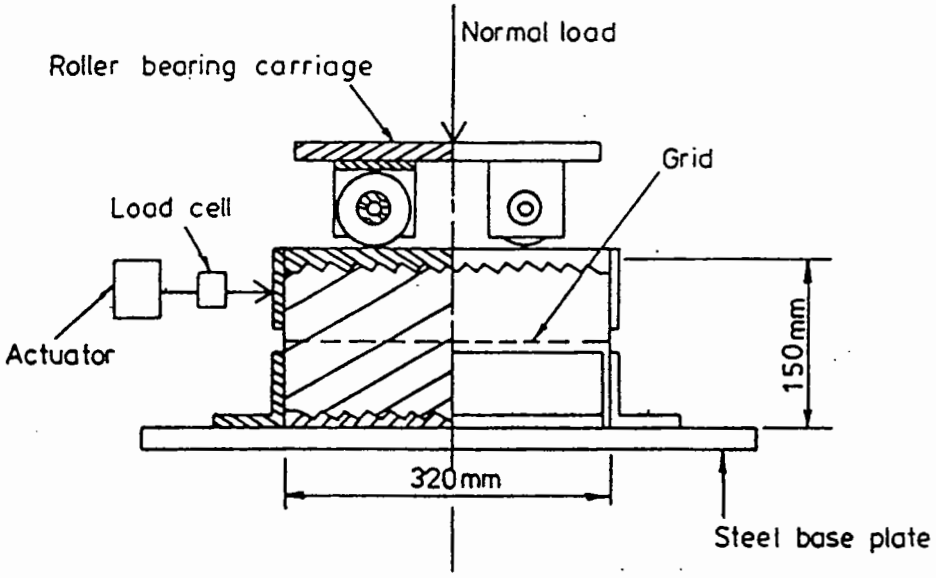

Figure 4.1 Shear Box Apparatus Configuration (after Hughes (44))

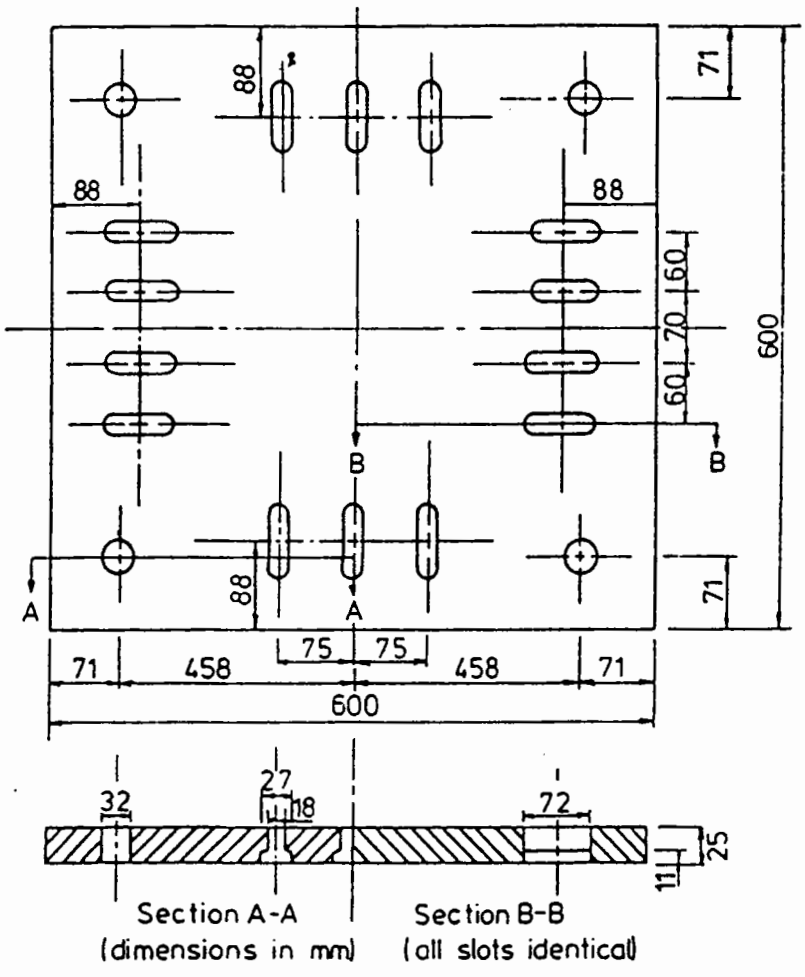

Figure 4.2 Steel Base Plate Arrangement (after Hughes (44))

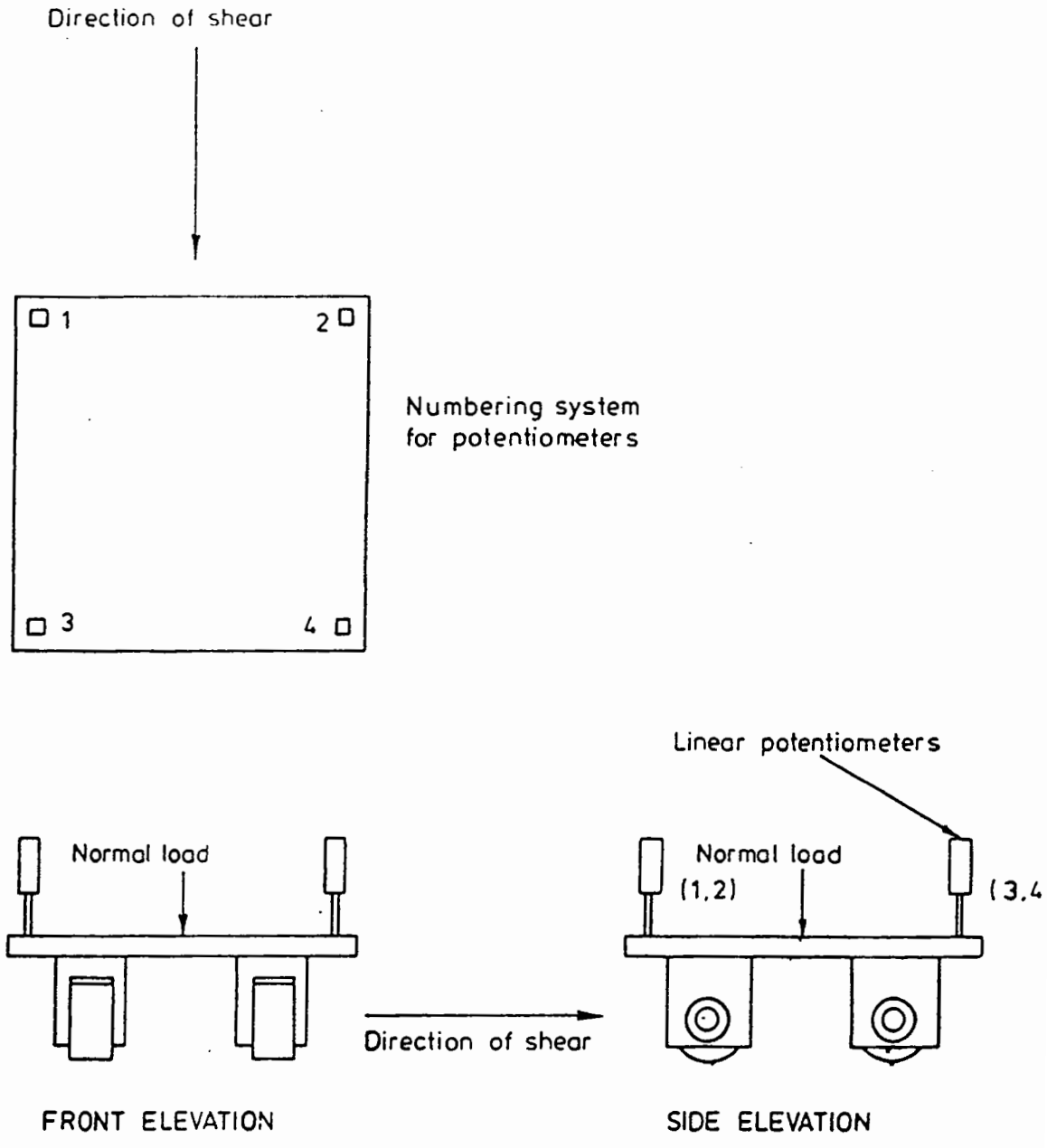

Figure 4.3 Roller Bearing Carriage and Linear Potentiometer Arrangement (after Hughes (44))

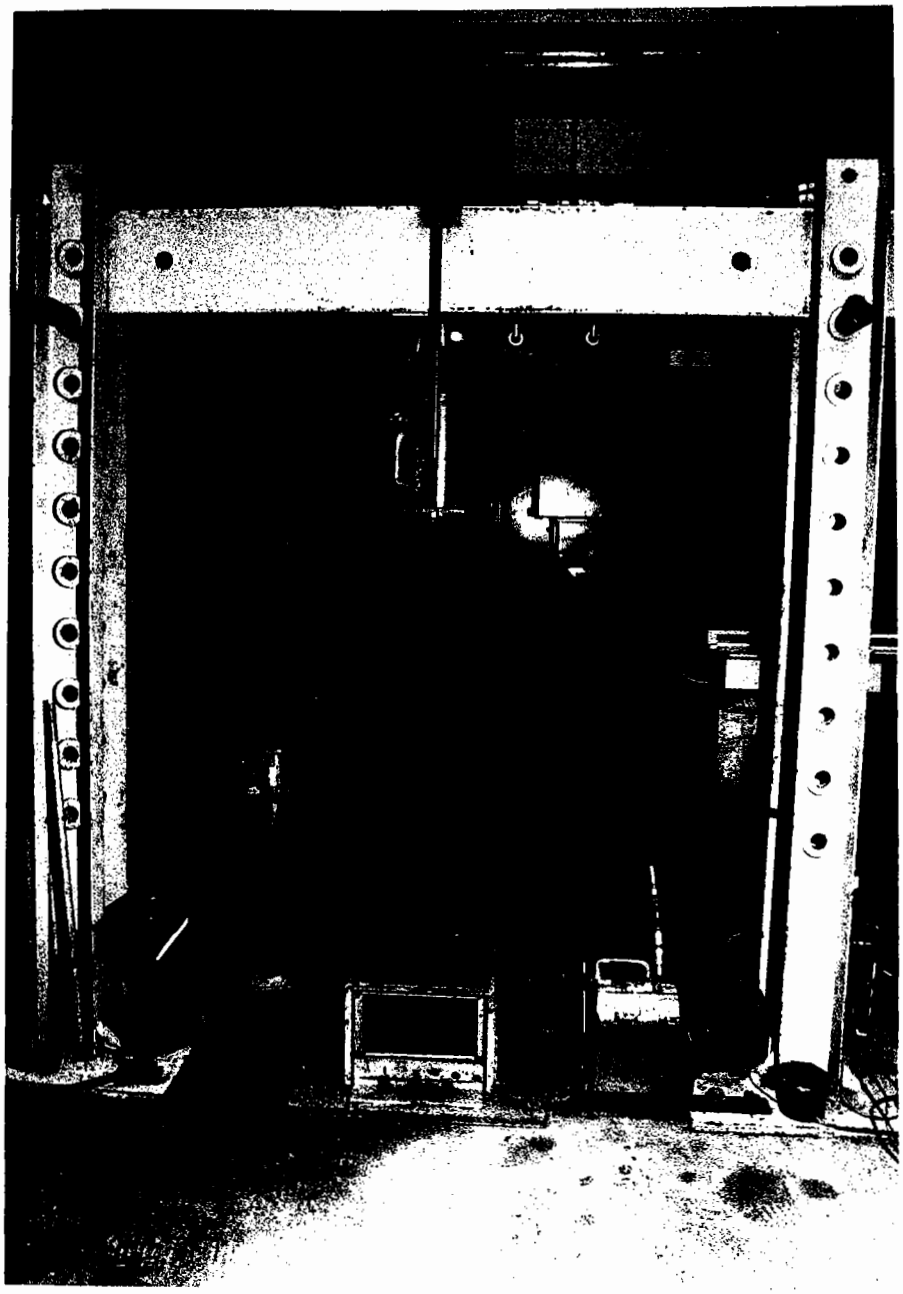

Plate 4.1 Timber Mould Set -Up Ready for Placement of Asphaltic Concrete

The general loading arrangement for the shear box test is illustrated in Figure 4.4. A constant normal stress was applied to the top plate through a system of four roller bearings which allow horizontal movement of the top asphaltic layer while still applying a vertical or normal load.

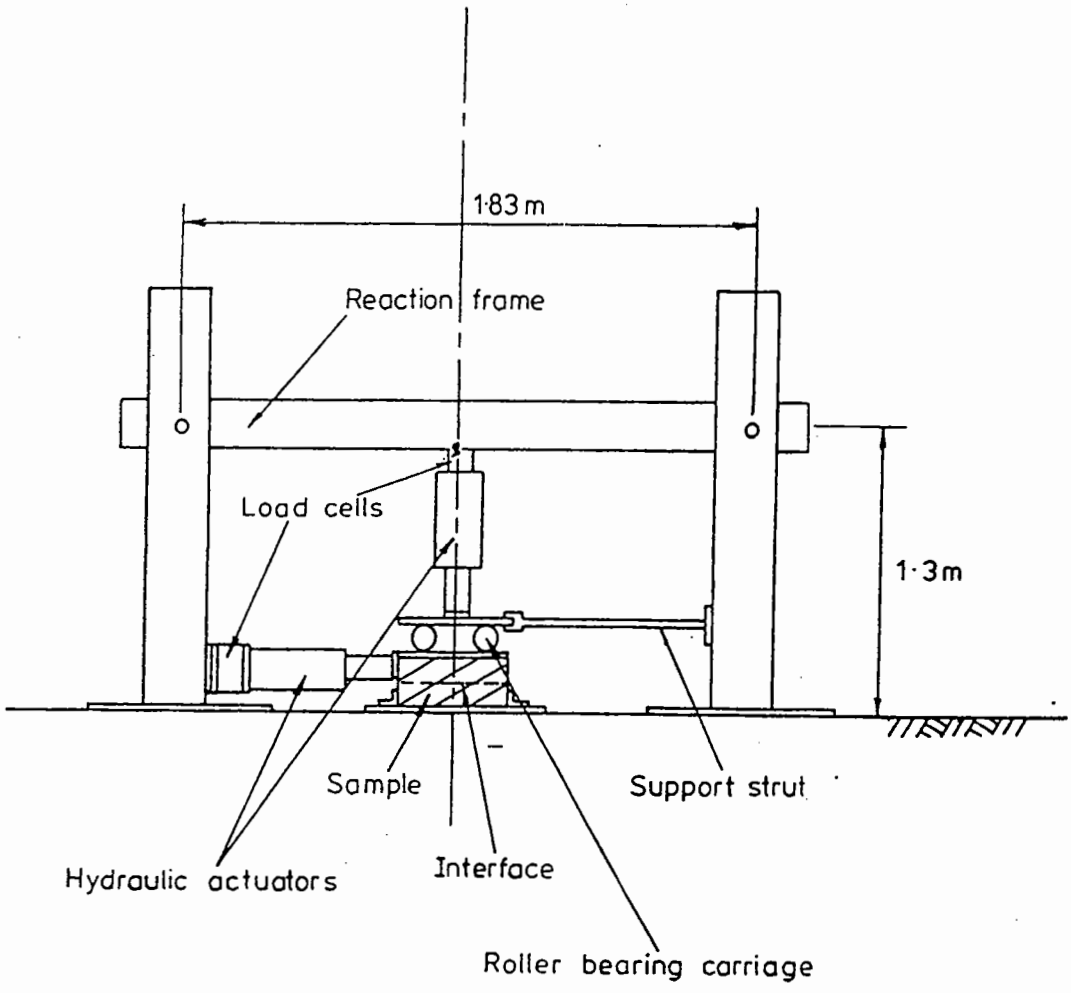

Figure 4.4 General Loading Arrangement for the Shear Box (after Hughes (44))

Linear potentiometers were placed on the corners of the roller bearing carriage to monitor any tilting of the top plate during the shearing process. Both normal and shearing stresses are applied through hydraulic actuators monitored by load cells. A shearing rate of 5mm per min was consistently used by Hughes for all tests.

4.2.3 Shear Box Developments

As part of this research work the following developments were made:-

(a) A method of compaction involving the use of a vibrating hammer with a square foot attachment was used for all layers of material. The vibrating hammer provided a closer approximation to field compaction than static plate compaction.

(b) The hydraulic equipment used to regulate the horizontal jack was able to apply a shearing rate of 3mm per minute to the sample.

(c) Values of interface shear strength were obtained for all materials and interlayers incorporated in the testing program. One further interface test condition was analysed by using a timber block 75mm thick with the same plan dimensions as the sample (320mm x 320mm). Emery paper of the same grade proposed for use in the beam and slab test facilities was affixed to the surface of the timber block. The purpose of this device was to establish the frictional qualities of the emery paper and compare this to the asphalt overlay bond to an existing pavement surface (control sample).

The basic hardware associated with the shear box remained unchanged from that used by Hughes. The experimental set up is illustrated in Plate 4.2 (a). Monitoring of the linear potentiometers and shear stress was carried out by chart recorders. The vertical load was monitored by a digital read-out and kept constant at 400 kPa. Plate 4.2 (b) shows the monitoring equipment used for all tests.

4.3 BEAM TESTING FACILITY

4.3.1 Beam Testing at Nottingham University

The general testing arrangement for beams made from asphaltic concrete used by Hughes (44), Brunton and Brown (50) and SWK(PE) (51) is illustrated in Figure 4.5. Specimen preparation utilized a steel mould of dimensions 525mm long x 150mm width with the specimen height set at 100mm. The asphaltic material was compacted using a vibrating hammer with a square foot attachment.

Two high quality plywood boards with emery paper glued to them were used as bases for the asphaltic beam and included a 10mm preset gap in the middle of the beam. The movement across this 10mm gap was monitored using a displacement transducer. A 24mm thick soft rubber resilient support was provided under the beam to simulate the response of a subgrade overlaid with a pavement structure.

A servo hydraulic machine was used to load the beam in a sinusoidal manner. A minimum load of 1.3 kN was applied to the beam because of difficulties in control of the hydraulics at zero load. The maximum load applied was 8.3 kN. A load cell between the ram and rigid loading frame provided feedback to the servo hydraulic actuator which controlled the cycling under a load control arrangement. A rubber backed steel loading platen 200mm x 150mm was used to transfer a maximum contact stress of 275 kPa to the sample. This load was applied at a rate of 5 Hz which corresponds to a vehicle speed of approximately 30 km/hr. The entire servo hydraulic device is contained within a temperature controlled cabinet which was maintained at 20°C ± 1°C for the duration of testing.

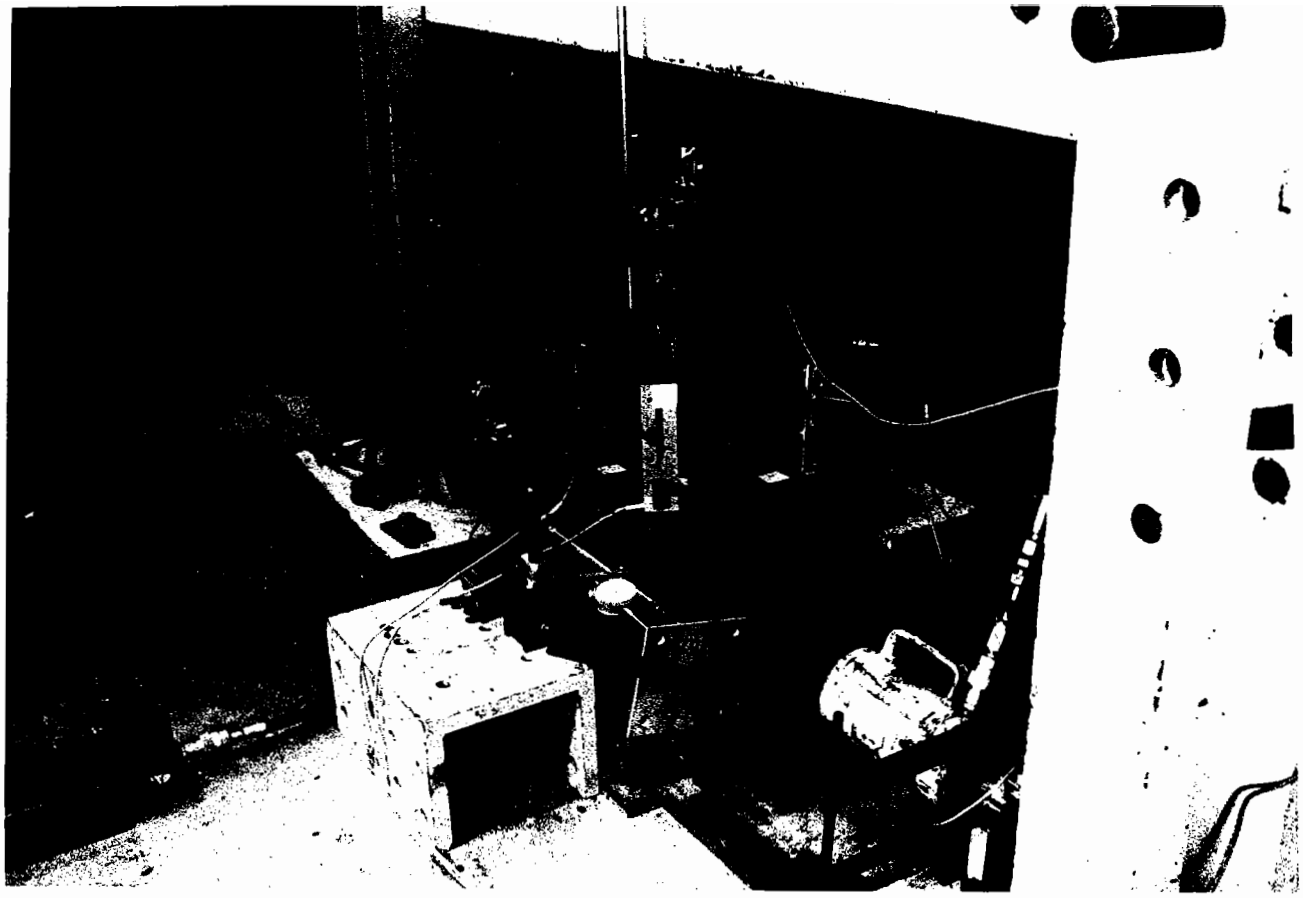

(a) Shear Box Arrangement for Testing

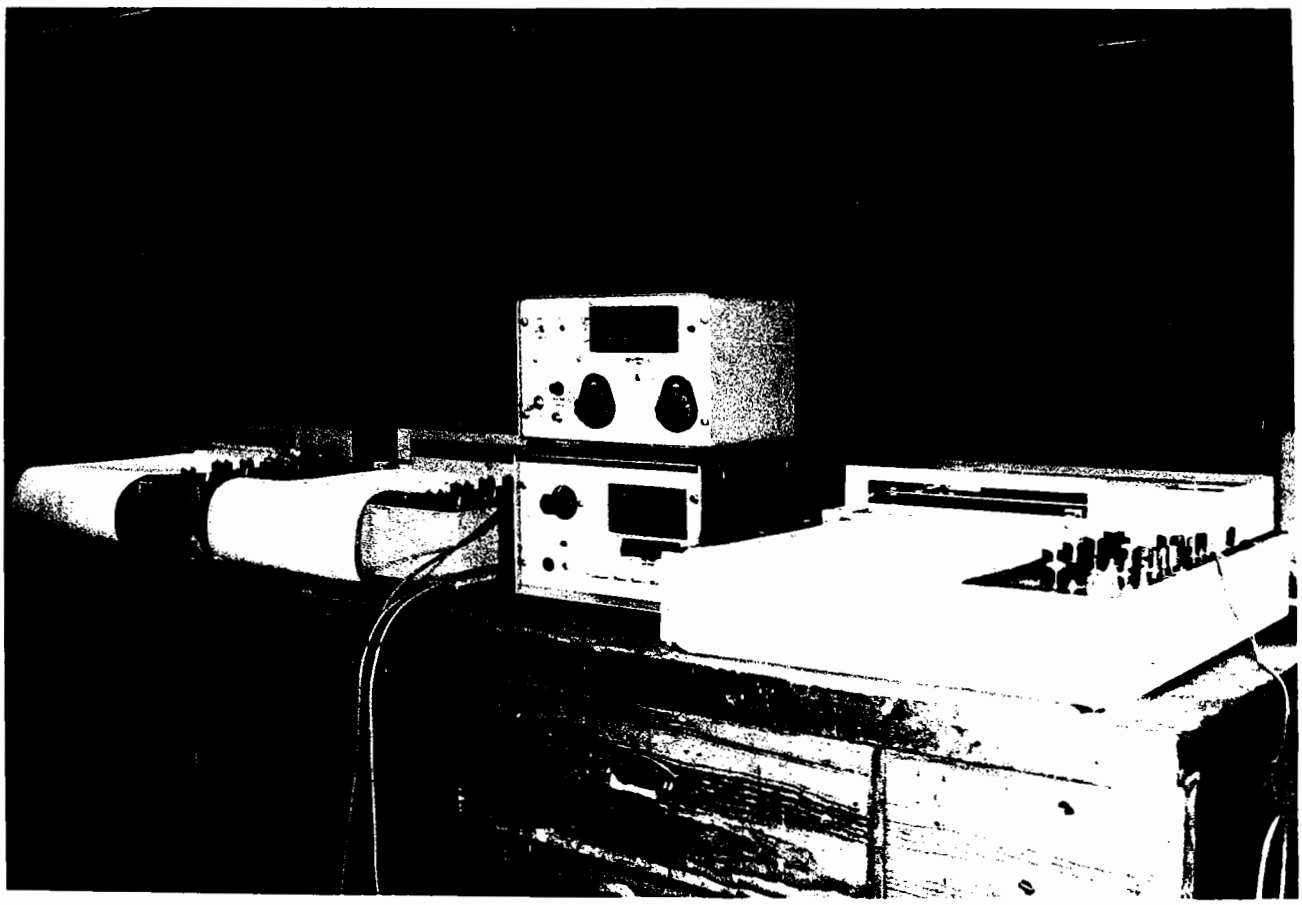

(b) Chart Recorders and Digital Readout Devices

Plate 4.2 Experimental Testing Arrangement and Recording Devices Used During Shear Box Testing

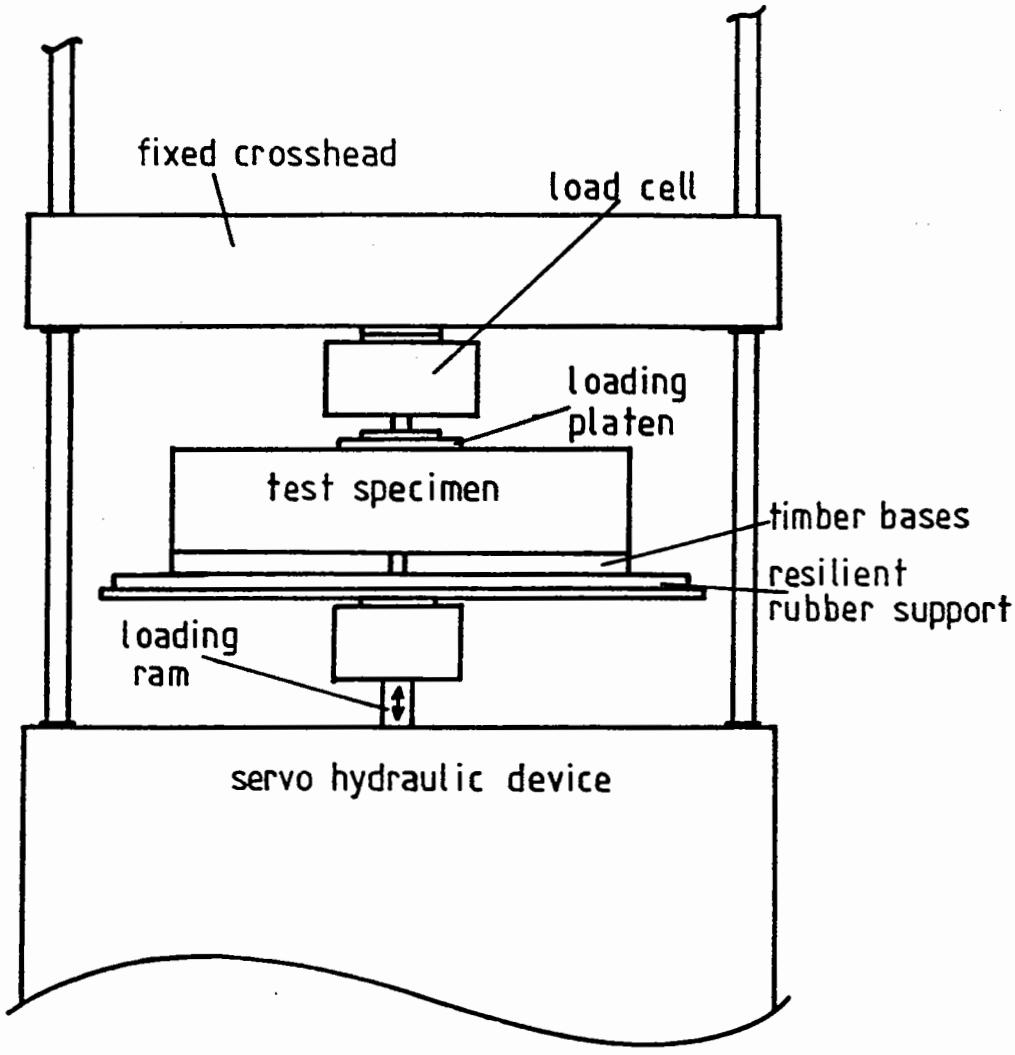

Figure 4.5 General Beam Testing Arrangement used by Others ((44), (50), (51))

In summary the following conditions prevailed for the testing conducted by others (44), (50), (51).

(i) Beams were made by compaction in a steel mould using a vibrating hammer.

(ii) Dimensions of the beams were 525m x 150mm x 100mm height.

(iii) Timber boards covered in emery paper were used as bases for the beams and had a preset gap of 10mm.

(iv) A soft rubber support 24mm thick was provided under the beams.

(v) Loading was applied sinusoidally between 1.3 kN and 8.3 kN at 5 Hz.

(vi) The loading platen measured 200mm x 150mm and had a rubber backing.

(vii) The loading ram was connected to a platform under the beam arrangement as shown in Figure 4.5 thus pushing the beam arrangement up onto a fixed cross head, during each loading cycle.

(viii) Temperature 20°C ± 1°C.

4.3.2 Modification to the Beam Testing Facility

4.3.2.1 Introduction

The process of evaluating how best to simulate field conditions in a laboratory test situation necessarily means that close attention must be paid to the following effects:-

(a) Specimen Manufacture.

(b) Thermal Movements.

(c) Traffic Loading.

(d) Combined Thermal and Traffic Induced Stresses.

(e) Temperature Regime.

(f) Crack Propagation.

A study of the relevant literature as presented in Chapter 2 has aided in the development of the beam testing facility where all of the above mentioned effects have been considered and accounted for during the development and testing program.

4.3.2.2 Specimen Manufacture

With the asphaltic mix, binder content and mixing process already defined in Chapter 3 the remaining variables to be considered for the manufacture of specimens were the method of compaction and the mould dimensions. The three modes of compaction available for beam specimens were vibratory hammer, static plate and roller compactor. The method that best simulates field conditions and has the ability to give consistent results throughout a testing program is the roller compactor.

The Nottingham University roller compactor produces slabs of asphaltic concrete that are 400mm long x 280mm wide x desired thickness (maximum 125mm). The required compaction standard can be achieved by varying the quantity of mix used for the specified volume of the mould. Plate 4.3 illustrates the general arrangement of the roller compactor device and also provides a close up view of the mould and compaction plate.

Asphaltic concrete once mixed is placed in five splitter trays each of equal mass that fill the roller compactor mould. Compaction is achieved by a pneumatically controlled curved plate which moves in the vertical plane with the mould fixed to a steel tray on rollers that is moved in the horizontal plane. The rolling effect achieved is designed to simulate the movement of an asphaltic concrete mat under the action of a steel drum roller.

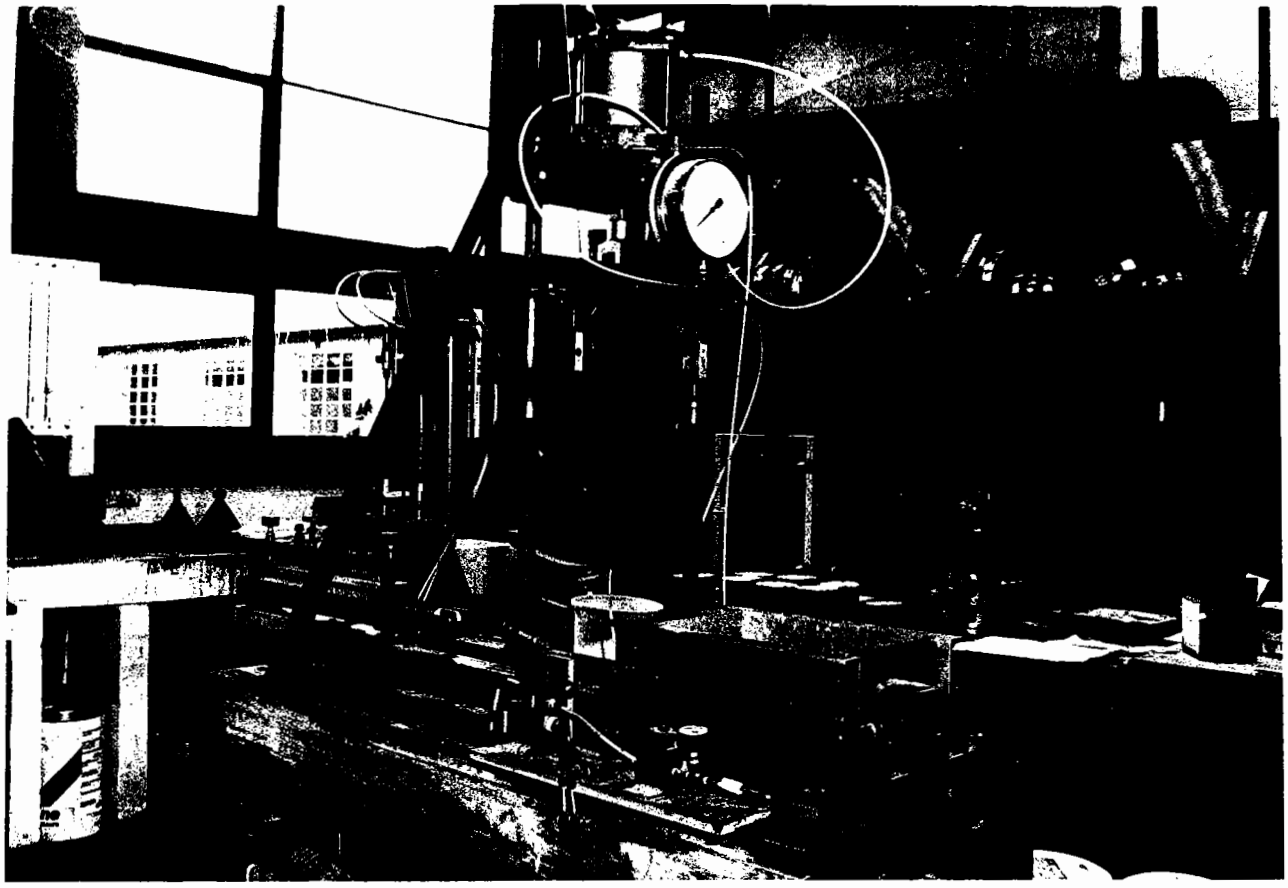

(a) General Arrangement

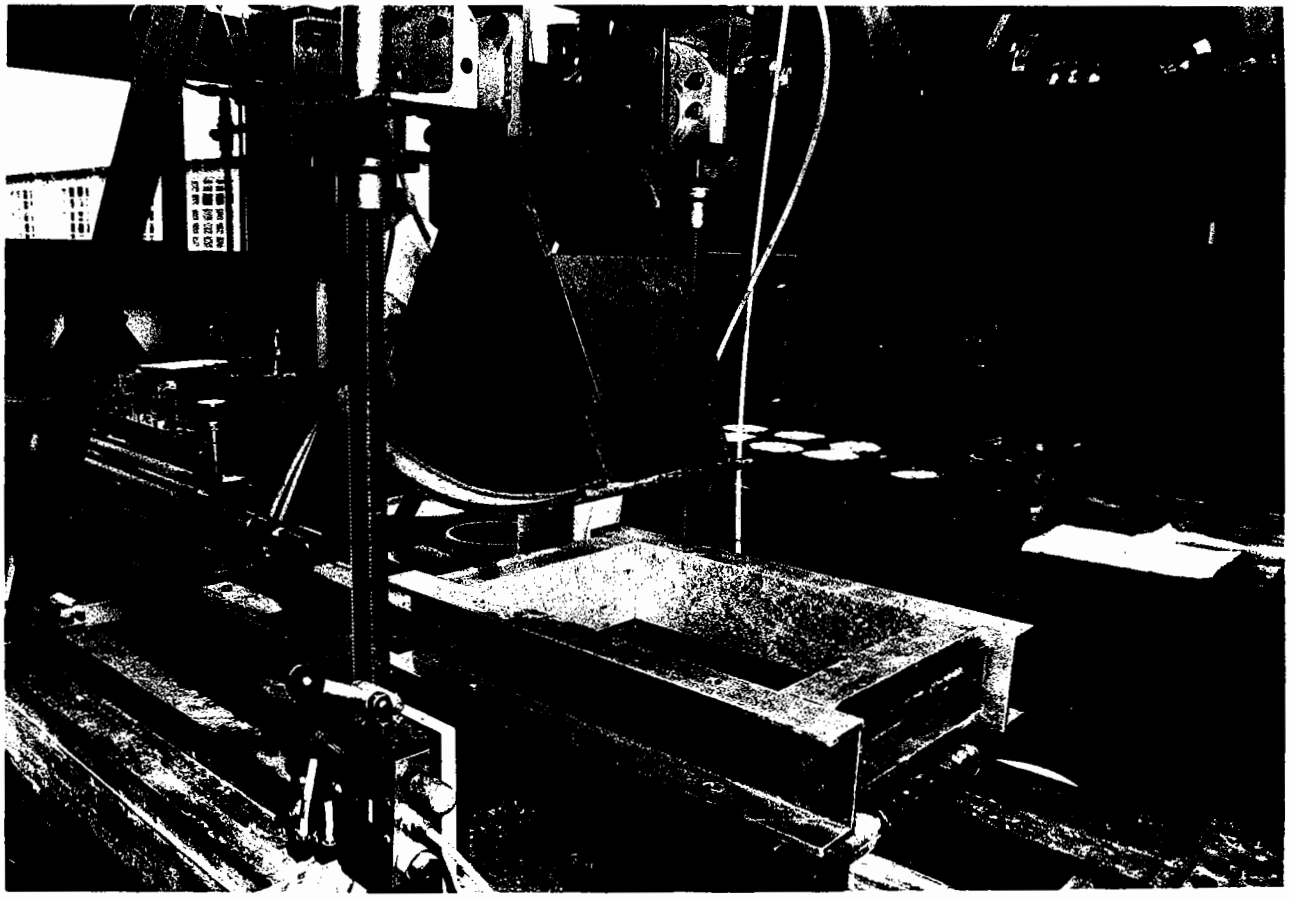

(b) Compaction Mould and Rolling Plate

Plate 4.3 Roller Compaction Equipment

The restraint imposed by the mould itself limits the free movement of the mix under the action of the compaction plate but this method forms a closer approximation of field conditions than either the vibratory hammer or static compaction methods.

As the standard plan area of the mould is 400mm x 280mm, sawing the completed slab in half gave two beam samples 400mm x 136mm. This process was completed using a circular saw and had the added advantage that one face of each beam was left smooth allowing cracks to be easily detected.

4.3.2.3 Thermal Movement

In a pavement with a predominant cement treated base or sub-base layer, transverse cracking due to thermal movements and natural shrinkage of the cementitious fines will generally occur at 5-7 metre intervals for a material with compressive strength less than 5 MPa at 7 days, Williams (58), Murphy et al (59). Figure 4.6 shows how this movement is distributed along the length of a pavement indicating that at mid slab there is zero relative movement.A method and test apparatus that induces thermal stresses in the asphaltic concrete beam were developed to mirror field conditions.

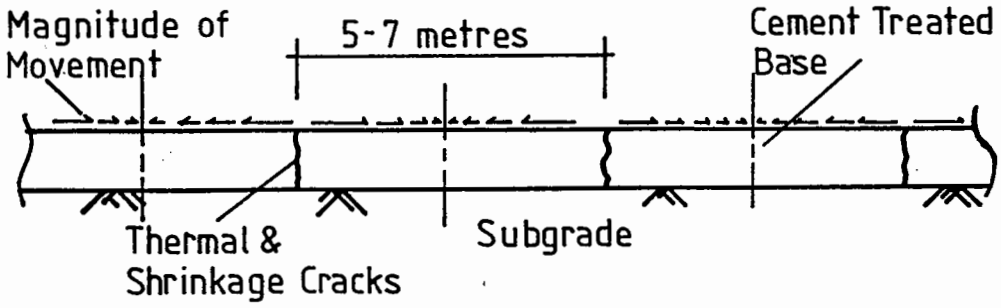

Figure 4.6 Stresses Induced in Cement Treated Pavement Layers

To simulate this type of movement in a testing rig requires the use of an elastic material that will display differential movements and then recover to be used in subsequent tests. This material used as a base under the asphaltic concrete overlay must also be relatively stiff in the vertical plane to act as a support to the overlay.

Approaches were made to several epoxy manufacturers, however no product was proposed that could fulfil the testing requirements. A further study of available products revealed that a rubber compound produced by "Devcon" called "Flexane 94 Liquid" appeared to have the following desired qualities:-

(i) Rigidity: The rubber hardness was 94 according to the shore hardness test ASTM D2240 which has a maximum of 100. This hardness was required to simulate a cement treated base.

(ii) Elongation and tensile strength: The rubber was able to provide good resilient properties coping with many induced thermal movements.

(iii) Heat resistance: A maximum operating temperature of 121°C allowed the rubber to be used as a base material when covered with emery paper as it was able to withstand asphaltic concrete placing temperatures.

A trial rubber base was produced to conduct preliminary tests to determine its suitability to perform the required movements. The testing configuration can be seen in Figure 4.7. An 18 gauge aluminium sheet was cut and folded to form an end piece for the base. The reinforcement at the end was designed to perform the following three functions:-

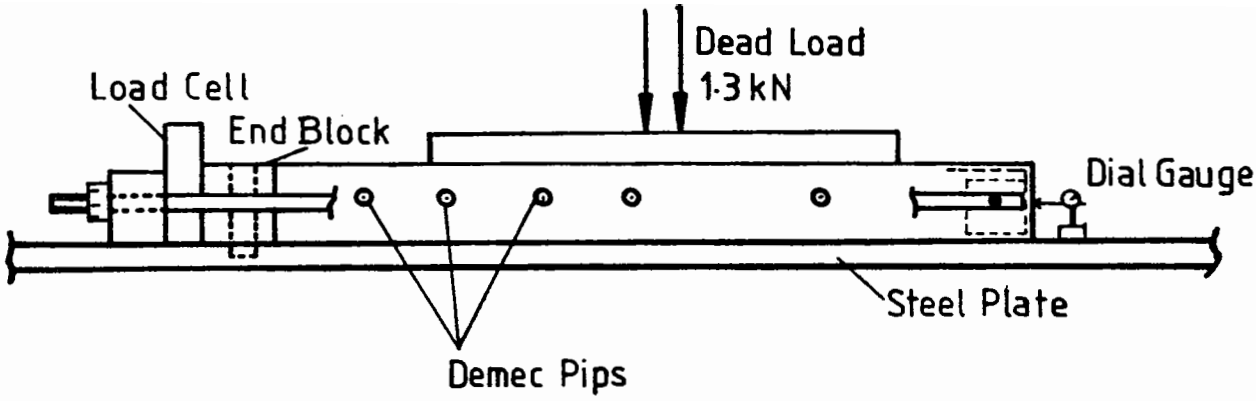

Elevation Trial Rubber Base

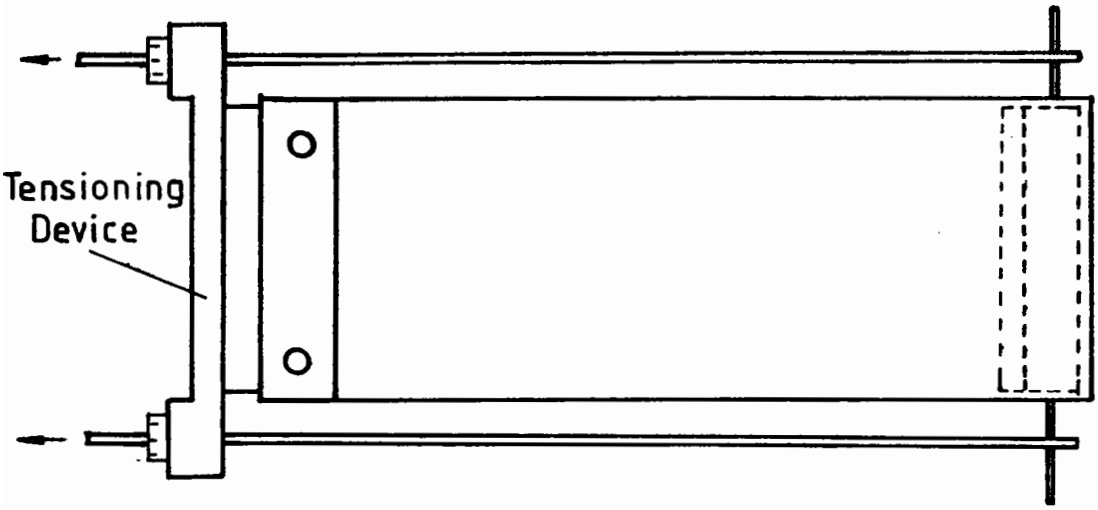

Plan View Tension Arrangment

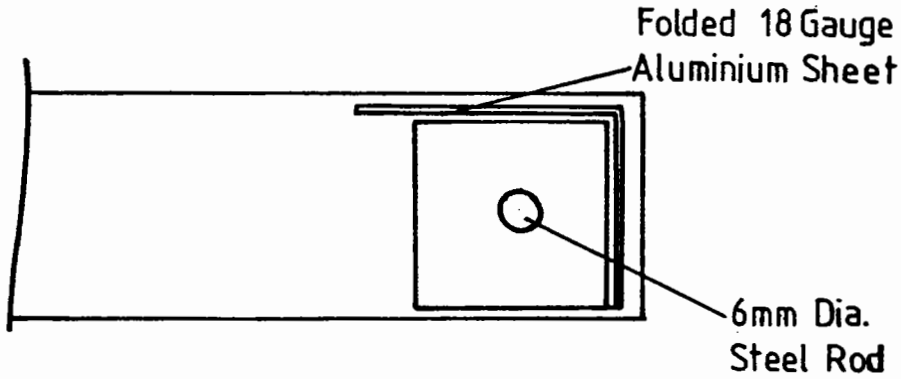

End Section Reinforcment

Figure 4.7 Trial Rubber Base Arrangement

(i) to provide a stiff end at the gap to stop excessive deformation of the base in this zone,

(ii) to ensure that the rubber end moved as a single body when tensioned, and

(iii) to reinforce the zone around the 6mm diameter steel rod that was used to apply loads to the trial base.

The trial base was loaded to simulate the typical movements in a cement treated base. A load of 1.3 kN was applied normal to the base as this would be the minimum load acting at any time. The results of this process are summarized in Table 4.1

Table 4.1 Rubber Base Trial Results

Dial Gauge Reading (mm)	Applied Load kN	Movement of Demec Pips (mm)				
		1	2	3	4	5
Initial base length 200mm	Initial Position	(28)	(54)	(79)	(104)	(130)
1	0.52	0.46	0.44	0.48	0.61	0.71
2	1.12	0.63	0.79	0.81	0.90	1.15
3	1.55	0.69	0.84	1.02	1.26	1.43
4	2.05	0.84	0.98	1.22	1.59	1.96

Clearly from these results the differential movement required to model field conditions can be achieved with the Devcon material. Elastic recovery was also observed thus allowing continued use of the same base sections. Vertical movement of the rubber base along its length as a result of the compressive load was not observed and was thus not considered significant.

The actual rubberized bases used for testing beams differ in design from the preliminary base as the tensioning device shown previously in Figure 4.7 would have been unsuitable due to the external nature in which the rubber bases were loaded. Monitoring of the preset 8-10mm gap would have been difficult because of fixation problems for the linear variable displacement transducer (LVDT). An obscuring from view of the interface conditions would also have prevailed with the trial loading arrangement.

A method of applying a thermal movement to the rubber bases was devised that incorporated the use of a steel end section and 10mm diameter steel rod. The steel end section performed the same function as that for the aluminium gauge it replaced. A greased and threaded steel rod was inserted centrally in the steel end section prior to casting of the rubber. An extension for this rod was secured to the end of the embedded rod and passed through a vertically slotted steel end block and tensioning plate.

Steel end blocks were positioned at the two ends of the test specimen and bolted to the steel base plate. This provided a location where there was zero movement, thus ensuring relative movement along the rubber base was achieved during the tensioning process.

The tensioning plate has a milled surface that was designed to allow rotational movement of the central tensioning rod. This rotational movement occurs as the beam is cycled under the action of a traffic induced load. Figures 4.8 and 4.9 provide details of the rubber base arrangement and the general beam configuration with tensioning plates and steel end blocks.

Plate 4.4 illustrates the steel end sections used in the manufacture of the rubber bases, and a view of the steel base plate with end blocks and tensioning plates.

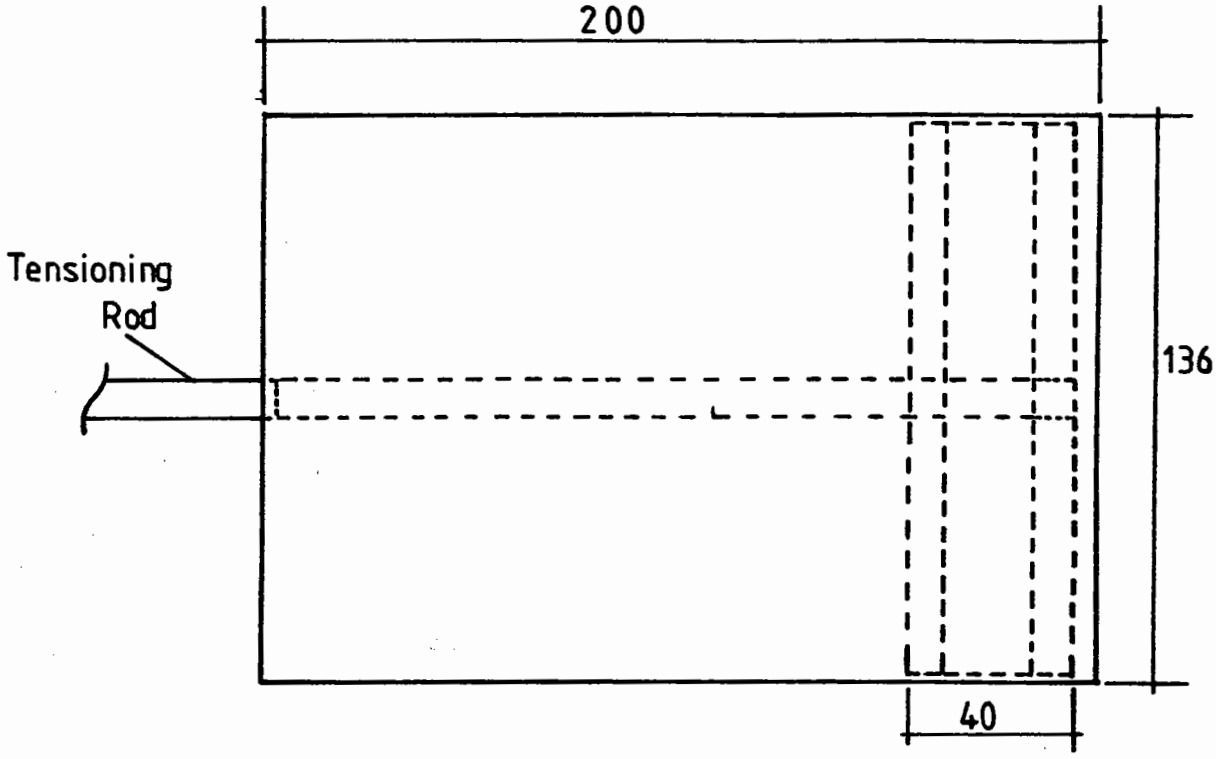

Plan View Rubber Base for Beam Testing

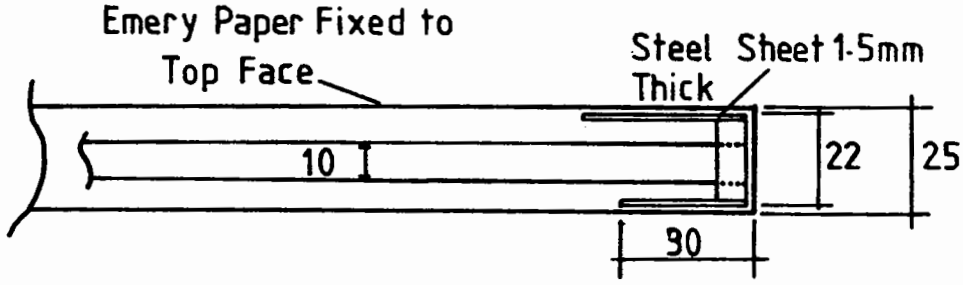

Elevation End Section

Connection of Tensioning Rods

Figure 4·8 General Arrangement of Rubber Bases

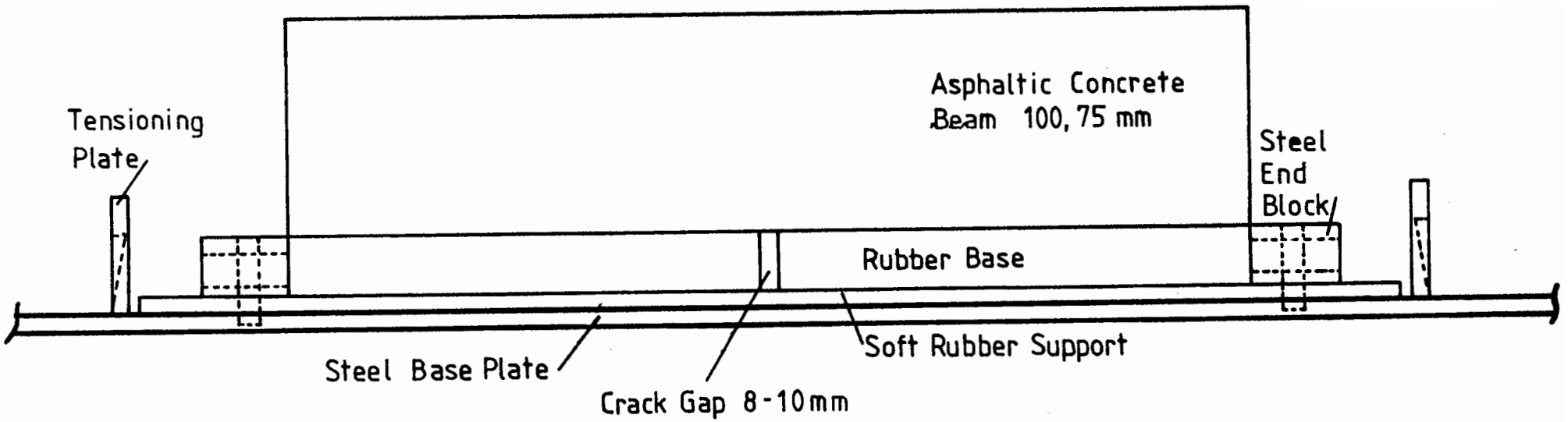

Elevation General Beam Arrangement

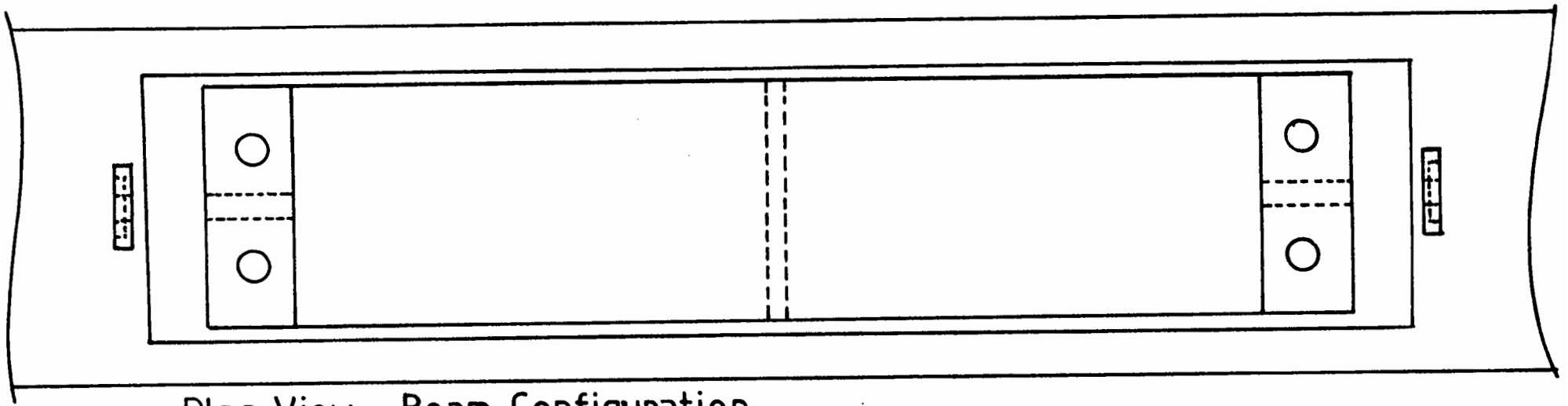

Plan View Beam Configuration

Figure 4.9 Initial Beam Test Arrangement

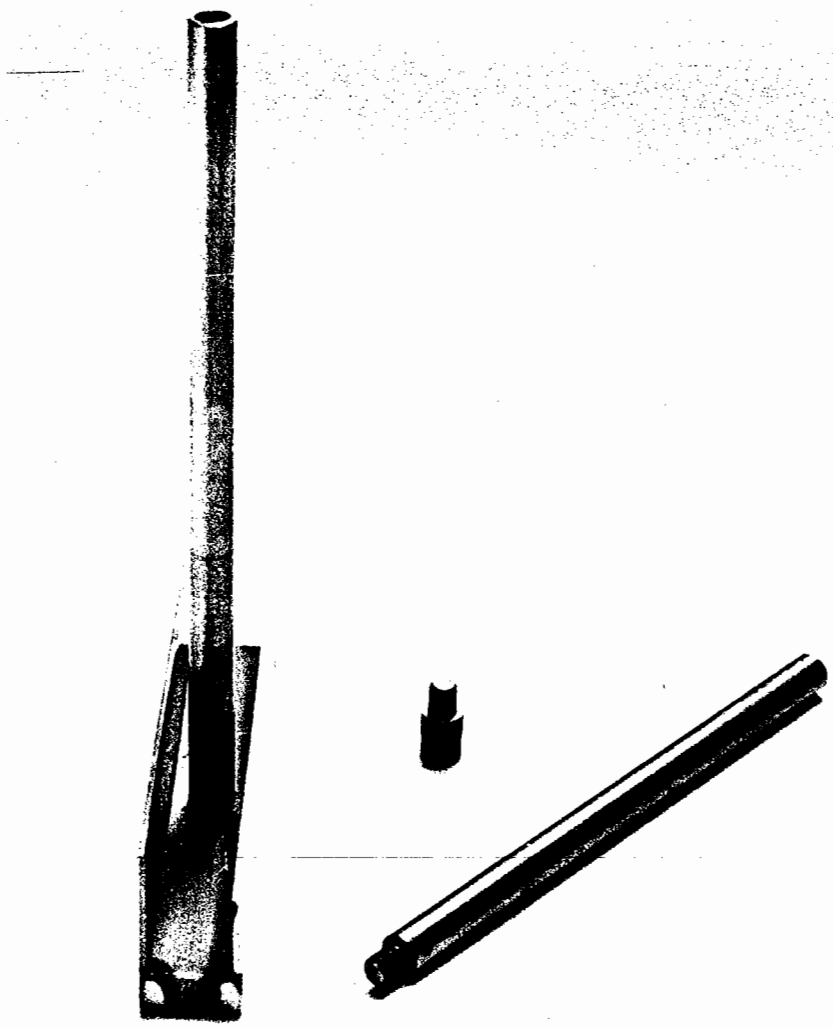

(a) End Piece and Tensioning Rod for the Rubber Base

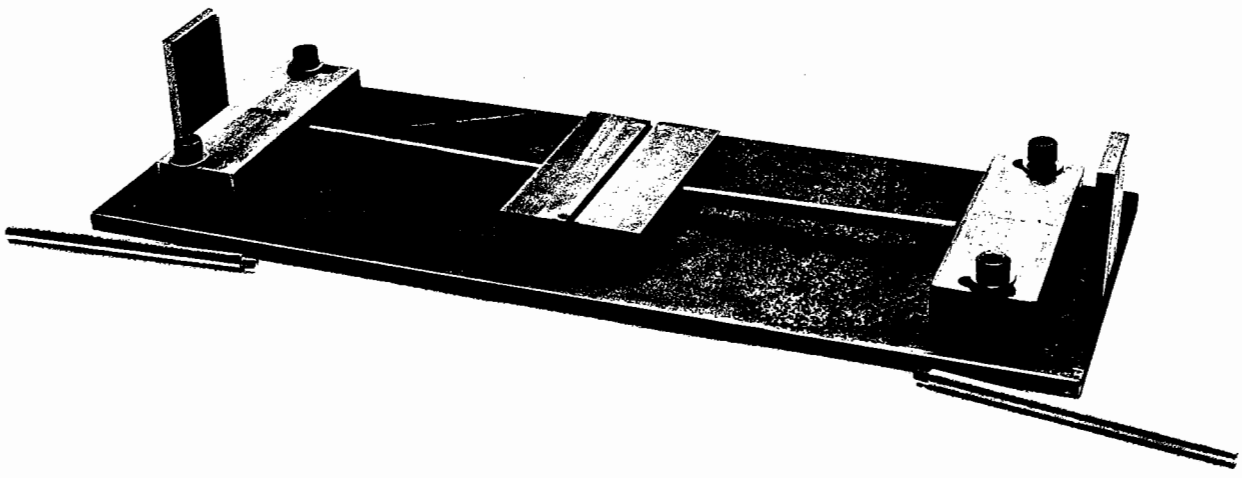

(b) General Base Plate Arrangement

Plate 4.4 Manufactured Steel Sections for the Application of Thermal Loads

The tensioning process involved the tightening of a nut on the threaded tensioning rod, against the tensioning plate. Both ends of the beam were tensioned simultaneously to give an extension of between 1.0 and 1.5mm as read on the transducer indicator which was connected to the LVDT spanning the preset gap of 8-10mm between rubber bases.

4.3.2.4 Total Loading Arrangement

To incorporate both thermal and traffic loads on the specimen it was necessary to make the specimen physically independent of the traffic load application. This was achieved by building a yoke arrangement connected to the loading ram thus loading the specimen from the top.

The yoke arrangement is made from 75mm square hollow section with a wall thickness of 5mm and had a half ball arrangement welded to it, through which the traffic induced loading was applied to the sample. Figure 4.10 illustrates the yoke loading arrangement in detail and a typical beam specimen.

Negligible losses occurred during load transfer through the yoke as checked with a load cell placed in the specimen location. The results of this test appear in Table 4.2.

Table 4.2 Load Transfer Through Yoke Arrangement

Applied load through servo hydraulic machine load cell (kN)	Resultant load transferred to the specimen (kN)
2.0	1.98
4.0	3.99
6.0	5.96
8.0	7.96

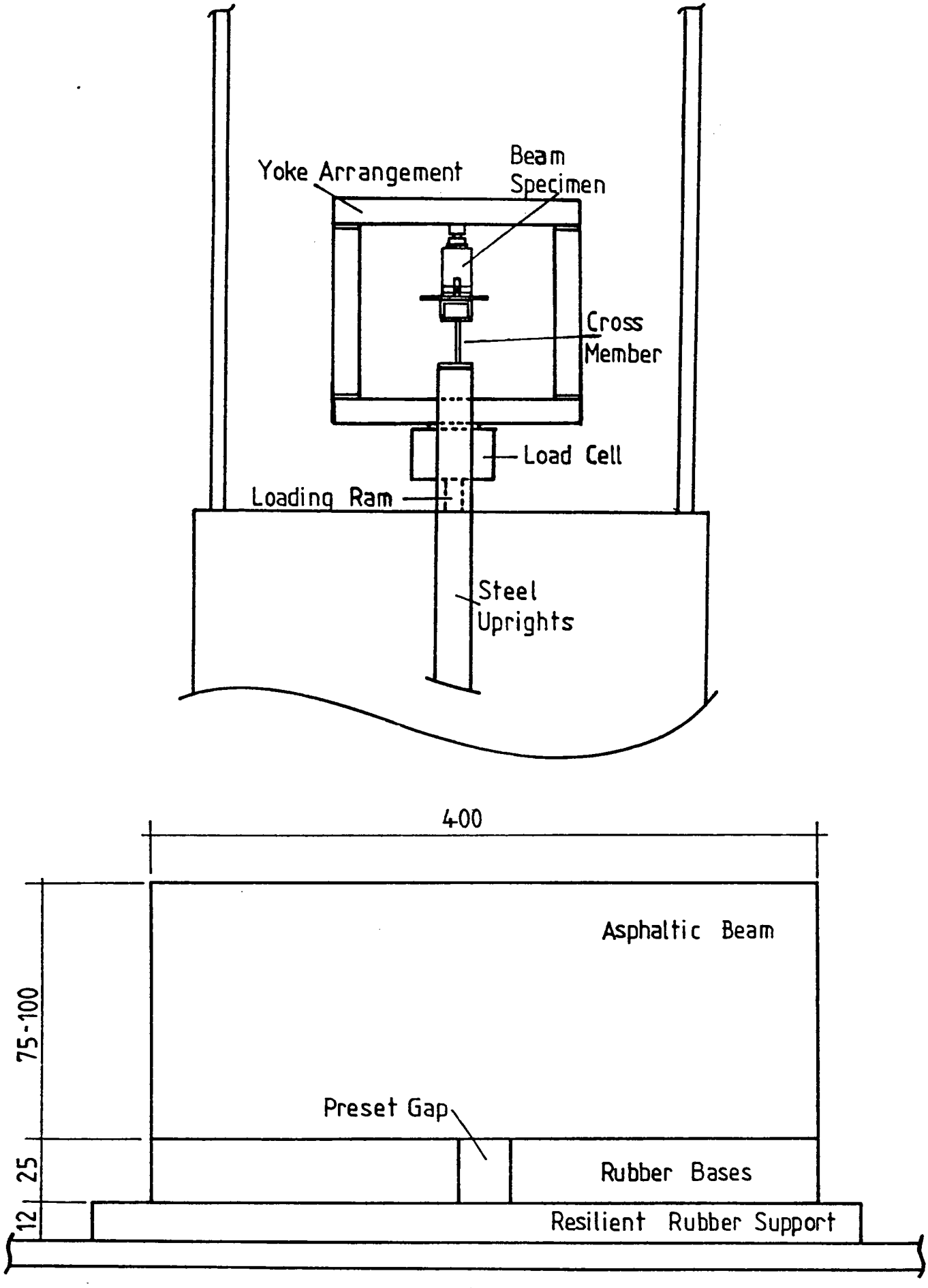

Figure 4.10 Yoke and General Loading Arrangement for Beam Testing Facility, and a Typical Beam Test Specimen

The rate at which the traffic loads were applied to the sample was initially set at 5 Hz as used by previous researchers (44), (50), (51). This rate of loading was increased to 10 Hz for two reasons:-

(a) to enable a greater number cycles to be performed in a day, and

(b) to give the higher effective vehicle speed that 10 Hz produces, which is approximately 60 km/hr. This allows performance at this speed and known temperature to be equated to an elastic stiffness as determined in the Nottingham Asphalt Tester (NAT). This device and results obtained are further detailed in Appendix A.

Some instabilities in the loading arrangement were experienced at this faster loading rate, however these were eliminated by bracing the vertical supports of the specimen arrangement and centring the half ball on the yoke directly in the middle of the beam specimens.

4.3.2.5 Crack Detection

Detection of cracking as it propagated up the beam face was completed on a visual basis only by Hughes (44). Brunton and Brown (50) visually monitored the crack propagation and also used demec pips placed on the face of the beam to monitor crack opening. Foulkes (20) and Vecoven (45) made use of thin aluminium self adhesive strips to monitor crack growth by voltage drop as the strips, which were connected to an electrical circuit, broke with crack propagation in the specimen.

As beam testing in this experimental program was designed to continue overnight on a 24 hour basis, a detection mechanism was required to monitor crack growth. An electrical circuit was designed and built in accordance with the circuit diagram shown in Figure 4.11. This circuit provided a 9 volt output across each metallic strip that was attached to the face of the beam. As the crack propagated up the beam face and broke

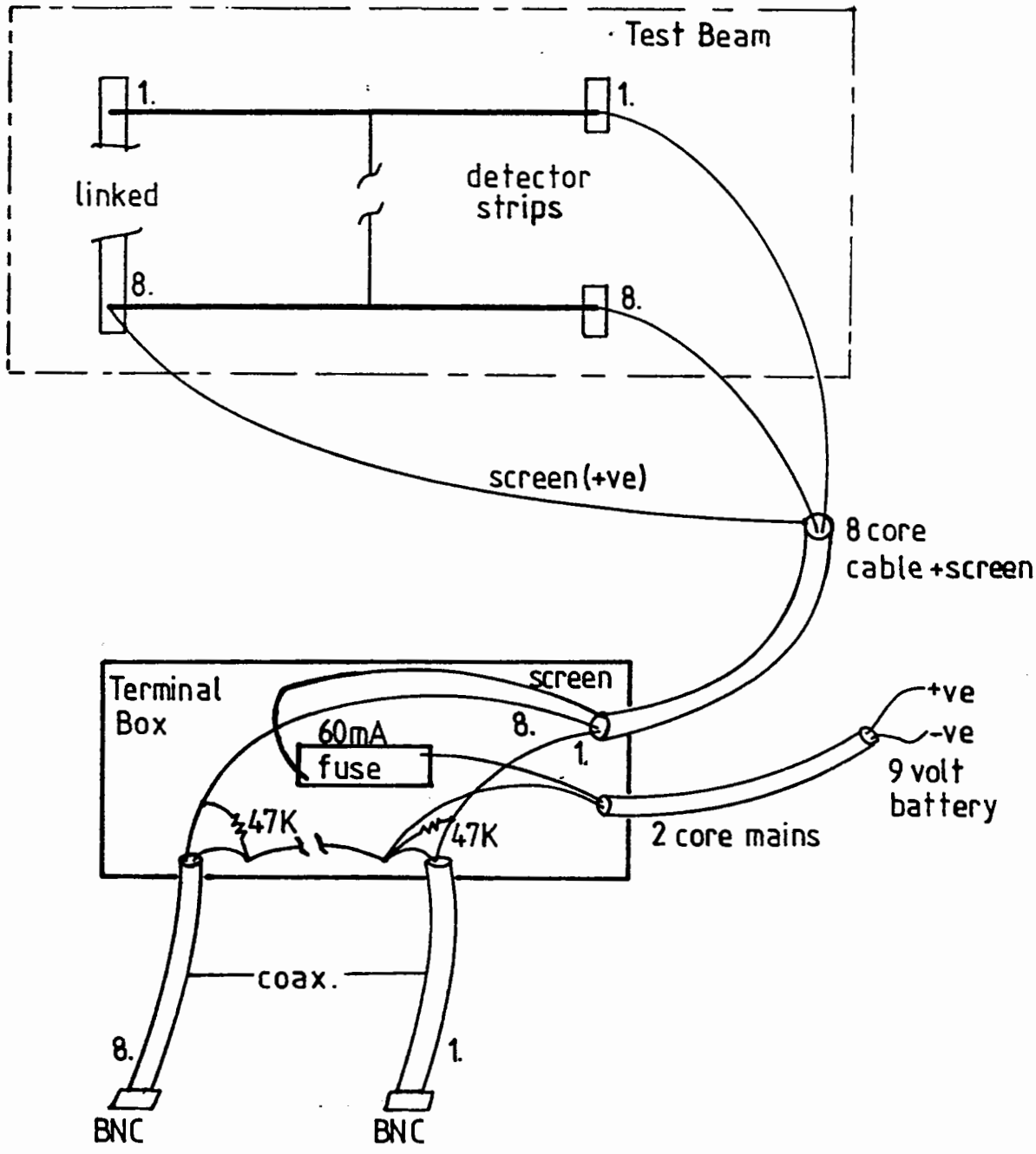

Figure 4.11 Circuit Diagram for Crack Detection Device

each strip successively the voltage dropped to zero across each strip. The voltage was monitored through an A-D converter, together with the LVDT readings across the preset gap by a HP85 computer program. The program sends a signal through the A-D converter and detects if there has been a voltage drop, then prints out the strip number and time of breakage. Every five minutes the computer prints out the LVDT offset and amplitude values.

The flow chart for the program appears in Figure 4.12 with the program listing contained in Appendix B. A typical section of input and output for the program are presented in Figure 4.13.

4.3.2.6 Preliminary Beam Testing

Evaluation of the following test parameters through a series of beam test trials was necessary prior to obtaining any meaningful results.

(i) Temperature of testing.

(ii) Crack detection strip type.

(iii) Load platen size.

(iv) Debonding potential.

The evaluation process took place over the first six beams and can be summarized as follows:-

1. Beam Test One was used primarily as a trial for the selected test temperature of 30°C ± 1°C. This value of 30°C ± 1°C was selected as it represents the weighted mean annual pavement temperature (WMAPT) for the Brisbane region of Queensland [Dickenson (60)] where the field trials described previously (23), (24), (25) were conducted.

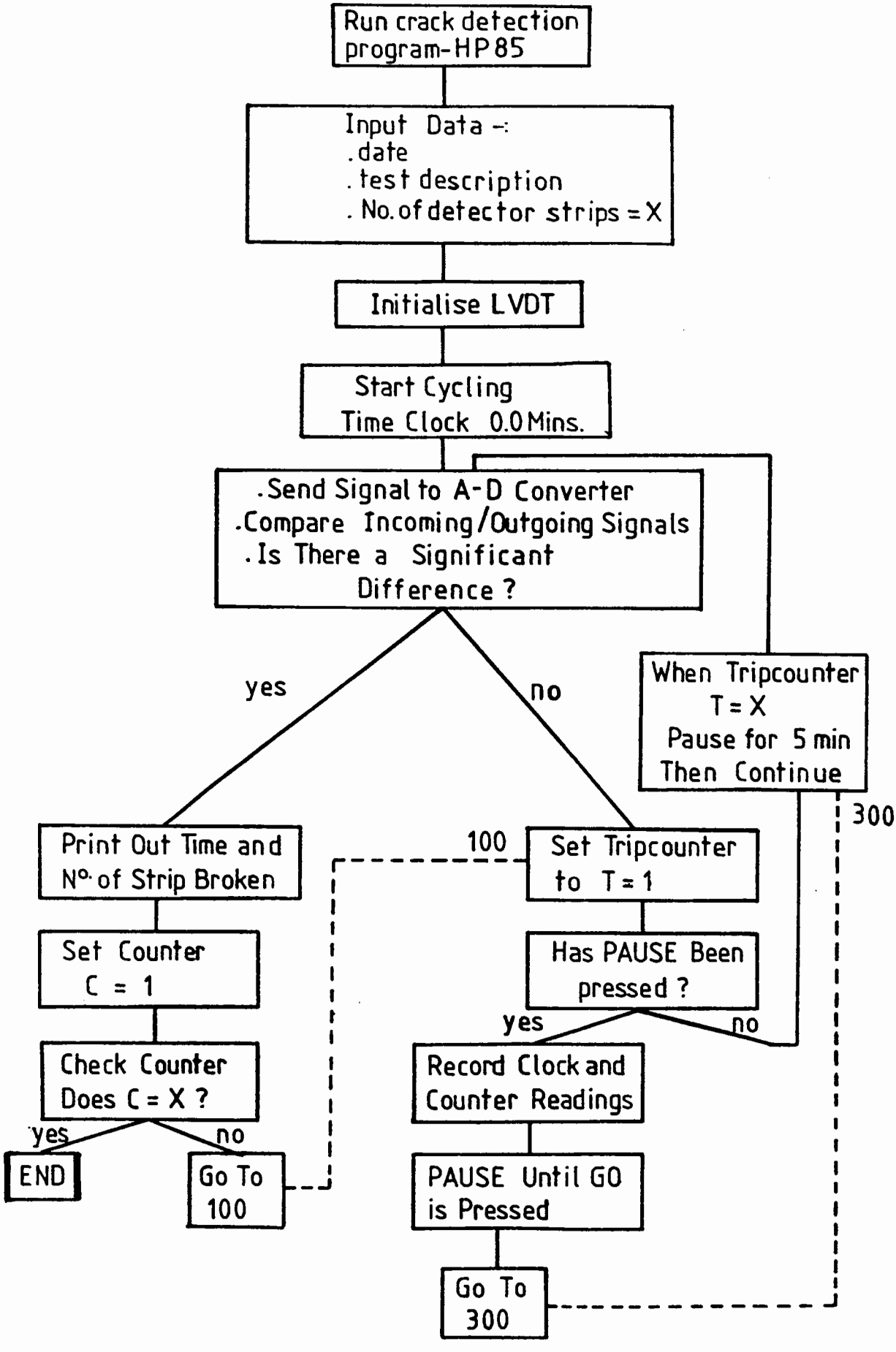

Figure 4.12 Flowchart for Computer Program to Detect Crack Propagation

Input : Date = ...

Specimen = ...

No. of Strips = ...

press Start to Initialize LVDT.

press Start cycling begins.

Results: Time = 5 mins

Amplitude = 0.0250mm

Offset = 0.8201mm

Time = 10 mins

Amplitude = 0.0270mm

Offset = 0.9702mm

At 12 minutes

Strip 1 broken

Time = 15 mins

Amplitude = 0.0293mm

Offset = 0.9947mm

Figure 4.13 Input Data and Output Results for Crack Detection Program

Initial test conditions were:-

- 100mm asphaltic concrete.
- Width of loading platen 140mm.
- End blocks in place.
- Traffic loading 1.3 kN - 8.3 kN, 10 Hz.
- Temperature 30°C.
- Crack detection strips, self adhesive aluminium 2mm width.

Prior to the use of aluminium strips as crack detectors a conductive paint was sprayed onto the surface of a test section through a template, however, no circuit connection could be achieved.

As the first beam specimen was tensioned the bottom two aluminium strips broke, not yielding to allow for the increase in strain due to tensioning.

Soon after cycling under traffic induced loads the sample showed signs of permanent deformation in the upper surface. Cracking was observed in the aluminium strips in several locations. Bulging of the sample sides soon followed, causing the crack detection strips to lift off the surface of the beam. Testing ceased after only 137,800 cycles, the beam experiencing a crushing failure. Plate 4.5 (a) shows beam one at the completion of testing.

The test temperature of 30°C ± 1°C proved too high for the prevailing test conditions and was subsequently lowered. Performance of the aluminium detector strips during the tensioning process was reviewed and the use of copper coil winding wire was incorporated in the testing program.

2. Beam Test Two examined aspects of the beam testing facility that included temperature, crack detection strips, and load platen width. Table 4.3 displays the methods of fixing crack detection devices to the face of the trial beam.

Table 4.3 Crack Detection Strips

Material Used / Method of Fixation	Aluminium Strips 2mm width	Copper Coil Wire 38 gauge 0.15mm dia.	Copper Coil Wire 39 gauge 0.08mm dia.
Self Adhesive	✓	-	-
Epoxy	-	✓	✓
Emulsion Painted	-	✓	✓

Initial testing conditions can be summarized as set out below:-

- 100mm asphaltic concrete.
- Loading platen width 140mm, 75mm, 53mm.
- End blocks in place.
- Traffic loading 1.3 kN - 8.3 kN, 10 Hz.
- Temperature 10°C, 20°C.
- Crack detection strips, various.

Initially the 140mm width loading platen was used with the temperature held constant at 10°C ± 1°C. After 996,300 cycles at this temperature no cracking had been observed. The loading platen was changed to a smaller 75mm width and the temperature raised to 20°C ± 1°C. A further 196,400 cycles were completed with no evidence of cracking in the sample, however some

permanent deformation was observed in the upper surface around the load platen.

Loading conditions were again changed to incorporate the use of a 53mm loading platen with the temperature remaining unchanged at 20°C ± 1°C. Cracking was quickly recorded once load cycling commenced under these new conditions. Testing was stopped after 88,700 cycles.

The total number of cycles for the sample was 1,281,400. Plate 4.5 (b) shows the cracking observed and the different types of detector strips used for crack monitoring. Analysis of detector strip performance showed that:-

(a) Aluminium strips tended to be too brittle and broke before cracking in the asphaltic material propagated past them.

(b) Epoxy fixing methods did not allow the wire embedded to break as the asphaltic material cracking propagated.

(c) Both 38 and 39 gauge copper wire proved adequate in detecting crack propagation when fixed to the face of the beam using an emulsion paint.

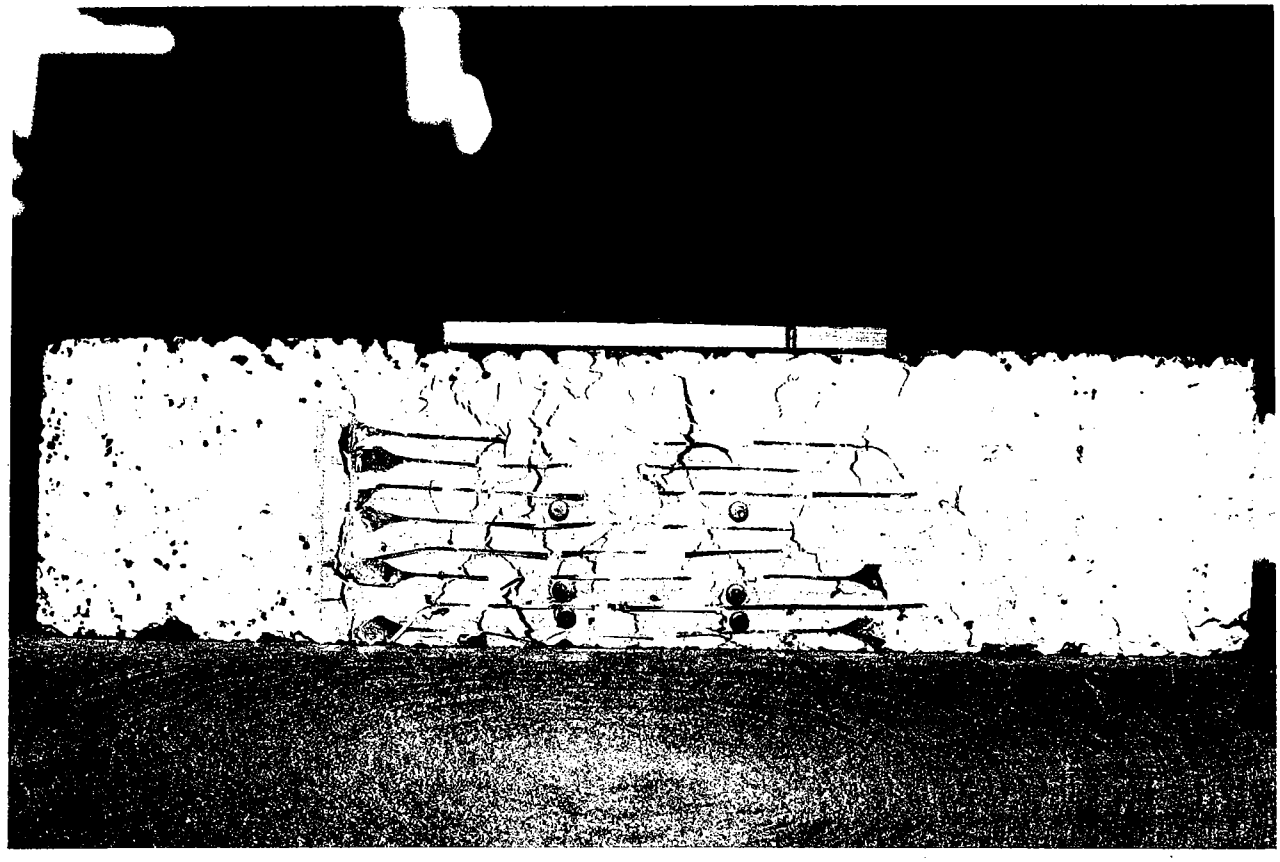

Plate 4.5 (a) Beam Test One ; 100mm Asphaltic Concrete
30 C Test Temperature
137,800 Cycles

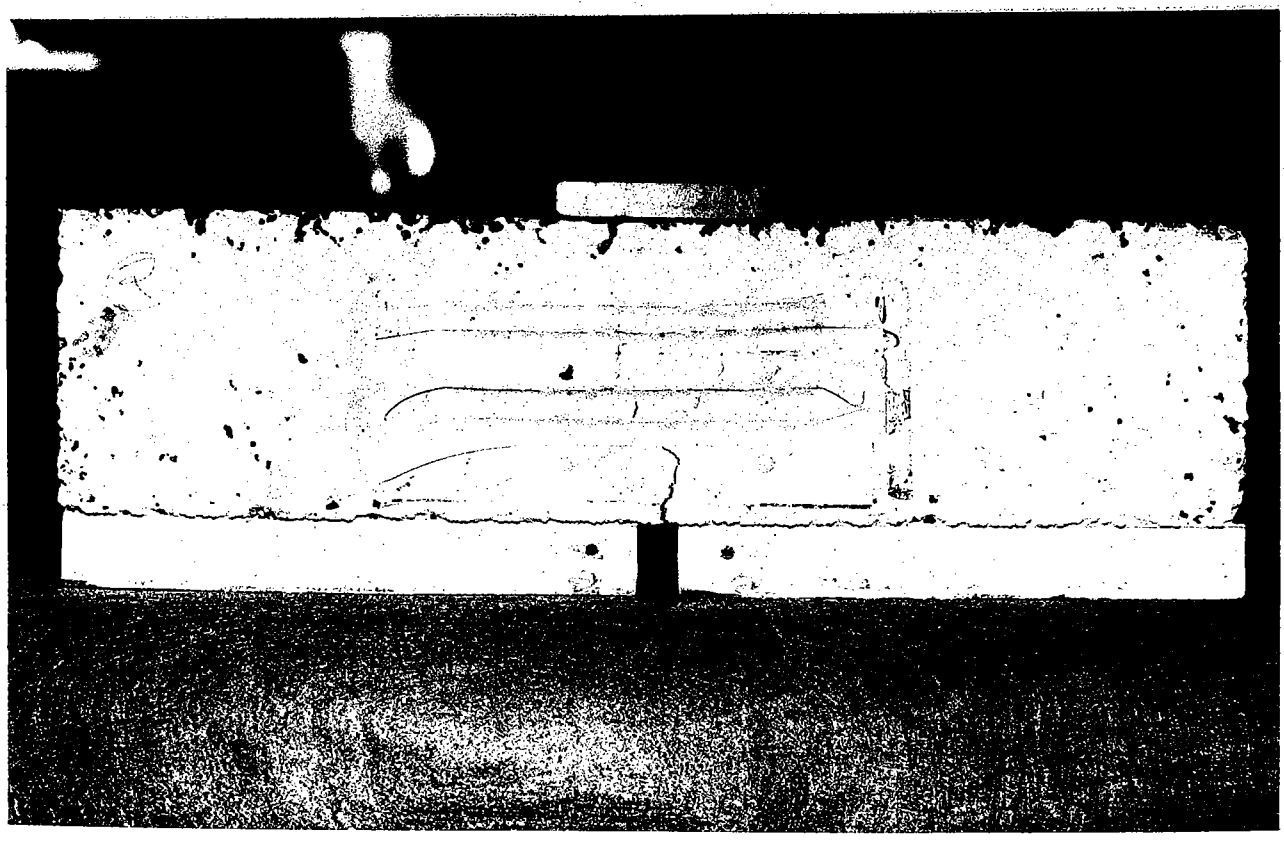

Plate 4.5 (b) Beam Test Two ; 100mm Asphaltic Concrete
Trial on Crack Detection Devices

3. Beam Test Three incorporated the use of a 75mm platen and the following initial test conditions :-

- 75mm asphaltic concrete.
- Width of loading platen 75mm, 53mm.
- End blocks initially in place.
- Traffic loading 1.3 kN - 8.3 kN, 10 Hz.
- Temperature 20°C ± 1°C.
- Crack detection, 39 gauge wire painted on with white emulsion.

After 761,400 cycles no cracking was evident in the beam, however, debonding of the asphaltic concrete beam ends from the rubber bases was quite extensive.

Debonding was a result of the combined effects of the tensioning force and frictional resistance at the connection between tensioning rod and tensioning plate, exceeding the friction and bond strengths between the rubber bases and asphaltic concrete. Figure 4.14 displays the relative beam movements associated with this debonding process.

A smaller 53mm load platen was then used and the steel end blocks removed to observe any reduction in lifting of the asphalt from the rubber bases. No such decrease in lifting was observed, however, cracking did propagate quickly through the sample under these conditions.

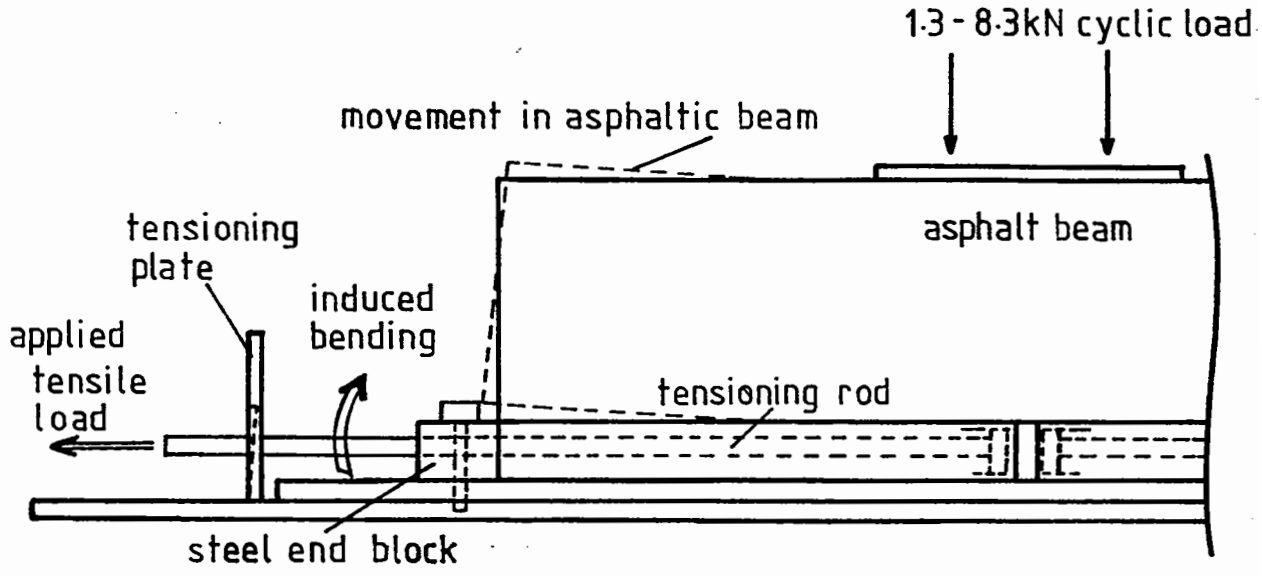

Figure 4.14 Beam Debonding Problems

4. Beam Test Four was set up without the steel end blocks in place. A dial gauge was used to evaluate the degree of differential movement in the rubber bases during the tensioning process. Figure 4.15 illustrates the new configuration during this process.

The initial test conditions were:-

- 75mm asphaltic concrete.
- Width of loading platen 53mm.
- End blocks not in use.
- Traffic loading 1.3 - 8.3 kN, 10 Hz.
- Temperature 20°C ± 1°C.
- Crack detection, 39 gauge wire painted on with white emulsion.

The results of the tensioning process undertaken are displayed in Table 4.4. It can be seen that a differential movement from the preset gap to the end of the rubber base is still achieved without the presence of steel end blocks, although not to the same extent as previously recorded.

Table 4.4 Rubber Base Movement

LVDT Across Gap (mm)	Dial Gauge (mm)
0.97	0.40
1.98	0.88
2.56	0.92

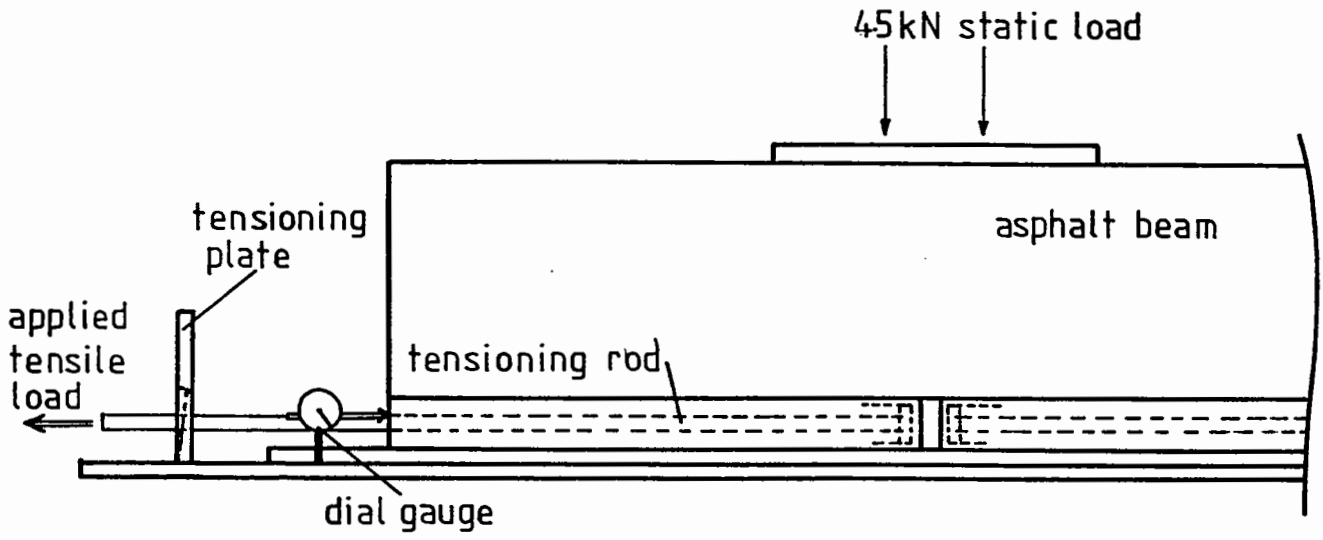

Figure 4.15 Relative Movement of the Rubber Base without End Blocks

Debonding again proved to be an immediate problem despite the absence of end blocks. Cracking of the sample was quite severe after only 65,400 cycles and consequently stopped any further testing on the sample. Plate 4.6 (a) shows the cracking pattern evidenced in this beam, both reflection cracking from the predefined gap and cracking from high stresses around the loading platen can be seen.

5. Beam Test Five and beam test six were primarily used to resolve the debonding problem of the asphalt material lifting from the rubber bases. Initial test conditions for beam test five were:-

- 100mm asphaltic concrete.
- Width of loading platen 75mm.
- End blocks not in use.
- Traffic loading 1.3 kN - 8.3 kN, 10 Hz.
- Temperature 20°C ± 1°C.
- Crack detection, 39 gauge wire painted on with white emulsion.

Lugs were threaded into the steel baseplate and protruded into the rubber bases which were similarly adjusted to ensure a snug fit. Figure 4.16 illustrates where and how the lugs fitted into the rubber bases.

The use of two lugs in each of the rubber bases was designed to allow vertical movement but not any significant horizontal movement during the loading of the specimen. Despite these efforts debonding of the asphaltic concrete from the bases still occurred. Lugs were abandoned from further testing.

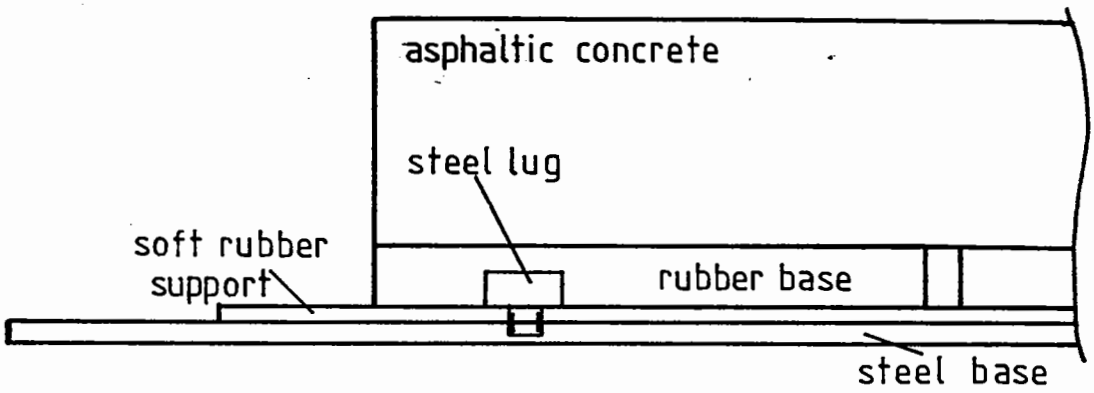

Beam test specimen with steel lugs.

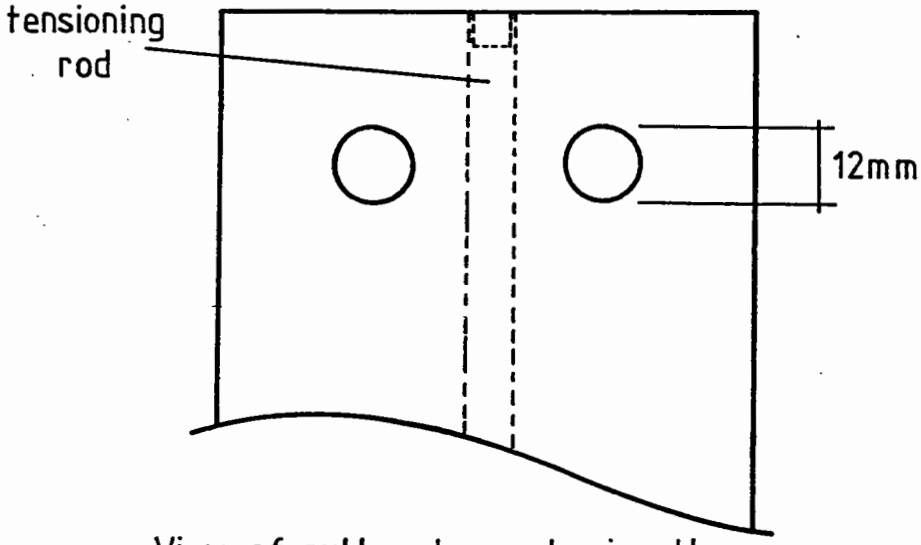

View of rubber base showing the location of lugs.

Figure 4.16 Steel Lugs use in an Attempt to Arrest Debonding Problems

6. Beam Test Six began after the design, construction and placement of end restraints on the beam had been completed. The end restraints were designed to tie the asphaltic concrete to the rubber bases. This was achieved by incorporating an angle iron 35mm x 35mm and steel plate sections in an arrangement where the angle iron clamped over the asphaltic concrete end and the extended steel plate section was connected to the tensioning rod.

This system was tightened using caver clamps to compress the ends of the beam then adjusting the tensioning nuts on the end restraints. Figure 4.17 shows the end restraint arrangement. Once the end restrains were fixed to the specimen and the test conditions as outlined below had been established, testing commenced.

- 100mm asphaltic concrete.
- Width of loading platen 75mm.
- End restraints on.
- End blocks not in use.
- Traffic loading 1.3 kN - 8.3 kN, 10 Hz.
- Temperature 20°C ± 1°C.
- Crack detection, 39 gauge wire painted on with white emulsion.

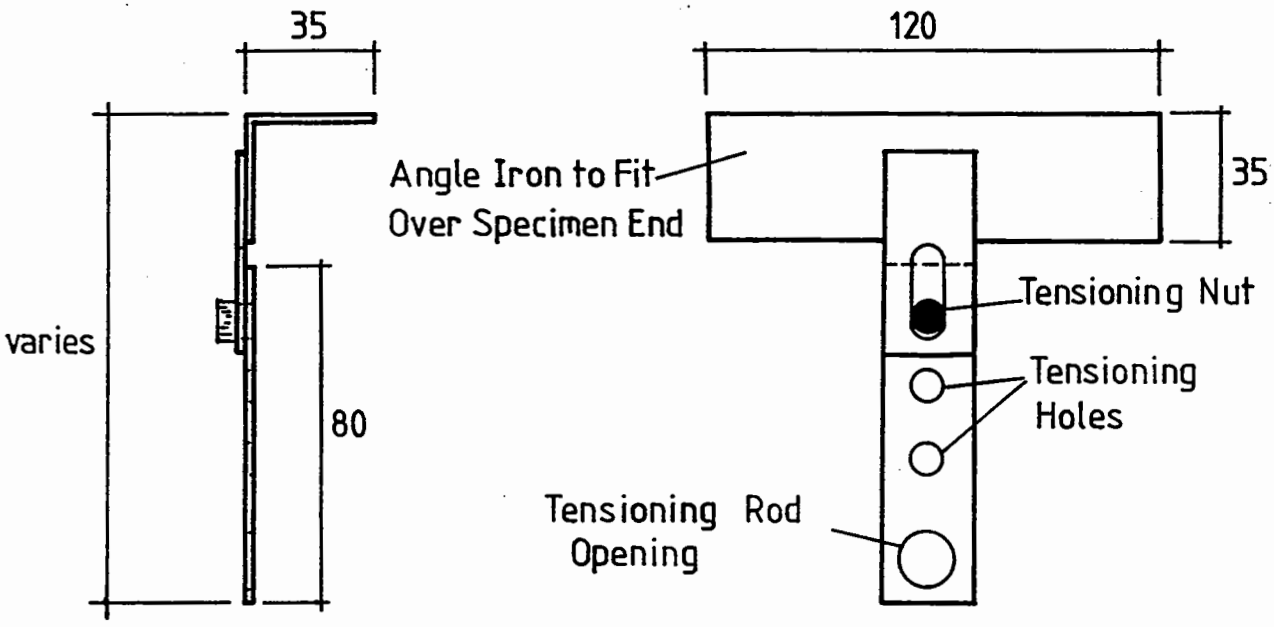

Figure 4.17 Schematic Diagram of End Restraints

Debonding did not occur during the 669,300 cycles applied to the sample. Plate 4.6 (b) shows the end restraint used to prevent debonding, together with a tensioning rod.

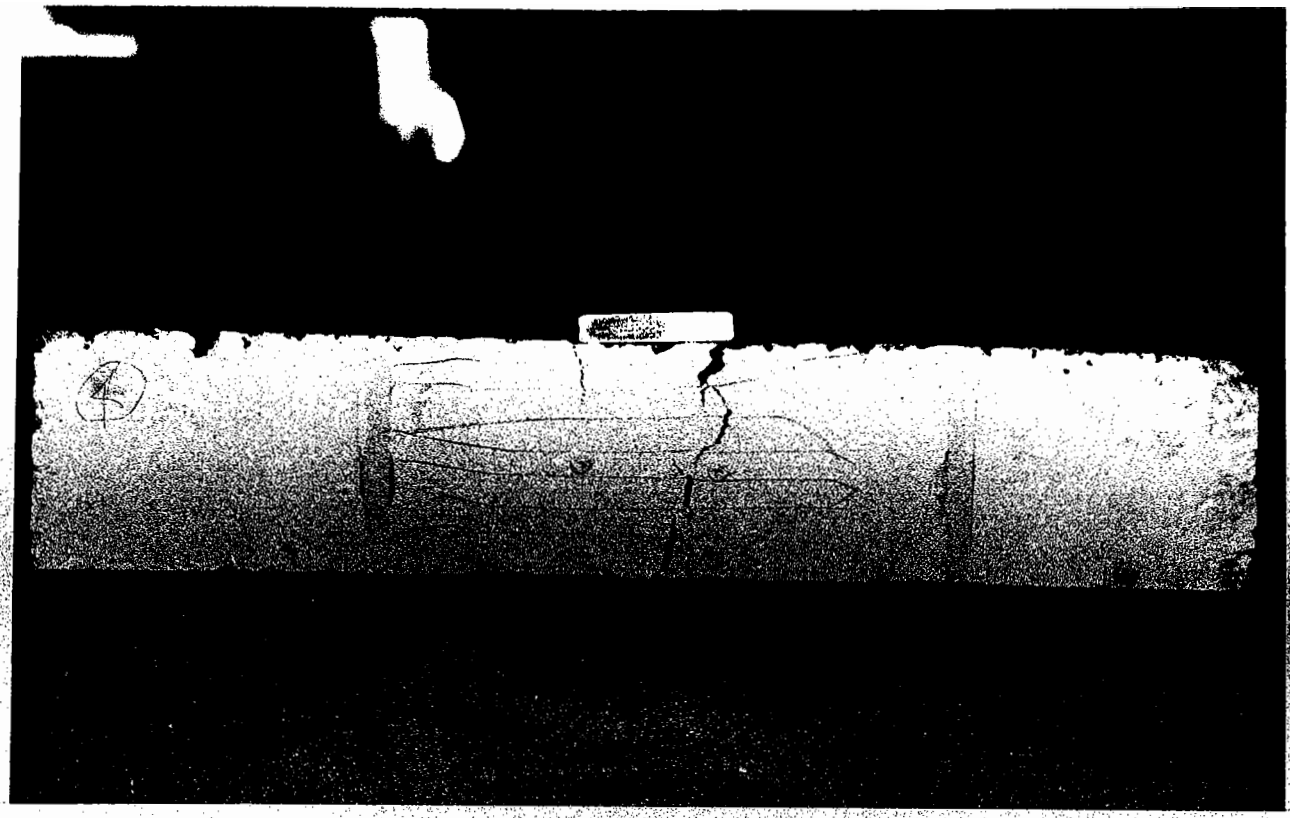

Plate 4.6 (a) Beam Test Four ; 75mm Asphaltic Concrete
Small Loading Platen
65,400 Cycles

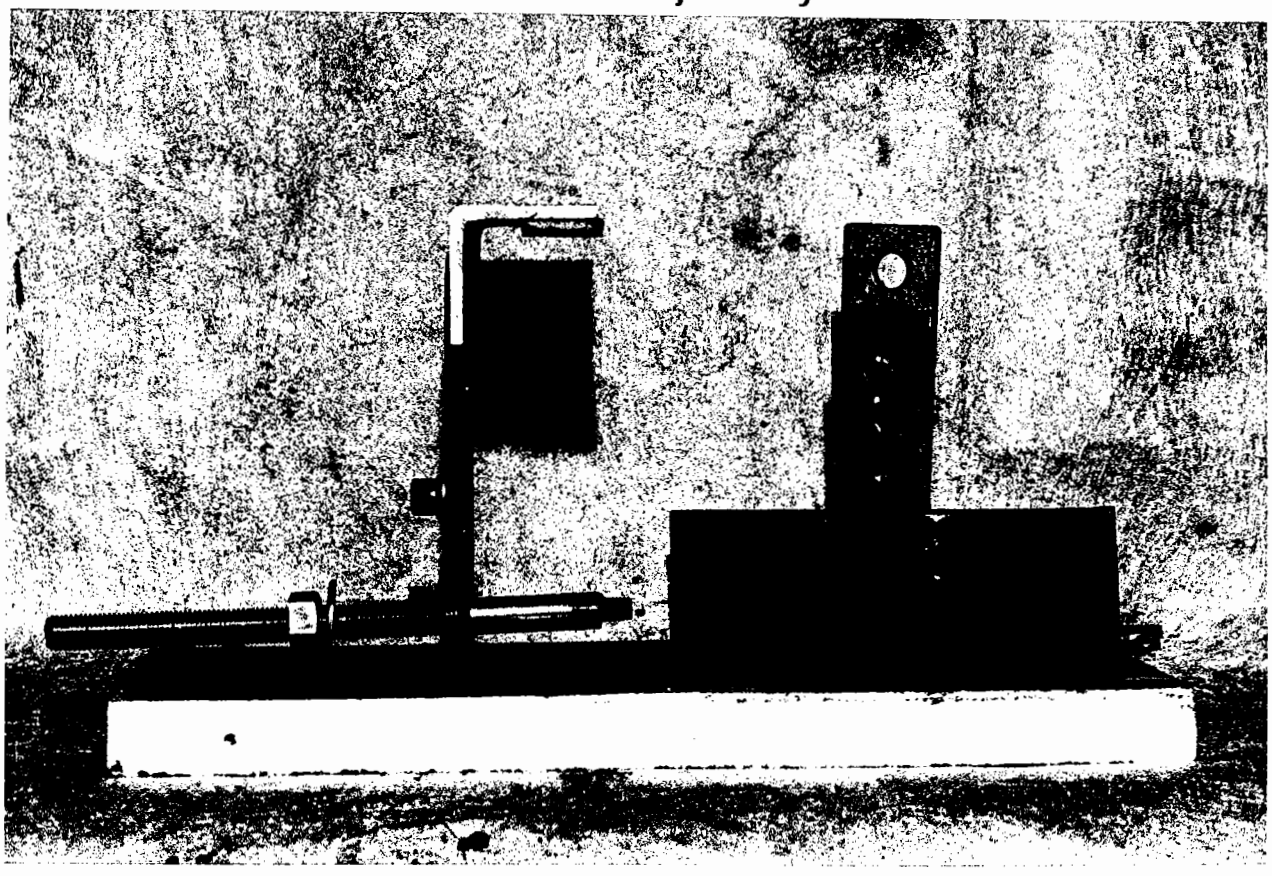

Plate 4.6 (b) End Restraints Manufactured to Prevent Debonding of the Asphaltic Concrete from the Rubber Bases

4.3.3 Summary of Modifications to the Beam Test Facility

4.3.3.1 Introduction

The first six beams as previously detailed were successfully used to develop a sound procedure that allows beam testing to accurately and consistently predict crack growth rates in asphaltic concrete specimens. Plates 4.7 (a) and (b) show the general arrangement of the beam testing rig and a close up view of a beam fully instrumented ready for the commencement of load cycling. Plates 4.8 (a) and (b) illustrate the crack detection equipment and HP85 computer, together with the servo hydraulic machine control unit.

4.3.3.2 Review of Variables

The development procedure for the beam test has been a culmination of the following variables being adequately defined:-

(a) Specimen Manufacture

Use has been made of the Nottingham roller compactor to produce two identical beams from a single compacted slab. These beams have been compacted in a manner that attempts to simulate field rolling conditions.

(b) Thermal Movements

Thermal movements have been modelled by the use of a high quality 'Devcon' rubber product that was cast into two beams that form the base for an asphaltic concrete overlay. When making these bases a steel end section was embedded with a steel tensioning rod to allow the end of the beam at the preset gap to move in a manner that reflects the types of movements occurring in pavements with cement treated layers.

(c) Combined Thermal and Traffic Loads

The ability to combine both thermal and traffic loads was achieved through the development of a yoke arrangement. The yoke provided a means of separating the specimen and the induced traffic loading.

The tensioning process to induce thermal movements extended the preset gap by between 1.0 and 1.5mm. This was measured by an LVDT and transducer indicator with the LVDT attached to the rubber bases either side of the gap.

Traffic loads were induced in the specimen through a load platen of dimensions 136mm x 75mm width producing a contact stress on the sample of 810 kPa (max). Later in the testing program as outlined in Chapter 6 a larger loading platen was incorporated to reduce the maximum contact stress to 555 kPa, a value equivalent to a standard axle load.

Both loading platens were made from composite steel and rubber. The thin rubber was placed in contact with the asphaltic surface to avoid any stress concentrations, likely to develop with a plain steel platen.

(d) Temperature

After experimentation with temperatures of 30°C, 20°C and 10°C it was found that the temperature best suited to crack propagation in the test facility was 20°C ± 1°C.

(e) Debonding

Severe debonding of early beam tests led to the development of an end restraint device which effectively tied the asphaltic concrete beam to the rubber base at both ends of the specimen. Plate 4.6 (b) previously illustrated the end restraint and how the tensioning rod was fitted.

(f) Crack Detection

The method of affixing strips of 39 gauge copper winding wire has been established as the most suitable for the detection of crack propagation on the beam faces.

4.3.3.3 Set Up Procedures for Beam Tests

To ensure that all beams were tested on the same basis it was essential that a strict set up procedure was established for all testing.

After sawing a roller compactor slab in half to form two test specimens the following procedure was adhered to:-

(1) Affix all crack detection devices to the face of the beam and the LVDT to the bases.

(2) Place the beam centrally in the testing rig and connect the electrical circuitry for the crack detection devices.

(3) Connect the steel tensioning rods to the rubber bases through the tensioning plate, ensuring that the end restraints are also affixed.

(4) Tighten the end restraints through the use of caver clamps on the beam ends.

(5) Apply a 4.5 kN dead load to the specimen.

(6) Tension the rubber bases by 1.0 to 1.5mm as read by the LVDT on the transducer indicator.

(7) Start cyclic loading at 10 Hz between 1.3 and 8.3 kN, and start the computer program initialising the start point.

This procedure was followed for beam tests 7 through 32.

Plate 4.7 (a) General Loading Arrangement for Beam Testing

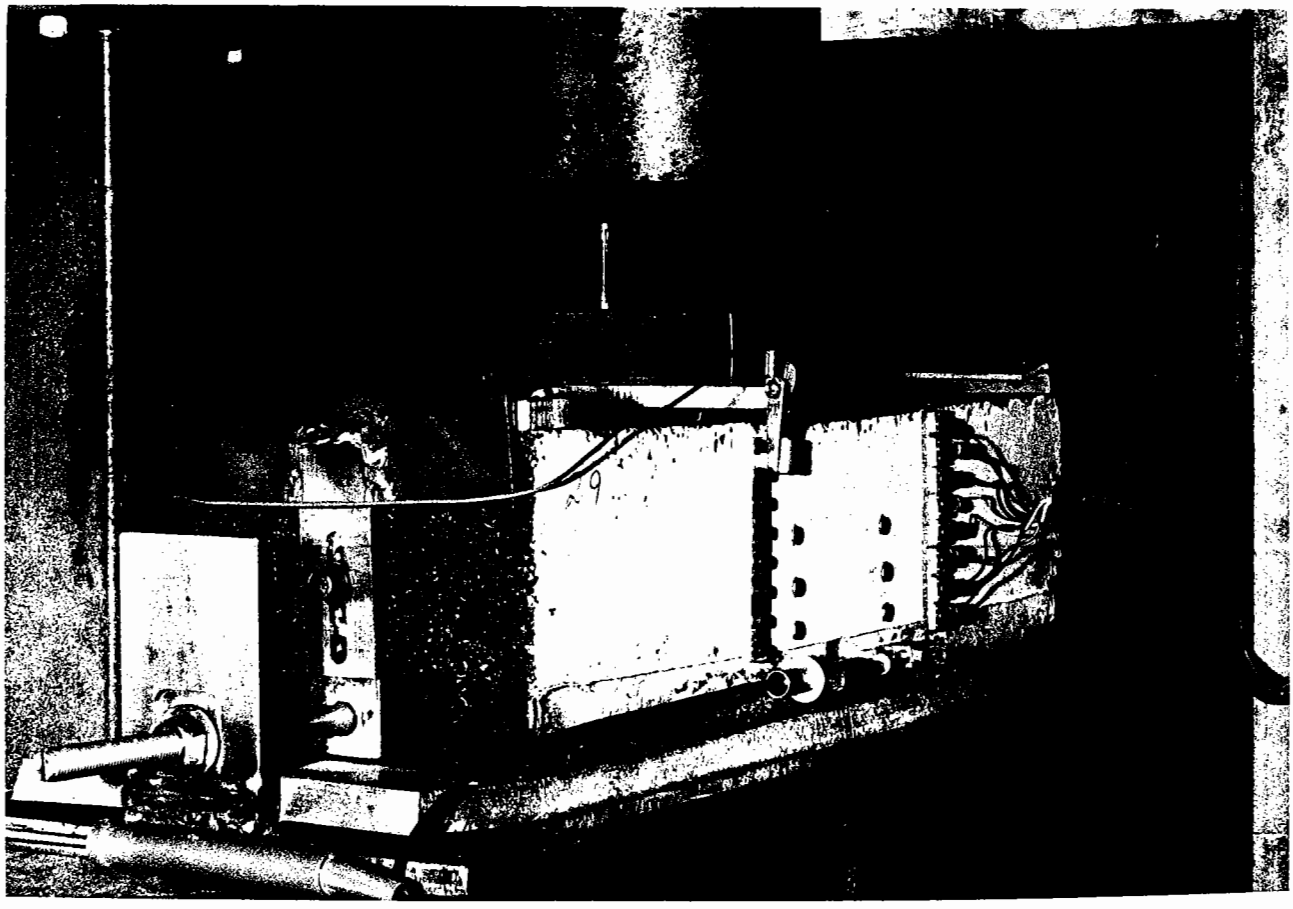

Plate 4.7 (b) Beam Configuration During Testing

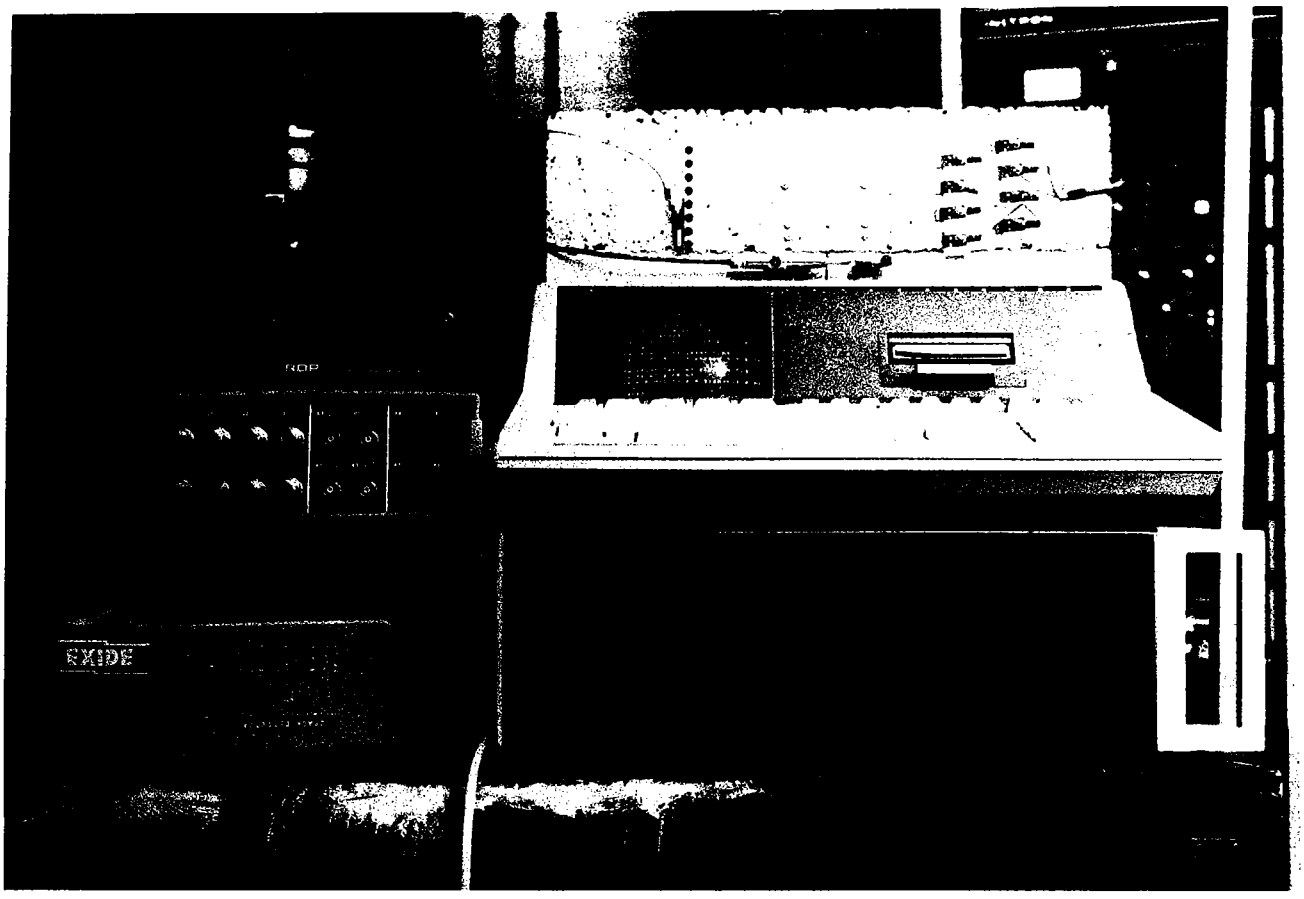

Plate 4.8 (a) Crack Detection Hardware for Beam Testing

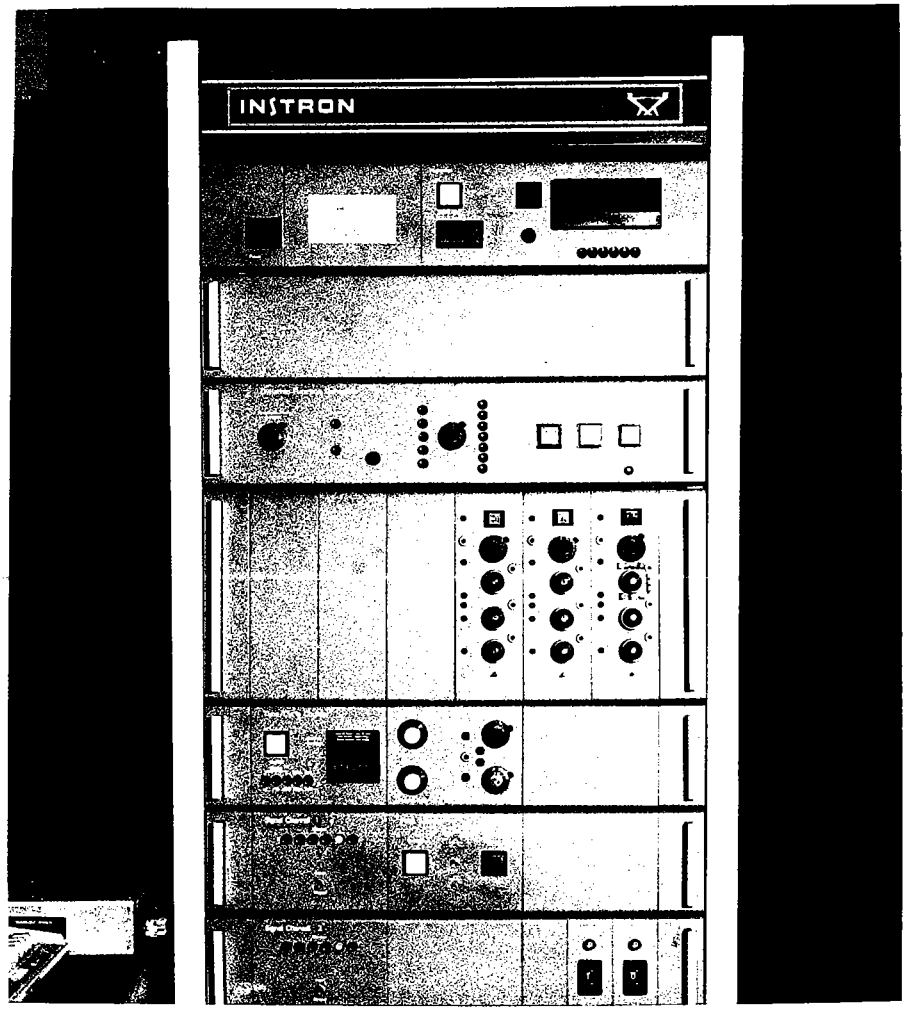

Plate 4.8 (b) Servohydraulic Control Unit

4.4 SLAB TESTING FACILITY

4.4.1 Introduction

The Nottingham University slab test facility simulates traffic loading by passing a moving wheel of variable load and speed over a slab of asphaltic concrete. The action of a moving wheel allows shearing stresses induced by lower pavement layer deficiencies to be transferred into the upper pavement layers. Figure 4.18 displays the typical induced stresses in the base of the overlay due to a moving wheel.

4.4.2 The Slab Test Facility

The existing slab test facility as used by others (44), (54) is illustrated in Figures 4.19 and 4.20 and consists of an integrated servo hydraulically controlled actuator to apply the load and an hydraulic controlled motor which determines wheel velocity through a cable and drum arrangement. A displacement transducer produces a voltage that is proportional to the location of the wheel as it travels along the slab. This signal when differentiated produces an output proportional to velocity. It is velocity that is set from the control unit thus the incoming signal is compared to the setting and adjusted accordingly. Triggers are set at each end of the slab, which reverse the direction of travel. This system produces movement of the wheel at a constant speed over the slab.

The loading frame which contains the wheel is pivoted at one end requiring the actuator to apply a constantly varying response in order to maintain the load as the wheel traverses the slab. This is achieved through the use of a load cell positioned in line with the actuator, providing a feedback voltage to the control unit which is compared to the setting and adjusted accordingly.

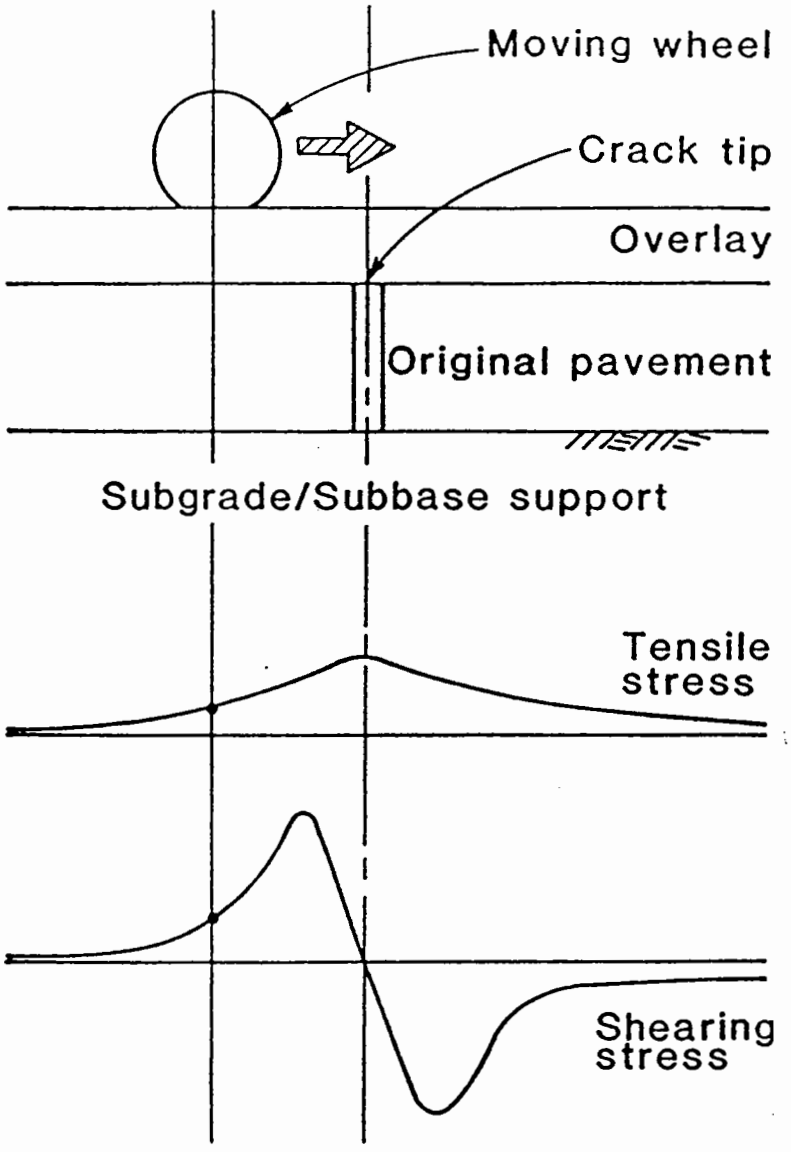

Figure 4.18 Stresses Induced at the Crack Under the Action of a Moving Wheel

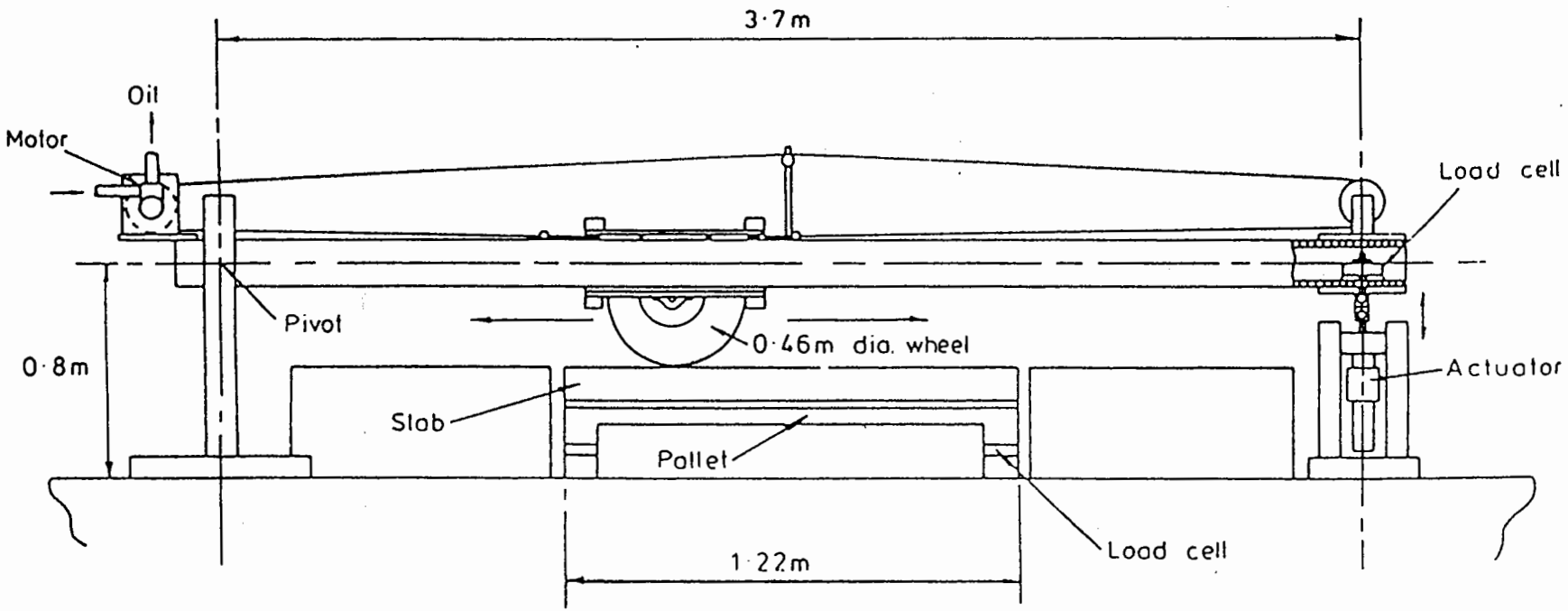

Figure 4.19 Slab Testing Facility General Arrangement

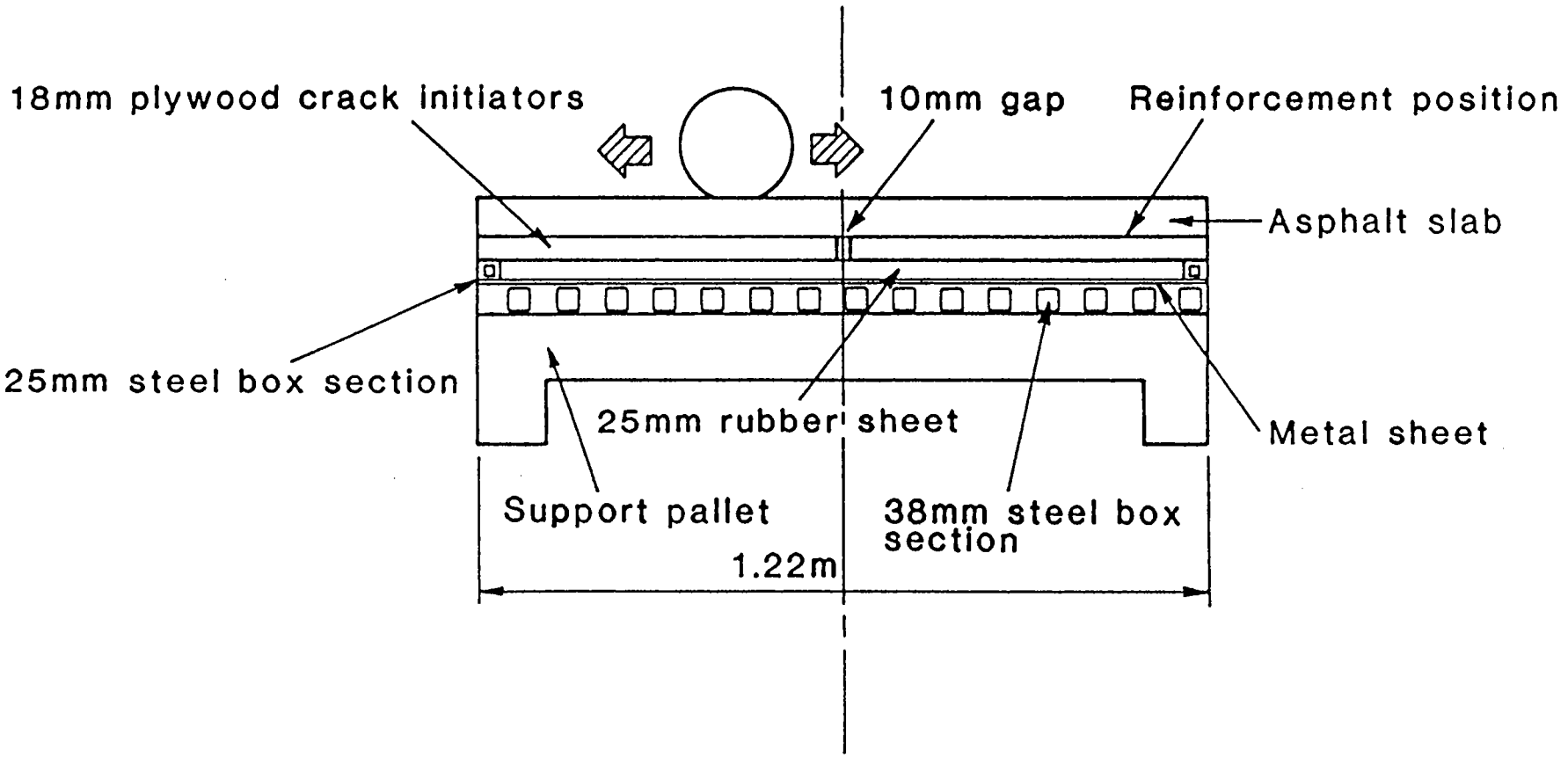

Figure 4.20 Specimen Arrangement in Slab Test Facility used by Hughes (44)

4.4.3 Previous Work Completed with the Slab Test Facility

Hughes (44) used the slab test facility to observe and monitor reflection crack propagation through slabs of asphaltic concrete. These slabs were cast in pairs, one including a geogrid and the other a control section. Each slab was 1.22m long x 0.86m wide x varying thickness from 40mm to 100mm and all had a predefined gap of 10mm in the bases which were made from high quality plywood. Hughes experienced difficulties with hogging and debonding of the asphaltic material, resulting in surface cracks and no cracking propagation from the gap. These problems were overcome by the placement of a rigid section under the ends of the slab in place of the soft resilient rubber.

Guo et al (54) used slabs of similar dimensions 1.0m length x 0.5m width and encountered debonding problems of the asphaltic mix from the timber bases. Guo overcame this problem by applying end restraints in the form of angle sections which clamped the slab ends to the steel pallet.

4.4.4 Slab Testing Developments

The work conducted as part of this study aimed to determine the benefit or otherwise of interlayer treatments in the prevention of reflection cracking under the action of a moving wheel. A slab was produced with two gaps allowing direct comparisons to be made between interlayer treatments and control sections in the same slab. This concurrent testing has the following advantages:-

(a) Identical load and vehicle speed for both sections.

(b) Same mix used for the entire slab.

(c) Compaction using a single drum vibratory roller for the whole slab.

Figure 4.21 displays the general slab testing arrangement with two gaps in the base.

The slab dimensions were 1.22m length x 0.6m width and a thickness of 75mm. Plate 4.9 (a) shows the mould and emery covered boards awaiting placement of the asphaltic mix. Plate 4.9 (b) illustrates the compacted slab at the completion of rolling with the Bomag 55 single drum vibratory roller. One side of the slab subsequently had 50mm sawn off to allow visual detection of crack growth from the predefined gaps. Plate 4.10 (a) shows the arrangement for sawing one face of the slab.

Once the slab is mounted in the slab test facility LVDT's are fitted to both gaps and the sawn face is painted white with emulsion to better detect crack propagation.

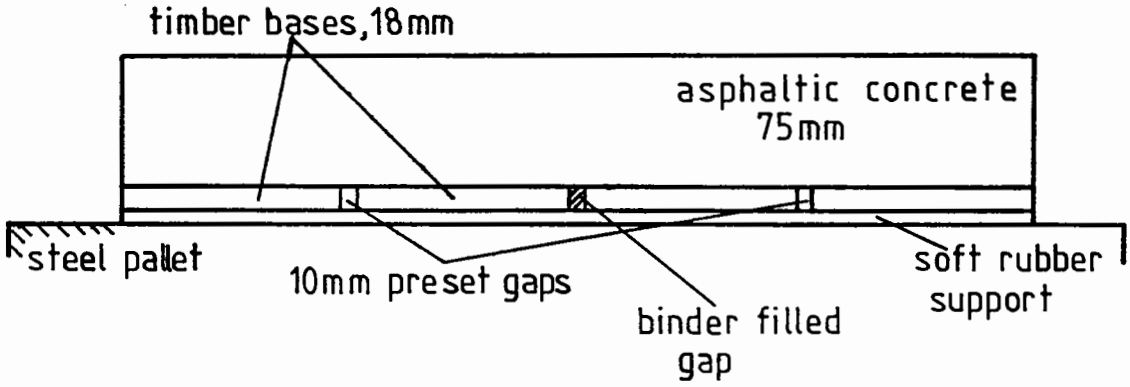

Figure 4.21 Slab Test Specimen with Two Crack Initiators

The wheel load was set at 3 kN which corresponded to a contact pressure of 315 kPa. Wheel speed was approximately 3 km/hr, although no run off beams were provided so this speed was only achieved over a short distance of the slab. Plate 4.10 (b) shows the general testing arrangement.

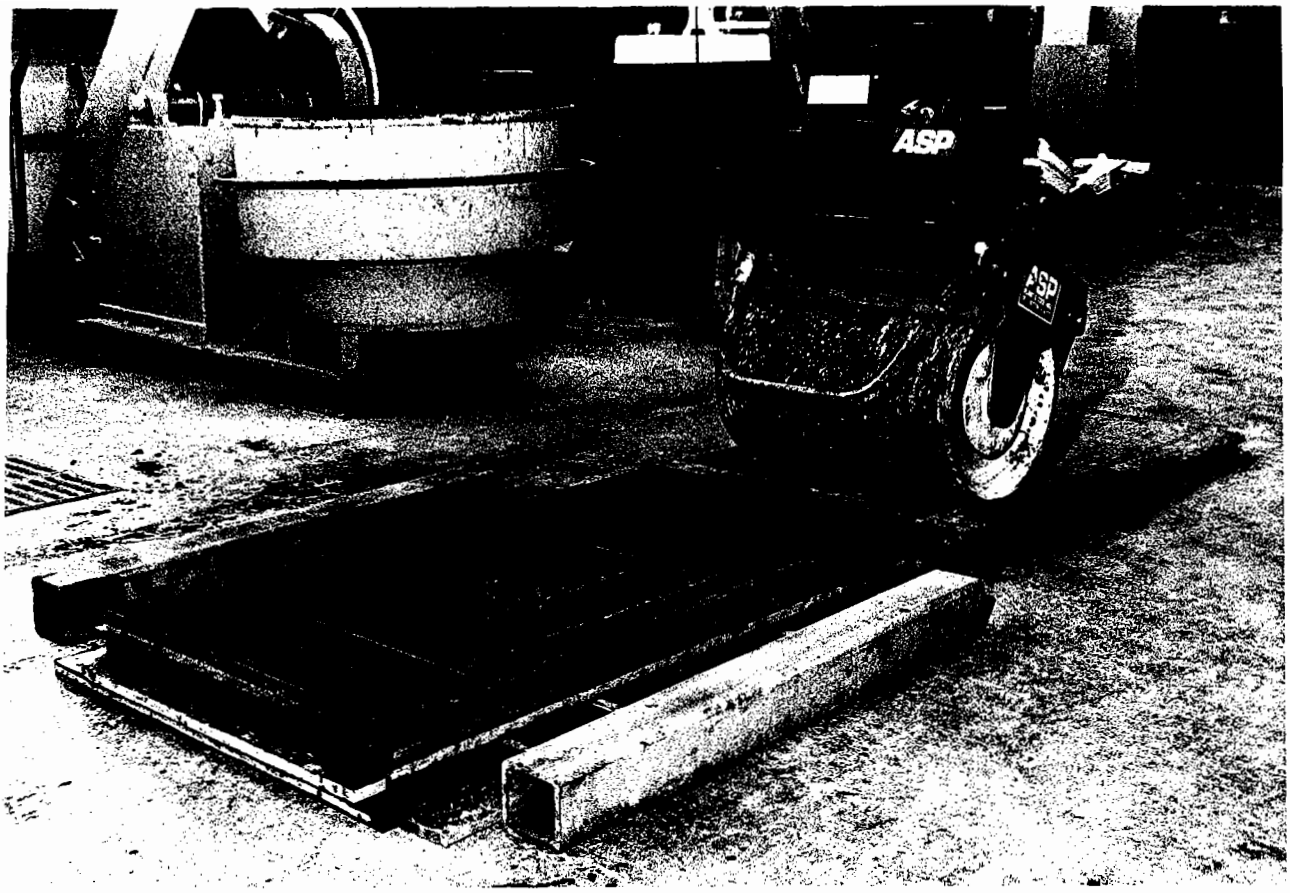

Plate 4.9 (a) Slab Test Specimen Mould

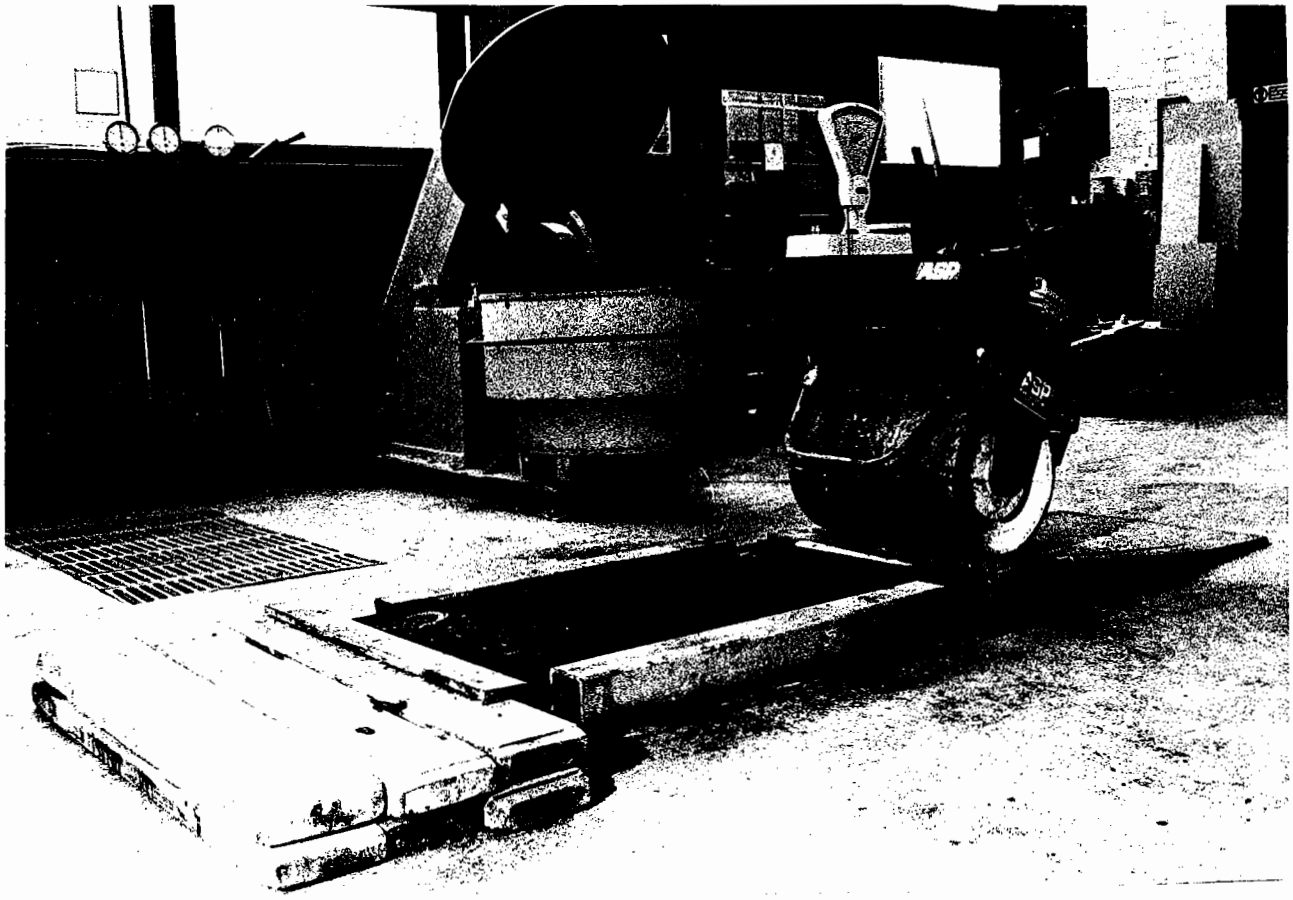

Plate 4.9 (b) Compacted Slab Test Specimen
1.22m Length x 0.6m Width

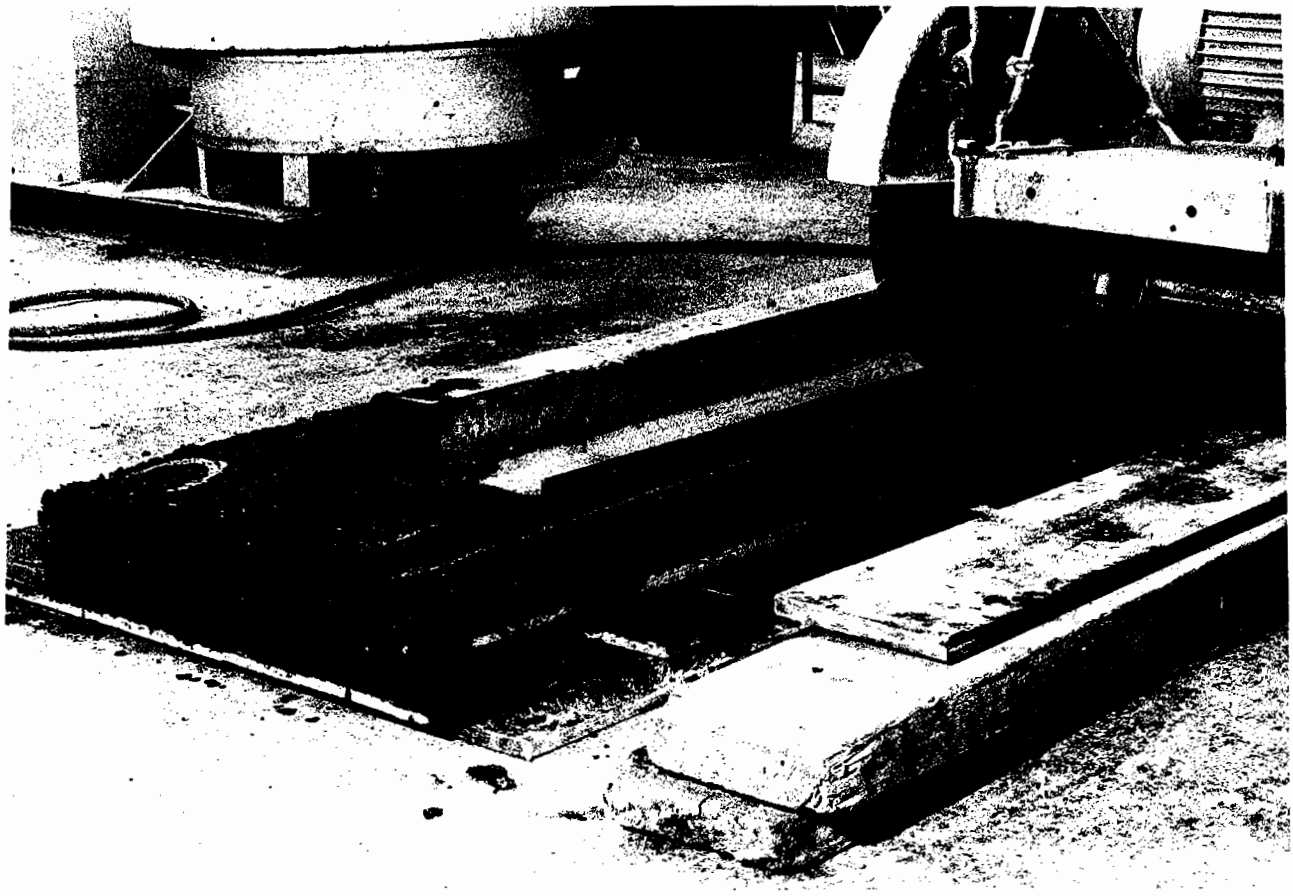

Plate 4.10 (a) One Face of the Slab Was Sawn to Better Facilitate the Viewing of Crack Propagation

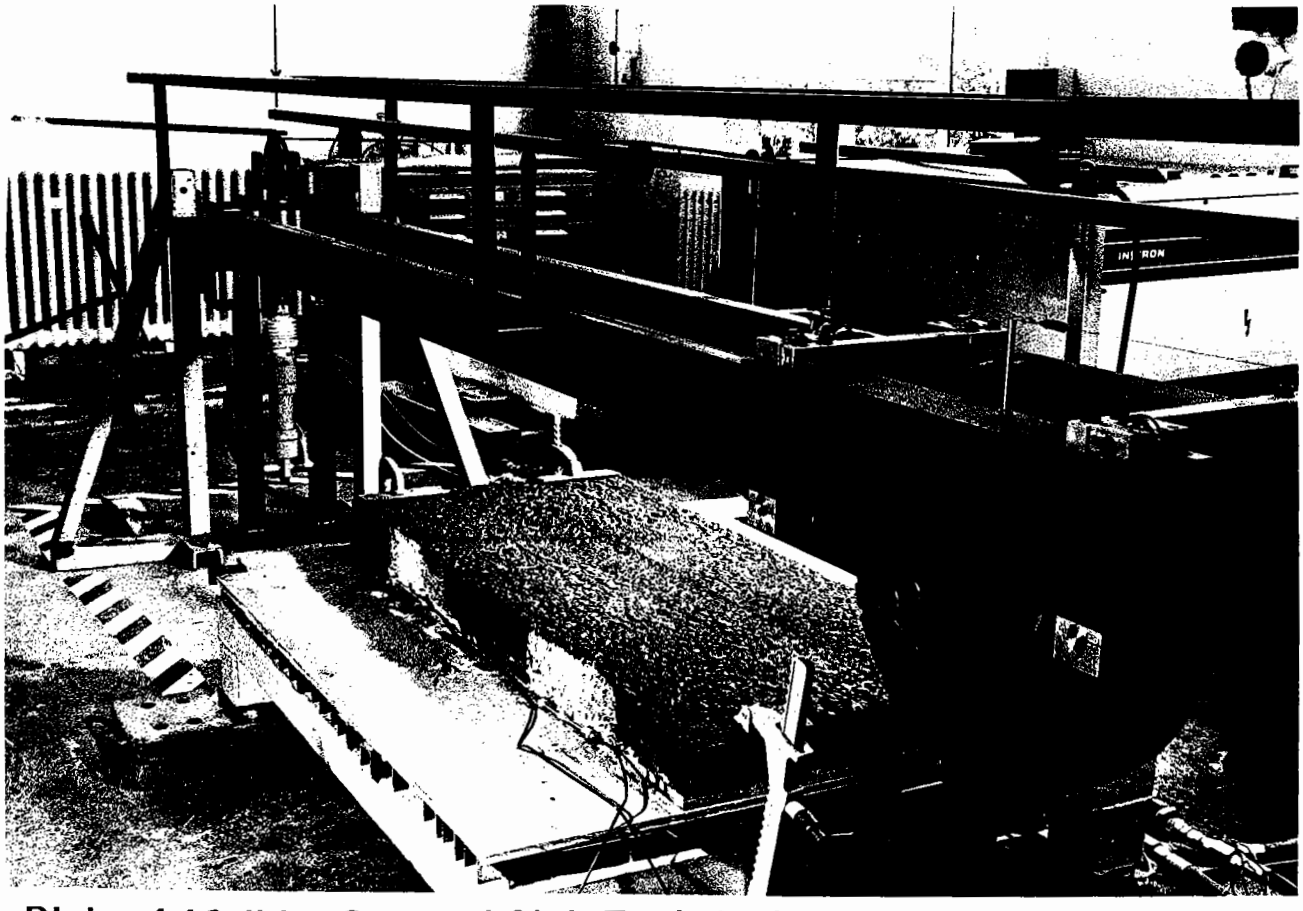

Plate 4.10 (b) General Slab Test Facility Arrangement With LVDT's on Each Gap and End Restraints in Use.

During the testing of the first and second slabs debonding problems were experienced either side of the gaps with extensive debonding evidenced in both control and interlayer treatments. Hogging of one slab was also noticed. Changes were made to the resilient rubber support in an effort to reduce the vertical movements, this did not however have the desired effect of reducing debonding problems.

Two further beam tests were subsequently carried out using a single gap as a crack initiator after the failure to stop debonding in the dual gap slabs. Plate 4.11 (a) and (b) illustrate the control unit and LVDT calibration equipment used for all test facilities.

The full set of results for this program of testing is presented in Chapter 7.

Plate 4.11 (a) Control Unit for the Slab Test Facility

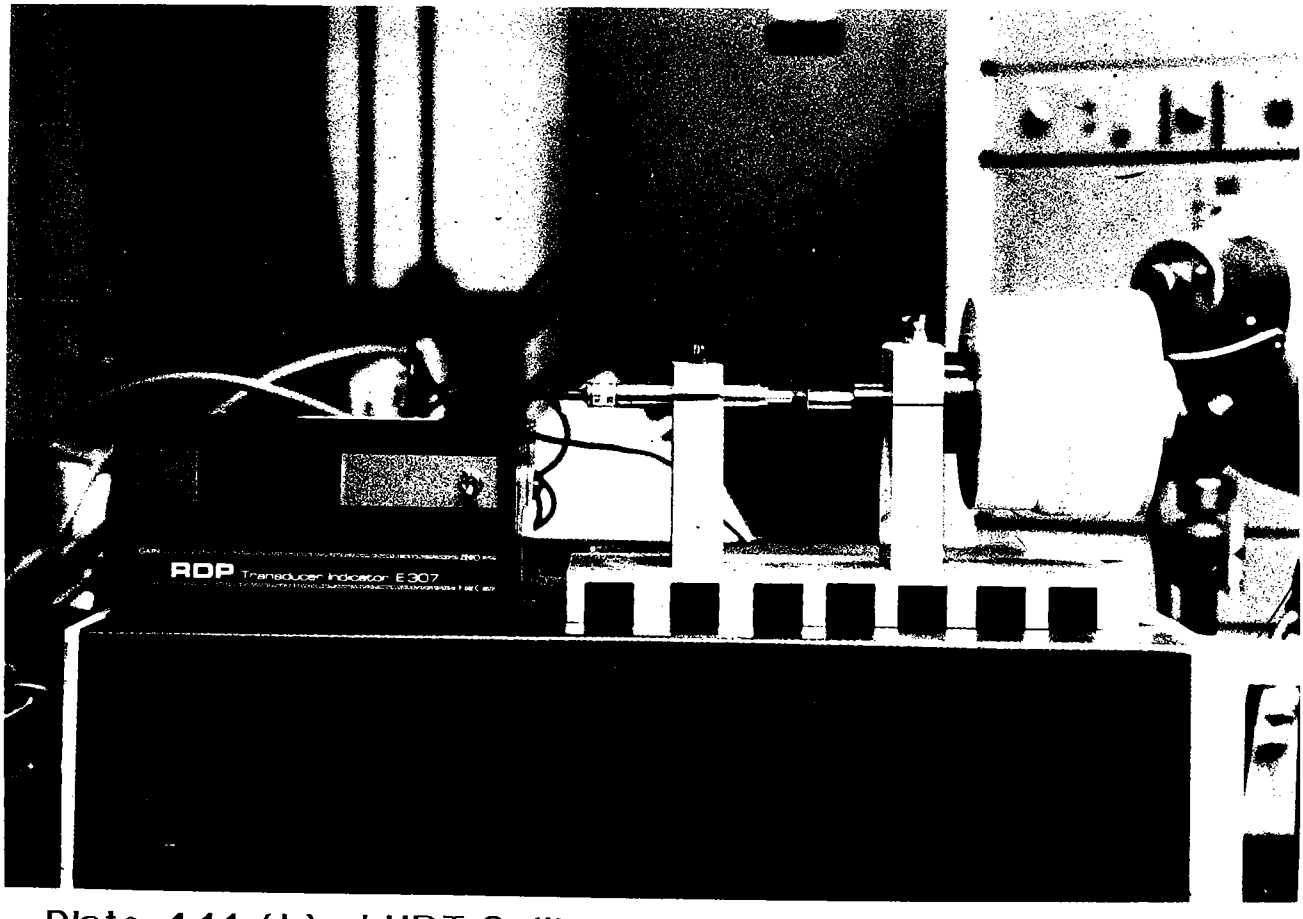

Plate 4.11 (b) LVDT Calibration Process

CHAPTER 5

SHEAR BOX TESTING

5.1 INTRODUCTION

The importance of interface friction between successive pavement layers has been outlined in section 4.2.1. The inclusion of an interlayer material will alter the bond between successive asphaltic concrete layers. Reports from Vicelja (29), (30) suggest that caution is necessary when applying tack coats prior to the placement of geotextiles, as excessive tack will lead to a slippage of the overlay under heavy braking or around sharp corners.

This part of the experimental program had a two fold aim.

(a) to determine the interface shear strength for materials used to prevent reflection cracking, and

(b) to evaluate the interface friction for a standard overlay, then test emery paper proposed for use in beam and slab testing to try and mirror field interface conditions.

5.2 TEST METHOD AND EQUIPMENT USED

As previously outlined in Section 4.1 the hardware associated with the use of the shear box remained unchanged from previous testing (44). Changes were made to the compaction method with a vibrating hammer used in lieu of static pressure and a constant normal stress of 867 kPa or 400 kPa was used.

The tests performed were completed with the following arrangement of interlayer conditions:-

(a) Asphaltic concrete/emulsion (tack coat)/Asphaltic concrete.

(b) Asphaltic concrete/emulsion (tack coat)/Polymer Modified Binder asphaltic concrete.

(c) Asphaltic concrete/Geogrid-emulsion chip seal/Asphaltic concrete.

(d) Asphaltic concrete/Geogrid-bituminous chip seal/Asphaltic concrete.

(e) Asphaltic concrete/Geotextile-emulsion (tack coat)/ Asphaltic concrete.

(f) Timber base-emery paper/emulsion (tack coat)/Asphaltic concrete.

Chart recorders were used to monitor four linear potentiometers placed at the corners of the roller bearing carriage to monitor the dilation of the sample during testing. A chart recorder was also used to plot the shear stress as the top layer of the specimen was sheared at a rate of 3mm per minute from the bottom layer, which was held fixed to the base plate. Plates 4.2 and 4.3 in Section 4.2.3 showed the general arrangement of the shear box.

5.3 RESULTS FROM TESTING

Testing in the shear box began with the application of an 867 kPa normal load which, as the results show was too high as it caused the failure of the sample in a saw tooth or "slip-grip" fashion. Figure 5.1 is a typical representation of the shear stress plot for this testing arrangement.Three tests were conducted at this high normal load, and the results are displayed in Table 5.1.

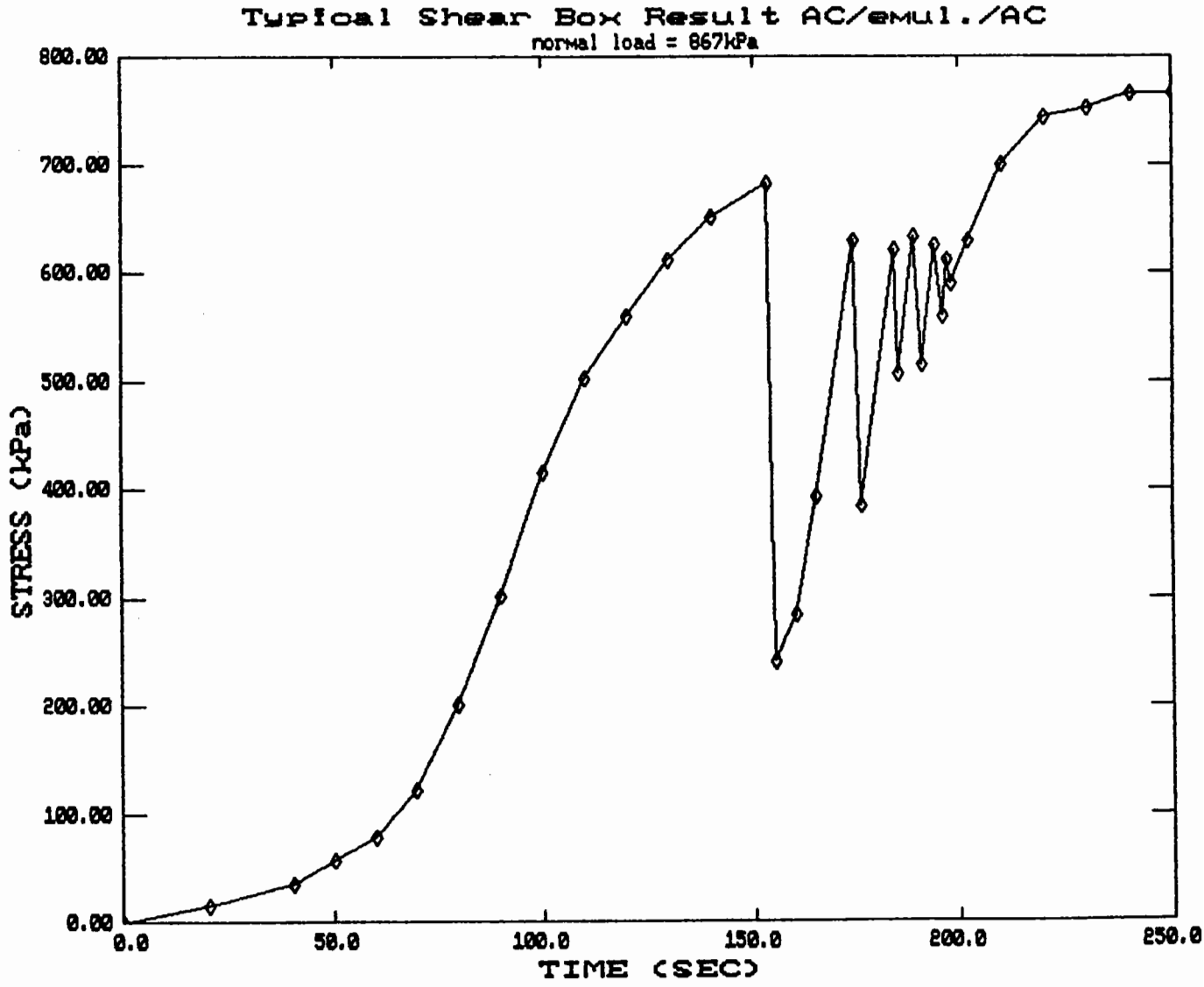

Figure 5.1 Stress vs Time Plot for Asphaltic Concrete Overlay, No Interlayer. High Normal Load of 867 kPa

Table 5.1 Shear Box Results; 867 kPa Normal Stress

Test Type			Stress on Sample	
Bottom Layer	Inter Layer	Top Layer	Normal Stress (kPa)	Shear Stress (kPa)
Timber - emery paper	emulsion	Asphaltic concrete	867	672*
Asphaltic concrete	emulsion	Asphaltic concrete	867	785
Asphaltic concrete	emulsion	Asphaltic concrete	867	764

* Shearing occurred between the timber base and emery paper.

The normal load was reduced to 400 kPa after the three tests at 867 kPa. Subsequent testing in the shear box for all configurations showed consistent results at the lower normal loading level. A plot of the typical curve for each group of interlayer treatments is presented in Figures 5.2, 5.3, 5.4, 5.5 and 5.6. Movement of the top loading plate during testing as recorded by the linear potentiometers is illustrated in Figure 5.7 as a plot of dilation against time.

The tests conducted in the shear box device at a normal load of 400kPa are summarized in Table 5.2. The individual results for each test are presented in Appendix C in graphical form. Subsequent to the completion of each test, cores were taken from both layers of the asphaltic material. These cores were analysed for density and mechanical properties with the results presented in Appendix A.

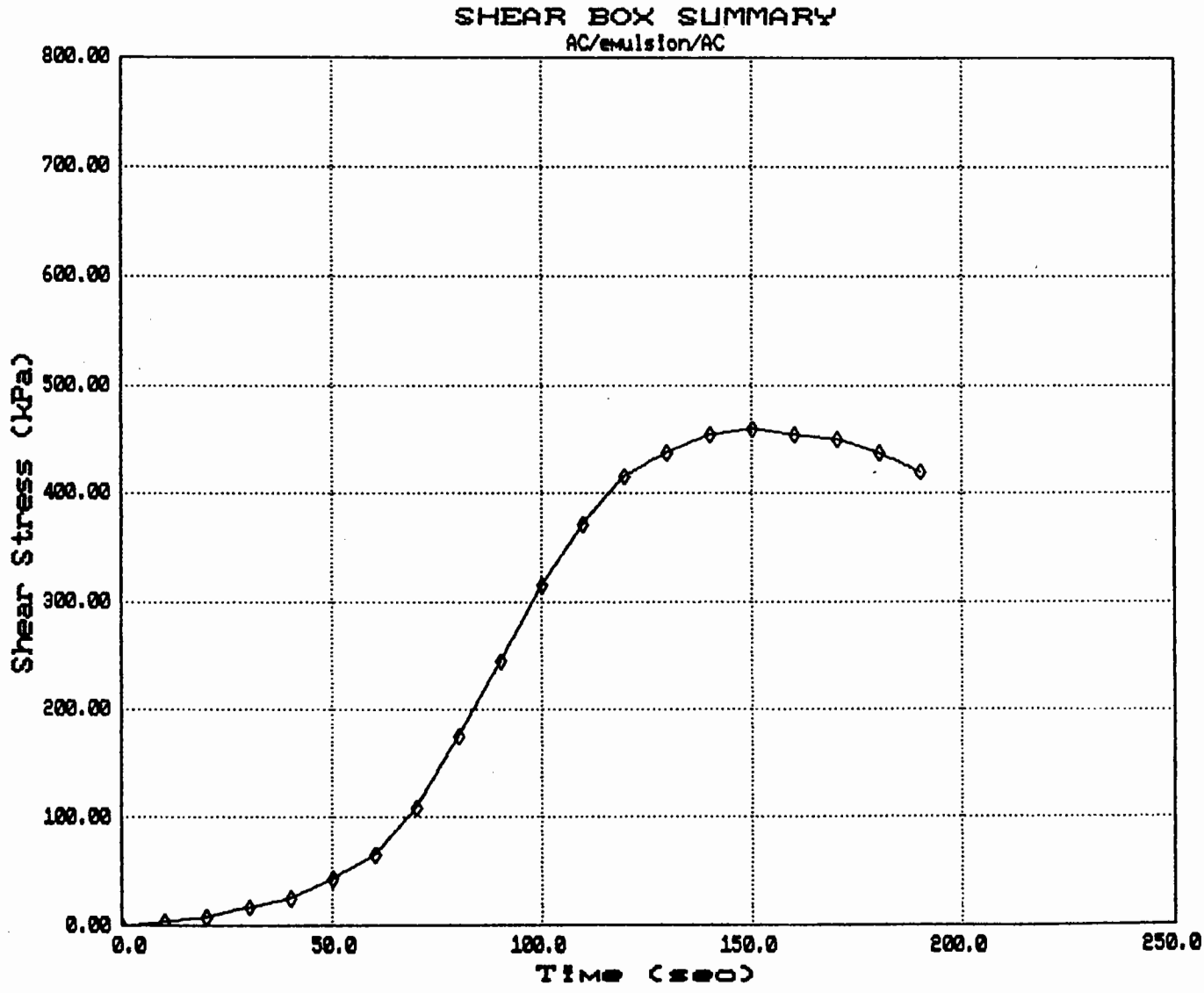

Figure 5.2 Stress vs Time Plot for Averaged Shear Box Results.
Interlayer Type - Emulsion

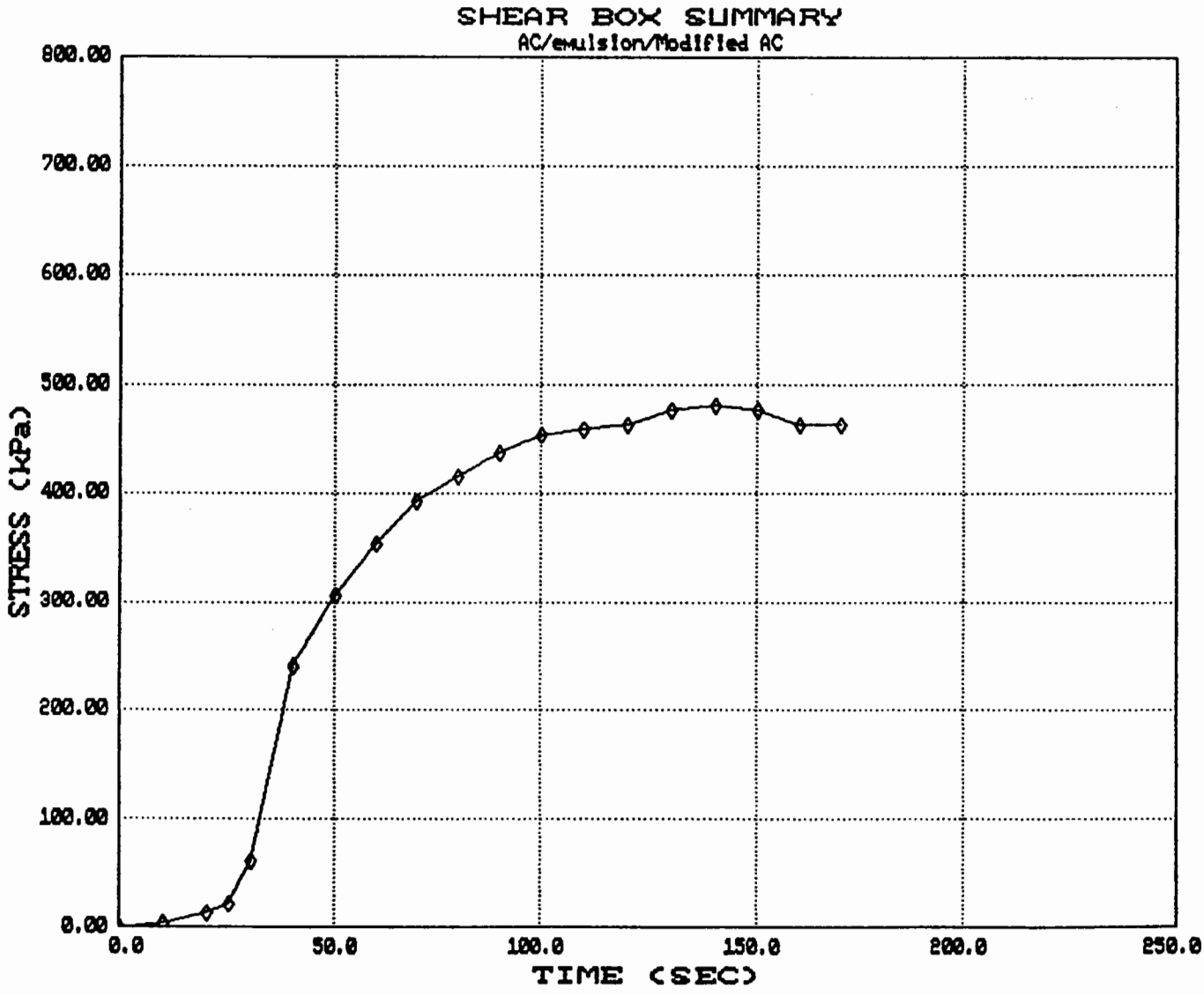

Figure 5.3 Stress vs Time Plot for Average Shear Box Results.
Interlayer Type - Emulsion,
Polymer Modified Binder Asphaltic Concrete

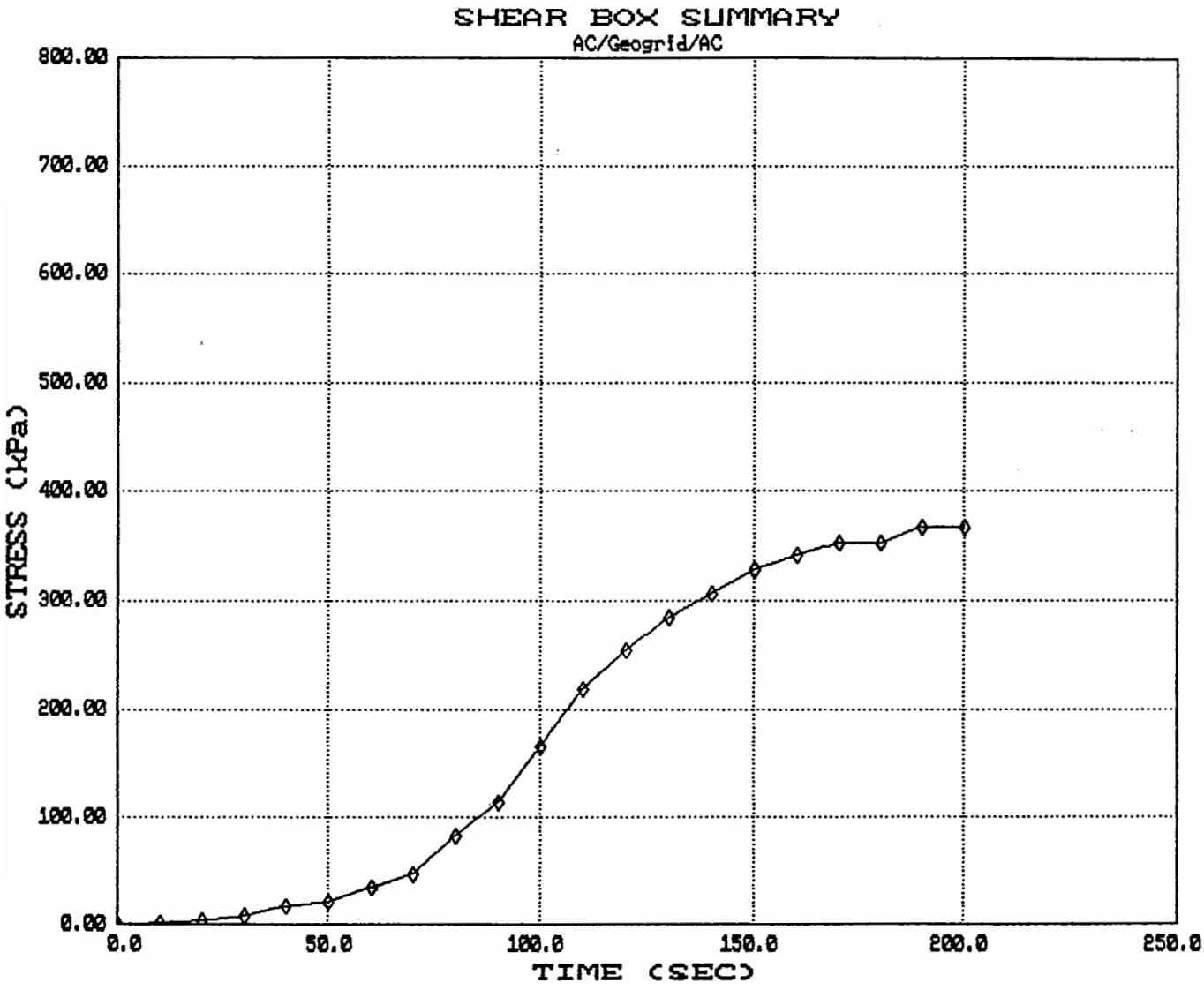

Figure 5.4 Stress vs Time Plot for Average Shear Box Results.

Interlayer Type - Bituminous Chip Seal, Geogrid

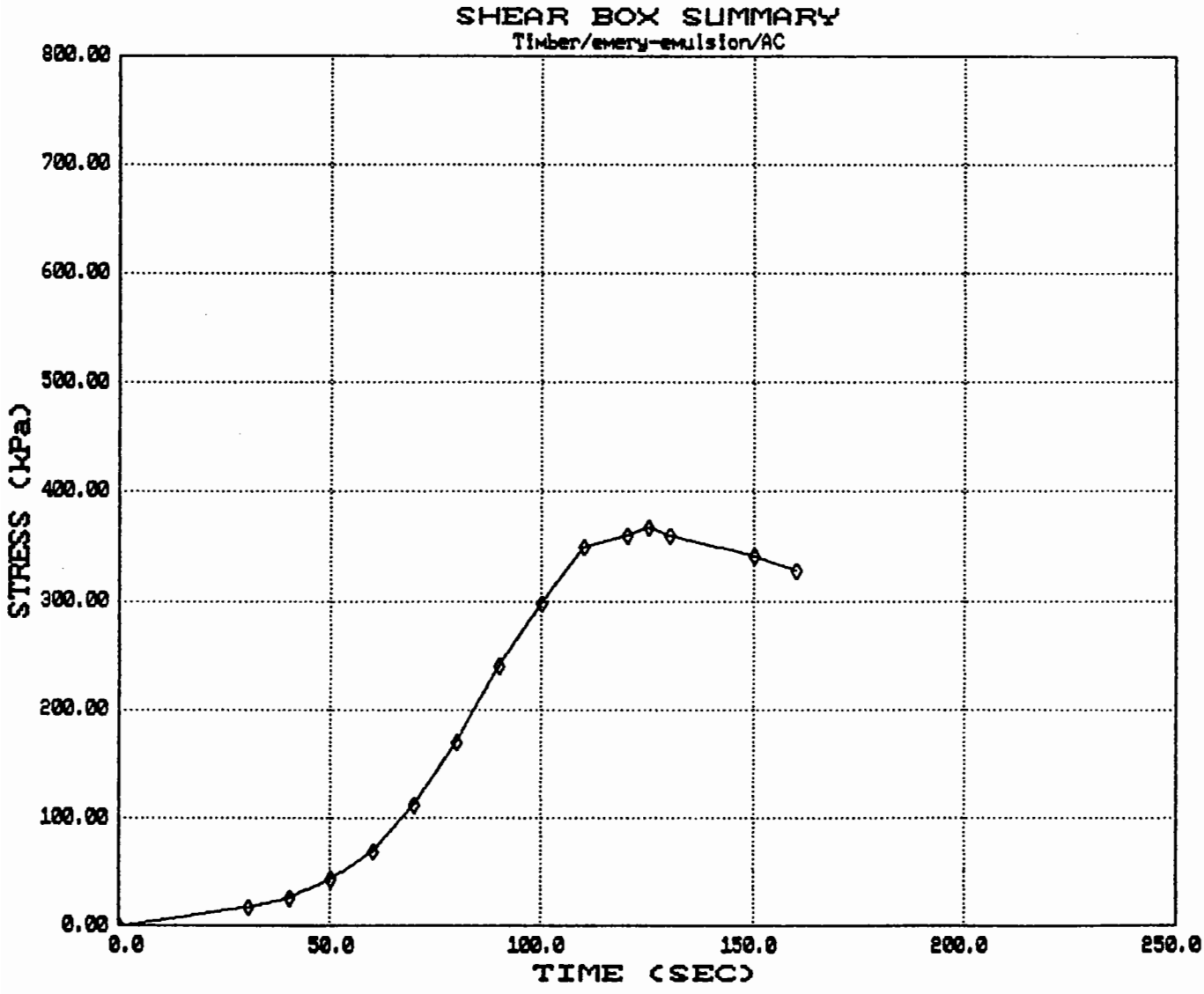

Figure 5.5 Stress vs Time Plot for Averaged Shear Box Results.

Interlayer Type - Emulsion, Emery Paper on Timber

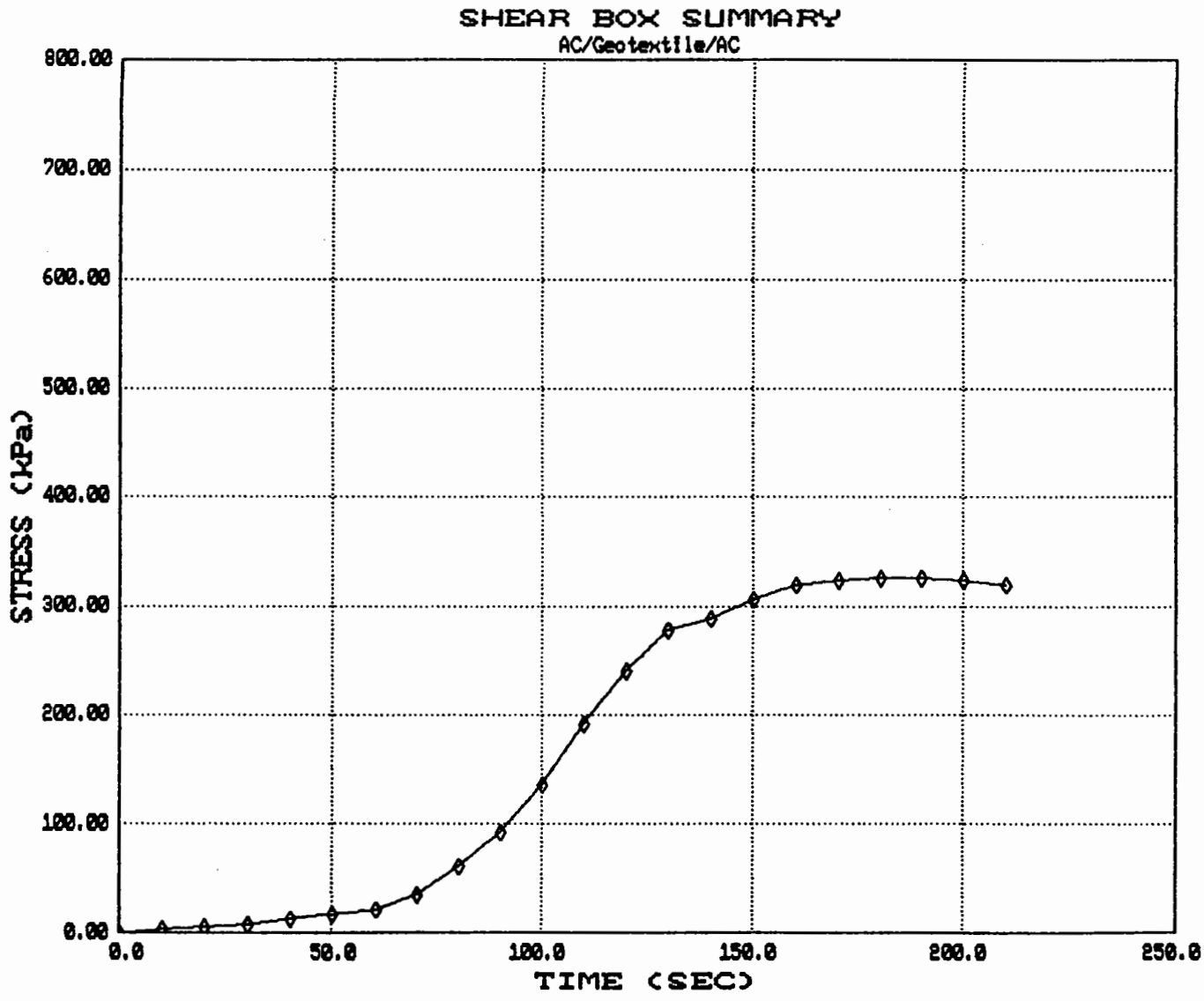

Figure 5.6 Stress vs Time Pot for Averaged Shear Box Results.

Interlayer Type - Bitumen Seal, Geotextile

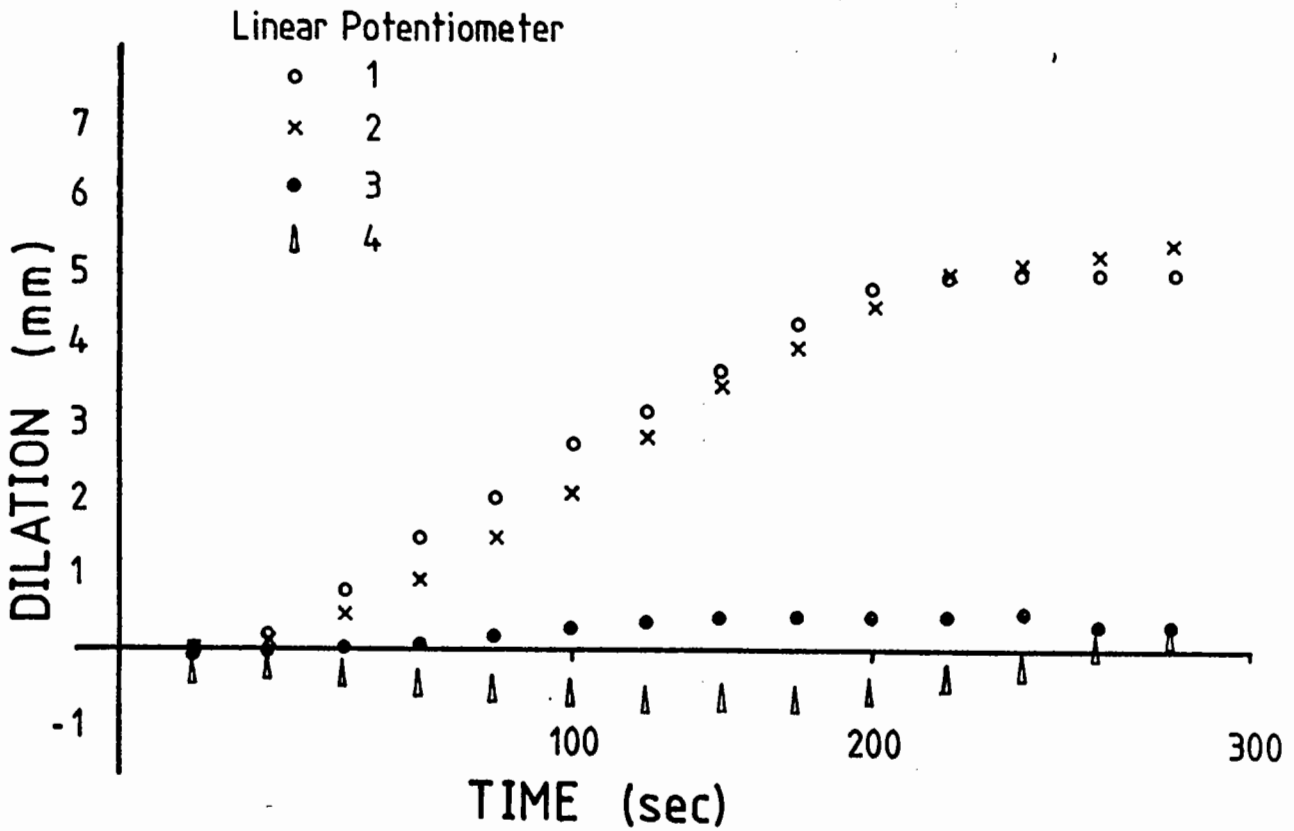

Figure 5.7 Typical Plot of Dilation vs Time for the Top Loading Plate
(Figure 4.3 Displays the Position of the Potentiometers)

Table 5.2 Shear Box Test Results; 400 kPa Normal Stress

Test Type			Stress on Sample	
Bottom Layer	Inter Layer	Top Layer	Normal Stress (kPa)	Shear Stress (kPa)
Timber - emery paper	emulsion (tack)	Asphaltic concrete	400	336
Timber - emery paper	emulsion (tack)	Asphaltic concrete	400	371
Asphaltic concrete	emulsion (tack)	Asphaltic concrete	400	458
Asphaltic concrete	emulsion (tack)	Asphaltic concrete	400	445
Asphaltic concrete	geogrid - emulsion chip seal	Asphaltic concrete	400	371
Asphaltic concrete	geogrid - bituminous chip seal	Asphaltic concrete	400	353
Asphaltic concrete	geogrid - bituminous chip seal	Asphaltic concrete	400	371
Asphaltic concrete	geotextile - emulsion	Asphaltic concrete	400	327
Asphaltic concrete	geotextile - bituminous seal	Asphaltic concrete	400	325
Asphaltic concrete	emulsion (tack)	Polymer Modif. A.C.	400	463
Asphaltic concrete	emulsion (tack)	Polymer Modif. A.C.	400	481

The average result for each type of interlayer treatment showed a clear trend between the shear strengths for each treatment. The average results are presented in Table 5.3.

Table 5.3 Averaged Shear Box Results

Test Type			Sample Stresses		
Bottom Layer	Inter Layer	Top Layer	No. of Results	Normal Stress (kPa)	Average Shear Stress (kPa)
Asphaltic concrete	emulsion (tack)	Asphaltic concrete	2	400	452
Asphaltic concrete	emulsion (tack)	Polymer Modif. A.C.	2	400	472
Asphaltic concrete	geogrid - chip seal	Asphaltic concrete	3	400	365
Timber - emery paper	emulsion (tack)	Asphaltic concrete	2	400	354
Asphaltic concrete	geotextile - seal	Asphaltic concrete	2	400	326

To better compare these results Table 5.4 presents the results as a percentage of the Asphaltic Concrete/emulsion (tack)/Asphaltic Concrete control test.

Table 5.4 Average Shear Stress Results with Respect to Asphaltic Concrete/Emulsion (tack)/Asphaltic Concrete

Test Type			
Bottom Layer	Inter Layer	Top Layer	Percentage of Control Test
Asphaltic concrete	emulsion (tack)	Asphaltic concrete	100
Asphaltic concrete	emulsion (tack)	Polymer Modif. A.C.	104
Asphaltic concrete	geogrid - chip seal	Asphaltic concrete	81
Timber - emery paper	emulsion (tack)	Asphaltic concrete	78
Asphaltic concrete	geotextile - seal	Asphaltic concrete	72

It can be seen from the results presented in Table 5.4 that with respect to the control test all interlayer treatments showed a reduction in shear strength of between 19% for geogrids to 28% for geotextiles. The polymer modified binder used in the asphaltic mix showed an increase in shear strength of 4%.

Density results taken on cores from shear box testing fell within a range of 6.8% air voids to 12.7% air voids. The average for 40 cores tested was 9.0% air voids. Although this value is higher than that required to meet the specification, the density testing method for cores could have given a result up to two percent higher than the actual value. This difference is primarily a result of the aluminium foil used to cover specimens trapping air voids during the wrapping process.

5.4 CONCLUSIONS

The greatest reduction in shear strength was recorded for the geotextile interlayer placed with a bituminous seal in accordance with the manufacturers recommendations. This reduction was approximately 30% of the control sample shear strength. The geogrid interlayer with chip seal, and the timber/emery paper interlayer showed a reduction of approximately 20% in shear strength from the control sample.

Hughes (44) found that for a geogrid with chip seal a reduction of 10% was observed when compared to a control sample of asphaltic concrete but no emulsion tack coat was placed. Thus it would seem that the latest set of results are in approximate agreement with those found by Hughes (44) who also had a greater shearing rate of 5mm per minute and a normal stress of 430 kPa.

Reductions in shear strength of the order of 20-30% obtained for laboratory testing should not cause any problems with overlay slippage for insitu conditions, as field loading rates are significantly higher than the shearing rate used during testing.

Emery paper, type P40, proved to be an effective way of simulating the asphaltic concrete bond to lower pavement layers and was successfully used in beam and slab testing facilities.

CHAPTER 6

BEAM TESTING

6.1 INTRODUCTION

Assessment of the relative performance of interlayers to delay the propagation of cracking through asphaltic concrete overlays was the prime objective of the beam testing program. To achieve this objective a test facility was developed as described in section 4.0 that was capable of applying thermal and simulated traffic loads on the test specimens.

6.2 TEST METHOD AND EQUIPMENT USED

The servo-hydraulic device used to apply the simulated traffic loading had been used by others (44), (50), (51) for this purpose, but with a different sample configuration. Modifications were made as previously outlined in Section 4.0. These initial modifications formed the first iteration in the development process that continued for the first six beams tested.

Controls on testing parameters, previously described in Section 2.6 ensured that consistency in mix properties was achieved, thus eliminating this source of error from influencing the results. By following the set up procedure outlined in Section 4.3.3.2 a consistent method of handling beam specimens once manufactured was devised to avoid errors arising from this source. The experimental set-up and equipment in use to monitor load application and crack propagation were previously illustrated in plates 4.7 and 4.8.

6.3 RESULTS OF TESTING

6.3.1 Introduction

During the testing sequence a continuous process of beam specimen evaluation was undertaken incorporating the following readings.

(i) LVDT amplitude and offset readings across the gap in the bases were taken automatically as part of the computer program described in Section 4.

(ii) Crack growth was measured by visual observation and the use of a digital vernier caliper on a regular basis.

(iii) Movements on the beam face as the crack progressed were measured using a digital vernier caliper placed on sets of demec pips fixed to the face of the beam.

The total testing program was split into three series of tests as outlined below:-

(a) Series A; beam thickness 100mm,
applied traffic load 810 kPa (max).

(b) Series B; beam thickness 75mm,
applied traffic load 810 kPa (max).

(c) Series C; beam thickness 75mm,
applied traffic load 555 kPa (max) one standard axle.

These three series evaluated not only the performance of the interlayers used but also the effect of thickness on crack growth as well as the accelerating effects of increased traffic loading. For each of these series, testing was conducted on a minimum of eight beams made up of specimens as follows:-

. Control, standard asphaltic concrete x 2

. Polymer modified binder x 2

. Geotextile interlayer x 2

. Geogrid interlayer x 2

The individual results for each beam test were collated and combined in tabular form as presented in Table 6.1. Each of these tabulations was used to plot graphs of crack growth against number of cycles and strain on the beam face against number of cycles. Figures 6.1 and 6.2 represent typical output plots for crack growth and strain against number of cycles. All graphs showing the individual results for each beam are presented in Appendix D.

Subsequent to the test completion each beam was cored and measurements of density taken. The cores were then subjected to mechanical testing in the Nottingham Asphalt Tester (NAT) to measure values of elastic stiffness and deformation resistance, through indirect tensile testing and creep testing respectively. A summary of these mechanical test results together with an explanation of the NAT's operations appear in Appendix A.

6.3.2 Results for Series A

Ten beams of 100mm thickness were tested during this part of the testing program as outlined below:-

- Control x 2
- Control, high tension x 2
- Polymer Modified Binder x 2
- Geotextile x 2
- Geogrid x 2

The control samples tested with a high tensile value were completed to assess the effects of large thermal movements induced in the overlay.

Results of the individual beam tests are summarized in Table 6.2. Figure 6.3 illustrates the averaged curves for each pair of beams tested.

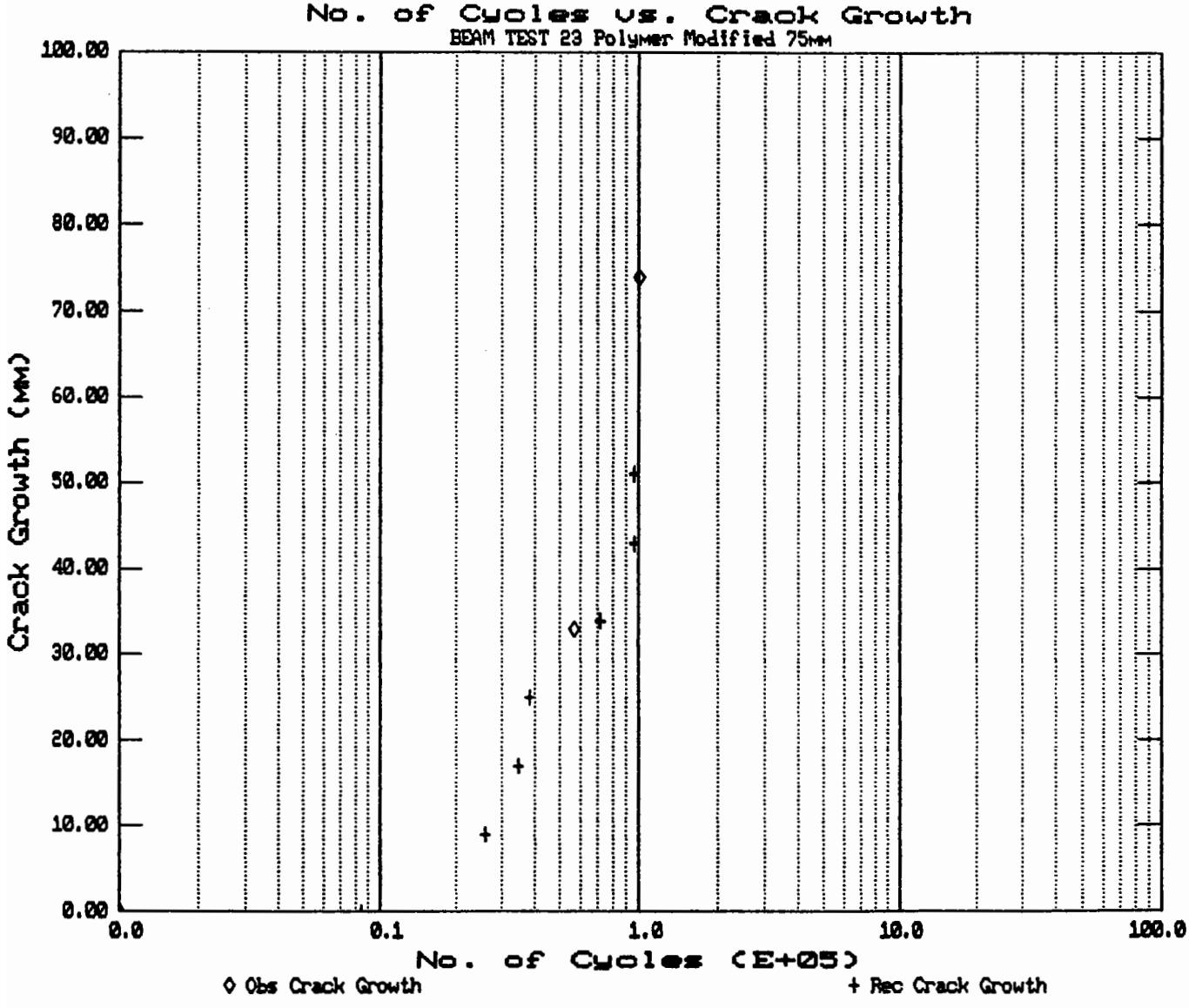

Figure 6.1 Typical Plot of Crack Growth vs Number of Cycles

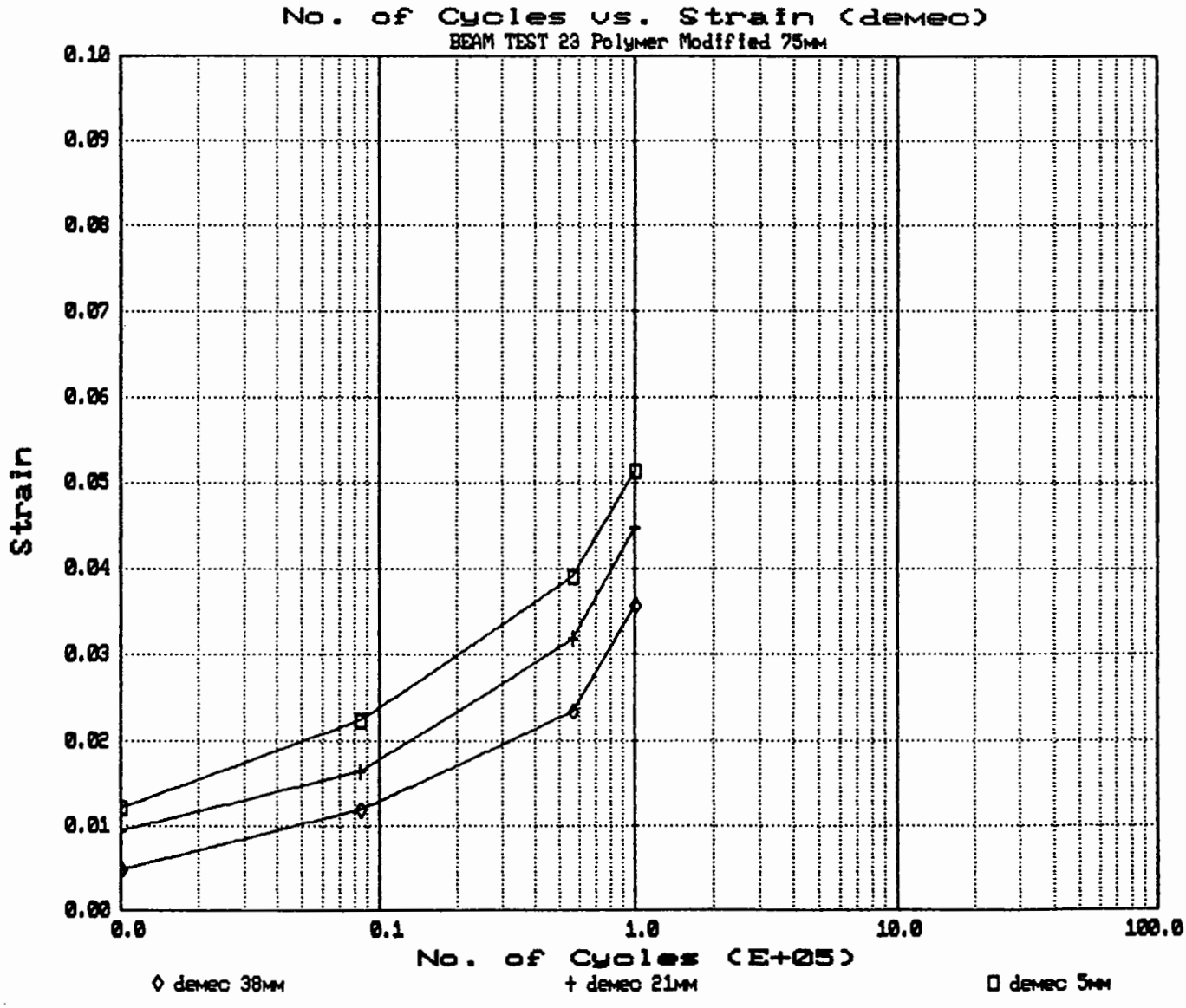

Figure 6.2 Typical Plot of Strain on the Beam Face vs Number of Cycles (Demec Positions Were Measured From the Base of the Asphalt)

Table 6.1 Results of Beam Test 7

				Strip Broken LVDT Reading (mm)				Visual Crack Length		
Load (kN)	No. of Cycles	Demec Readings (mm)	Diff. from Beg.	No.	Crack Length (mm)	Ampl. (mm)	Offset (mm)	Front (mm)	Rear (mm)	Comments
0	0	1. 45.15 2. 45.76 3. 46.24	- - -			0.0	0.0			Initial conditions
4.5	0	1. 45.71 2. 45.92 3. 46.27	0.56 0.16 0.03			0.0	1.17			Tensioning of rubber under dead load
4.5	0	-	-			0.0	0.0			LVDT set to zero
8.3-1.3	1200	-	-	4	0.0	0.005	0.150	0.0	0.0	Strip 4 broken due to araldite from Demec
8.3-1.3	41400	-	-	1	4.0	0.025	1.140			
8.3-1.3	42400	1. 46.96 2. 47.10 3. 46.73	1.81 1.34 0.49				1.180	6.0	10.5	
8.3-1.3	65300	1. 47.37 2. 47.10 3. 46.99	2.22 1.65 0.75				1.56	22.5	15.0	
8.3-1.3	66000	-	-	2	13.0	0.020	1.563			
8.3-1.3	81600	1. 47.53 2. 47.45 3. 46.99	2.38 1.69 0.75				1.773	25.0	45.5	Front face, distress in paint up to 45mm
8.3-1.3	109800	-	-	3	22.5	0.020	2.041			
8.3-1.3	128400	1. 47.93 2. 47.83 3. 47.24	2.78 2.07 1.00				2.183	27.0	46.0	
8.3-1.3	168600	1. 48.73 2. 48.72 3. 47.67	3.58 2.96 1.43				2.803	40.0	51.0	
8.3-1.3	206400	1. 48.98 2. 48.85 3. 47.83	3.83 3.09 1.59				3.027	50.0	71.0	Cracking past strips
8.3-1.3	222000	1. 48.99 2. 48.92 3. 47.87	3.84 3.16 1.63				3.073	50.0	71.0	Crack width 2mm at level of strip 1
FINISHED CYCLING AT THIS POINT										
Totals 8.3-1.3	222000		3.84 3.16 1.63				4.24	50.0	71.0	Crack width at base of AC adj to rubber 4.5mm

Table 6.2 Results of Series A; Beam Test

Treatment Type	Beam No	LVDT Tension & Dead Load (mm)	LVDT Final (mm)	No of Cycles Completed	Crack Length (mm)
Control*	13	2.12	5.22	92,600	90
Control*	14	2.23	4.38	79,600	95
Control	7	1.17	4.24	222,000	71
Control	8	0.36**	3.30	193,000	50
Polymer Modif. Binder	15	1.21	3.09	803,200	60
Polymer Modif. Binder	16	1.33	4.83	981,000	100
Geotextile	11	1.49	3.66	956,400	18
Geotextile	12	1.66	4.30	821,400	19
Geogrid	9	1.93	2.29	1,114,400	0
Geogrid	10	1.33	2.08	1,196,700	15

* large tensile force applied. ** no tension applied.

The cracking observed in both the geogrid and geotextile treated beams consisted of no more than a hair line crack that did not break the crack detection strips.

From the summary curves in Figure 6.3 it is possible to evaluate the relative benefits of modifications to the asphaltic concrete and the effects of increased tension or large thermal movements on asphaltic concrete beam specimens.

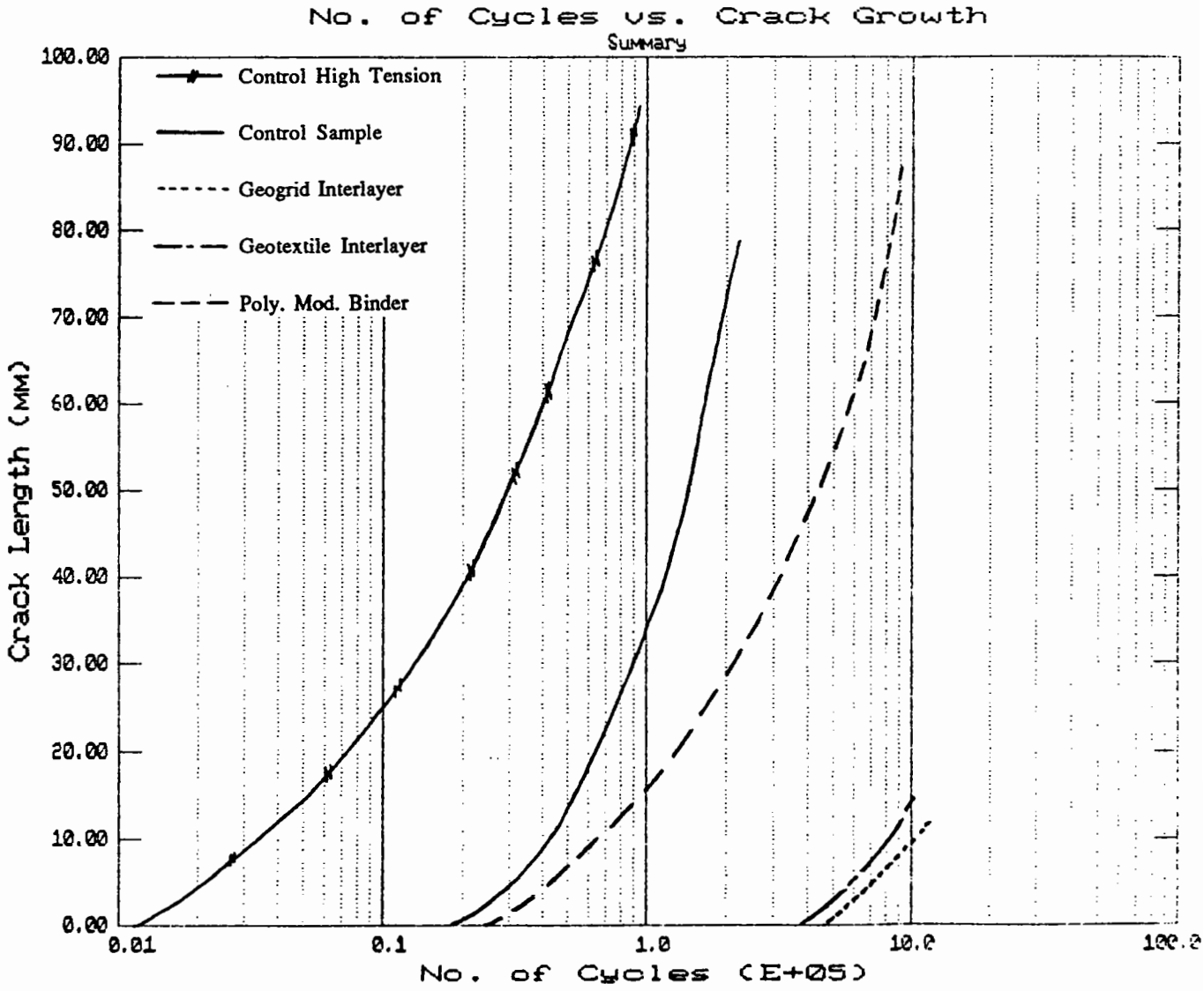

Figure 6.3 Summary Curves of Crack Length vs Number of Cycles for Test Series A , 100mm Asphaltic Concrete, 810 kPa Traffic Load

Table 6.3 expresses the crack growth against number of cycles as a life comparison with the control beams. Geogrid and geotextile interlayer treated beams are not included as the evidence of cracking is not considered significant.

Table 6.3 Comparison of Life for Series A

	Increase in Control Life		
Crack Length (mm)	Control	Control High Tension	Polymer Modified Binder
30	1.0	0.15	2.4
50	1.0	0.20	3.1
75	1.0	0.29	3.6

The increase in tension by a factor of two as previously shown in Table 6.2 produced a decrease in life by a factor of approximately five for the control beams. This result reflects the experiences of maintenance Engineers who claim that a sudden severe cold spell tends to "bring out" reflection cracking in road pavements.

The benefits of a polymer modified binder in an asphaltic concrete mix appear from Table 6.3 to be an increase in life of three times for a control mix.

The final LVDT offsets as shown previously in Table 6.2 can be directly related to the material performance. Geogrids had the lowest offset values even though the initial strain levels imposed were similar to all other treatments.

A representative view from each of the four basic groups of beams can be seen in Plates 6.1 (a), (b) and 6.2 (a), (b). These plates illustrate the cracking patterns observed at the completion of testing.

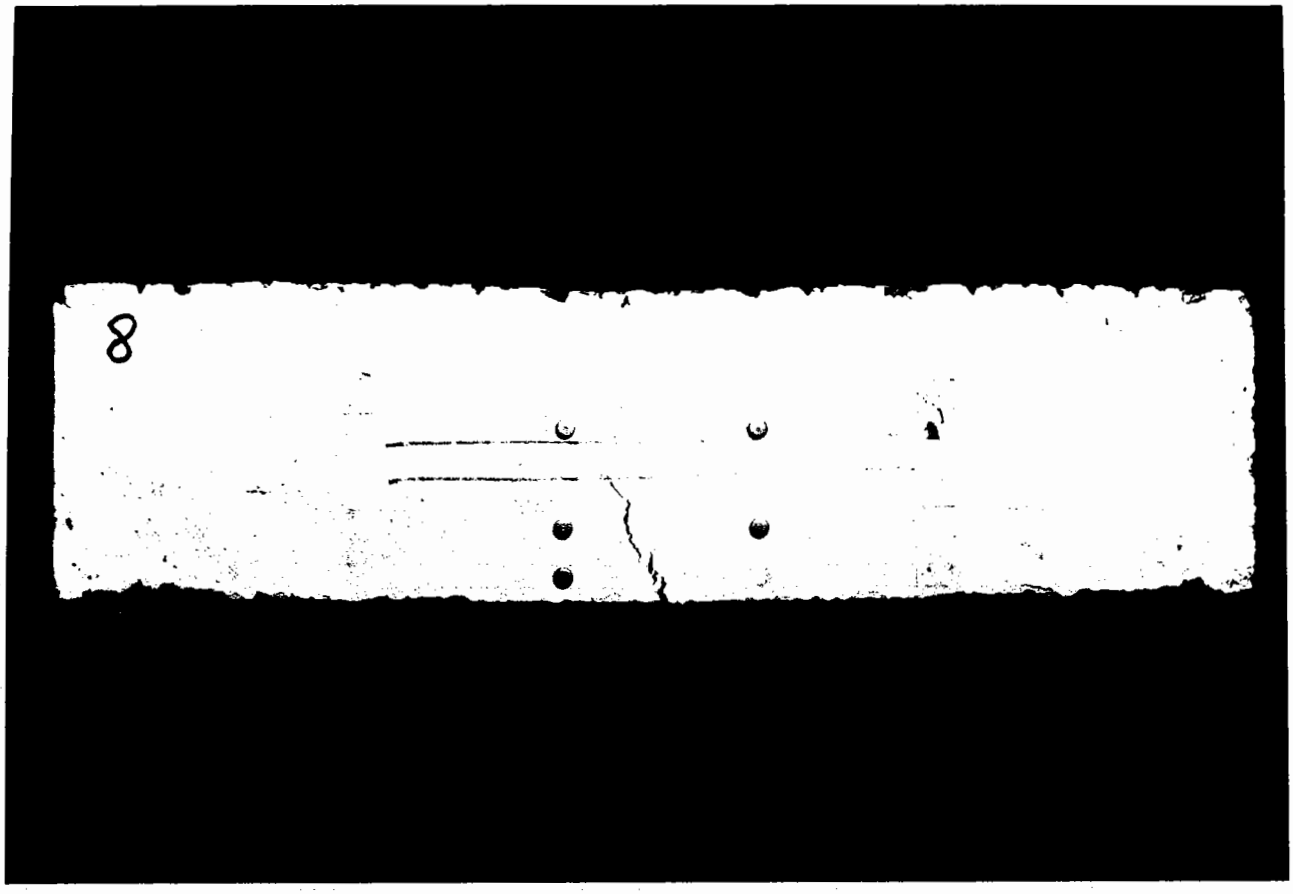

Plate 6.1 (a) Beam Test 8 ; 100mm Control Sample
193,000 Cycles

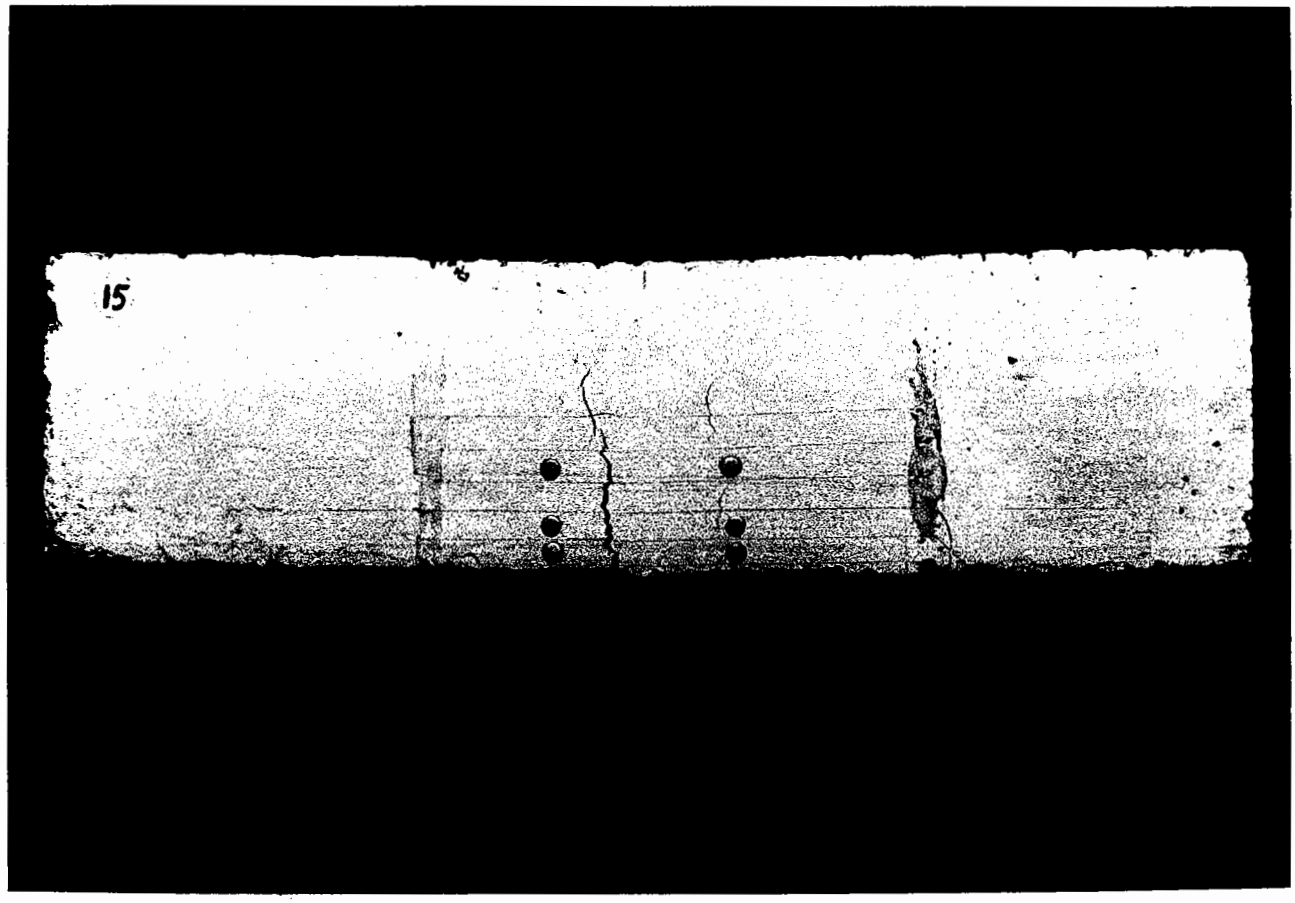

Plate 6.1 (b) Beam Test 15 ; 100mm Polymer Modified Binder
803,200 Cycles

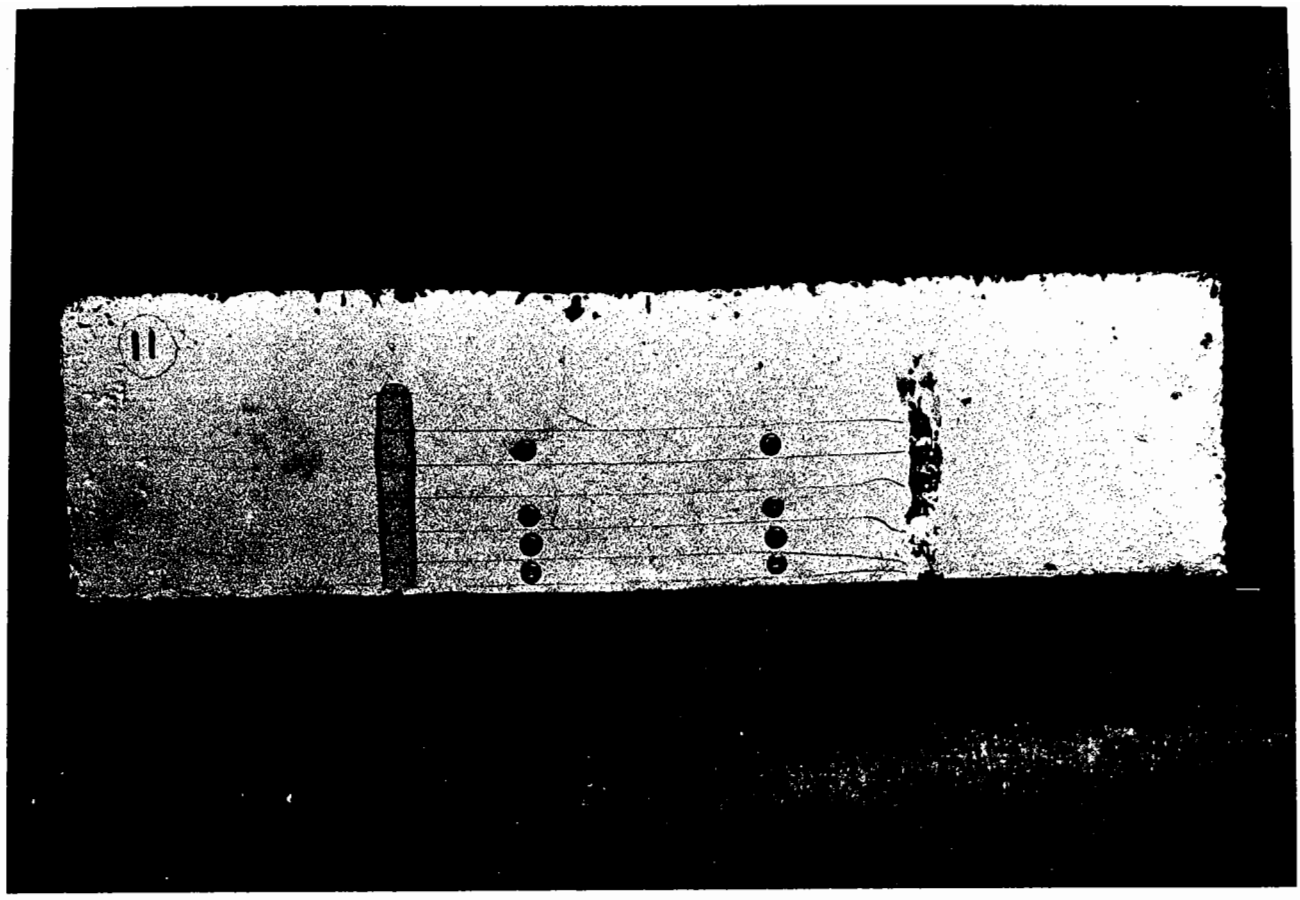

Plate 6.2(a) Beam Test 11 ; 100mm Geotextile Interlayer
956,400 Cycles

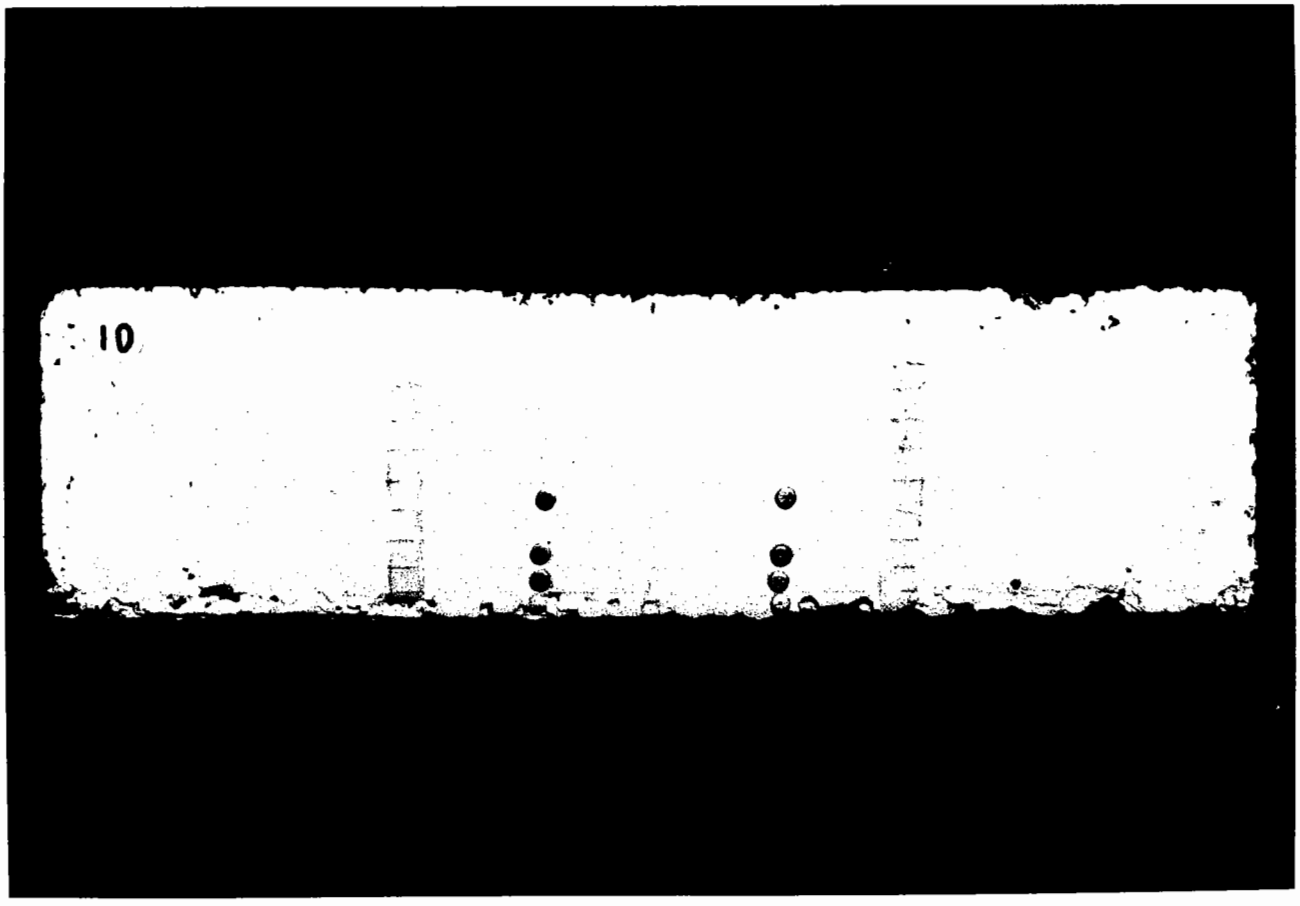

Plate 6.2 (b) Beam Test 10 ; 100mm Geogrid Interlayer
1,196,700 Cycles

6.3.3 Results for Series B

This series of tests was based on a 75mm thickness asphaltic layer and consisted of eight beams as outlined previously in Section 6.3.1. The individual beam test results are presented in Table 6.4 and a visual representation of the averaged crack growth rates can be seen in Figure 6.4.

Table 6.4 Results of Series B; Beam Tests

Treatment Type	Beam No	LVDT Tension & Dead Load (mm)	LVDT Final (mm)	No of Cycles Completed	Crack Length (mm)
Control	19	1.27	4.20	65,000	75
Control	20	1.39	4.19	40,200	75
Polymer Modif. Binder	23	1.42	4.14	100,600	75
Polymer Modif. Binder	24	1.42	5.48	86,000	75
Geotextile	21	1.53	3.77	759,900	75
Geotextile	22	1.42	3.17	785,700	60
Geogrid	17	1.41	1.91	998,000	30
Geogrid	18	1.45	2.06	1,004,000	40

Within this testing group three sets of specimens cracked to full depth, the only exception being the geogrid interlayer beams.

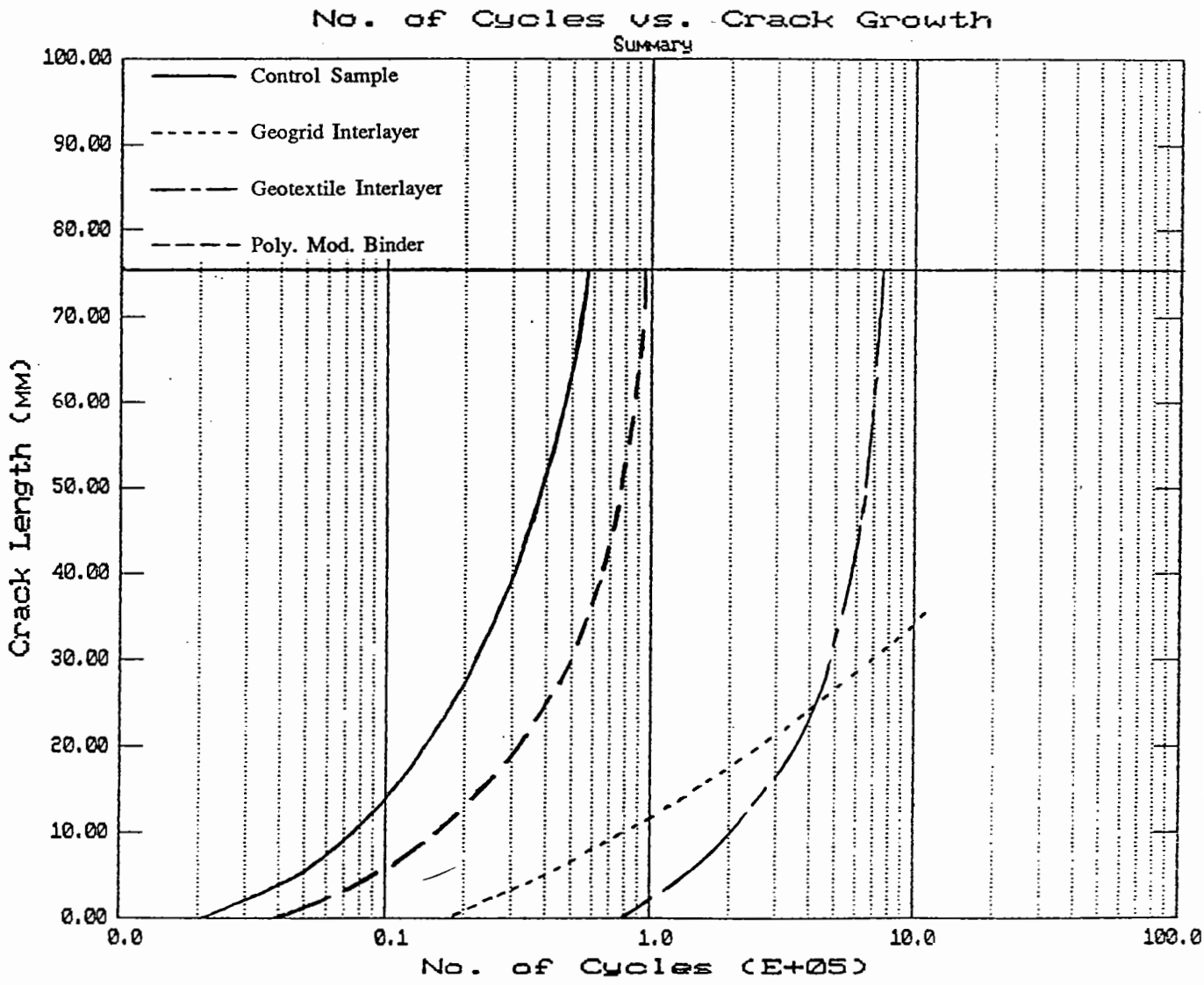

Figure 6.4 Summary Curves of Crack Length vs Number of Cycles for Test Series B, 75mm Asphaltic Concrete, 810 kPa Traffic Load

It can be seen from the plotted curves displayed in Figures 6.3 and 6.4 that a consistent failure pattern exists for the averaged results of beams that cracked to full depth. The geogrid material again did not show extensive crack propagation with an early appearance of cracking due primarily to the presence of a chip seal that had a height of approximately 15mm when the geogrid thickness was taken into account.

Table 6.5 shows a summary of extended lives when compared to the control beams as a function of crack growth and number of cycles.

Table 6.5 Comparison of Life for Series B

	Increase in Control Life			
Crack Length (mm)	Control	Polymer Modified Binder	Geotextile	Geogrid
30	1.0	2.3	22.7	31.8
50	1.0	2.0	17.1	
75	1.0	1.7	13.6	

The increase in lives of the interlayer treatments can be better defined by considering the latter part of the individual crack growth curves. This gave the following average lives as an increase over the control beams

(a) Polymer Modified Binder 2.0

(b) Geotextile 15.0

(c) Geogrid 31.0

The decrease in thickness from 100mm in series A to 75mm in series B had the effect of decreasing the life at a 75mm cracking level from 210,000 cycles to 55,000 cycles in the control samples.Thus it would seem that a 25% increase in thickness gives approximately a 400% increase in life.

No comparisons are able to be made for the interlayer treatments as no significant cracking occurred for the 100mm thick samples after one million cycles.Plates 6.3 and 6.4 illustrate the cracking patterns in representative beams for this series of tests.

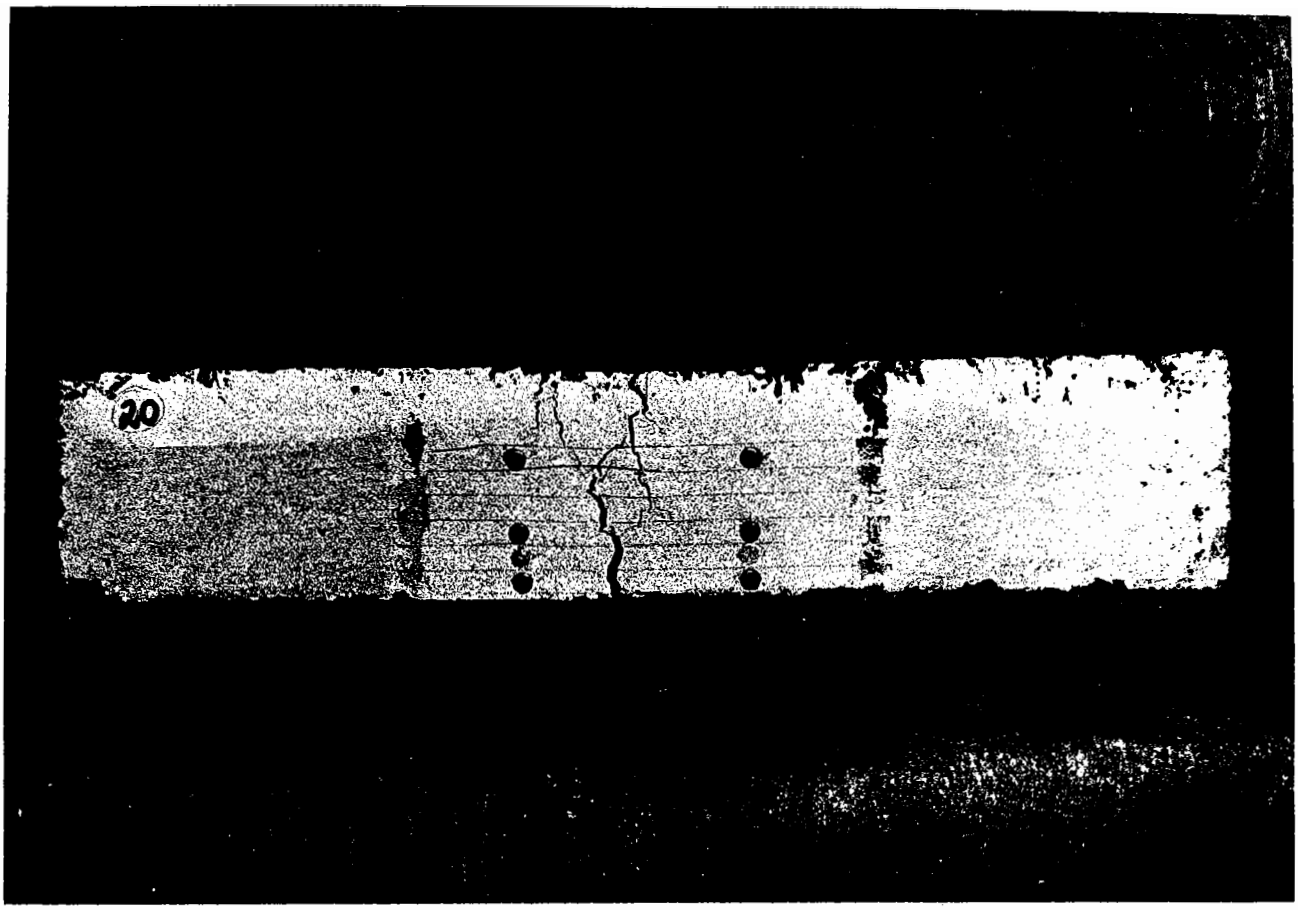

Plate 6.3 (a) Beam Test 20 ; 75mm Control Sample
40,200 Cycles

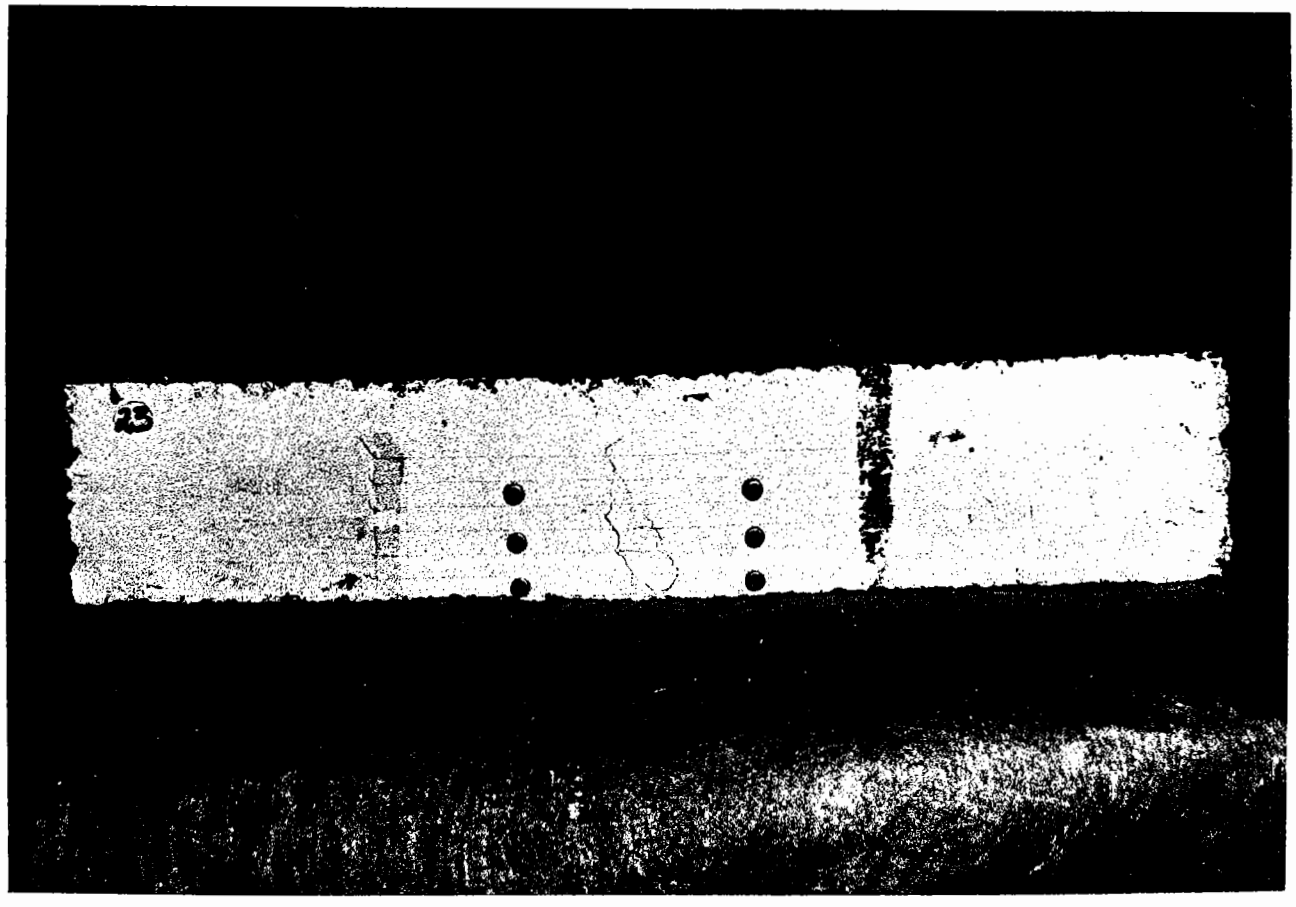

Plate 6.3 (b) Beam Test 23 ; 75mm Polymer Modified Binder
100,600 Cycles

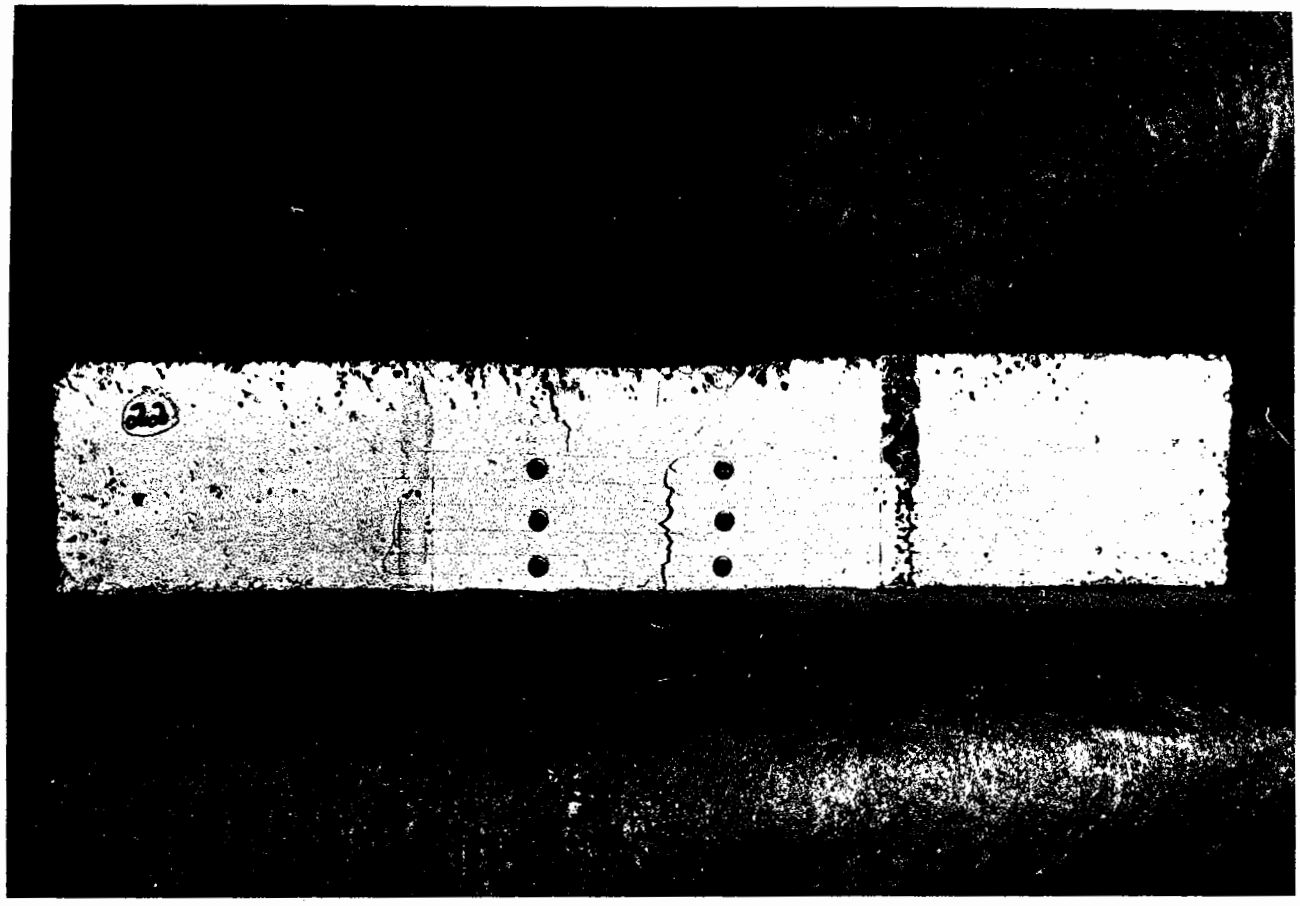

Plate 6.4 (a) Beam Test 22 ; 75mm Geotextile Interlayer
785,700 Cycles

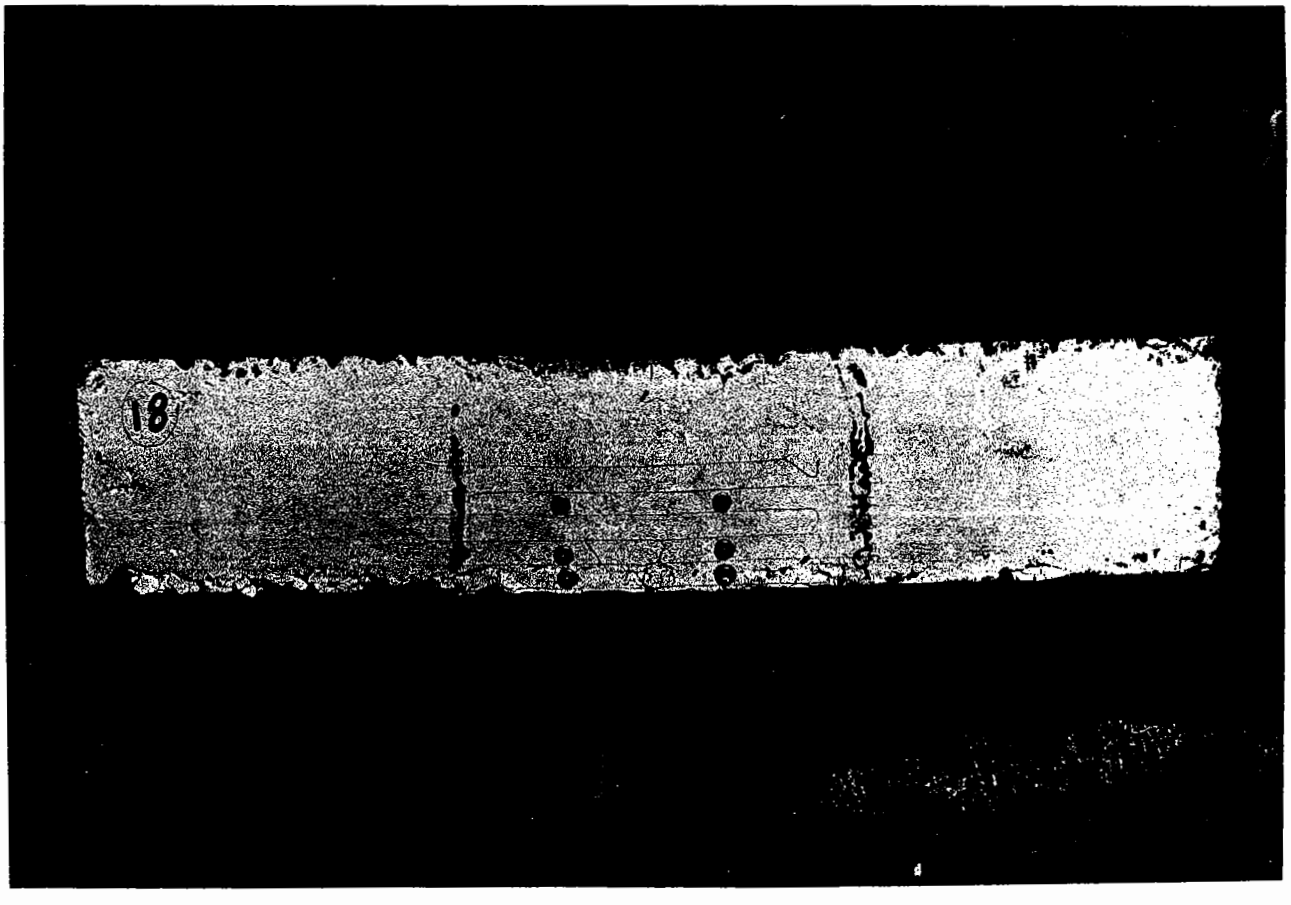

Plate 6.4 (b) Beam Test 18 ; 75mm Geogrid Interlayer
1,004,000 Cycles

6.3.4 Results for Series C

The use of a larger loading platen for this series of tests produced a simulated traffic loading of approximately one standard axle. The results achieved from this testing regime are displayed in Table 6.6.

Table 6.6 Results of Series C; Beam Tests

Treatment Type	Beam No	LVDT Tension & Dead Load (mm)	LVDT Final (mm)	No of Cycles Completed	Crack Length (mm)
Control	25	0.97	3.43	1,562,000	75
Control	26	1.41	3.86	728,300	75
Polymer Modif. Binder	27	1.31	2.47	3,108,700	75
Polymer Modif. Binder	28	1.43	2.64	3,402,500	70
Geotextile	29	1.48	2.46	6,019,300	30
Geotextile	30	1.59	3.32	2,005,000	40
Geogrid	31	1.39	1.90	3,835,000	30
Geogrid	32	1.39	2.01	5,886,200	25

An extensive and lengthy program of testing was conducted for this series of treatments with the total number of cycles in excess of 24.5 million, taking more that 30 continuous days testing to complete. As a consequence of this procedure results have been obtained for crack growth rates that extend to all treatments used. Figure 6.5

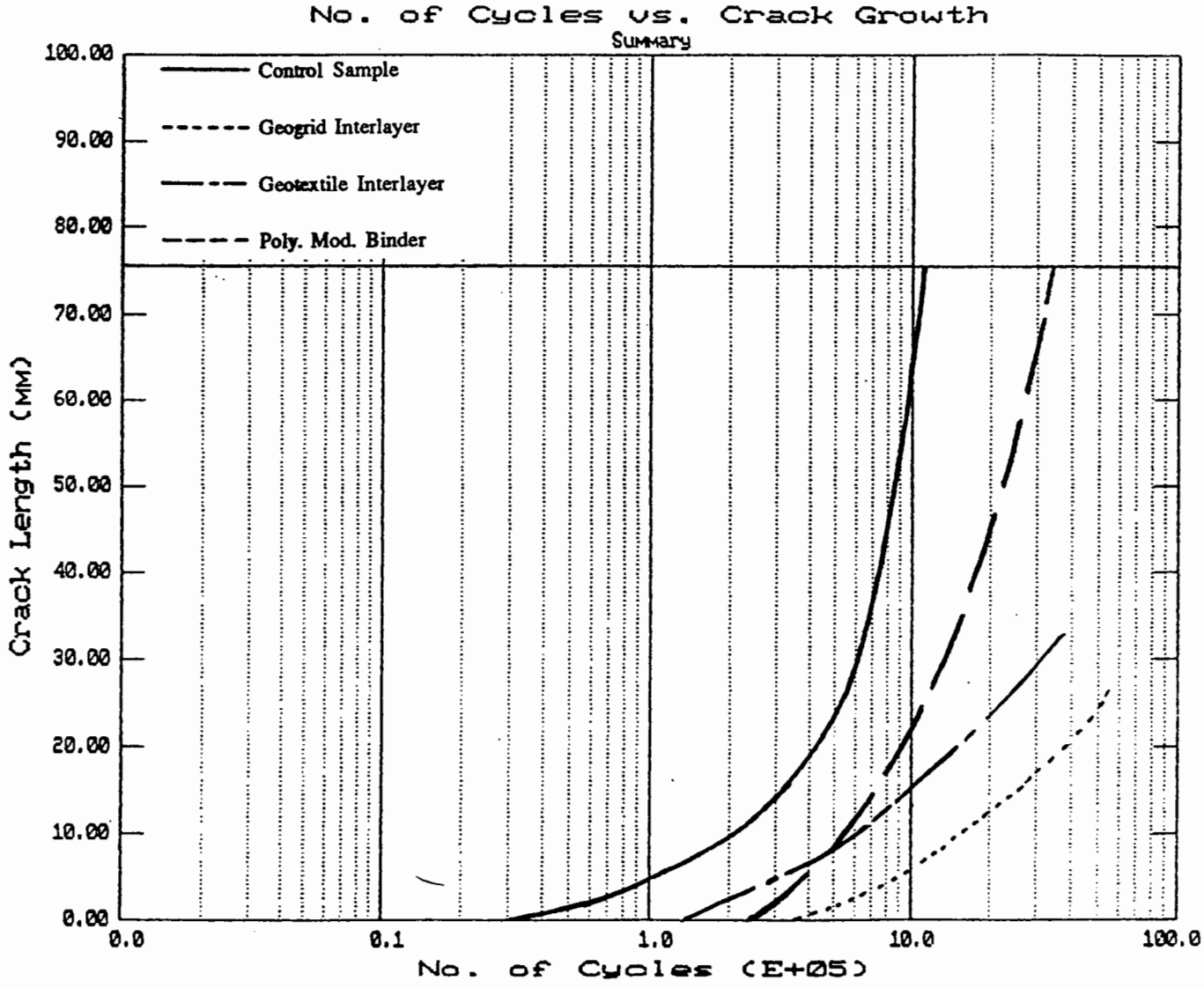

Figure 6.5 Summary Curves of Crack Length vs Number of Cycles for Test Series C, 75mm Asphaltic Concrete, 555 kPa Traffic Load

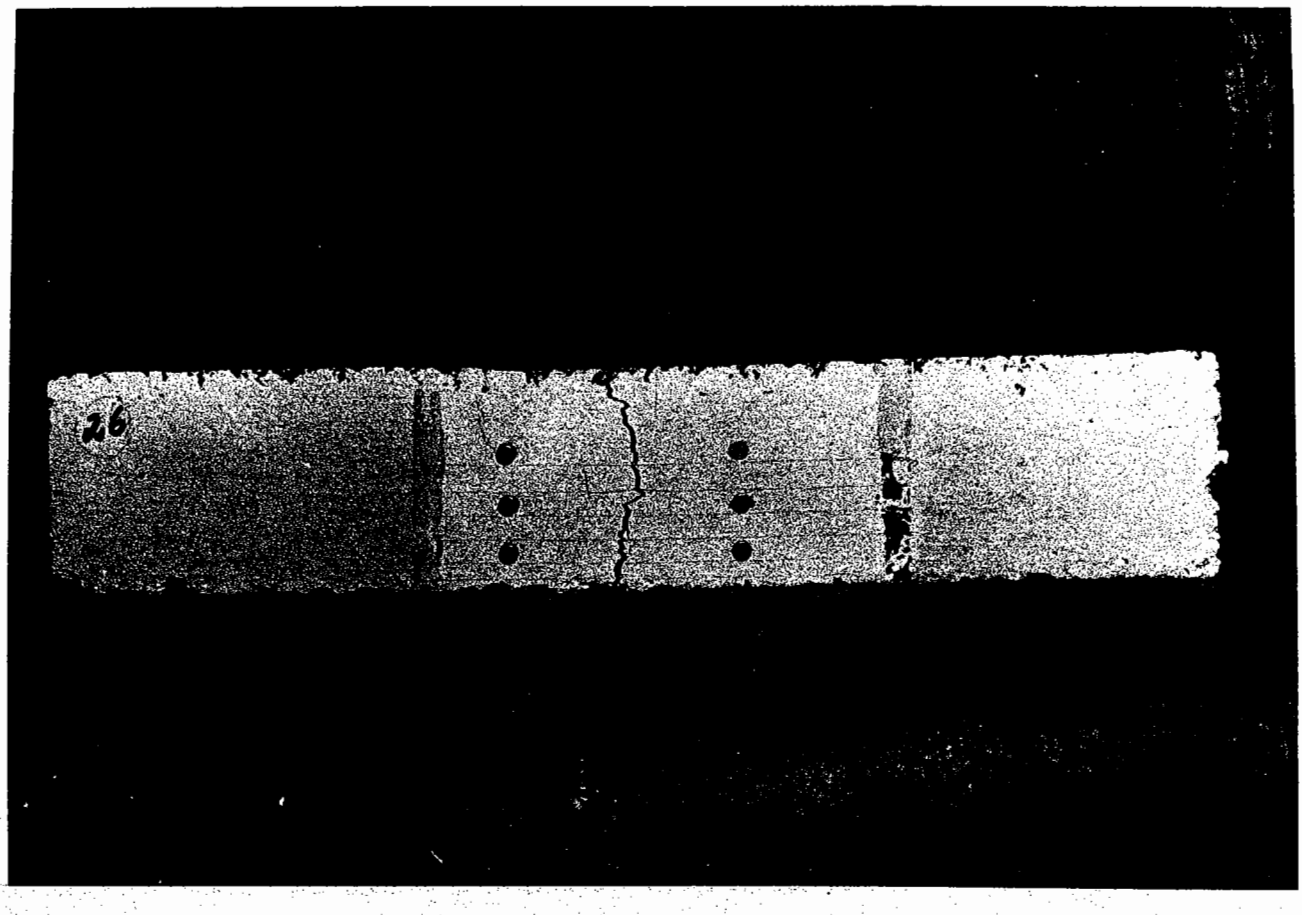

Plate 6.5 (a) Beam Test 26 ; 75mm Control Sample
728,300 Cycles

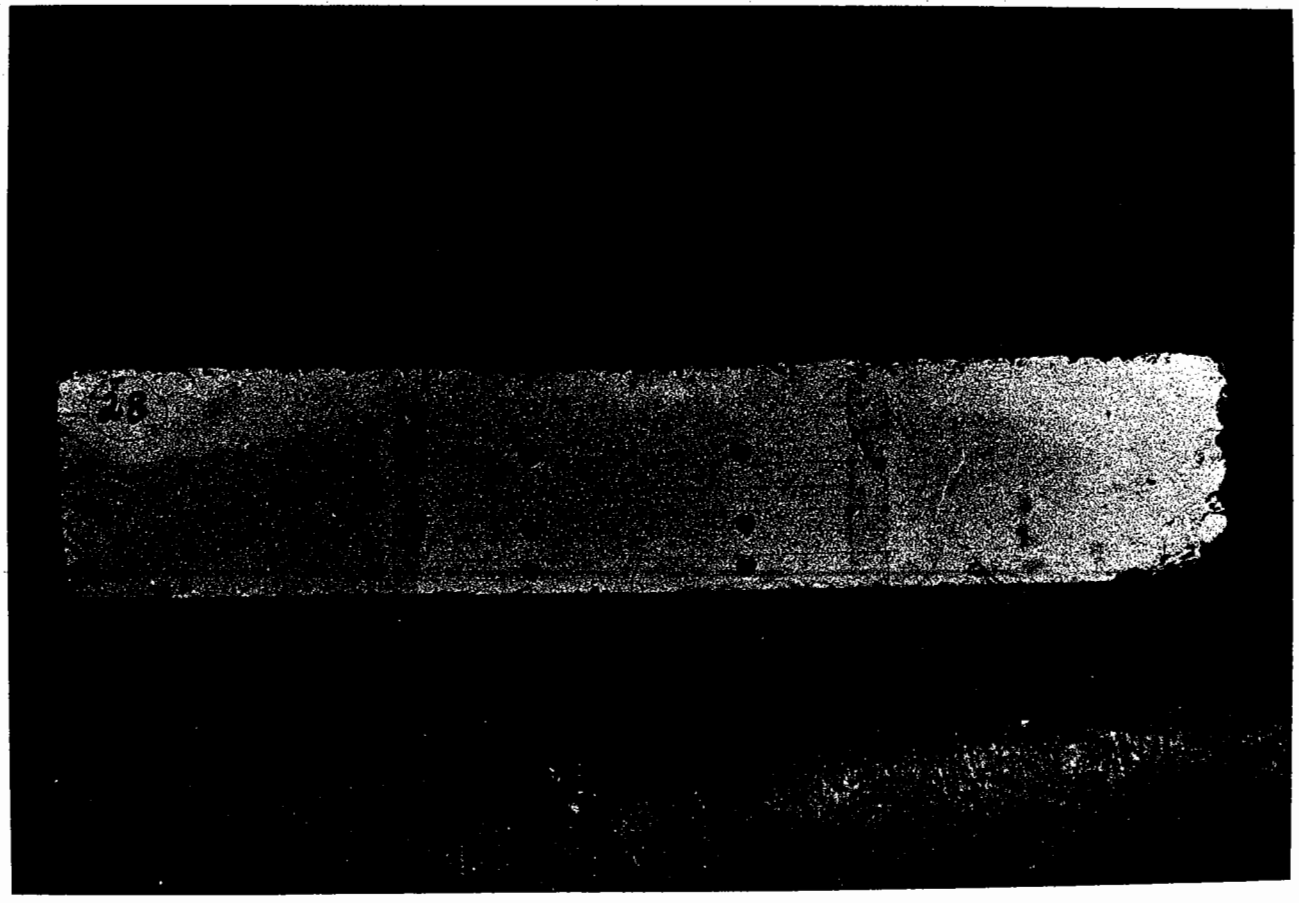

Plate 6.5 (b) Beam Test 28 ; 75mm Polymer Modified Binder
3,402,500 Cycles

shows the averaged resultant curves for crack growth rate against number of load cycles for series C.

A similar pattern of crack growth through the asphaltic concrete control section and polymer modified binder treatment has been seen previously in Figures 6.3 and 6.4. The increase in life for interlayer treatments is expressed in terms of control sample life in Table 6.7.

Table 6.7 Comparison of Life for Series C

	Increase in Control Life			
Crack Length (mm)	Control	Polymer Modified Binder	Geotextile	Geogrid
30	1.0	2.3	5.2	10.0
50	1.0	2.6	17.1	
75	1.0	3.2	13.6	

This series of tests conducted with simulated traffic loads approximating one standard axle gave lives that can be considered to best approximate field conditions.

Plates 6.5 and 6.6 illustrate typical cracking patterns for beams tested in series C.

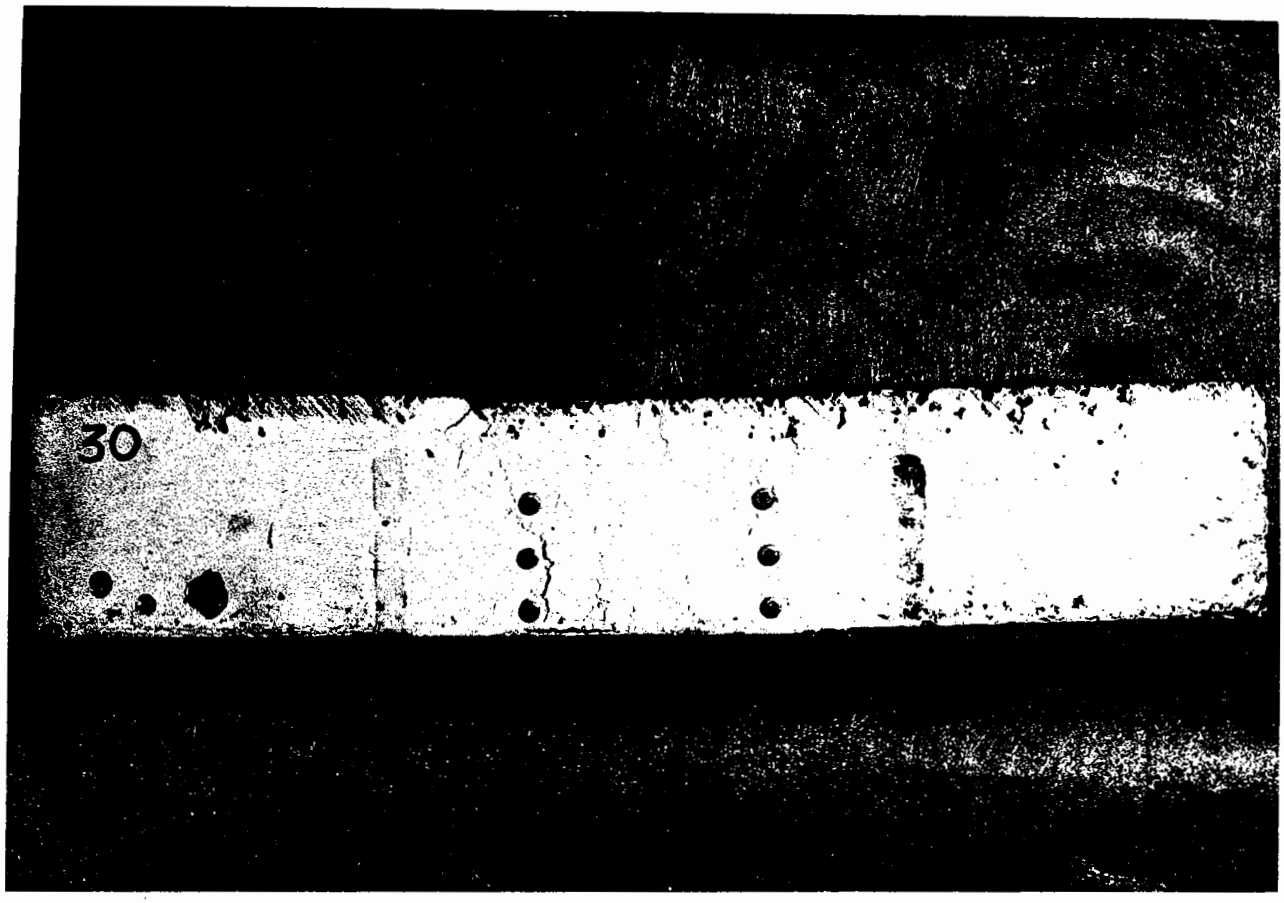

Plate 6.6 (a) Beam Test 30 ; 75mm Geotextile Interlayer
2,005,000 Cycles

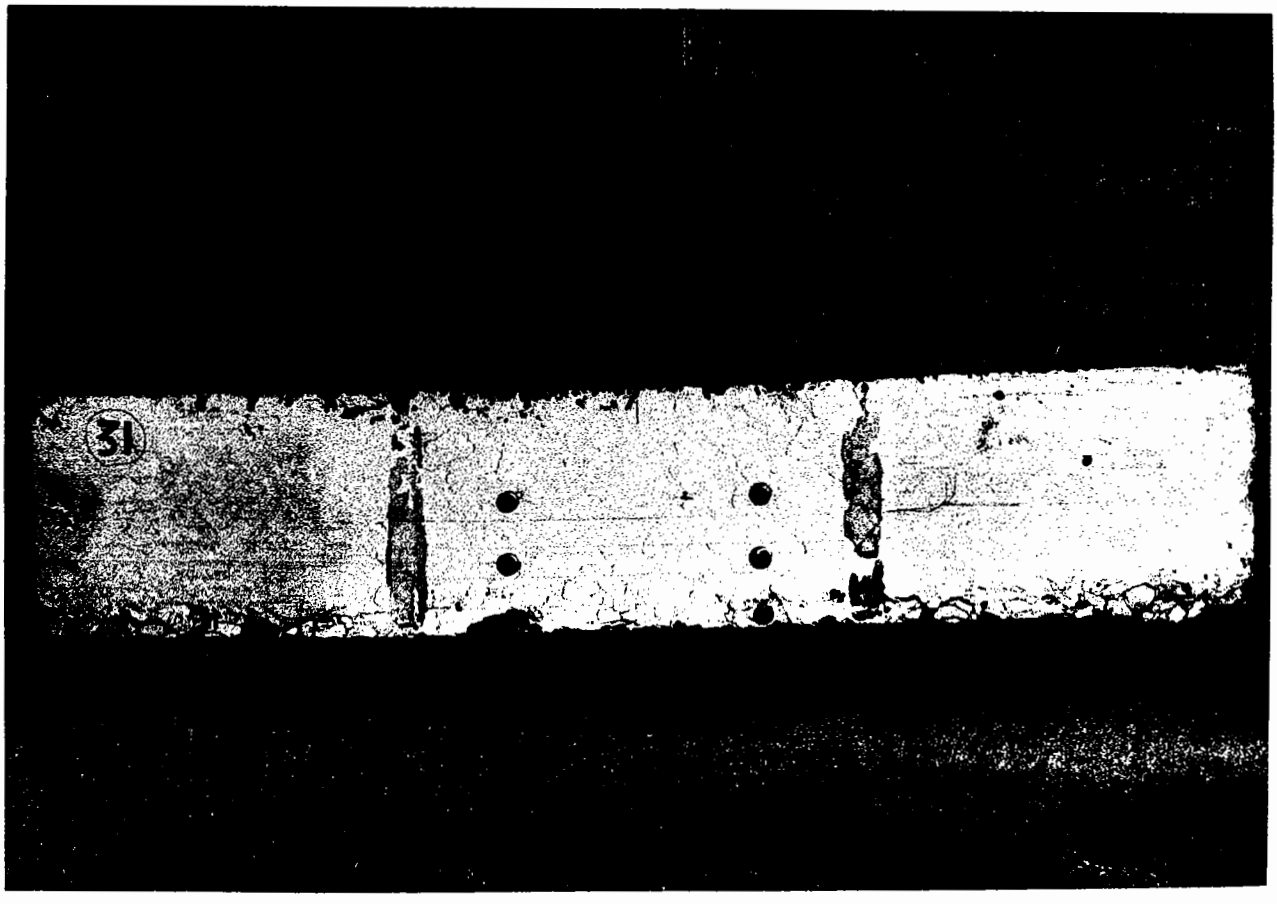

Plate 6.6 (b) Beam Test 31 ; 75mm Geogrid Interlayer
3,835,000 Cycles

6.3.5 Summary of Test Results

To satisfy the aim of this series of experiments a clear measure of relative performance between the different treatments used to inhibit the propagation of reflection cracking through asphaltic concrete overlays must be obtained.

A comparison of the number of cycles to failure for each test series can be seen in Table 6.8. Table 6.9 contains a summary of relative lives obtained for each test series. An entire summary of raw data from all three test series is contained in Table 6.10.

Table 6.8 Comparison of Summary Curves for Series A, B and C

	Number of Cycles (x 10^6)										
Crack Length (mm)	Series B 75mm				Series A 100mm				Series C 75mm Red. Stress			
	Control	Ply Md	Geotex	Geogrid	Control	Ply Md	Geotex	Geogrid	Control	Ply Md	Geotex	Geogrid
10	0.007	0.015	0.20	0.08	0.032	0.066	no significant cracking		0.22	0.59	0.65	1.80
20	0.015	0.035	0.35	0.28	0.062	0.13			0.44	0.95	1.6	3.9
30	0.022	0.050	0.50	0.70	0.088	0.21			0.60	1.4	3.1	6.0
40	0.030	0.065	0.58		0.11	0.30			0.72	1.8		
50	0.038	0.077	0.65		0.14	0.44			0.86	2.2		
75	0.055	0.095	0.75		0.21	0.76			1.1	3.5		

Table 6.9 Percentage Comparison of Life for Series A, B and C

	% of Control Life for Each Series										
Crack Length (mm)	Series B 75mm				Series A 100mm				Series C 75mm Red. Stress			
	Control	Ply Md	Geotex	Geogrid	Control	Ply Md	Geotext	Geogrid	Control	Ply Md	Geotex	Geogrid
10	1.00	2.1	28.6	11.4	1.00	2.1	no significant cracking		100	2.7	3.0	8.2
20	10.0	2.3	23.3	18.7	1.00	2.1			100	2.2	3.6	8.9
30	1.00	2.3	22.7	31.8	1.00	2.4			1.00	2.3	5.2	10.0
40	1.00	2.2	19.3		1.00	2.7			1.00	2.5		
50	1.00	2.0	17.1		1.00	3.1			1.00	2.6		
75	1.00	1.7	13.6		1.00	3.6			1.00	3.2		

TABLE 6.10 SUMMARY OF TEST DATA FROM BEAM SPECIMENS

	Series A 100mm Thickness, Load 810 kPa					Series B 75mm Thickness, Load 810 kPa					Series C 75mm Thickness, Loads 555 kPa				
Interlayer Type	Beam No.	LVDT Tension & Dead Load (mm)	LVDT Final (mm)	No. of Cycles Completed ($x10^6$)	Crack Length (mm)	Beam No.	LVDT Tension & Dead Load (mm)	LVDT Final (mm)	No. of Cycles Completed ($x10^6$)	Crack Length (mm)	Beam No.	LVDT Tension & Dead Load (mm)	LVDT Final (mm)	No. of Cycles Completed ($x10^6$)	Crack Length (mm)
Control	7	1.17	4.24	0.22	71	19	1.27	4.20	0.065	75	25	0.97	3.43	1.56	75
Control	8	0.36*	3.30	0.19	50	20	1.39	4.19	0.42	75	26	1.41	3.86	0.73	75
Polymer Mod. Binder	15	1.21	3.09	0.80	60	23	1.42	4.14	0.10	75	27	1.31	2.47	3.11	75
Polymer Mod. Binder	16	1.33	4.83	0.98	100	24	1.42	5.48	0.086	75	28	1.43	2.64	3.40	70
Geotextile	11	1.49	3.66	0.96	10	21	1.53	3.77	0.76	75	29	1.48	2.46	6.02	30
Geotextile	12	1.66	4.30	0.82	18	22	1.42	3.17	0.79	60	30	1.59	3.32	2.01	40
Geogrid	9	1.93	2.29	1.11	0	17	1.41	1.91	1.00	30	31	1.39	1.90	3.84	30
Geogrid	10	1.33	2.08	1.20	15	18	1.45	2.06	1.01	40	32	1.39	2.01	5.89	25

* no tension.

A summary of treatment performance related to an increase in life over the equivalent control beams for each series is presented in Table 6.11.

Table 6.11 Performance Relative to a Control Beam for all Three Test Series

	Increase in Control Life		
Treatment Type	Series C	Series B	Series A
Polymer Modified Binder	2.8	2.0	3.0
Geotextile	5.0	15.0	N/A
Geogrid	10.0	31.0	N/A

Series C provided the closest approximation to field conditions through the use of a 555 kPa load simulating one standard axle. To actually complete such an intensive program at the lower loading regime took a significant period of time. The accelerating effects of increasing the simulated traffic loading to 810 kPa gave a three fold increase in performance for the interlayer treatments over a similar control section. The ability to successfully accelerate the testing program allowed all three series to be completed within the time allowed.

The polymer modified binder asphaltic beam results show that the increase in life over a control section remained within the range 2.0 - 3.0 for all three test series. Figure 6.6 is a plot of crack growth against number of load cycles for tests conducted in all three series. The first 30 mm of cracking has for most tests been left out for clarity.

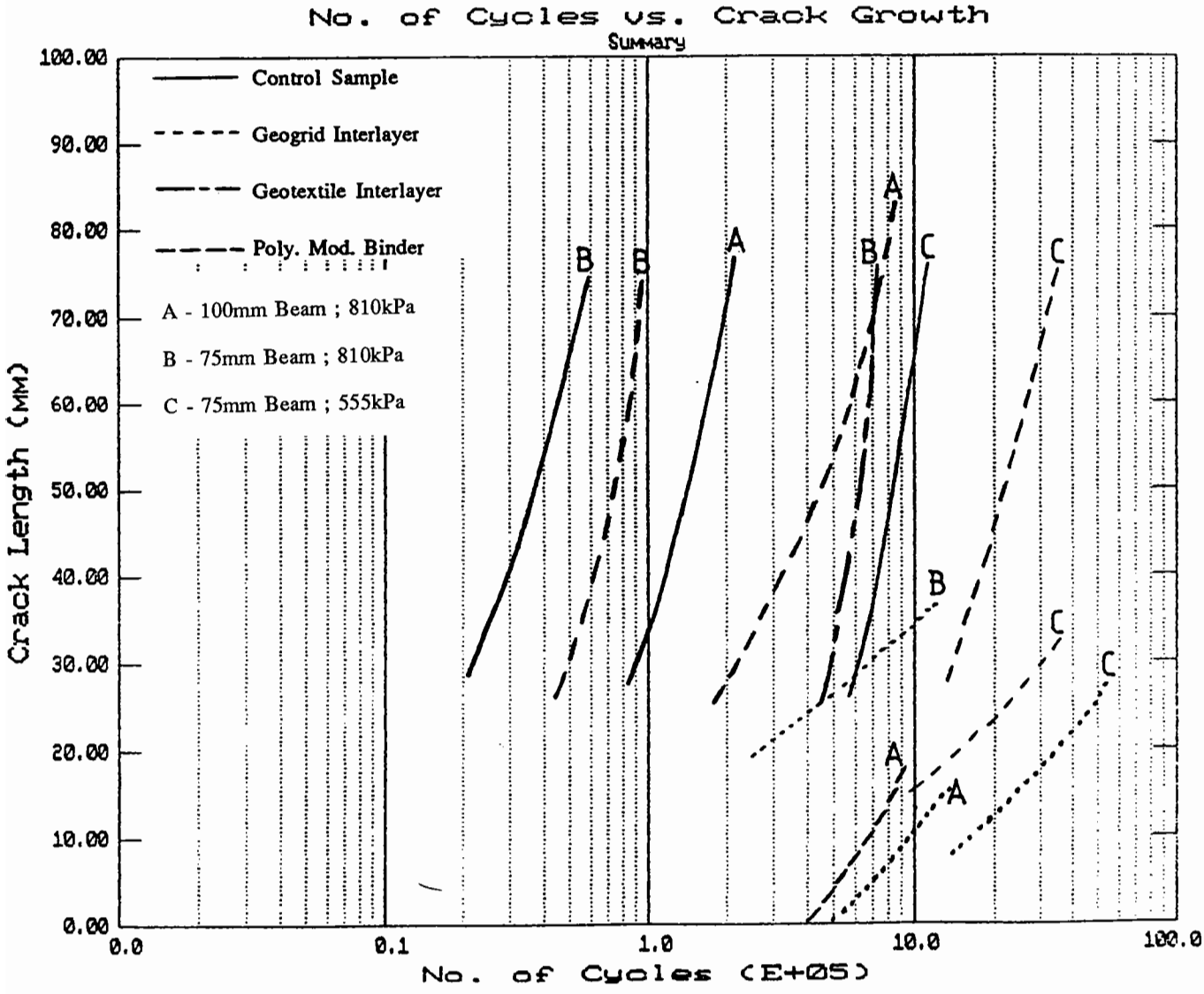

Figure 6.6 Summary Plots for all Testing Series,

Crack Length vs Number of Cycles

The results of density testing on cores taken from 30 beams gave an average air voids volume of 3.5%. The range of air voids was 2.0% - 6.6%. While these values are on the lower end of the specified standard (11.09, MRD (48)) they are never the less within the target range. Results of mechanical testing on all cores is presented in Appendix A. The mean value obtained for elastic stiffness was 4422 MPa with a standard deviation of 950 MPa.

6.4 CONCLUSIONS

Several trends have been established during the course of testing beam specimens. The following summary covers these areas:

(1) A doubling in the tension force or thermal load to the specimens resulted in a reduction of overlay life by a factor of five for control beams.

(2) An increase in asphaltic concrete thickness of 25% produced a corresponding increase in life for control beams of 400%.

(3) Asphaltic beams with geotextile interlayers had a life five times that of an equivalent control section.

(4) Asphaltic beams with geogrid interlayers had a life ten times that of an equivalent control section.

(5) Asphaltic concrete with a polymer modified (SBS) binder had an increase in life of 2.0-3.0 times that of an equivalent control section.

(6) Acceleration of the testing process by increasing the traffic induced loads can be successfully completed yielding meaningful results.

(7) Increasing the simulated traffic loading from 555 kPa to 810 kPa produced a three fold increase in the life of asphaltic concrete beams with geotextile or geogrid interlayers when compared to an equivalent control section.

(8) No increase in life for the polymer modified binder treatment relative to equivalent control sections was found for accelerated loading tests, thus indicating that the tensile strength of the interlayers had a marked effect on their performance under greater loads.

In a realistic pavement situation with a 20 year design life of 1 x 10^7 equivalent standard axles (ESA's) representing 720 vehicles per day, the results of this testing program predict that an ordinary asphaltic concrete overlay of 75mm thickness, on a cracked pavement, would last $1.1x10^6$ cycles of a standard axle which corresponds to 4 years life. Experience in field trials with 75mm thickness overlays is limited, however, information is available for 50mm thick overlays.

Reflection cracking through a 50mm overlay on top of a typical 350mm thick cement treated base pavement with 50mm of existing asphaltic material generally takes 1 to 1.5 years to reach the overlay surface, under environmental conditions that are similar to those in Queensland, Australia.

The summary performance curve for series C, indicated that a reduction in thickness of a 75mm overlay (1.1 x 10^6 cycles) by 25mm would give a life of approximately 0.28 x 10^6 cycles for full depth cracking. This corresponds to 1.1 years of overlay life which is in agreement with field observations. It would appear from this rough example that the testing arrangement developed has the capabilities of mirroring field conditions.

Further refinement of this process would obviously be required before any quantitative statements can be made, however this demonstration indicates that the combined effects of thermal and simulated traffic loads gave a close approximation to field conditions.

CHAPTER 7

SLAB TESTING

7.1 INTRODUCTION

The aim of conducting a series of laboratory experiments using the slab test facility was to correlate the results obtained from beam testing to a moving wheel arrangement which has the capability of inducing shear stresses around a predefined gap.

The slab testing arrangement as previously illustrated in Figure 4.20 consisted of a wheel moving on a pivoted loading carriage that traversed a specimen placed on a steel pallet 1.22m x 1.22m in area resting on four load cells.

This basic testing configuration had been used by Hughes (44) and Guo et al (54) to conduct tests assessing the relative performance of asphaltic concrete materials resistance to reflection cracking. Problems with debonding and sample hogging were evidenced by both researchers.

7.2 TEST RESULTS

The testing program for the slab test facility was initially based on the completion of the following tests:-

. Geogrid and control section in a single slab x 2

. Geotextile and control section in a single slab x 2

. Polymer modified binder and control section in a single slab x 2

However due to the problems experienced with debonding the following slabs were constructed and tested.

. Geogrid and control sections in a single slab. x 1

- Geotextile and control sections in a single slab. x 1
- Polymer modified binder and control sections in a single slab. x 1
- Control slab, 1 gap. x 1
- Geotextile interlayer slab, 1 gap. x 1

Slabs were originally produced with two crack gap initiators which were formed using steel spacers 10mm in width. The bases for this test were high quality plywood boards 18mm thick with P40 grade emery paper affixed to the upper surface. Interlayer treatments were placed on one half of the slab bases in accordance with manufacturers recommendations, in the same fashion as for beam tests.

The steel mould dimensions were 1.22m long x 0.6m in width x 0.075m thickness. Mixing for the slabs was carried out in accordance with the method established in Section 3.4. Great care was taken during the placement operation to avoid segregation of the mix. A small single drum vibratory roller was used to compact the mix with all areas receiving the same compactive effort. Cores were taken from all slabs at the completion of testing and the percentage of air voids obtained.

The average value of air voids for the slab tests was 9.5% with all results falling within a range of 8% - 12%. These results are slightly higher than would be expected for an overlay on a construction project but are quite acceptable for slab testing purposes.

Slab Test One incorporating a geogrid interlayer and control section completed 40,000 cycles of a 315kPa load with the results shown in Table 7.1.Debonding in both sections began after approximately 2000 cycles despite the presence of end restraints. Debonding in the specimen continued to extend until the test was terminated. The debonded length either side of the gap for both sections at the completion of the test was approximately 150-250mm.

Table 7.1 Results of Slab Test One

	LVDT Reading Amplitude (mm)		Observed Crack Growth (mm)	
Number of Cycles	Control	Geogrid	Control	Geogrid
613	0.36	0.27	0	0
4740	0.39	0.29	5	0
16110	0.32	0.20	10	5
19555	0.33	0.20	15	5
24630	0.37	0.20	15	5
40002	0.40	0.20	15	10

Some evidence of a delay in crack growth was recorded for the geogrid interlayer treatment however this was masked by the debonding problems experienced. Plate 7.1 (a) shows the cracking recorded in the geogrid section, also visible is the debonding over an extended length. Plate 7.1 (b) is a view of the control section in which vertical cracking and debonding can be seen.

Plate 7.2 (a) illustrates the base of the overlay after the timber bases were removed. The difference between the geogrid and control sections is clearly visible. Plate 7.2 (b) shows two typical cores taken after the completion of testing.

Plate 7.1 (a) Crack Patterns in Geogrid Section of Test Slab One

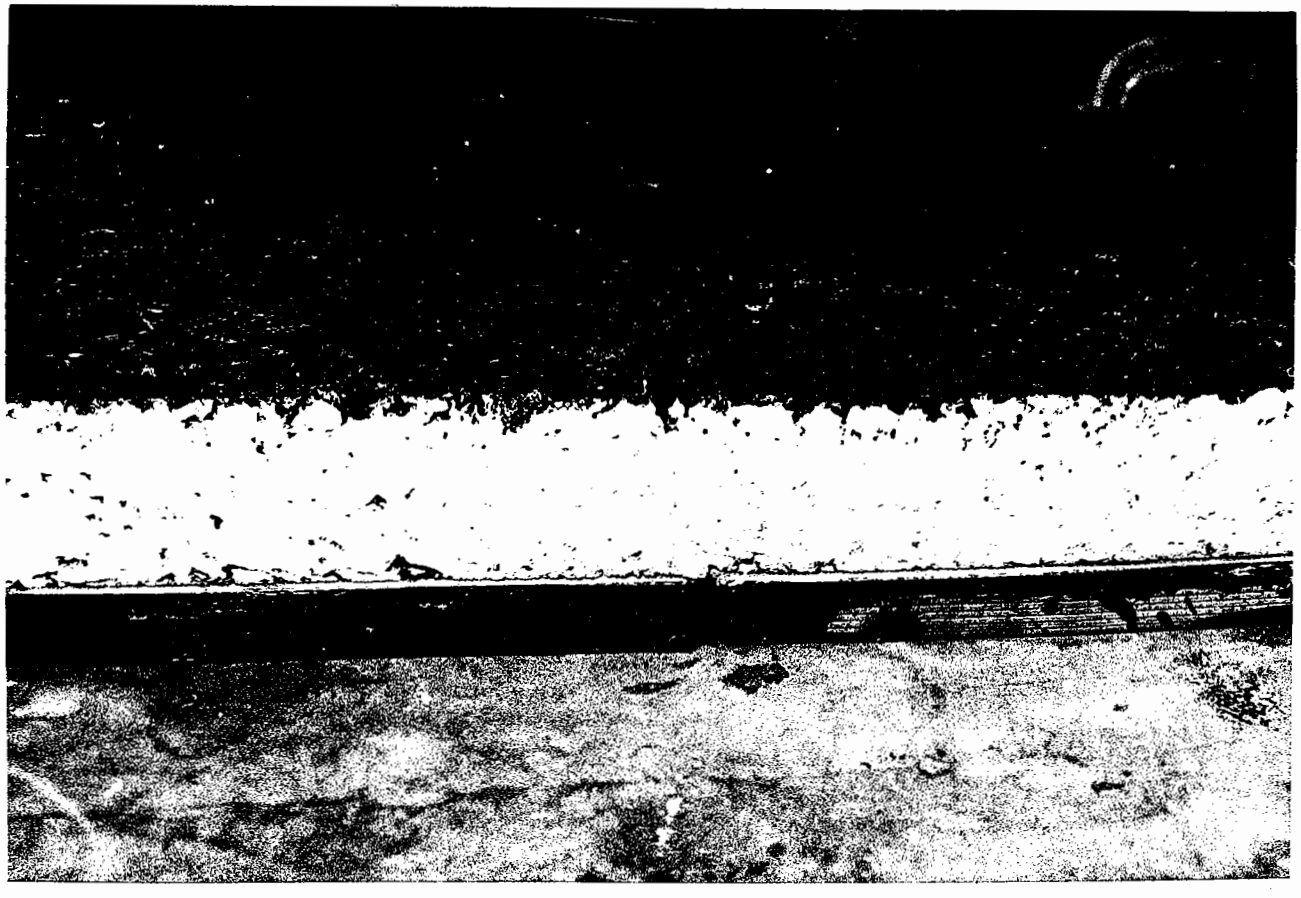

Plate 7.1 (b) Crack Patterns in Control Section of Test Slab One

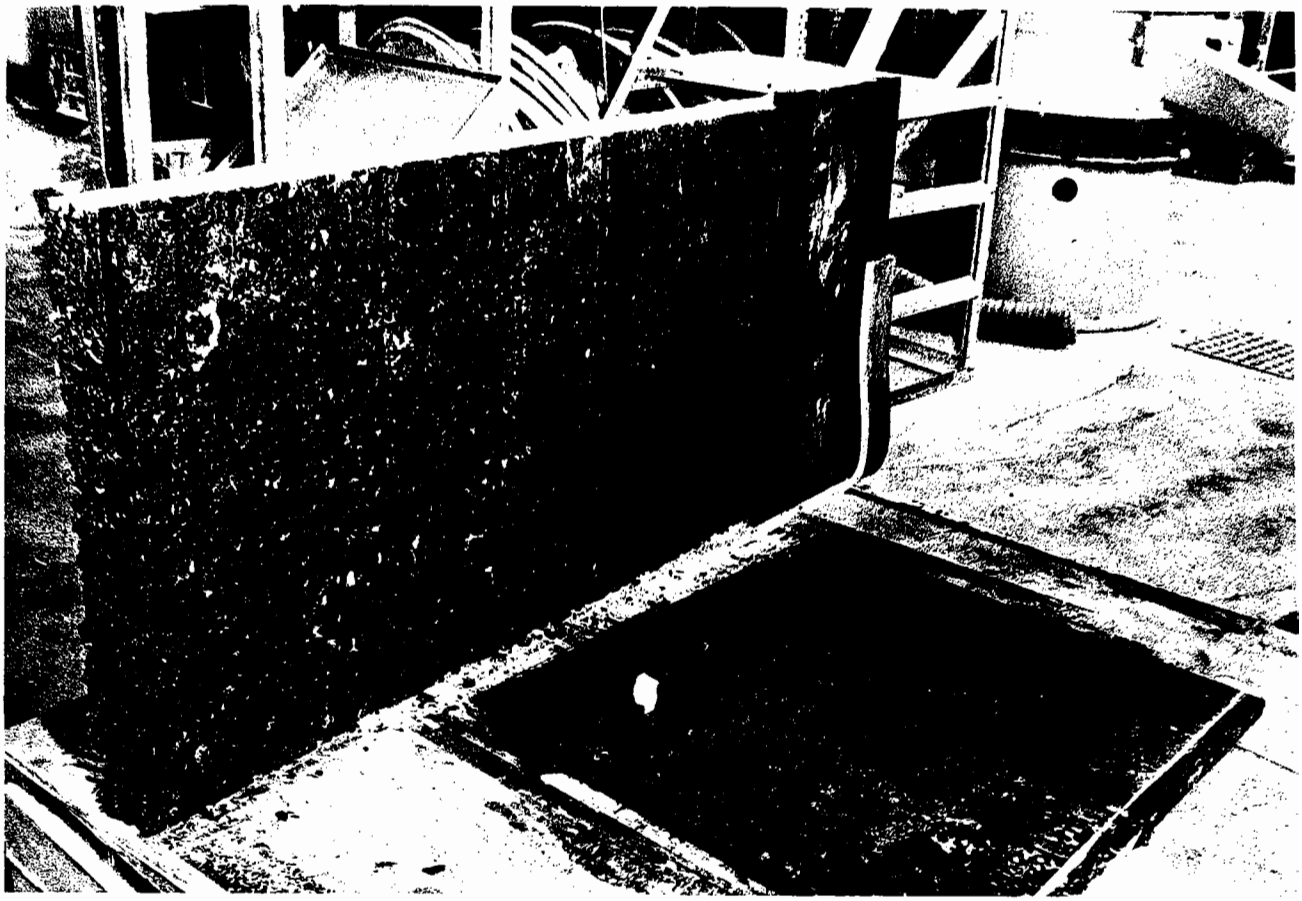

Plate 7.2 (a) Removal of Timber Bases Reveals a Clear Distinction Between Adjacent Sections

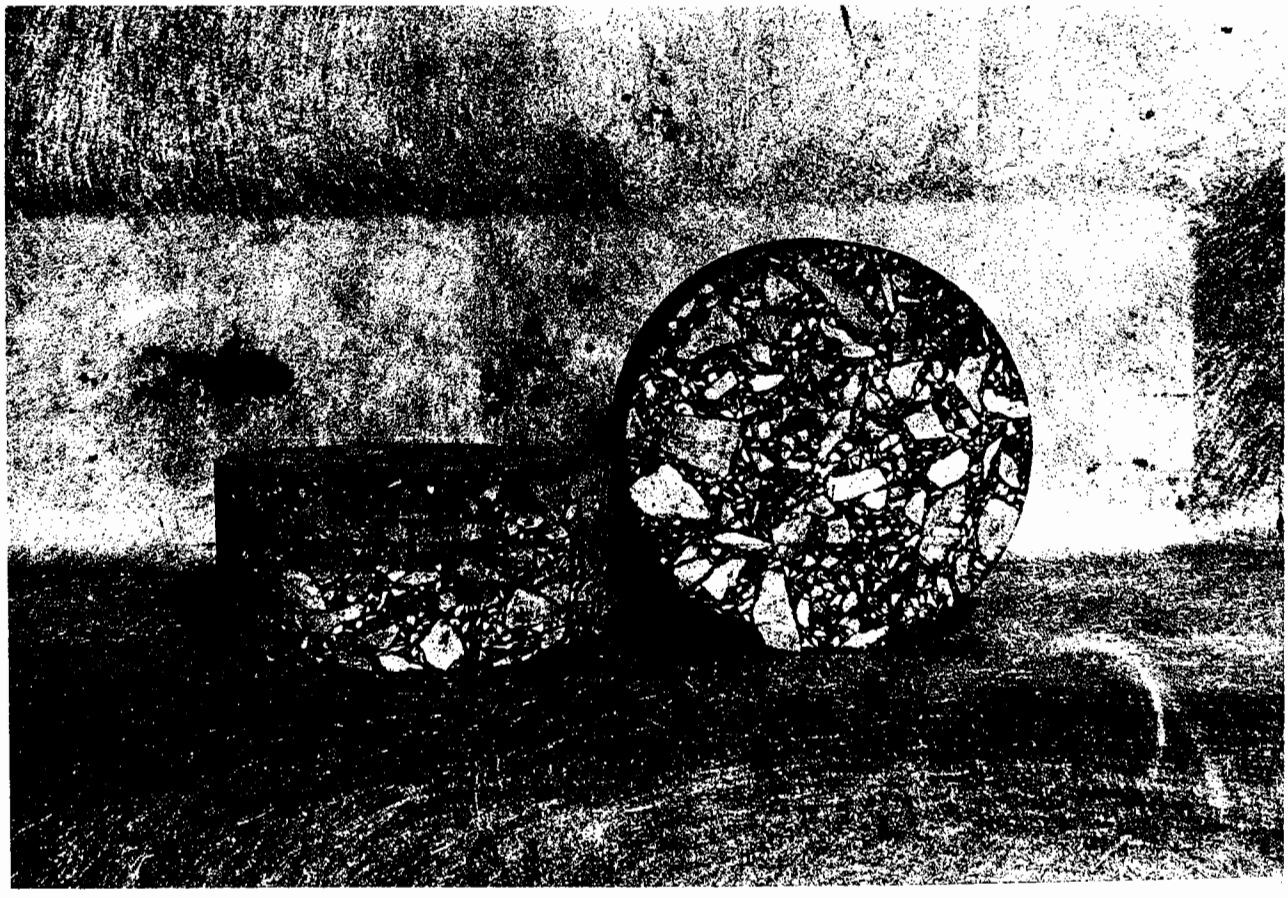

Plate 7.2 (b) Typical Cores Extracted for Further Testing

Table 7.3 Results of Slab Test Three

	LVDT Reading Amplitude (mm)		Observed Crack Growth (mm)	
Number of Cycles	Control	Polymer Mod. Binder	Control	Polymer Mod. Binder
919	0.09	0.11	0	0
11765	0.17	0.20	0	0
28322	0.17	0.16	5	(10)
44800	0.16	0.16	10	(15)
59450	0.20	0.21	10-15	(35)

( ) cracking from the slab surface down.

Cracking in this slab was observed to propagate down from the surface of the polymer modified asphaltic concrete. This cracking was due to a hogging effect induced in the slab. Debonding was again observed in both sections of the slab. No firm conclusions can be drawn from this test regarding the effectiveness of the modified asphaltic treatment due to the hogging problem experienced.

Plate 7.3 (a) illustrates the cracking observed in the modified asphaltic concrete section which propagated down from the asphalt surface and plate 7.3 (b) shows the cracking evidenced in the control section.

Slab Test Four was the first of two slabs using a single gap to initiate crack propagation under the action of a moving wheel.This slab was produced using the control mix and had dimensions of 1.22m length x 0.4m width x 0.075m thickness. The thinner rubber

Slab Test Two was a dual gap slab incorporating a geotextile interlayer section and a control section. The same loading conditions of a 315 kPa wheel load at a speed of 3 km/hr were applied to this slab. A great deal of care was taken with the preparation of this slab to eliminate any minor level discrepancies in the timber bases that might have contributed to the debonding process. Table 7.2 displays the results for slab test two.

Table 7.2 Results of Slab Test Two Results

	LVDT Reading Amplitude (mm)		Observed Crack Growth (mm)	
Number of Cycles	Control	Geotextile	Control	Geotextile
5120	0.18	0.12	0	0
15625	0.23	0.20	15	5
22345	0.31	0.21	20	5
39700	0.30	0.20	20	10
60600	0.30	0.18	20-25	10

The observed crack lengths in the control section again proved larger than those evidenced in the interlayer section. Debonding of both sections was again prevalent and served to make any firm conclusions regarding relative crack growth quite difficult.

Slab Test Three was constructed from a polymer modified binder asphaltic mix and a control section. The rubber used to provide a resilient base under the test specimens was changed from a 12mm thick soft rubber to a 5mm thick stiffer grade of rubber. This change was made to reduce the vertical movement in an attempt to prevent debonding from occurring. Table 7.3 presents the results from this test.

Plate 7.3 (a) Crack Pattern in Polymer Modified Binder Section of Slab Test Three

Plate 7.3 (b) Crack Pattern in Control Section of Slab Test Three

previously described was used under this slab for the duration of the test. A load of 315 kPa travelling at approximately 3 km/hr was applied to the slab as for all other slab tests conducted as part of the program. After some 20,000 passes of the load evidence of debonding was recorded but no vertical crack growth had occurred. The test was terminated at 60,500 load cycles with no vertical crack growth, however evidence of debonding was visible either side of the gap.

Slab Test Five was conducted under slightly different set-up conditions to previous tests. The original 12mm thick soft rubber support was replaced under the slab for this test. Steel end sections were made to fit under the ends of slab to provide a solid support for both ends of the slab, thus eliminating any likelihood of hogging in the sample. Figure 7.1 shows the slab testing arrangement for slab test five, which included a geotextile interlayer.

After 2100 cycles small horizontal movements either side of the gap were observed. At 23,600 cycles 50mm of debonding was observed either side of the 10mm gap in the bases. This movement was generally less than that previously observed for other slab specimens with the recorded LVDT movement equal to 0.15mm. An extended wheel tracking program of 95,000 cycles was completed, however no reflection cracking was observed in the specimen. Debonding along the base of the sample had extended to approximately 200-300mm either side of the gap at the completion of wheel tracking.

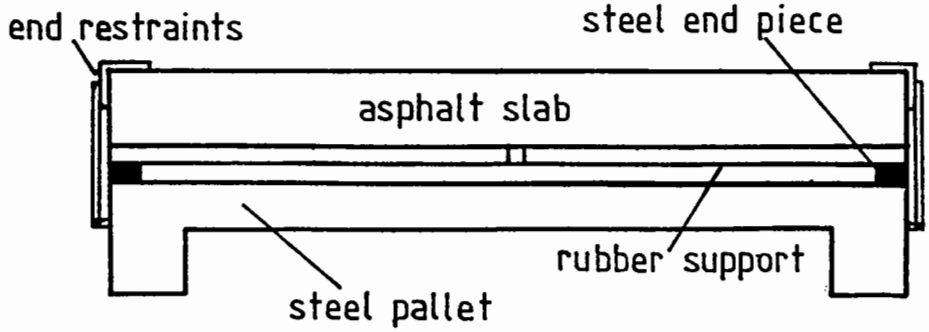

Figure 7.1 Testing Arrangement in use for Slab Test Five

7.3 SUMMARY OF TEST RESULTS

The problems encountered during the testing program can be listed as follows:-

(a) Debonding between overlay and timber bases.

(b) Hogging of a specimen with two crack initiators.

(c) Masking of crack growth rates by the above mentioned problems.

These deficiencies have not allowed a comprehensive set of test data to be collated. The limited test results available indicate that there may be some reduction in crack growth with the inclusion of an interlayer treatment. A definite reduction in relative movement across the gaps in the timber bases, for both interlayer treatments, was recorded by the LVDT's in place. This reduction was approximately one half of that recorded for the control sections.

Potential solutions to the problems experienced during this testing program are listed below:-

(i) Specimen manufacture should be conducted on a levelled surface to avoid any inconsistencies in timber base alignment.

(ii) The testing wheel should be set up with run-off steel rails to avoid the deceleration and acceleration effects occurring on the test specimen. This will also ensure that the wheel travels at a constant speed over the full length of slab.

(iii) Use of steel end pieces placed under the end of each slab does prevent hogging of the sample and should be combined with the use of end restraints.

(iv) A 12mm soft rubber can successfully be used if the debonding problems are overcome. This soft rubber is necessary to adequately represent subgrade conditions.

Unfortunately, time was not available to investigate these factors as part of this work. Further use of the slab testing facility would be well served by analysing the factors listed above at the inception of a testing program.

CHAPTER 8

DISCUSSION AND CONCLUSIONS

8.1 DISCUSSION

To successfully conduct a laboratory investigation into the relative effects of different interlayer treatments on reflection cracking through asphalt overlays it is necessary to firstly conduct a comprehensive study of the available literature. Such a study was undertaken as part of this work and concentrated on the following areas of interest:-

(a) field trial performance of interlayer treatments,

(b) design models for the prediction of reflection crack propagation, and

(c) laboratory testing of treatments to prevent reflection cracking.

This review revealed that installation techniques are vital to the success of interlayer treatments. Other researchers experimental arrangements and test results together with the data bank of information from field trials provided valuable input data for this research program.

The following parameters were carefully incorporated into this testing program in an effort to produce repeatable results that were also able to be correlated to in-situ field performance.

(1) Interface frictional qualities.

(2) Operational temperature.

(3) Loading regime (traffic).

(4) Thermal load application.

(5) Monitoring equipment for crack detection.

(6) Consistency in set-up procedure.

(7) Sample preparation techniques that reach a balance between modelling field conditions and the practicalities of laboratory scale testing.

At the completion of beam testing the treatments used to prevent reflection cracking were presented as the extension in life observed as a percentage of control beam specimens. Some indication of the relationship between increase in thickness and life was also obtained.

The recommendation of one product in preference to another is not solely based on product performance but must also include the economic implications of such a choice. Cost of raw materials and installation for the three treatments used in this laboratory study were obtained from the Main Roads Department field trial (23), as this was the only literature source which quoted such costs. These costs were presented per square metre of application above that for a control overlay section.

(a)	Polymer Modified Binder	$\$4.05/m^2$
(b)	Geotextile	$\$1.64/m^2$
(c)	Geogrid	$\$6.55/m^2$

The relative performance in terms of increased life of these treatments related to a control value of one were from the results presented in Section 6.0 found to be:-

(a)	Polymer Modified Binder	2.5
(b)	Geotextile	5.0
(c)	Geogrid	10.0

The geotextile interlayer treatment has the lowest installation and material cost and a life five times that of the control specimen. Geogrid interlayers with a cost four times that for a geotextile have a life ten times the equivalent control section.

The difficulty in relating the cost-benefit of these products lies in the maintenance considerations that must be made depending on the overlay design life.

Confirmation of these results was sought from the slab test facility, using slab specimens that incorporated two gaps initiating cracks in both interlayer and control sections.Unfortunately results from this testing program were incomplete and time did not allow further development of the testing facility.

8.2 CONCLUSIONS

Conclusions from the testing program conducted at Nottingham University to determine the relative performance of various treatments in their ability to inhibit reflection cracking are presented as follows.

1. Shear box testing has shown that the grade of emery paper chosen for beam and slab testing can adequately model interlayer friction between successive layers of asphaltic concrete.

2. Reductions in shear strength due to the effects of interlayers were found to be:-

   20% for geogrids placed with a bituminous chip seal.

   30% for geotextiles placed with a bituminous seal.

   An increase in shear strength of 4% was recorded for polymer modified binder asphaltic concrete. These shear box tests were conducted at a low shearing rate of 3mm per minute.

3. A beam testing facility has been developed that can simulate the combined effects of thermal and simulated traffic loads on a beam specimen of asphaltic concrete.

4. Consistency and repeatability of beam testing has allowed a successful series of beam tests to be completed. An extension in life for the treatments tested was related to the control specimen life which was taken as one. The increases in life measured during experimentation are listed below.

   (a) 2.5 times for polymer modified binder asphaltic concrete,

   (b) 5.0 times for geotextile interlayers, and

   (c) 10.0 times for geogrid interlayers.

5. The effect of accelerating beam testing by increasing the simulated traffic load from 555 kPa to 810 kPa produced a decrease in life by a factor of 20.0 for the control beams. The lives of interlayer treatments and polymer modified binder asphaltic concrete relative to the control specimens were:-

   (a) 2.5 times, polymer modified binder asphaltic concrete.

   (b) 15.0 times, geotextiles interlayer.

   (c) 31.0 times, geogrid interlayer.

   This represents an increase in relative life for the interlayer treatments of three times that previously found. The tensile effects of the interlayer treatments would appear to have increased their relative lives. The life of the polymer modified binder remained constant with respect to the control beams.

6. Some direct correlation may exist between results obtained for reflection crack propagation in control beams and experience gained of overlay life in field situations.

7. Slab testing with two crack initiators gave some indication that interlayer treatments would reduce the rate of reflection crack propagation.

8. The slab testing specimens for the most part showed signs of debonding as a result of the experimental arrangement.

The beam testing equipment developed for the testing of interlayer treatments has successfully performed the dual function of applying thermal and simulated traffic loads on a single beam specimen. Results indicate that definite benefits can be obtained from all treatments used to inhibit the propagation reflection cracks.

CHAPTER 9

RECOMMENDATIONS FOR FUTURE WORK

9.1 MODIFICATIONS TO EXISTING EQUIPMENT

9.1.1 Shear Box Device

The shear box device has been successfully operated to evaluate the relative shear strengths of treatments used to prevent reflection cracking through asphalt overlays. This has been achieved by shearing one layer of asphaltic concrete over another.

In Australia, France and South Africa a predominant form of construction involves the use of full depth cement treated base pavements with thin asphaltic concrete wearing courses (58). In an attempt to prevent reflection cracking from propagating through the surfacing layer preventive treatments, including interlayers, may be included as part of the construction of the pavement, not as a remedial measure subsequent to the appearance of surface cracking.

An adjustment of frictional interlayer properties for modelling purposes may be required as a result of the cement treated base/asphaltic concrete interface. The shear box could successfully be used to conduct such a testing program by incorporating a layer of cement treated base material in the bottom of the testing device. This extension to the capabilities of the shear box widens the scope for accurate modelling in the beam test facility.

9.1.2 Beam Testing Facility

The current beam test facility as outlined previously in Chapter 4 can be modified to incorporate the effects of 24 hour cyclic thermal movements and a moving load across the top of the beam simulating a wheel load.

Cyclic temperature movements can be incorporated into the current facility through the use of a specially geared motor which is able to be connected to the tensioning rod through a series of couplings. There already exists the software capable of running such a device controlled by an LVDT that monitors the base movements (20).The ability to conduct beam tests with a cyclic thermal loading would enhance the prediction of insitu overlay performance.

Simulation of a moving wheel across a small beam sample can be achieved through the use of multiple loading points on the top surface of the beam. The use of loading platens placed a) centrally above the predefined gap and b) either side of the gap, will develop the typical shearing and bending loads, as previously illustrated in Figure 4.18, above a predefined discontinuity due to the effects of a moving wheel.

This loading can be achieved through the use of a three piston arrangement that is able to cycle across the beam at 9 cycles of load each second. A pneumatically controlled set of actuators may be required to achieve this loading frequency.

Detailed monitoring of crack growth and determinations of crack tip movements would also prove to be of great benefit in future analysis work. A more accurate interpretation of the movements on the beam face would be possible by the use of photographic equipment. A video or camera arrangement could provide visual information on crack growth through the use of a closely spaced crosshair pattern. This arrangement could be installed in the current temperature controlled cabinet.

9.1.3 Slab Testing Facility

Further development of the slab testing facility is required to establish a set of standard procedures that will ensure the successful completion of any slab arrangement placed in the facility.

The debonding problems experienced during slab testing may be at least partly attributed to the acceleration and deceleration of the loading wheel within the confines of the slab itself. To alleviate this problem run-off beams should be provided thus ensuring that the wheel is moving at constant speed across the slab.

The steel pallet which currently supports the specimens during testing operations, needs to be stiffened with larger transverse steel members to ensure that the full capacity of the slab test facility is used. Brief use of the moving wheel at or about one standard axle load (550kPa) caused excessive deflections in the supporting members of the pallet.

Upon completion of these modifications a series of slab tests are required to fine tune the operations of the facility.

9.2 NEW EQUIPMENT DEVELOPMENT

There does not currently exist a device that can simulate the movements in a pavement with a cement treated layer under the action of cyclic thermal effects. Nunn (18) and Foulkes (20) report that cement treated pavement layers once cracked into slabs (10m-15m), warp under the action of thermal gradients from the surface layer to the base of the pavement configuration. This warping effect causes a tensile strain in the surface course, initiating cracking in the surface.

Nottingham University currently has a bridge deck expansion joint simulator that produces thermal movements in an asphaltic sample representative of bridge movements. Through modification of this device or the development of a new apparatus that can induce the movements in test slabs as shown in Figure 9.1, it should be possible to reproduce the type of movements that are claimed to occur in the pavement under thermal loads.

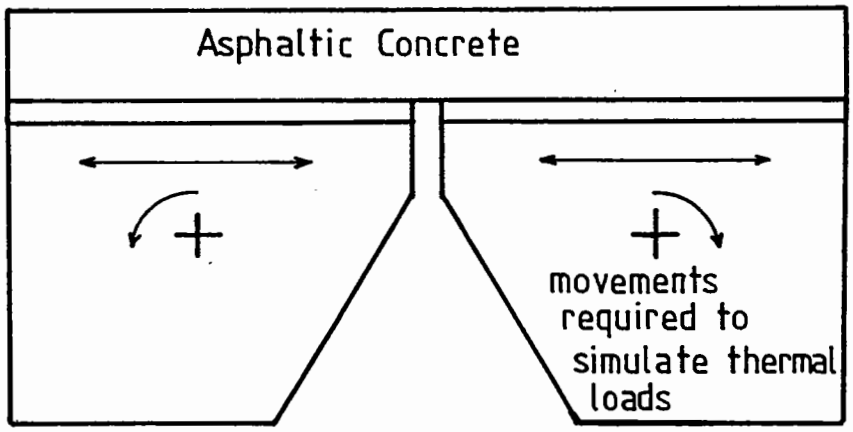

Figure 9.1 Movements in a Testing Device that Simulate Loads in the Pavement

9.3 OTHER WORK

Laboratory testing is the first step in an evaluation process that should provide the design Engineer with relevant product performance in terms of extended life for field conditions.

The laboratory testing process needs to be correctly correlated to field performance before this can occur. Correlation with field performance can be achieved through field trials or the use of accelerated loading facilities such as the South African Heavy Vehicle Simulator (HVS), the New Zealand CAPTIF or the Australian Accelerated Loading Facility (ALF) (61). Each of these devices has the capability of testing pavements in an as-constructed way, evaluating performance in a controlled manner.

Once this correlation process is complete the laboratory testing of different treatments to prevent reflection cracking can be evaluated and the results directly related to field performance.

REFERENCES

1. VON QUINTUS H L, TREYBIG H J and McCULLOUGH B F, "Reflection Cracking Analysis for Asphaltic Concrete Overlays", Proc. AAPT, Vol. 48, February 1979.

2. MAURER D A and MALASHESKIE G J, "Field Performance of Fabrics and Fibres to Retard Reflective Cracking", Trans. Research Board, Annual Meeting, January 1989.

3. BECKHAM W K, MILLS W H, "Cotton Reinforced Roads", Engineering News Record, Vol. 115, 1935.

4. LUTHER M S, MAJIDZADEH K, and CHANG C W, "Mechanistic Investigation of Reflection Cracking of Asphalt Overlays", Transp. Research Board, Report No. 572.

5. RUST F C, "State of the Art of Rehabilitating Reflection Cracking in Cemented Pavements", Technical Report RP/29, National Inst. for Transport and Road Research, CSIR, South Africa, April 1986.

6. HAAS R and PONNIAH E J, "Design Oriented Evaluation of Alternatives for Reflection Cracking through Pavement Overlays", Rilem Conference, Reflective Cracking in Pavement, March 1989.

7. MOLENAAR A A A, "Effects of Mix Modifications, Membrane Interlayers and Reinforcements on the Prevention of Reflective Cracking of Asphalt Overlays", Rilem Conference Reflective Cracking in Pavements, March 1989.

8. SICARD D, "Remontée des Fissures dans les Chaussées. Essai de Comportement en Laboratoire pour Flexions sur Barreaux", Rilem Conference Reflective Cracking in Pavements, March 1989.

9. GOACOLOU H and MARCHAND J P, "Fissuration des Couches de Rourement 5 éme Conference Internationale sur les Chaussees Bitumineuses, Delf, 1982.

10. MARKER V, "Introductory Statement of the Problem, Non-Traffic Load Associated Cracking of Asphalt Pavements", Proc. AAPT, Vol. 35, February 1966.

11. COLOMBIER G, "Fissuration des Chaussées: Nature et Origine des Fissures; Moyens pour Maîtriser Leur Remontée", Rilem Conference, Reflective Cracking in Pavements, March 1989.

12. GORDON R G and WYMAN A C, "Design of Pavement Rehabilitation with Particular Reference to Overlays", Main Roads Dept., Queensland, Northern Divisional Seminar, November 1981.

13. BROWN S F, TAM W S and BRUNTON J M, "Structural Evaluation and Overlay Design: Analysis and Implementation", 6th International Conference, Structural Design of Asphalt Pavements.

14. JAYAWICKRAMA P W, SMITH R E, LYTTON R L and TIRADO-CROVETTI M R, "Development of Asphalt Concrete Overlay Design Program for Reflection Cracking", Rilem Conference, Reflective Cracking in Pavements, March 1989.

15. PARIS P C and ERDOGAN F, "A Critical Analysis of Crack Propagation Laws", Trans. ASME Journ. Basic Engineering Series D, Vol. 85, 1963

16. VAN GURP C A P M and MOLENAAR A A A, "Simplified Method to Predict Reflective Cracking in Asphalt Overlays", Rilem Conference, Reflective Cracking in Pavements, March 1989.

17. CLAUWAERT C and FRANCKEN L, "Etude et Observation de la Fissuration", Rilem Conference, Reflective Cracking in Pavements, March 1989.

18. NUNN M E, "An Investigation of Reflection Cracking in Composite Pavements in the United Kingdom", Rilem Conference, Reflective Cracking in Pavements, March 1989.

19. YANDELL W O, CURISKIS, "Fabric Reinforcement to Extend Pavement Life", AAPT Annual Meeting, March 1983.

20. FOULKES M D, "Assessment of Asphalt Materials to Relieve Reflection Cracking of Highway Surfacings", Thesis submitted to the Council for National Academic Awards in Partial fulfilment of the requirements for the degree of Doctor of Philosophy, March 1988.

21. SCHMIDT R J, "The Relationship of the Low Temperature Properties of Asphalt to the Cracking of Pavements", Proc. AAPT, Vol. 35, February 1966.

22. MINER M A, "Cumulative Damage in Fatigue", Journal of Applied Mechanics No. 67, 1945.

23. MAIN ROADS DEPARTMENT, "Crack Control Trial on Cement Treated Base", Bruce Highway - Beerburrum Deviation, Ref. RP1200, Queensland, November 1987.

24. MAIN ROADS DEPARTMENT, "Beerburrum Deviation Crack Control Trial Condition Assessment", Report No. 1, Ref. RP1256, Queensland, May 1988.

25. MAIN ROADS DEPARTMENT, "Beerburrum Deviation Crack Control Trial Condition Assessment Report No. 2", Report Ref. RP1369, May 1989.

26. SADLIER M, FOCK G and WEBB T, "The Use of a Paving Grade Fabric as a Water Proofing and Crack Retarding Interlayer in Road Surfacing", AAPA, 1988.

27. DICKSON M G, "The Use of Geosynethetics in the Prevention of Reflective Cracking in Premix Overlays, Concrete Pavements and Spray and Chip Road Surfaces", Rilem Conference, Reflective Cracking in Pavements, March 1989.

28. VAN WIJK W, VICELJA J L, "Asphalt Overlay Fabrics, A Life Time Extension of New Asphalt Overlays", Rilem Conference, Reflective Cracking in Pavements, March 1989.

29. VICELJA J L, "Methods to Eliminate Reflection Cracking in Asphalt Concrete Resurfacing over Portland Cement Concrete Pavements", Proc. AAPT, Vol. 32, 1963.

30. VICELJA J L, "Pavement Fabric Interlayers: Benefits - Construction - Experience", Rilem Conference, Additional Paper, Reflective Cracking in Pavements, March 1989.

31. BUTTON J W, "Overlay Construction and Performance Using Geotextiles", Proc. 68th Annual Transportation Research Board Meeting, Washington DC, January 1989.

32. JOHANSSON S S, "Reinforcement of Bituminous Wearing Course with Geotextiles - A Research Project on Road 588 in Soderhamn, Sweden", Rilem Conference, Reflective Cracking in Pavements, March 1989.

33. FUKUOKA M, "Some Old Case Histories on Reflection Cracks in Japan", Rilem Conference Reflective Cracking in Pavements, March 1989.

34. ATKINSON D J and GORDON R G, "Evaluation of Measures for Prevention of Reflective Cracking", Rilem Conference, Reflective Cracking in Pavements, March 1989.

35. OLIVER T L H and BORONI M, "Tensile Reinforcement of Asphalt Using High Strength Polymer Geogrids", AAPA Conference, Brisbane, 1988.

36. GILCHRIST A J T, "Control of Reflective Cracking in Pavements by the Installation of Polymer Geogrids", Rilem Conference, Reflective Cracking in Pavements, March 1989.

37. KASSNER J, "Theory and Practical Experience with Polyester Reinforcing Grids in Bituminous Pavements Courses", Rilem Conference, Reflective Cracking in Pavements, March 1989.

38. WALSH I D, "Overbanding and Polymer Modified Asphalt in Overlay to Concrete Carriageways", Rilem Conference, Reflective Cracking in Pavements, March 1989.

39. SMITH G H, and CALTABIANO M A, "Cement Treated Base Trial Pavements",MRD Qld., Metropolitan Divisional Symposium, 1988.

40. PERFETTI J and SANGSTER T, "The Use of a Textile-Based System to Control Pavement Cracking", Proc. Geotextiles and Geomembrane, pp 165-178, 1988.

41. BROWN S F, BRUNTON J M and ARMITAGE R J, "Grid Reinforced Overlays", Proc. RILEM Conference on Reflective Cracking in Pavements, March 1989.

42. SMITH R D, "Laboratory Testing of Fabric Interlayers for Asphalt Concrete Paving: Interim Report", Transportation Research Record 916.

43. YAMAOKA I, YAMAMOTO D and HARA T, "Laboratory Fatigue Testing of Asphalt Concrete Pavements Containing Fabric Interlayers", Rilem Conference, Reflective Cracking Pavements, March 1989.

44. HUGHES D A B, "Polymer Grid Reinforcement of Asphalt Pavements", Thesis submitted to the University of Nottingham for the degree of Doctor of Philosophy, May 1986.

45. VECOVEN J H, "Methode D'Etude de Systems Limitant la Remontee de Fissures dans les Chaussées", Rilem Conference Reflective Cracking in Pavements, March 1989.

46. WRIGHT D C, "Hot Mixed Asphalt Paving in Queensland", Main Roads Dept. of Queensland, April 1987.

47. BS 4987, Specification for Coated Macadam for Roads and Other Paved Areas.

48. MAIN ROADS DEPARTMENT, "Hot Rolled Asphalt Pavements - Specification No. 11.09 8/88".

49. HUGHES D A B, GILCHRIST A J F and BROWN S F, "Polymer Grid Reinforcements of Asphalt Pavements", Proc. Sino - British Highways and Urban Traffic Conference, Beijing, November 1986.

50. BRUNTON J M and BROWN S F, "Design of Asphalt Pavements with Polymer Grid Reinforcement for North American Conditions", Report to the Tensar Corporation, October 1984.

51. SWK PAVEMENT ENGINEERING, "A Proposal for a Study into the Use of Hatelit in Bituminous Pavement Construction", 1986.

52. SWK PAVEMENT ENGINEERING, "Rehau Armapal Reflection Cracking, Beam Testing", 1988.

53. SWK PAVEMENT ENGINEERING, "The Asphapol Process and Asphapol 2000 Modified Bituminous Materials", Test Results and Engineering Information, 1988.

54. GUO Z, BRUNTON J M and BROWN S F, "Investigation of Sandwich Pavement Construction Incorporating Asphalt Mixtures with Modified Binder", Nottingham University, 1989.

55. KADAR P, Discussions held at the University of Nottingham, November 1989.

56. BISHOP A N, "A Large Shear Box for Testing Sands and Gravels", Proc. 2nd Int. Soil Mech. Conference, Rotterdam, 1948.

57. UZAN J, LIEEH M and ESHED Y, "Investigation of Adhesion Properties Between Asphaltic Concrete Layers", Proc. AAPT, 1978.

58. WILLIAMS R I T, "Cement Treated Pavements, Materials, Design and Construction", Elsevier Applied Science Publications.

59. MURPHY H W, BARAN E and GORDON R, "Cement Treated Bases for Pavements", Inst. of Engineers, 21 pp 1-9, Australia, 1980.

60. DICKENSON E J, "Pavement Temperature Regimes in Australia", Special Report 23, ARRB, 1981.

61. WRIGHT D, "Bitumen Surfacing on Geofabrics", Main Roads Department, Queensland, Australia, November 1988.

62. COOPER K E and BROWN S F, "Development of Simple Apparatus for the Measurement of the Mechanical Properties of Asphalt Mixes", 4th Eurobitume Symp., Vol. 1, October 1989.

63. DE BATS F Th, "The Computer Program PONOS and POEL. A Computer Simulation of Van der Poels Nomograph", External Report, Koninklijke/Shell Laboratorium, Amsterdam 1972.

64. VAN DER POEL C, "A General System Describing the Visco-Elastic Properties of Bitumen and its Relation to Routine Test Data", Journ. App. Chem. 4, 1954.

65. COOPER K E, BROWN S Fand POOLEY G R, "Design of Aggregate Gradings for Asphalt Basecourses", AAPT, February 1985.

66. ARRB, "The Callington ALF Trial", ALF Bulletin No. 15, September 1989.

67. BRADY K C, AWCOCK I and WIGHTMAN N R, "A Comparison of Shear Strength Measurements Using Two Sizes of Shear Box", TRRL Laboratory Report 1105.

68. COOPER K E, "The Effect of Mix and Testing Variables on the Fatigue Strength of Bituminous Mixes", Thesis submitted to the Univ. of Nottingham for the Degree of Master of Philosophy, July 1976.

69. SCHAPERY R A, "A Theory of Crack Growth in Viscoelastic Media", Report MM 2764-73-1, Texas A & M University, March 1983.

70. MONISMITH C L, "Symposium - Non Traffic Load Associated Cracking of Asphalt Pavements, Introductory Remarks", Proc. AAPT, Vol. 35, February 1966.

71. ABD EL HALIM A O, "A New Approach Towards Understanding the Problem of Reflection Cracking", Rilem Conference, Reflective Cracking in Pavements, March 1989.

72. BROWN S F, BRODRICK B V and HUGHES D A B, "Tensar Reinforcement of Asphalt: Laboratory Studies", Univ. of Nottingham, Symposium on Polymer Grid Reinforcement in Civil Engineering, Inst. of Civil Engineers, March 1984.

73. BROWN S F, BRUNTON J M, HUGHES D A B and BRODRICK B V, "Polymer Grid Reinforcement of Asphalt ", Proc. AAPT Annual Meeting, February 1985.

74. EDWARDS J M, "Bitumen Specifications and Quality", Proc. Conference on Road Engineering in Asia and Australia, Kuala Lumpur, June 1973.

75. MAJIDZADEH K, ILVES G J and LUTHUR M S, "Reflection Cracking Models: Review and Laboratory Evaluation of Engineering Fabrics", Transportation Research Record No. 916.

76. KOLIAS S and WILLIAMS R I T, "Cement Bound Road Materials: Strength and Elastic Properties Measured in the Laboratory", TRRL Supplementary Report No. 344.

77. THE EARTHMOVER AND CIVIL CONTRACTOR, "Geosynthetics in Asphalt Pavements", AAPA Conference Review, September 1989.

78. DOWNES M S W, KOOLE R C, MULDER E A and GRAHAM W E, "Some Proven New Binders and Their Cost Effectiveness", AAPA Conf., Brisbane, August 1988.

79. JONES G M, DARTER M I and LITTLEFIELD G, "Thermal Expansion - Contraction of Asphaltic Concrete", Proc. AAPT, Vol. 37, 1968.

80. THE ASPHALT INSTITUTE, "Asphalt Overlays and Pavement Rehabilitation", (MS-17) College Park, Maryland 2nd Ed., 1983.

81. STATE OF CALIFORNIA DEPARTMENT OF TRANSPORTATION, "Method of Test to Determine Overlay Requirements by Pavement Deflection Measurements", California Test Method 356, Manual of Test, Vol. 2, Sacramento, California.

82. KENNEDY C K and LISTER N W, "Prediction of Pavement Performance and the Design of Overlays", TRRL Laboratory Report No. 833, 1978.

83. AUSTIN RESEARCH ENGINEERS INC., "Asphalt Concrete Overlays of Flexible Pavements", Vols. 1 and 2, US Federal Highway Administration Report No. FHWA-RD-77-66, 67, 1981.

84. CLAESSEN A I M and DITMARSCH R, "Pavement Evaluation and Overlay Design, the Shell Method", Proc. 4th Inst. Conf. Structural Design of Asphalt Pavements, University of Michigan, August 1977.

85. COETZEE N F and MONISMITH C L, "Analytical Study of Minimization of Reflection Cracking in Asphalt Concrete Overlays by Use of a Rubber Asphalt Interlayer", Transportation Research Board, TRB 700, 1979.

86. BS 594, Specification for Hot Rolled Asphalt for Roads and Other Paved Areas, Part 1, 1985.

87. MOLENAAR A A A, MOENS J, VANDER WALLE M and VAN DRONGELEN J, "Steel Reinforcement for the Prevention of Reflective Cracking in Asphalt Overlays", Rilem Conference, Reflective Cracking in Pavements, March 1989.

88. BOFINGER H E and SULLIVAN G A, "An Investigation of Cracking in Soil-Cement Bases for Roads", TRRL Report LR379.

89. KELLY J E, "Cracking of Asphalt Concrete Pavements Associated with Volume Changes in Underlying Materials and Base Courses", Proc. AAPT, Vol. 35, February 1966.

90. PELL P S and BROWN S F, "The Characteristics of Materials for the Design of Flexible Pavement Structures", Proc. 3rd Int. Conf. on the Structural Design of Asphalt Pavements, London, 1972.

91. MAJIDZAHEH K, KAUFFMANN E M and CHANG C W, "Verification of Fracture Mechanics Concepts to Predict Cracking of Flexible Pavements", Final Report, No. FHWA RD73-91, Prepared for Federal Highway Administration, 1973.

92. KENNEPOHL G J A and LYTTON R L, "Pavement Reinforcement with Tensar Geogrids for Reflection Cracking Reduction", Proc. Tsukuba Science City, Japan, October 1984.

93. AUSTIN G E, "Reflective and Premature Cracking of Bituminous Paving Practically Solved with Fibre Reinforced Materials", Seminar at Inst. of Highway Inc. Engineers (ICIE), Univ. of Nottingham.

94. BROWN S F, "Improved Asphalt Pavement Engineering", Proc. AAPA Conference, Brisbane, 1988.

95. FROMM H J and PHANG W A, "A Study of Transverse Cracking of Bituminous Pavements", Proc. AAPT, Vol. 41, 1972.

96. GULDEN W, "Rehabilitation of Plain Portland Cement Concrete Pavements with Asphaltic Concrete Overlays", Proc. AAPT, Vol. 47, February 1978.

97. BRUNTON J M, BROWN S F and PELL P S, "Developments to the Nottingham Analytical Design Method for Asphalt Pavements", 6th International Conference - Structural Design of Asphalt Pavements.

98. BINGFU L, "Reducing or Eliminating Reflection Cracking by Rubberized Asphalt Membrane", Rilem Conference, Reflective Cracking in Pavements, March 1989.

99. POWELL D W, POTTER J F, MAYHEW H C and NUNN M E, "The Structural Design of Bituminous Roads", TRRL Report 1132, 1984.

100. DEPARTMENT OF ENVIRONMENT, "Road Note 29 - A Guide to the Structural Design of Pavements for New Roads -Third Edition 1970", Road Research Laboratory.

101. THE EARTHMOVER AND CIVIL CONTRACTOR, "Cracking and Seating Rehabilitating Concrete Pavement", AAPA Conference Review, September 1989.

102. ATKINSON D J, "Measures for Prevention of Reflective Cracking", South East Divisional Symposium, Main Roads Dept., Queensland, August 1988.

103. ZUBE E, "Cracking of Asphalt Concrete Pavements Associated with Absorptive Aggregates", Proc. AAPT, Vol. 35, February 1966.

APPENDIX A

NOTTINGHAM ASPHALT TESTER

APPENDIX A

NOTTINGHAM ASPHALT TESTER (NAT)

A.1 INTRODUCTION

The mechanical properties of mix stiffness and deformation resistance for asphaltic concrete are required for the analytical design of pavement structures. A repeated load testing apparatus has been developed at Nottingham University to test cored or manufactured specimens in creep or indirect tension.

NAT testing conducted as part of this project was completed for two reasons as outlined below.

(1) Assessment of elastic stiffness for beam tests specimens was necessary to ensure compatibility between individual beam tests. Elastic stiffness provides a measure of the load spreading ability of the material, hence a difference in beam stiffness may have affected crack propagation rates.

(2) A move to analytical pavement design procedures world-wide has necessitated the evaluation of stiffness and deformation values for asphaltic mixes. The emergence of end product specifications will also require a means of obtaining mix stiffness and deformation properties for acceptance of the placed material. The testing device used to produce these results must be reliable, accurate, user simple, cost effective and provide quick repeatable answers.The NAT device has the capability of meeting these requirements and through this series of tests the author has gained an appreciation of the relative magnitudes of results obtained from the testing of continuously graded asphaltic cores.

A.2 NOTTINGHAM ASPHALT TESTER (NAT)

A.2.1 Introduction

The NAT test apparatus is capable of testing cores of material up to 150mm diameter in repeated load indirect tension, static uniaxial creep and repeated load uniaxial creep conditions. The loading arrangement consists of a pneumatic actuator controlled by a microcomputer.A single operator is needed to provide the input requirements and adjust the LVDT's which are used to record specimen deformation.

A.2.2 Indirect Tensile Test

The indirect tensile test is used for elastic stiffness evaluation of asphaltic concrete cores. The device used at Nottingham University was developed by Cooper and Brown (62) and Figure A.1 is a diagramatic representation of the test equipment.

Figure A.1 illustrates the specimen location in the testing rig such that a loading strip is able to apply a pulsed load along one diameter. Figure A.2 shows the load pulse application and subsequent indirect tensile movement on the opposite diameter where deformation is measured. Five pulse loads are applied to the specimen with the deformations due to each load recorded. Elastic stiffness is then determined as a function of the applied load and resultant deformation. Figure A.3 illustrates the load and deformation response recorded during cycling.

A typical output from the testing of a cored beam sample is shown in Figure A.4. Upon the completion of indirect tensile testing the cores can be used for either creep testing or compositional analysis as the indirect tensile testing procedure is non-destructive.

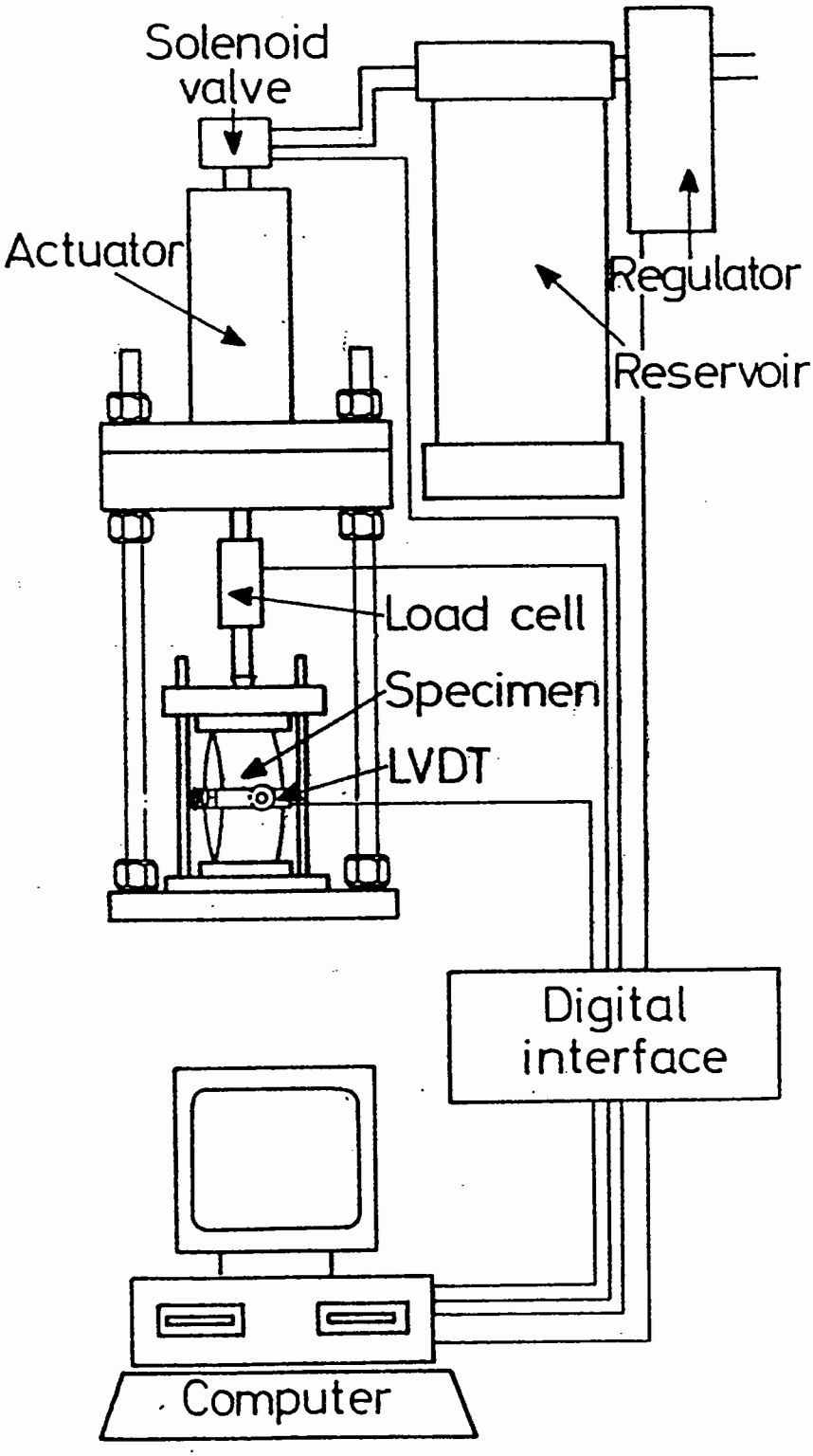

Figure A.1 Diagrammatic Layout of Repeated Load Indirect Tensile Test Equipment (after Cooper and Brown (62))

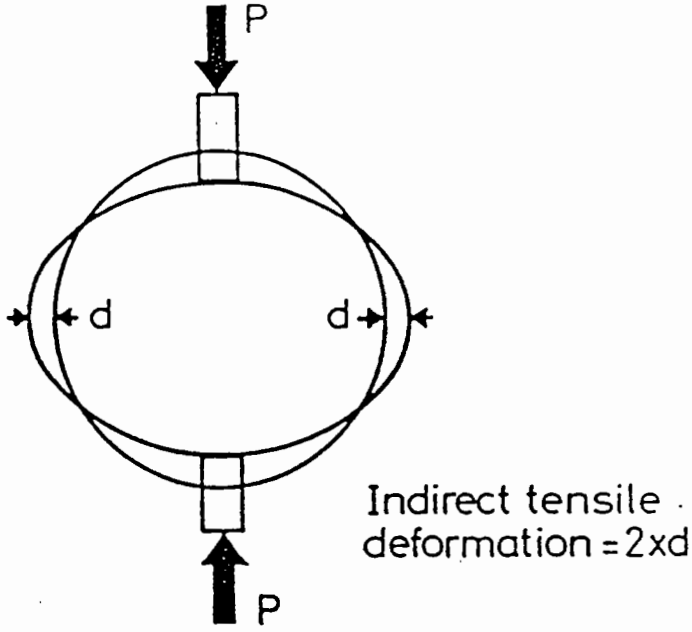

Figure A.2 Loading Configuration of Indirect Tension Specimen Cores

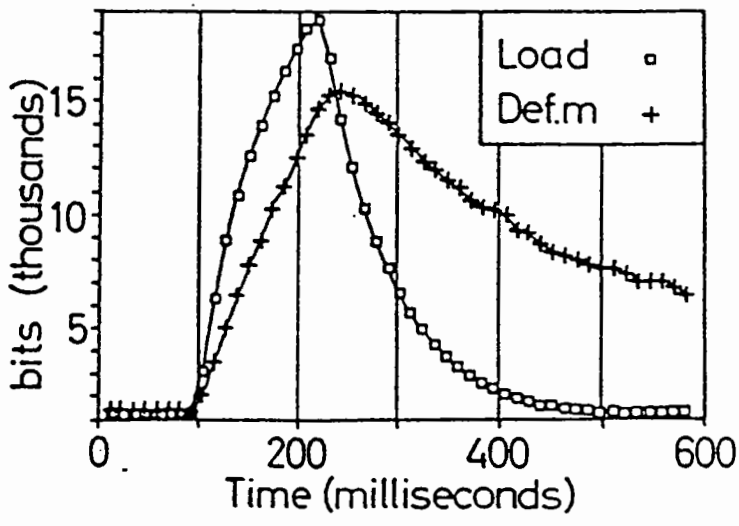

Figure A.3 Typical Load and Deformation Responses for Indirect Tension Testing

NOTTINGHAM ASPHALT TESTER
REPEATED LOAD INDIRECT TENSILE TEST

(calibration factors reviewed on 9 Sept 89)

Date is 8/2/90
Temperature = 20 Celsius
Specimen dia. = 99 mm
Poissons ratio = 0.35
No. cond. pulses = 5
Pressure scale = 5 Rise time scale = 5

Specimen is beam 31
Specimen thickness = 39 mm
1.4000000000E+00 1.6000000000E+00
1.3000000000E+00 1.5000000000E+00
1.4000000000E+00 1.5000000000E+00
1.4000000000E+00 1.6000000000E+00
1.4000000000E+00 1.5000000000E+00

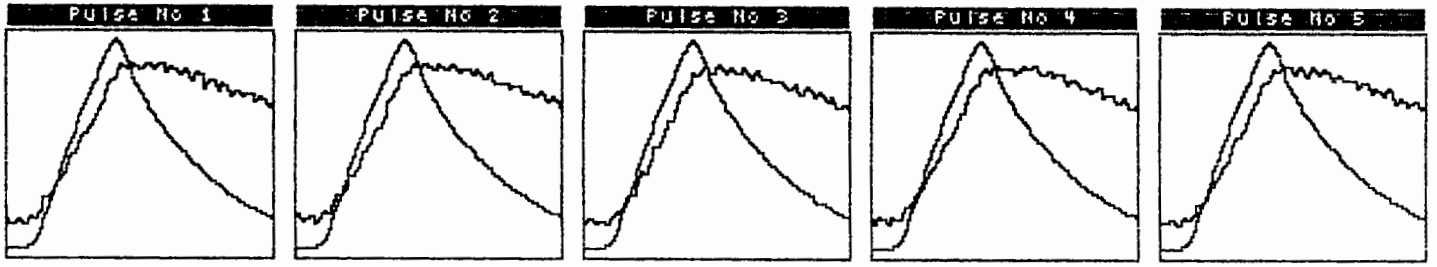

Pulse No.	Vertical Force (kN)	Tensile Stress (kPa)	Rise Time (M.secs)	Elastic Stiffness (MPa)
1	1.22	201.09	121.6	6241
2	1.25	205.45	121.6	6850
3	1.24	205.05	121.6	6629
4	1.25	205.82	121.6	6352
5	1.24	205.07	121.6	6569
Mean	1.24	204.50	121.6	6528

Figure A.4 Typical Output Curves for Beam Cores

A.2.3 Uniaxial Creep Test

The NAT is capable of conducting two types of creep tests

(a) uniaxial static creep, and

(b) uniaxial repeated load creep testing.

The static creep and repeated load creep arrangements both have the same specimen configuration as illustrated in Figure A.5. The difference in the test procedures lies in the loads imposed on the samples. The static creep test applies a 100kPa load to the specimen for a period of one hour. The uniaxial repeated load test provides a 100 kPa load in a cyclic one second on, one second off configuration which approximates a square wave. As a result of this load cycling, which better approximates traffic conditions, the aggregate matrix plays a more significant role in determining the residual, non recoverable deformation which occurs during each load application.

Typical output values obtained for static creep and repeated load creep testing of beam specimen cores are illustrated in Figures A.6 and A.7 respectively.

A.3 TEST RESULTS

A.3.1 Indirect Tensile Results

The results of indirect tensile testing have been split into two categories, (a) beam testing cores and (b) shear box cores. The differences in compaction method and order of magnitude of voids volume were the reasons for separating these two sets of data.

(a) The indirect tensile test results obtained from beam cores are presented in Table A.1 and show the beam number, voids volume and elastic stiffness of data.

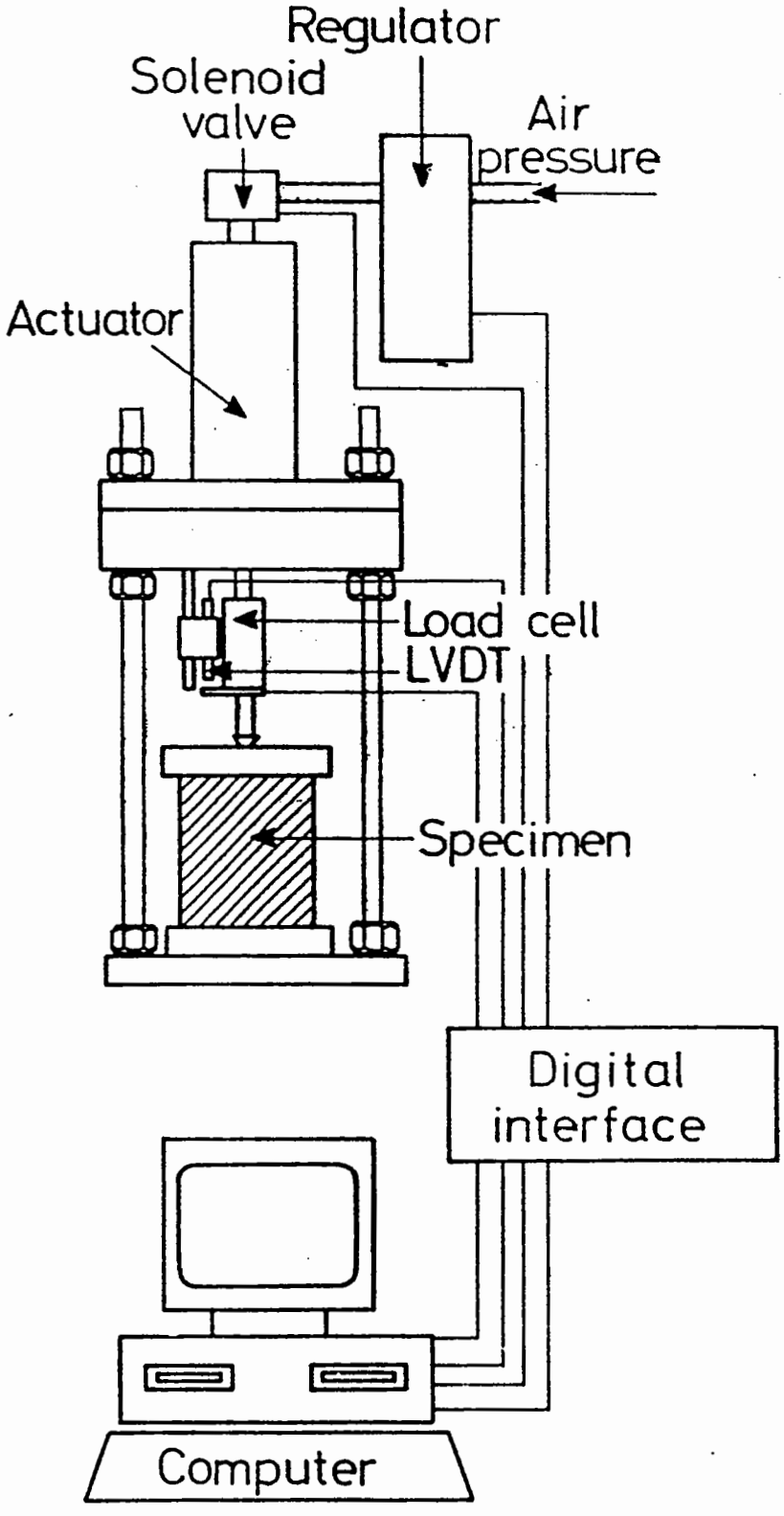

Figure A.5 Diagrammatic Layout of Uniaxial Creep Equipment (after Cooper and Brown (62))

Figure A.6 Typical Output from Uniaxial Static Load Creep Test

```
        NOTTINGHAM ASPHALT TESTER
          UNIAXIAL CREEP TEST

Conditioning period to be used

Date is 18 Jan 90
Specimen is 13\A
Temperature = 40 Celsius
Specimen height = 58 mm
Specimen dia. = 100 mm
Axial test stress = 100 kPa

Axial strain during conditioning =   4064.1

At       2 secs     axial microstrain =     917.6
At       4 secs     axial microstrain =    1331.7
At       6 secs     axial microstrain =    1569.6
At       8 secs     axial microstrain =    1735.6
At      10 secs     axial microstrain =    1867.4
At      20 secs     axial microstrain =    2276.0
At      40 secs     axial microstrain =    2708.5
At      60 secs     axial microstrain =    2983.3
At      80 secs     axial microstrain =    3180.7
At     100 secs     axial microstrain =    3338.4
At     200 secs     axial microstrain =    3828.0
At     300 secs     axial microstrain =    4123.1
At     400 secs     axial microstrain =    4343.5
At     500 secs     axial microstrain =    4509.5
At     600 secs     axial microstrain =    4657.1
At     700 secs     axial microstrain =    4779.7
At     800 secs     axial microstrain =    4883.0
At     900 secs     axial microstrain =    4976.2
At    1000 secs     axial microstrain =    5070.2
At    1100 secs     axial microstrain =    5145.9
At    1200 secs     axial microstrain =    5220.6
At    1300 secs     axial microstrain =    5280.5
At    1400 secs     axial microstrain =    5342.3
At    1500 secs     axial microstrain =    5396.7
At    1600 secs     axial microstrain =    5450.2
At    1700 secs     axial microstrain =    5505.5
At    1800 secs     axial microstrain =    5559.0
At    1900 secs     axial microstrain =    5601.4
At    2000 secs     axial microstrain =    5647.5
At    2100 secs     axial microstrain =    5693.6
At    2200 secs     axial microstrain =    5737.0
At    2300 secs     axial microstrain =    5773.9
At    2400 secs     axial microstrain =    5816.3
At    2500 secs     axial microstrain =    5846.7
At    2600 secs     axial microstrain =    5879.9
At    2700 secs     axial microstrain =    5910.4
At    2800 secs     axial microstrain =    5940.8
At    2900 secs     axial microstrain =    5974.0
At    3000 secs     axial microstrain =    6005.3
At    3100 secs     axial microstrain =    6046.8
At    3200 secs     axial microstrain =    6073.6
At    3300 secs     axial microstrain =    6111.4
At    3400 secs     axial microstrain =    6130.8
At    3500 secs     axial microstrain =    6159.3
At    3600 secs     axial microstrain =    6180.6

**** Start of relaxation period ****

At    3700 secs     axial microstrain =    5622.6
At    3800 secs     axial microstrain =    5560.8
At    3900 secs     axial microstrain =    5537.8
At    4000 secs     axial microstrain =    5510.1
At    4100 secs     axial microstrain =    5504.6
At    4200 secs     axial microstrain =    5492.6
At    4300 secs     axial microstrain =    5480.6
At    4400 secs     axial microstrain =    5472.3
At    4500 secs     axial microstrain =    5466.8

******* Test ended *******
```

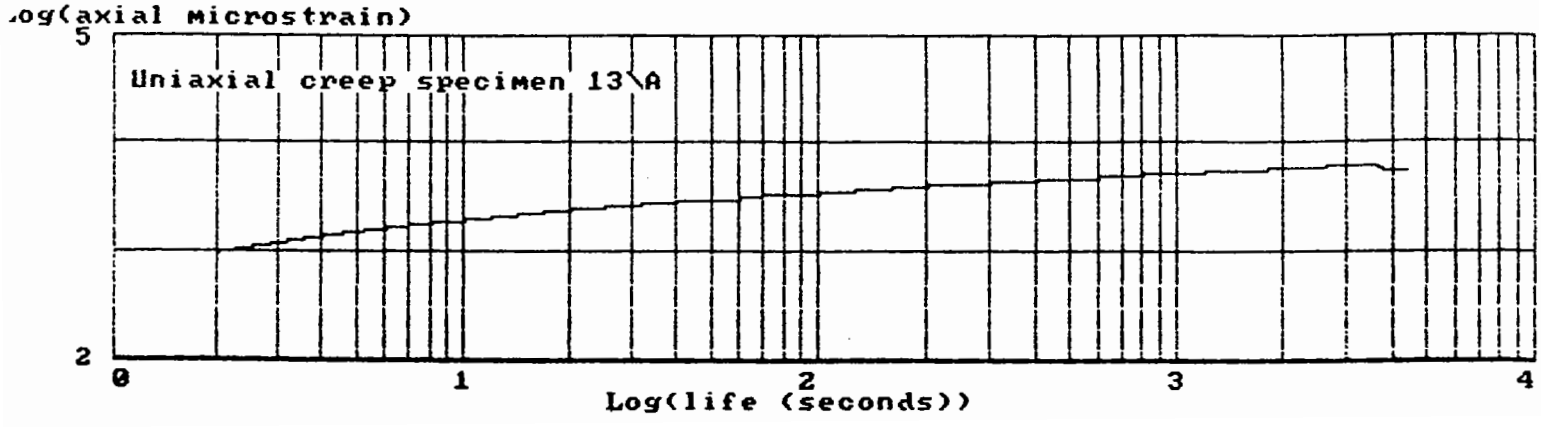

```
PULSED LOAD TEST - 1 sec on & 1 sec off
Date = 19\1\90
Specimen is 24
Specimen height =  45.8  (mm)
Specimen dia. =  100  (mm)
Peak stress =  100  kN/sq m

Cycles =  5        axial u.strain =  3213
Cycles =  10       axial u.strain =  4500
Cycles =  20       axial u.strain =  5606
Cycles =  40       axial u.strain =  6886
Cycles =  60       axial u.strain =  7604
Cycles =  80       axial u.strain =  7997
Cycles =  100      axial u.strain =  8470
Cycles =  200      axial u.strain =  9610   E.stiff =  25140  Pa
Cycles =  300      axial u.strain =  10244  E.stiff =  25654  Pa
Cycles =  400      axial u.strain =  10638  E.stiff =  25992  Pa
Cycles =  500      axial u.strain =  10971  E.stiff =  26209  Pa
Cycles =  600      axial u.strain =  11228  E.stiff =  26408  Pa
Cycles =  700      axial u.strain =  11396  E.stiff =  26516  Pa
Cycles =  800      axial u.strain =  11566  E.stiff =  26659  Pa
Cycles =  900      axial u.strain =  11742  E.stiff =  26755  Pa
Cycles =  1000     axial u.strain =  11868  E.stiff =  26907  Pa
Cycles =  1100     axial u.strain =  11996  E.stiff =  26940  Pa
Cycles =  1200     axial u.strain =  12123  E.stiff =  26953  Pa
Cycles =  1300     axial u.strain =  12171  E.stiff =  27005  Pa
Cycles =  1400     axial u.strain =  12261  E.stiff =  27130  Pa
Cycles =  1500     axial u.strain =  12394  E.stiff =  27192  Pa
Cycles =  1600     axial u.strain =  12469  E.stiff =  27316  Pa
Cycles =  1700     axial u.strain =  12491  E.stiff =  27359  Pa
Cycles =  1800     axial u.strain =  12578  E.stiff =  27380  Pa
Cycles =  1900     axial u.strain =  12624  E.stiff =  27387  Pa
Cycles =  2000     axial u.strain =  12711  E.stiff =  27392  Pa
Cycles =  2100     axial u.strain =  12756  E.stiff =  27426  Pa
Cycles =  2200     axial u.strain =  12778  E.stiff =  27551  Pa
Cycles =  2300     axial u.strain =  12783  E.stiff =  27591  Pa
Cycles =  2400     axial u.strain =  12784  E.stiff =  27604  Pa
Cycles =  2500     axial u.strain =  12795  E.stiff =  27608  Pa
Cycles =  2600     axial u.strain =  12840  E.stiff =  27612  Pa
Cycles =  2700     axial u.strain =  12912  E.stiff =  27630  Pa
Cycles =  2800     axial u.strain =  13036  E.stiff =  27692  Pa
Cycles =  2900     axial u.strain =  13070  E.stiff =  27768  Pa
Cycles =  3000     axial u.strain =  13083  E.stiff =  27805  Pa
Cycles =  3100     axial u.strain =  13127  E.stiff =  27824  Pa
Cycles =  3200     axial u.strain =  13191  E.stiff =  27828  Pa
Cycles =  3300     axial u.strain =  13224  E.stiff =  27853  Pa
Cycles =  3400     axial u.strain =  13239  E.stiff =  27907  Pa
Cycles =  3500     axial u.strain =  13304  E.stiff =  27923  Pa
Cycles =  3600     axial u.strain =  13347  E.stiff =  27926  Pa

Test terminated
```

Figure A.7 Typical Output from Uniaxial Repeated Load Creep Test

Table A.1 NAT Results for Beam Testing

Beam No.	Voids Volume (%)	Loading Time (sec)	Frequency (Hz)	Speed (km/hr)	Elastic Stiffness (MPa)
3	5.2	0.121	8.3	52	4520
4	4.6	0.127	7.7	50	3275
5	6.6	0.124	8.1	51	3519
6	5.9	0.133	7.5	47	3931
7	4.0	0.121	8.3	52	3846
8	3.0	0.115	8.7	55	5248
9	2.9	0.115	8.7	55	4001
10	2.5	0.115	8.7	55	4105
11	3.0	0.115	8.7	55	4500
12	3.0	0.115	8.7	55	4823
13	2.8	0.121	8.3	52	3632
14	2.7	0.115	8.7	55	4304
15*	2.5	0.115	8.7	55	2823
16*	3.0	0.115	8.7	55	2880
17	3.4	0.115	8.7	55	3598
18	2.0	0.115	8.7	55	4236
19	2.0	0.115	8.7	55	4451
20	2.0	0.115	8.7	55	4235
21	5.5	0.115	8.7	55	3587
22	4.0	0.115	8.7	55	3749
23*	4.5	0.115	8.7	55	2109
24*	4.5	0.115	8.7	55	1882
25	4.0	0.115	8.7	55	4210
26	4.6	0.110	9.1	57	3501
27*	3.0	0.115	8.7	55	2645
28*	3.0	0.115	8.7	55	2265
29	3.0	0.121	8.3	52	4538
30	3.0	0.121	8.3	52	6833
31	3.0	0.121	8.3	52	6528
32	2.5	0.121	8.3	52	6977

*Polymer Modified Binder.

The results showing lower values of elastic stiffness were obtained from cores containing a polymer modified binder. This is not an unexpected result as the penetration of this binder was 81 compared with 65 pen for all other cores.

Reasonable agreement was found for beams produced from the same roller compactor slabs. In general a consistency in elastic stiffness values for beam testing cores was recorded.

(b) Indirect tensile test results from shear box cores are contained in Table A.2

Table A.2 Shear Box NAT Test Results

Date of Test	Voids Volume (%)	Loading Time (sec)	Frequency (Hz)	Speed (km/hr)	Elastic Stiffness (MPa)
5.9.89	7.1	0.139	7.2	45	2680
	7.4	0.139	7.2	45	3350
	6.8	0.139	7.2	45	3555
	7.0	0.139	7.2	45	3350
14.6.89	6.5	0.133	7.5	47	2455
	7.0	0.133	7.5	47	2780
	6.0	0.139	7.2	45	2330
	7.2	0.139	7.2	45	2080
16.6.89	11.8	0.142	7.0	44	1900
	11.4	0.139	7.2	45	1780
22.6.89	10.5	0.139	7.2	45	2750
	10.0	0.141	7.1	45	3440
	8.6	0.121	8.3	52	2383
	8.1	0.121	8.3	55	2526
	8.2	0.121	8.3	52	2394
	8.4	0.121	8.3	52	2329

(Continued over)

Date of Test	Voids Volume (%)	Loading Time (sec)	Frequency (Hz)	Speed (km/hr)	Elastic Stiffness (MPa)
7.7.89	9.8	0.115	8.7	55	2192
	8.3	0.115	8.7	55	2623
	10.5	0.115	8.7	55	2144
	8.7	0.115	8.7	55	2382
14.7.89	10.1	0.115	8.7	55	2114
	9.3	0.121	8.3	52	2901
	10.3	0.121	8.3	52	2193
	10.8	0.121	8.3	52	2148
20.7.89	12.1	0.127	7.9	50	2034
	11.0	0.127	7.9	50	2566
	8.5	0.127	7.9	50	3106
	8.7	0.122	8.2	52	2615
26.7.89	7.3	0.121	8.3	52	3719
	8.0	0.127	7.9	50	3763
	10.5	0.127	7.9	50	2888
	7.7	0.127	7.9	50	3922
1.8.90	9.3	0.127	7.9	50	3510
	11.2	0.127	7.9	50	2779
	8.0	0.122	8.2	52	4316
	10.3	0.127	7.9	50	3033
10.8.89	8.6	0.127	7.9	50	4428
	10.4	0.127	7.9	50	4076
	10.1	0.127	7.9	50	4234
	8.8	0.127	7.9	50	3844
16.10.89**	10.7	0.121	8.3	52	1250
*	12.4	0.121	8.3	52	894
	8.9	0.121	8.3	52	2010
	6.7	0.121	8.3	52	2592
18.10.90**	11.9	0.121	8.3	52	874
*	12.7	0.121	8.3	52	705
	11.6	0.121	8.3	52	1697
	10.3	0.121	8.3	52	1796

*Polymer Modified Binder

Again the lowest values for elastic stiffness were recorded for those cores with a polymer modified binder.

A distinctive trend is evident between voids volume and values of elastic stiffness as expected. A visual representation of both shear box and beam test results in which voids volume is plotted against mix stiffness can be seen in Figures A.8 and A.9.

A.3.2 Creep Testing Results

Creep testing is used to give an indication of the material's deformation resistance. The test temperature of 40°C and maximum load of 100 kPa are the same for both types of creep tests in use.

The static creep test provides a determination of the viscous flow of the core being tested. A typical deformation against time plot for a continuously graded sample was shown previously in Figure A.6. From these plots it is possible to determine the viscous modulus of the material and the deformation resistance, expressed as a Δ(3600sec - 200sec) value. A comparison of voids volume variation for cores compacted using different methods can be made for this experimental program. A measure of deformation resistance can be calculated for uniaxial repeated load test cores in the same manner as for static load test cores.

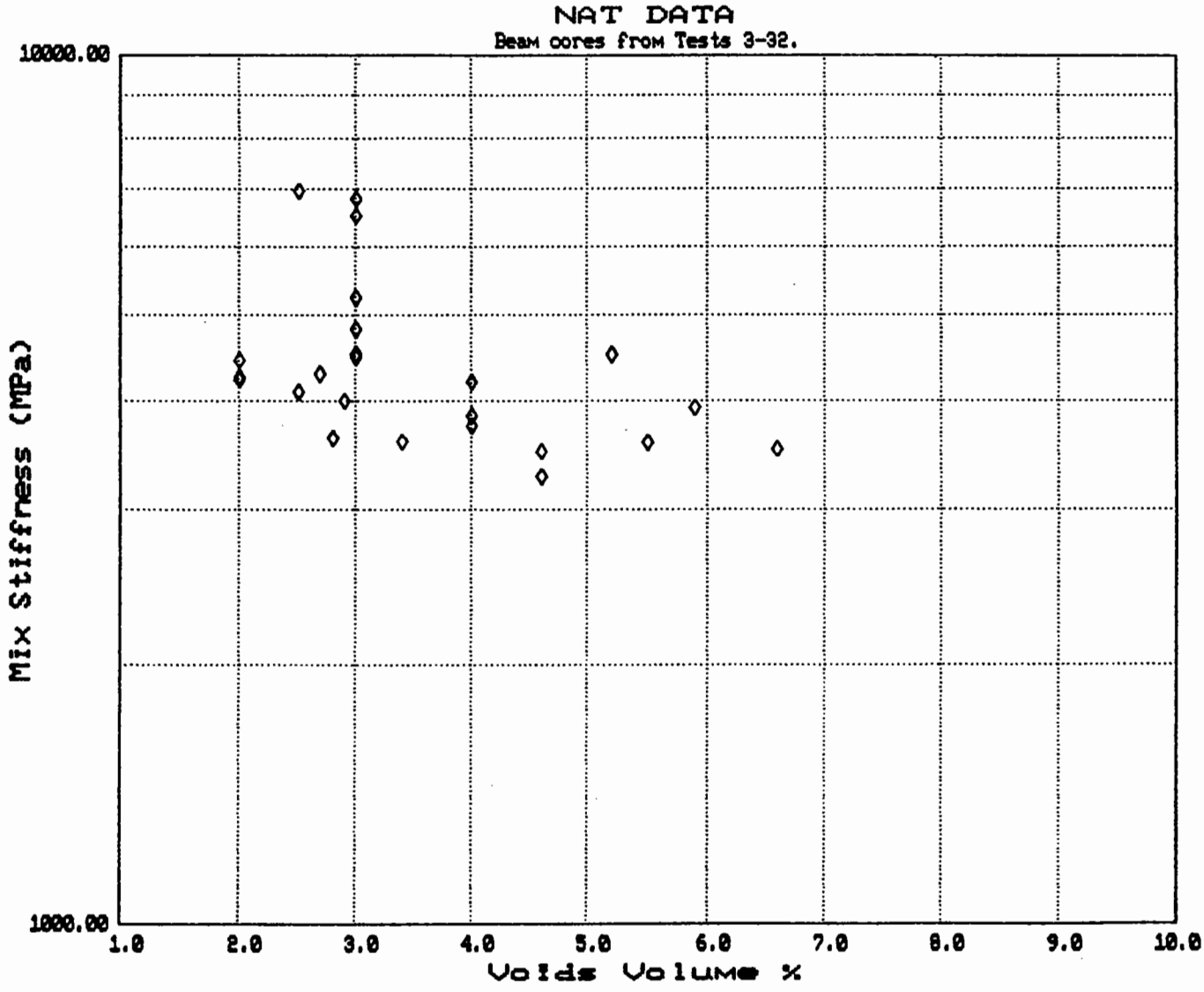

Figure A.8 Plot of all NAT Data from Beam Tests as Elastic Stiffness Against Voids Volume

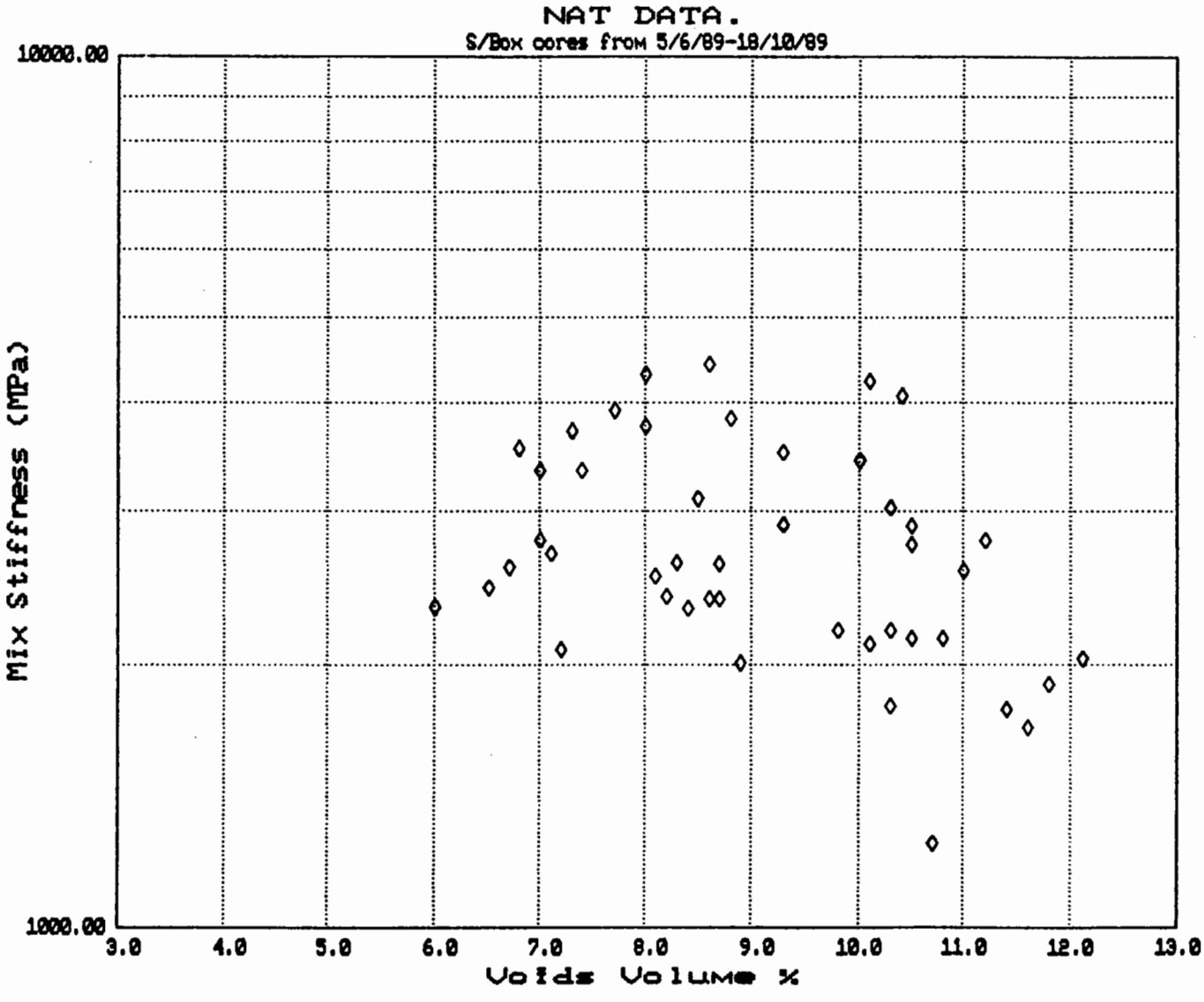

Figure A.9 Plot of all NAT Data from Shear Box Tests as Elastic Stiffness Against Voids Volume

A summary of results from the static creep testing completed is shown in Table A.3.

Table A.3 Results of Static Creep Testing

Specimen Type/Number	Axial Microstrain		Deformation Resistance (μm) Δ(3600-200)
	200 sec	3600 sec	
Beam 13*	3828	6181	2353
Beam 1	3947	5462	1515
Beam 2	6116	8378	2262
Beam 3	4075	5536	1461
Beam 4	4207	5636	1429
Beam 5	5288	6012	2724
Beam 6	3588	5430	1842
Shear Box 10/8 (1)	2836	3794	958
Shear Box 10/8 (2)	3399	4662	1263
Shear Box 26/7 (1)	3376	4500	1124
Shear Box 26/7 (2)	3310	4339	1029
Shear Box 20/7 (1)	2929	4116	1187
Beam 17	11186	15646	4460
Beam 20	8580	12515	3935
Beam 27*	4995	7130	2135
Beam 22	4583	6117	1534
Beam 11	5529	7304	1775
Shear Box 16/10 (1)	3433	4966	1533

* Polymer Modified Binder

The mean deformation values for Δ(3600-200) were calculated for both beam test cores and shear box cores with the results as detailed below.

(1) Beam test core deformation value 2269 microstrain.

(2) Shear box test core deformation value 1182 microstrain.

Thus it would seem that from these mean values the beam testing results with an average volume of voids, from cores used in creep testing, equal to 3.9% have almost twice the susceptibility to deformation than shear box cores with an average volume of voids of 9.4%. All materials have the same grading and binder contents but are compacted using different methods.

Repeated load test results are presented in Table A.4 for cores taken from beam testing, shear box testing and slab testing.

Table A.4 Results of Repeated Load Creep Testing

Specimen Name	Axial Microstrain		Δ(3600-200) microstrain
	200 cycles	3600 cycles	
Beam 16*	6368	9033	2665
Beam 13	6633	14941	8308
Beam 7	6116	8378	13127
Beam 26	9816	19765	9949
Beam 19	10550	16141	5591
Beam 21	11195	25332	14137
Beam 10	17717	26107	8390
Beam 24*	9610	13347	3737
Beam 25	11246	20493	9247
Shear Box 16/10 (1)	4152	6061	1909
Slab Test 2	5764	23710	17946
Slab Test 1	12471	44421	31950

*Polymer Modified Binder

Results from testing of the polymer modified binder cores showed that they performed significantly better than the standard binders in this repeated load test. This was not the case for the static load creep test. Beam test results from standard binders had a mean deformation of 9700 microstrain however the results vary from 14137 to 5591 microstrain.

Results from the slab test cores, showed high values of deformation indicating that the measured voids content of 9.0% and 10.2% for slab test two and one respectively have a marked effect on deformation resistance.

A.4 DISCUSSION

The determination of elastic stiffness values through the use of PONOS (63) a computer program based on Van der Poel's nomograph values (64) for bitumen stiffness were compared to the results obtained from NAT testing. Elastic stiffness at a known temperature and time of loading has been shown to be dependent on Bitumen stiffness and Voids in Mineral Aggregate (VMA) (Cooper et al (65)).

The PONOS (63) program requires input variables as shown in Figure A.10. Typical output values from the prediction program are contained in Figure A.11. By varying the air voids content and fixing the initial binder properties a plot of mix stiffness against traffic speed can be determined showing the effects of increasing air voids content. Figure A.12 presents the results of such a plot.

The program was used to calculate values of mix stiffness at traffic speeds of 40 and 60 km/hr as this represents the range of speeds effectively used during the testing of cores in the NAT. Comparisons are able to be made between the PONOS lines and the regression line obtained from NAT data.

```
OBITUMEN STIFFNESS FROM VAN DER POELS NOMOGRAPH
0
 INPUT DATA:
                        MODE  =      5

 INITIAL PENETRATION OF BITUMEN USED IN CALC

                     INITIAL PENETRATION  =    60.00
          NUMBER OF STEPS IN PENETRATION  =      1
                 PENETRATION TEMPERATURE  =     25.0

 INITIAL SOFTENING POINT RING AND BALL    =     52.0
 NUMBER OF STEPS IN S.P. RING AND BALL    =      1

                     INITIAL TEMPERATURE  =     20.0
          NUMBER OF STEPS IN TEMPERATURE  =      2
               STEP VALUE IN TEMPERATURE  =      1.0

  INITIAL DEPTH OF BITUMEN BOUND LAYER    =       .1
     NUMBER OF STEP INCREASES OF DEPTH    =      1

          INITIAL VALUE OF TRAFFIC SPEED  =     30.0
       NUMBER OF STEPS IN TRAFFIC SPEED   =      7
            STEP VALUE IN SPEED INCREASE  =      5.0

                   INITIAL BINDER CONTENT  =      .045
     NUMBER OF STEPS IN BINDER CONTENT     =      1

                              VOIDS VOLUME  =      .050
        NUMBER OF STEPS IN VOIDS VOLUME    =      1

                            AGGREGATE S.G.  =     2.780
                              BITUMEN S.G.  =     1.020
```

Figure A.10 PONOS Input Requirements

	PI	SOFTENING POINT R&B (DEG. C)	TEMP (DEG. C)	DEPTH OF BIT LAYER (MM)	TRAFFIC SPEED (KPH)	LOADING TIME (SEC)	PEN.	PEN. TEMP (DEG. C)	LOG STIFFNESS	BITUMEN STIFFNESS (N/M**2)	COMPUTED VISCOSITY (NS/M**2)	MIX STIFFNESS (MN/M**2)	B.C %	VV %
0	-.3	52.0	20.0	.1	30.0	.025	60.0	25.0	.728E+01	.191E+08	.161E+06	4083.	4.5	5.0
0	-.3	52.0	20.0	.1	35.0	.022	60.0	25.0	.732E+01	.208E+08	.152E+06	4308.	4.5	5.0
0	-.3	52.0	20.0	.1	40.0	.019	60.0	25.0	.735E+01	.225E+08	.145E+06	4512.	4.5	5.0
0	-.3	52.0	20.0	.1	45.0	.017	60.0	25.0	.738E+01	.241E+08	.139E+06	4699.	4.5	5.0
0	-.3	52.0	20.0	.1	50.0	.016	60.0	25.0	.741E+01	.255E+08	.133E+06	4870.	4.5	5.0
0	-.3	52.0	20.0	.1	55.0	.014	60.0	25.0	.743E+01	.267E+08	.127E+06	5002.	4.5	5.0
0	-.3	52.0	20.0	.1	60.0	.013	60.0	25.0	.744E+01	.278E+08	.122E+06	5122.	4.5	5.0
0	-.3	52.0	21.0	.1	30.0	.025	60.0	25.0	.721E+01	.161E+08	.136E+06	3685.	4.5	5.0
0	-.3	52.0	21.0	.1	35.0	.022	60.0	25.0	.725E+01	.176E+08	.129E+06	3890.	4.5	5.0
0	-.3	52.0	21.0	.1	40.0	.019	60.0	25.0	.728E+01	.190E+08	.122E+06	4076.	4.5	5.0
0	-.3	52.0	21.0	.1	45.0	.017	60.0	25.0	.731E+01	.203E+08	.117E+06	4247.	4.5	5.0
0	-.3	52.0	21.0	.1	50.0	.016	60.0	25.0	.733E+01	.216E+08	.113E+06	4405.	4.5	5.0
0	-.3	52.0	21.0	.1	55.0	.014	60.0	25.0	.736E+01	.228E+08	.109E+06	4553.	4.5	5.0
0	-.3	52.0	21.0	.1	60.0	.013	60.0	25.0	.738E+01	.240E+08	.105E+06	4692.	4.5	5.0

Figure A.11 Typical PONOS Output Data

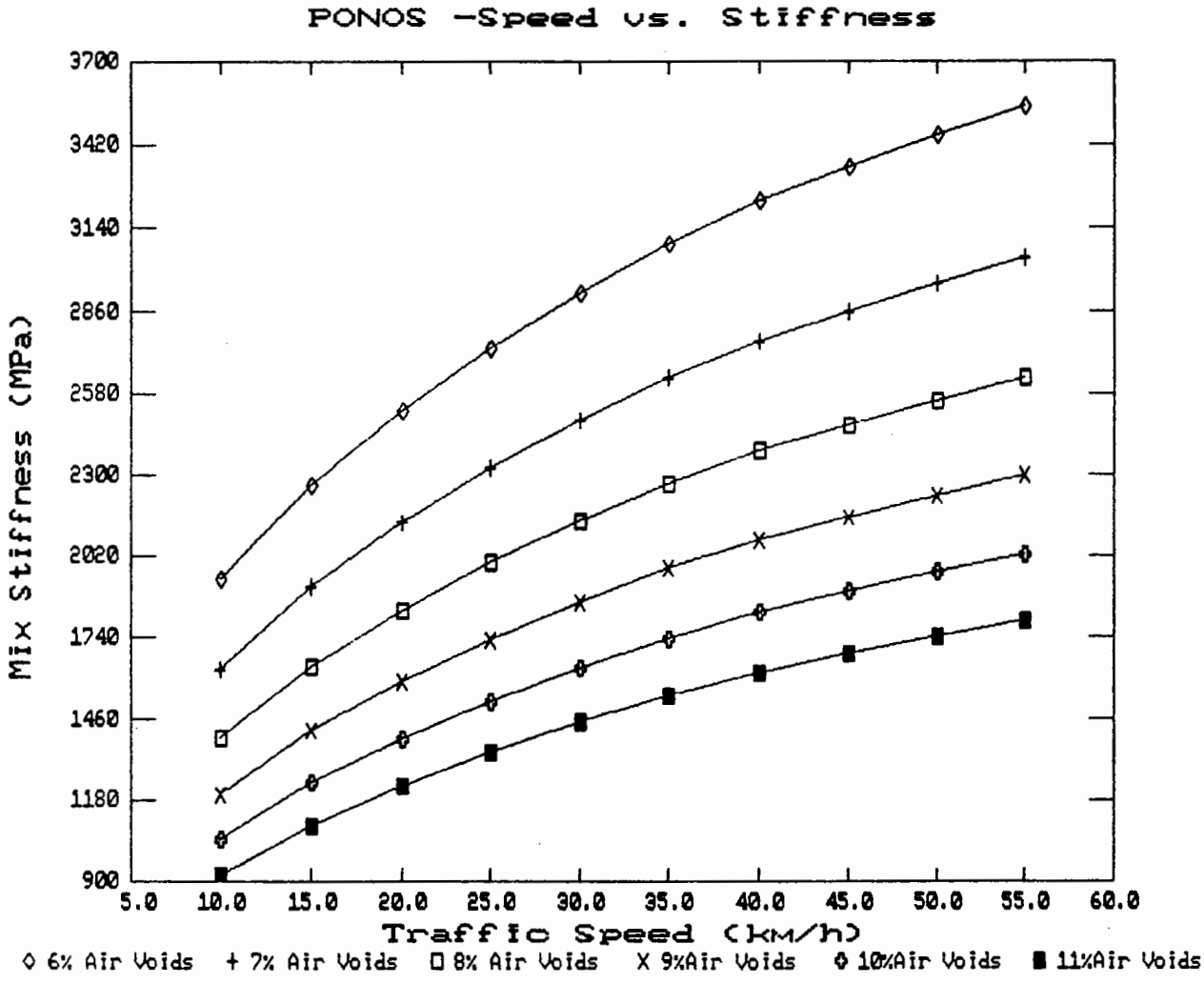

Figure A.12 **PONOS Data Plot of Mix Stiffness Against Traffic Speed Showing the Effects of Air Voids Content**

Two plots are presented in Figures A.13 and A.14 which represent NAT data from beam test cores and shear box test cores plotted with PONOS prediction data. It can be seen from this data that good agreement is achieved between the NAT evaluation of elastic stiffness and that predicted by PONOS for shear box core results. The same however is not true for beam testing cores. The voids contents for the beam cores were in the range 2.0- 6.6%, the lower end of this range is outside the prediction range for the PONOS program.

Creep testing results under static load conditions showed that beam testing cores had higher deformations than shear box cores despite having a lower void content.The reason for this difference in results may be due to the reduction in air voids as a result of the action of a 100 kPa load at 40°C. As the air void content passes the point at which the material displays maximum deformation resistance an increase due to lubrication between aggregate particles by the binder will result.

Figure A.15 shows diagrammatically the location of such a point on a plot of VMA against STRAIN. The shape of this curve is dependent on grading of the aggregate and other aggregate properties as well as volumetric proportions and compaction method used. (Cooper et al (65)).

The repeated load uniaxial creep test results had a greater scatter of results with the value of Δ(3600-200) ranging from 14137 microstrain to 5591 microstrain. The explanation for this variability may lie in the thickness of cores used which varied from 69mm to 38mm. With a decrease in core thickness the aggregate matrix composition may vary from cores that are thicker thus having a more representative matrix configuration.

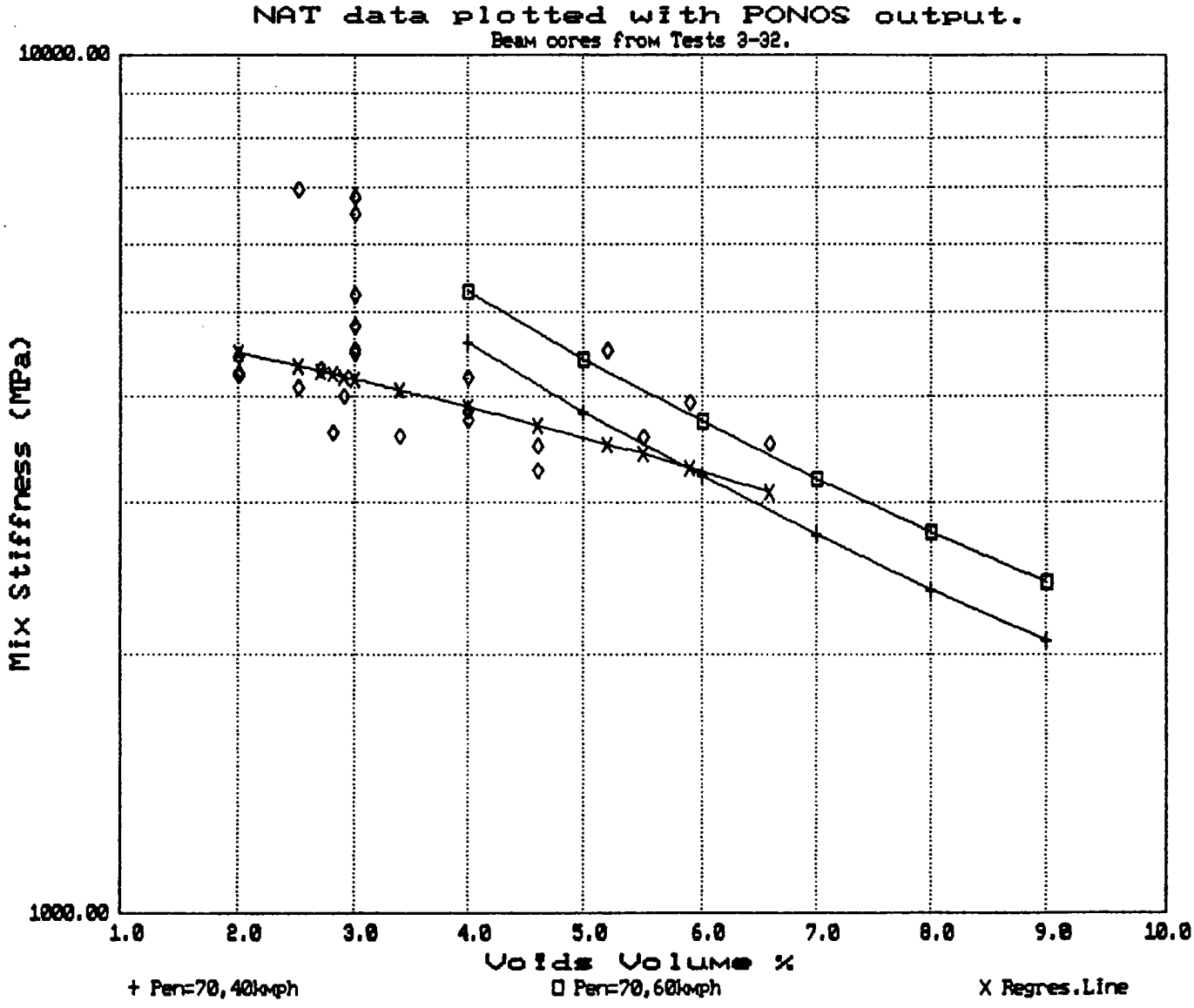

Figure A.13 Plot of Mix Stiffness Against Voids Volume for Beam Test Cores. PONOS Lines for 70 Pen Binder and Traffic Speeds of 40 and 60 km/hr Show Predicted Mix Stiffnesses

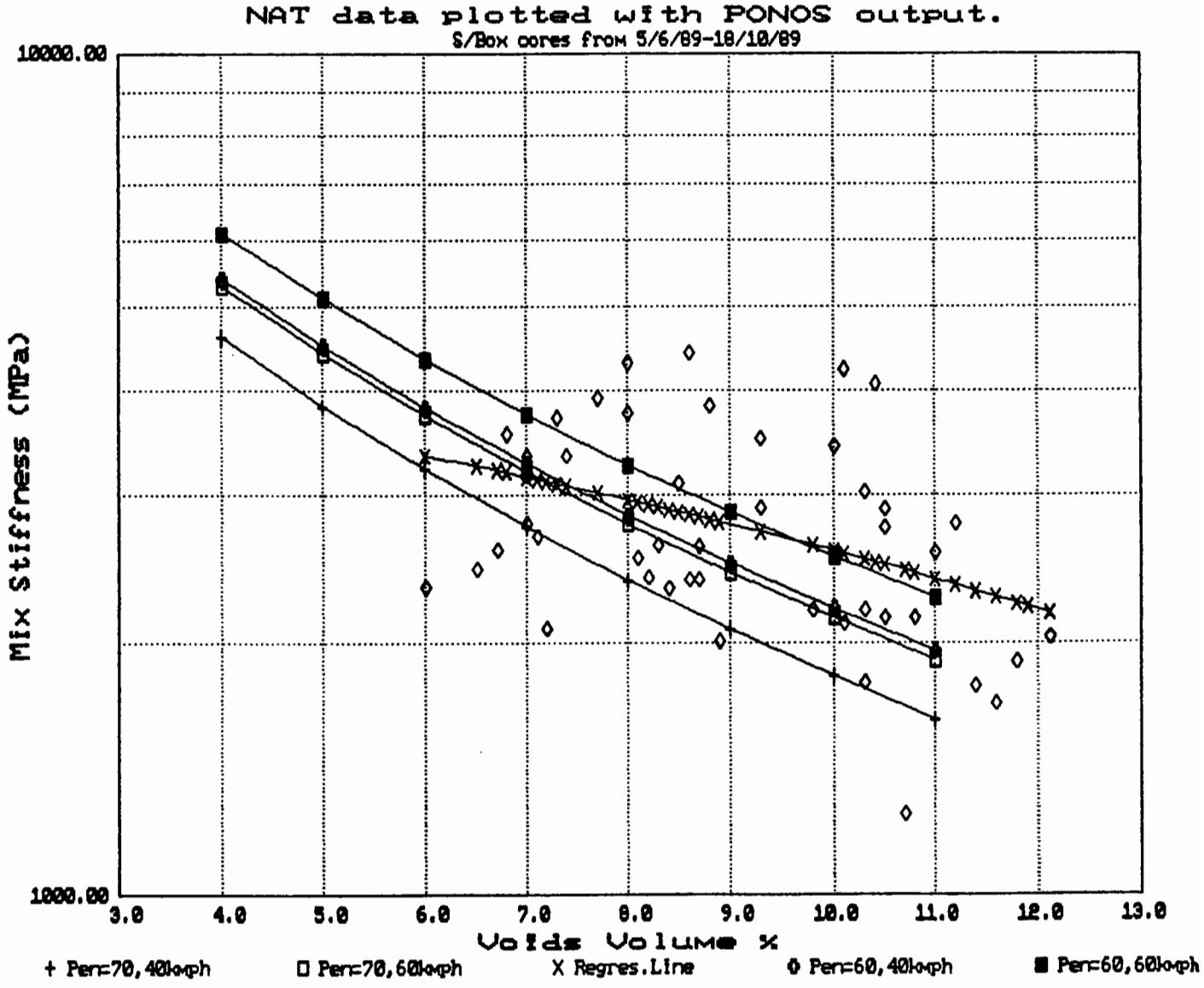

Figure A.14 Plot of Mix Stiffness Against Voids Volume for Shear Box Test Cores. PONOS Lines for Both 60 and 70 Pen Binder and Traffic Speeds of 40 and 60 km/hr Show Predicted Mix Stiffnesses

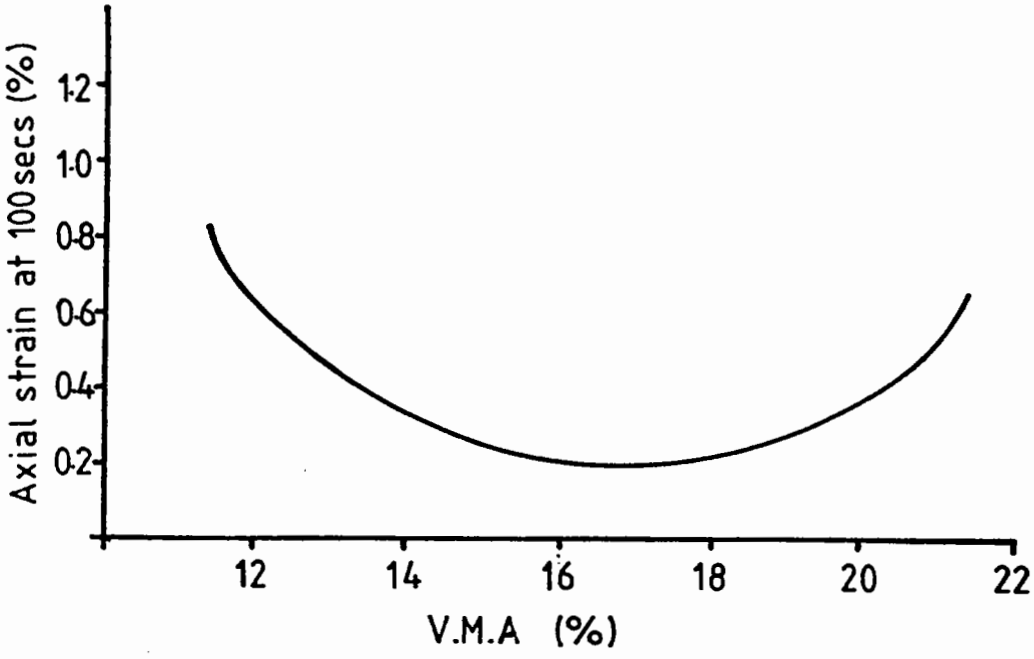

Figure A.15 **Typical Plot of the Effect of Compaction on Resistance to Deformation**

APPENDIX B

COMPUTER PROGRAM LISTING

```
120 PRINT @ PRINT @ PRINT
140 DIM A(2000),T(200)
160 CLEAR
180 DISP "DATE ?" @ INPUT D$
200 PRINT "Date= ";D$
220 DIM N$[40]
240 DISP "SPECIMEN NAME ? " @ IN
    PUT N$
260 PRINT "Specimen= ";N$
280 DISP "No. of strips ? " @ IN
    PUT S
300 PRINT "No. of strips= ";S
320 PRINT @ PRINT
340 FOR N=1 TO S @ S1(N)=-1 @ NE
    XT N
360 C=0 @ REM NO. OF READINGS
370 GOTO 2000
380 ON KEY# 1,"START" GOTO 480
400 ON KEY# 2,"PAUSE" GOSUB 1140
420 ON KEY# 3,"FINISH" GOSUB 120
    0
440 CLEAR @ KEY LABEL
450 DISP @ DISP @ DISP
455 DISP "Press 'START' when loa
    d"
456 DISP "cycling started"
460 GOTO 460
480 ON TIMER# 1,60000 GOTO 500
500 DIM A$[100]
520 A$="A,PA6144,G0,I0,I1,I2,I3,
    I4,I5,I6,I7, QS1,F1,IC2,0E"
    @ GOSUB 820
540 A$="PA6144,QI" @ GOSUB 820
560 ENTER 709 ; A(1),A(2),A(3),A
    (4),A(5),A(6),A(7),A(8)
580 SEND 7 ; UNT
600 RESUME 7
620 CLEAR @ KEY LABEL
640 FOR I=1 TO S
660 DISP I,A(I)
680 IF C=0 THEN B(I)=A(I)
700 NEXT I
720 T=C
740 DISP "Time= ";T;" minutes"
760 IF C>0 THEN GOSUB 940
780 C=C+1
800 GOTO 800
820 OUTPUT 709 ;A$
840 SEND 7 ; UNL
860 RESUME 7
880 RETURN
900 GOTO 480
920 END
940 REM
960 FOR J=1 TO S
980 IF A(J)>B(J)-15000 THEN 1100
1000 IF S1(J)>0 THEN 1100
1020 S1(J)=1
1040 PRINT
1060 PRINT "AT ";T;"minutes"
1080 PRINT "Strip ";J;" broke"
1100 NEXT J
1105 IF T<5 THEN GOSUB 1240
1110 IF T/5=INT(T/5) THEN GOSUB
     1240
1120 RETURN
1140 CLEAR @ DISP "PRESS 'CONT'
     TO CONTINUE"
1160 PAUSE
1180 RETURN
1200 CLEAR @ PRINT @ PRINT "TER
     INATED"
1220 END
1240 A$="A,PA6144,I0,I1,QS200 ,S
     0,F0,IC2,0E" @ GOSUB 1540
1260 A$="PA6144,QI" @ GOSUB 154
1280 X1=-30000 @ X2=30000
1300 Y1=-30000 @ Y2=30000
1320 FOR M=1 TO 200
1340 ENTER 710 ; X(M),Y(M)
1350 SEND 7 ; UNT
1355 RESUME 7
1360 IF X(M)>X1 THEN X1=X(M)
1380 IF X(M)<X2 THEN X2=X(M)
1400 IF Y(M)>Y1 THEN Y1=Y(M)
1420 IF Y(M)<Y2 THEN Y2=Y(M)
1440 NEXT M
1500 D1=ABS(X1-X2)*.000202
1510 D2=(X3-(X1+X2)/2)*.000202
1512 PRINT "Time= ";T;" mins"
1514 PRINT "Amplitude= ";D1;" m
     "
1516 PRINT "Offset= ";D2;" mm"
1517 PRINT
1520 RETURN
1540 OUTPUT 710 ;A$
1560 SEND 7 ; UNL
1580 RESUME 7
1600 RETURN
2000 CLEAR
2050 DISP @ DISP @ DISP
2060 DISP "Press 'START' to take
      zero"
2070 DISP "LVDT readings"
2100 ON KEY# 1,"START" GOTO 2200
2150 KEY LABEL
2160 GOTO 2160
2200 REM
2240 A$="A,PA6144,I0,I1,QS50 ,S0
     0,F1,IC2,0E" @ GOSUB 2540
2260 A$="PA6144,QI" @ GOSUB 2540
2270 X3=0
2320 FOR M=1 TO 50
2340 ENTER 710 ; X(M),Y(M)
2350 X3=X3+X(M)
2352 SEND 7 ; UNT
2355 RESUME 7
2440 NEXT M
2500 X3=X3/50
2510 OFF KEY# 1
2515 CLEAR
2520 GOTO 380
2540 OUTPUT 710 ;A$
2560 SEND 7 ; UNL
2580 RESUME 7
2600 RETURN
```

APPENDIX C

SHEAR BOX TEST RESULTS

APPENDIX D

BEAM TESTING RESULTS FOR BOTH CRACK GROWTH AND STRAIN VS NUMBER OF CYCLES

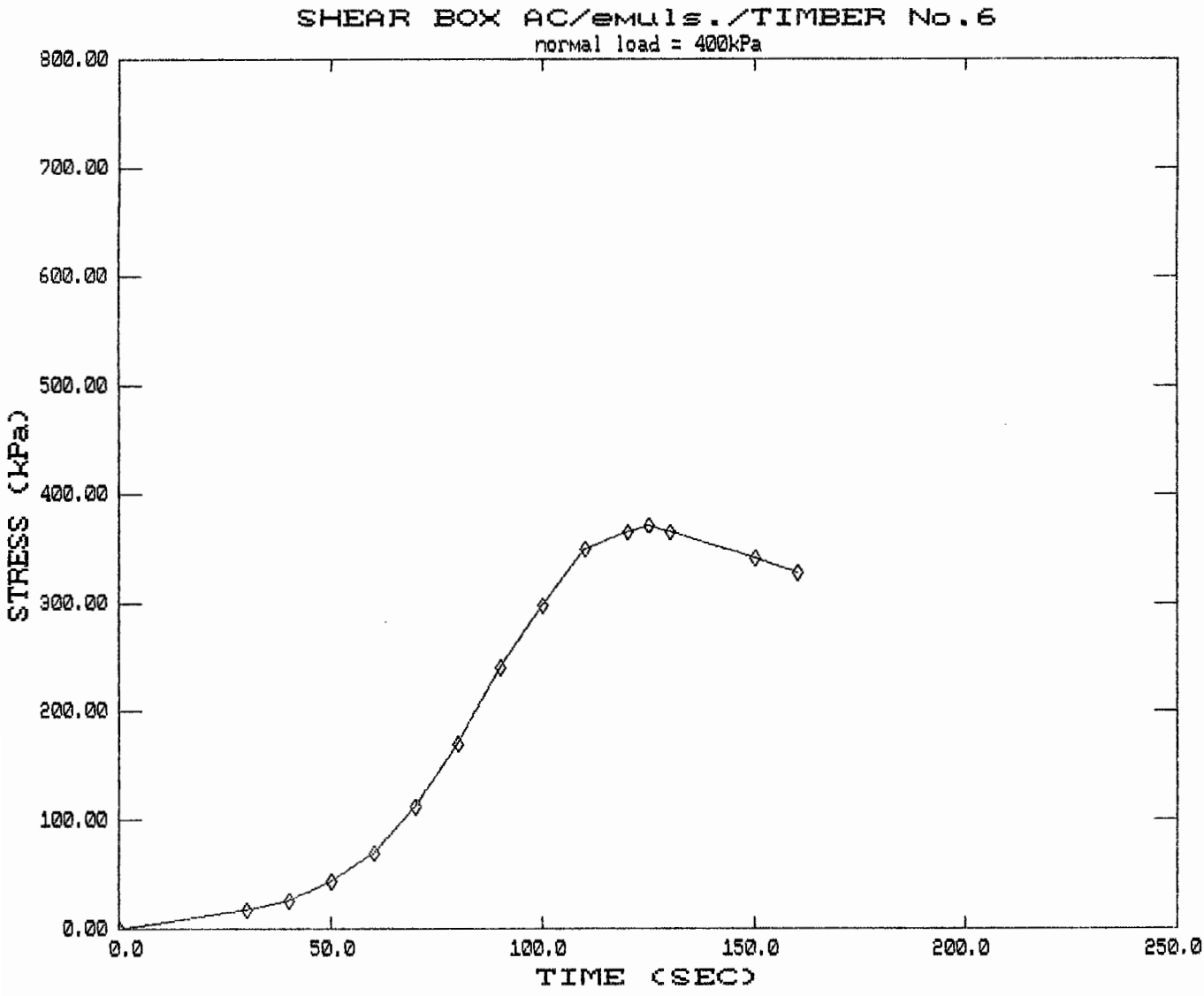
SHEAR BOX AC/emuls./TIMBER No.6
normal load = 400kPa
800.00
700.00
600.00
500.00
400.00
300.00
200.00
100.00
0.00
STRESS (kPa)
0.0
50.0
100.0
150.0
200.0
250.0
TIME (SEC)

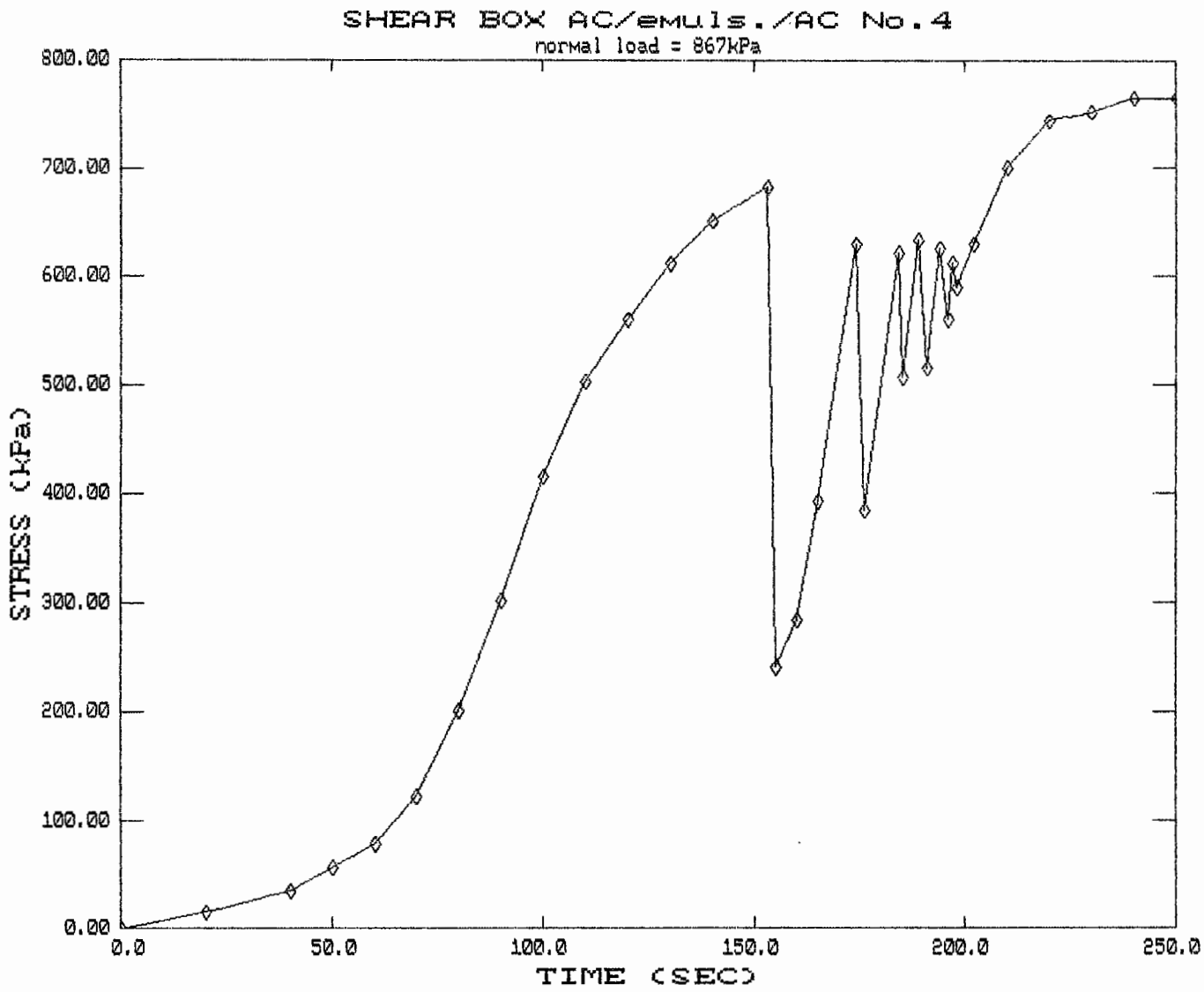
SHEAR BOX AC/emuls./AC No.4
normal load = 867kPa
800.00
700.00
600.00
500.00
400.00
300.00
200.00
100.00
0.00
STRESS (kPa)
0.0
50.0
100.0
150.0
200.0
250.0
TIME (SEC)

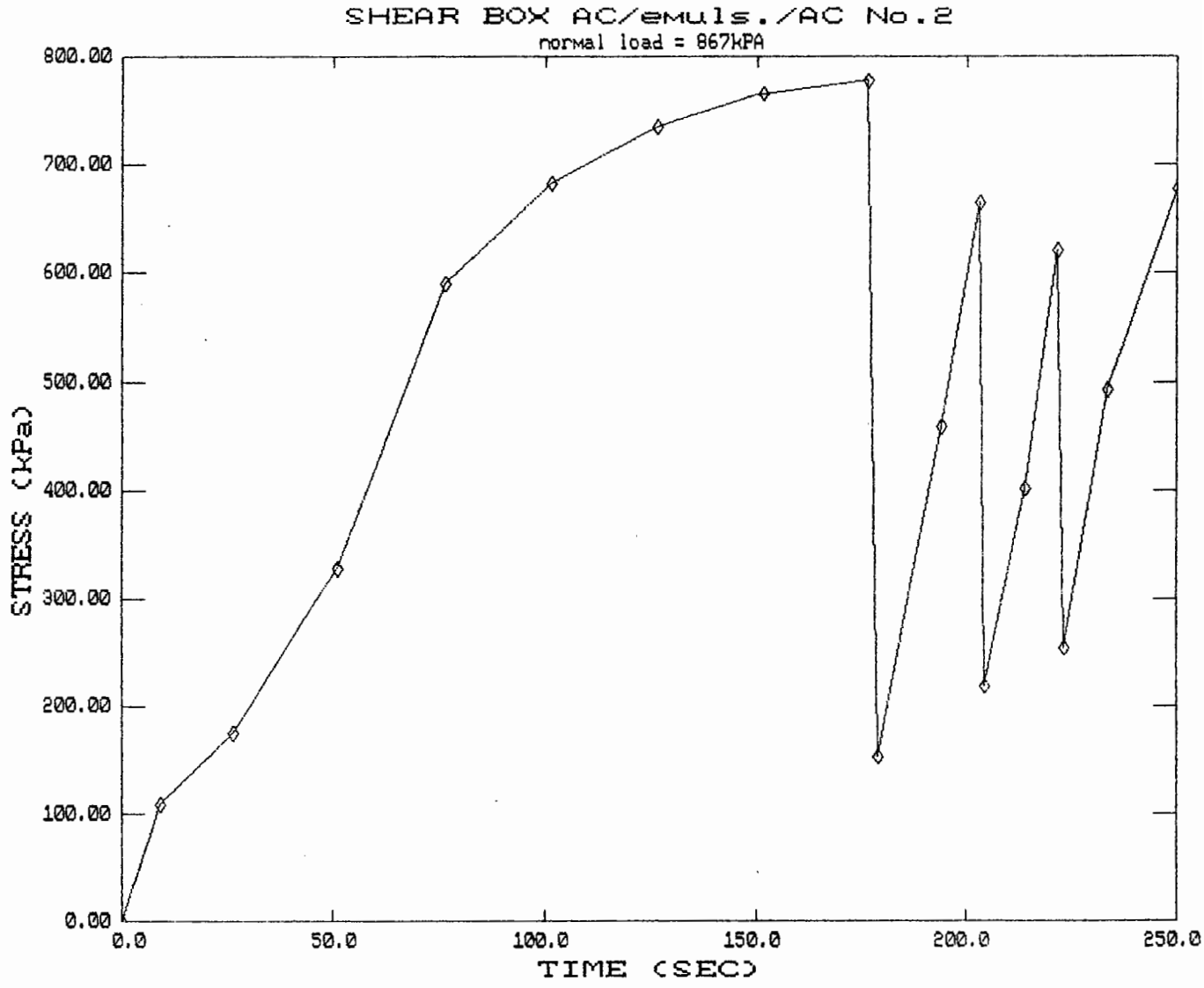
SHEAR BOX AC/emuls./AC No.2
normal load = 867kPA
STRESS (kPa)
800.00
700.00
600.00
500.00
400.00
300.00
200.00
100.00
0.00
0.0
50.0
100.0
150.0
200.0
250.0
TIME (SEC)

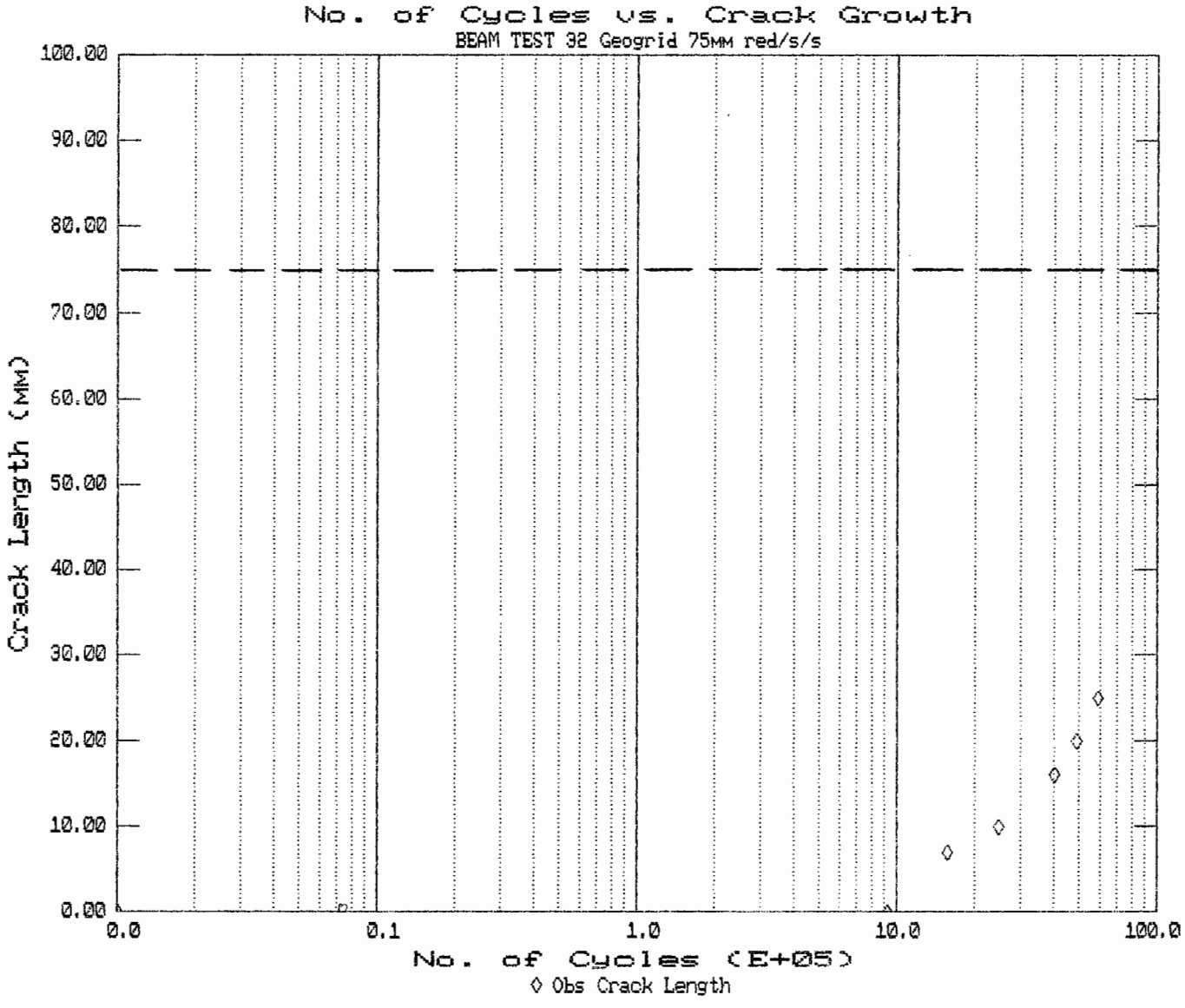
No. of Cycles vs. Crack Growth
BEAM TEST 32 Geogrid 75MM red/s/s
Crack Length (MM)
100.00
90.00
80.00
70.00
60.00
50.00
40.00
30.00
20.00
10.00
0.00
0.0
0.1
1.0
10.0
100.0
No. of Cycles (E+05)
◊ Obs Crack Length

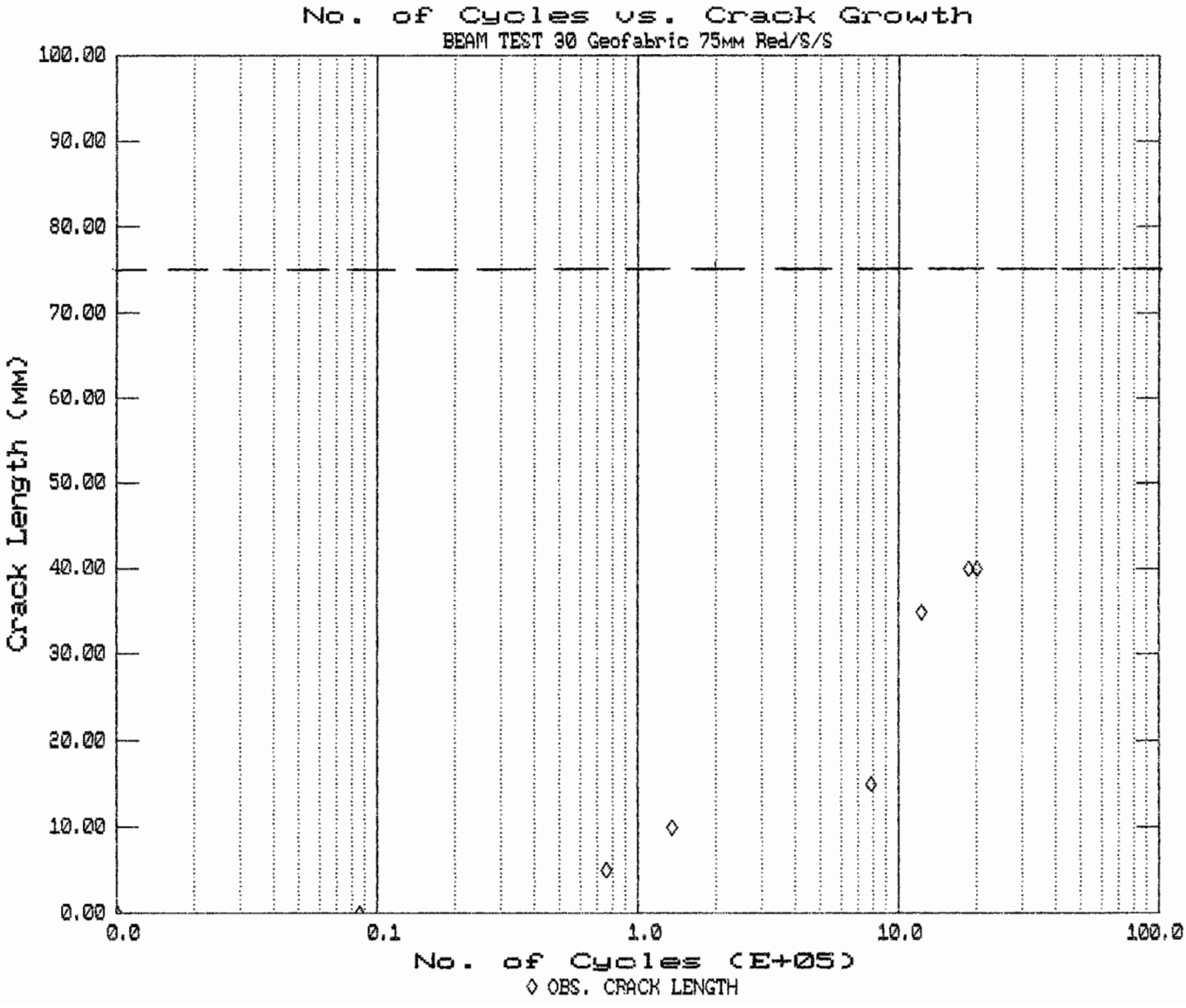
No. of Cycles vs. Crack Growth
BEAM TEST 30 Geofabric 75MM Red/S/S
100.00
90.00
80.00
70.00
60.00
50.00
40.00
30.00
20.00
10.00
0.00
Crack Length (MM)
0.0
0.1
1.0
10.0
100.0
No. of Cycles (E+05)
◊ OBS. CRACK LENGTH

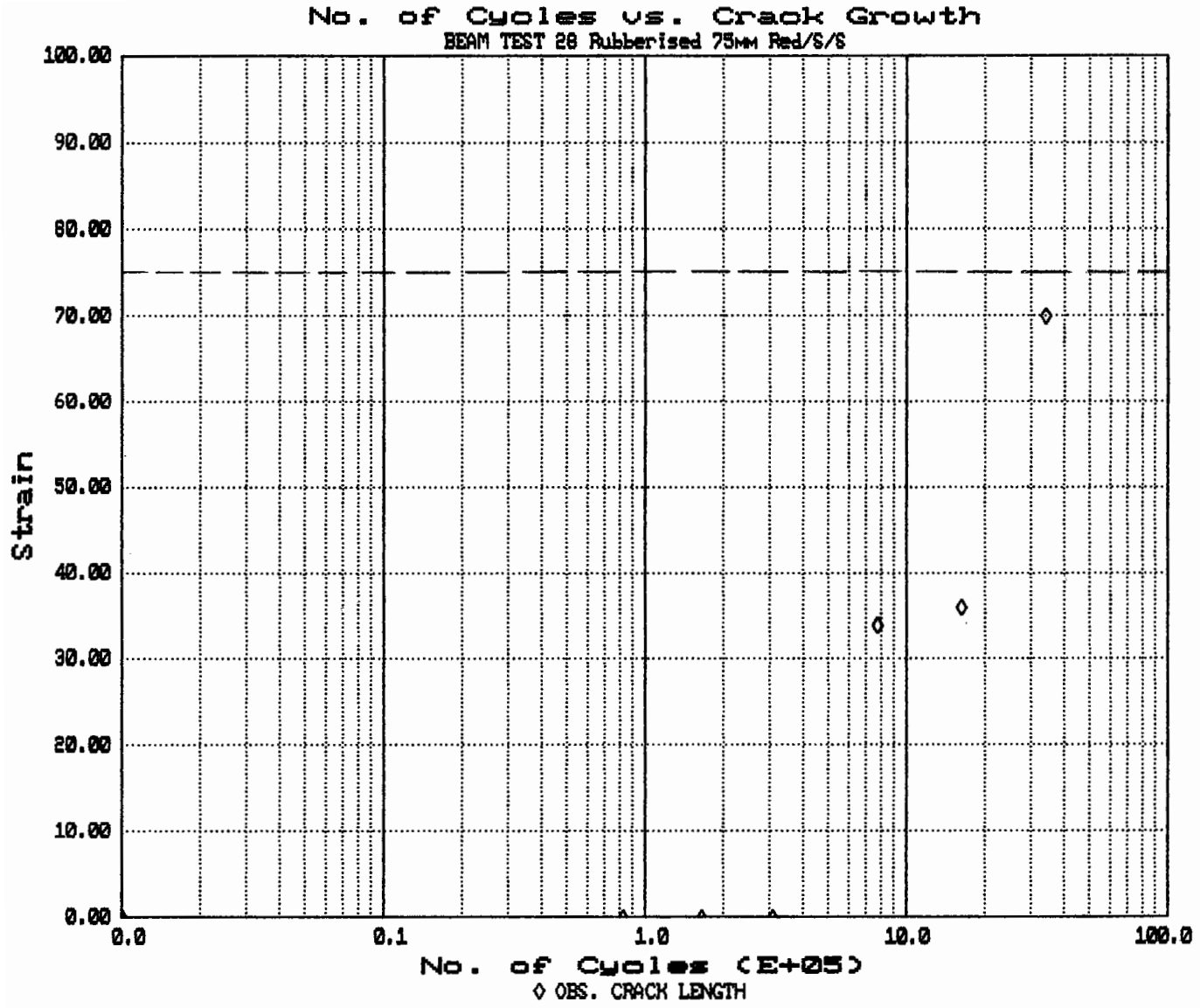
No. of Cycles vs. Crack Growth
BEAM TEST 28 Rubberised 75mm Rad/S/S
100.00
90.00
80.00
70.00
60.00
50.00
40.00
30.00
20.00
10.00
0.00
Strain
0.0
0.1
1.0
10.0
100.0
No. of Cycles (E+05)
◊ OBS. CRACK LENGTH

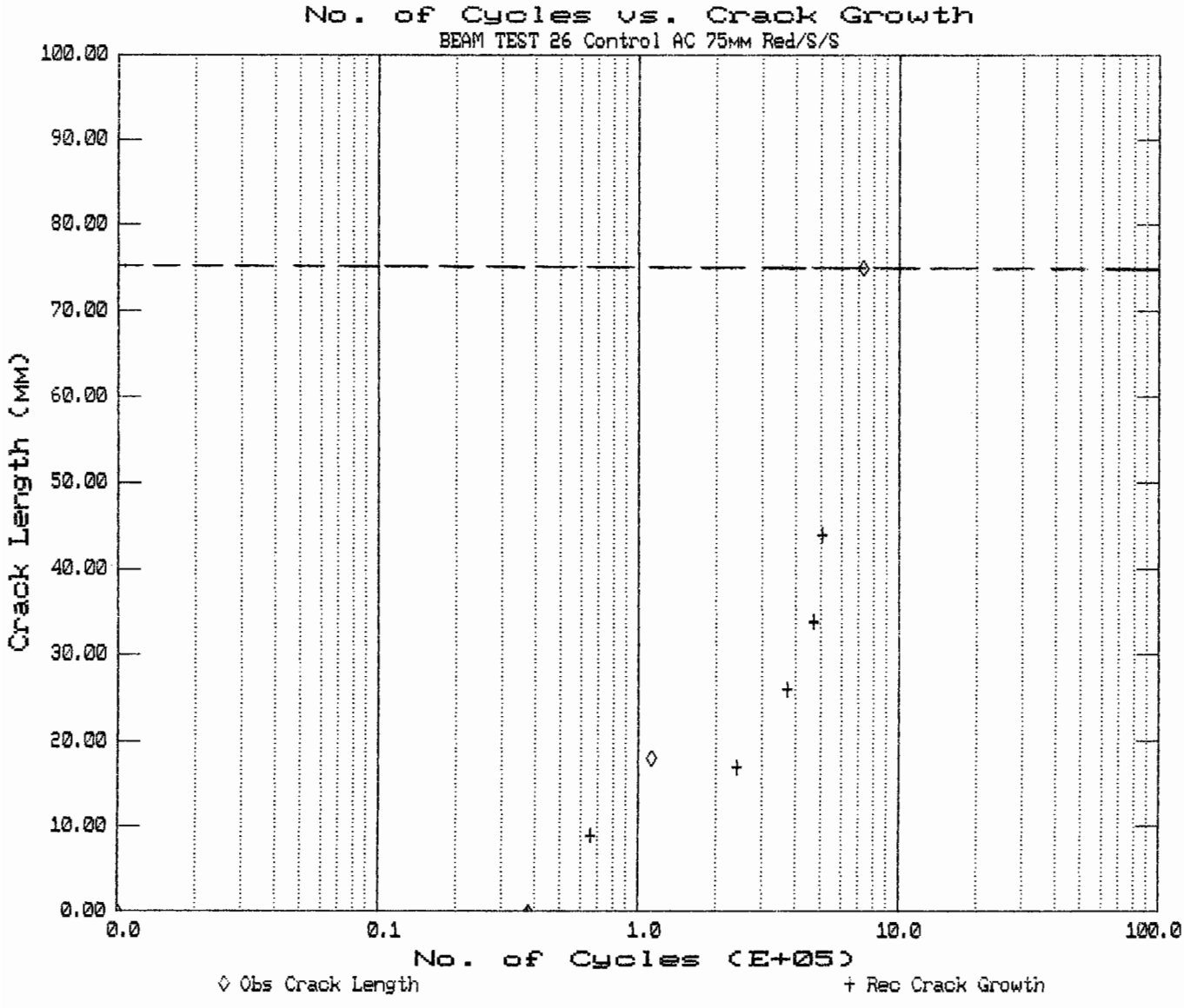
No. of Cycles vs. Crack Growth
BEAM TEST 26 Control AC 75MM Red/S/S
100.00
90.00
80.00
70.00
60.00
50.00
40.00
30.00
20.00
10.00
0.00
Crack Length (MM)
0.0
0.1
1.0
10.0
100.0
No. of Cycles (E+05)
◊ Obs Crack Length
+ Rec Crack Growth

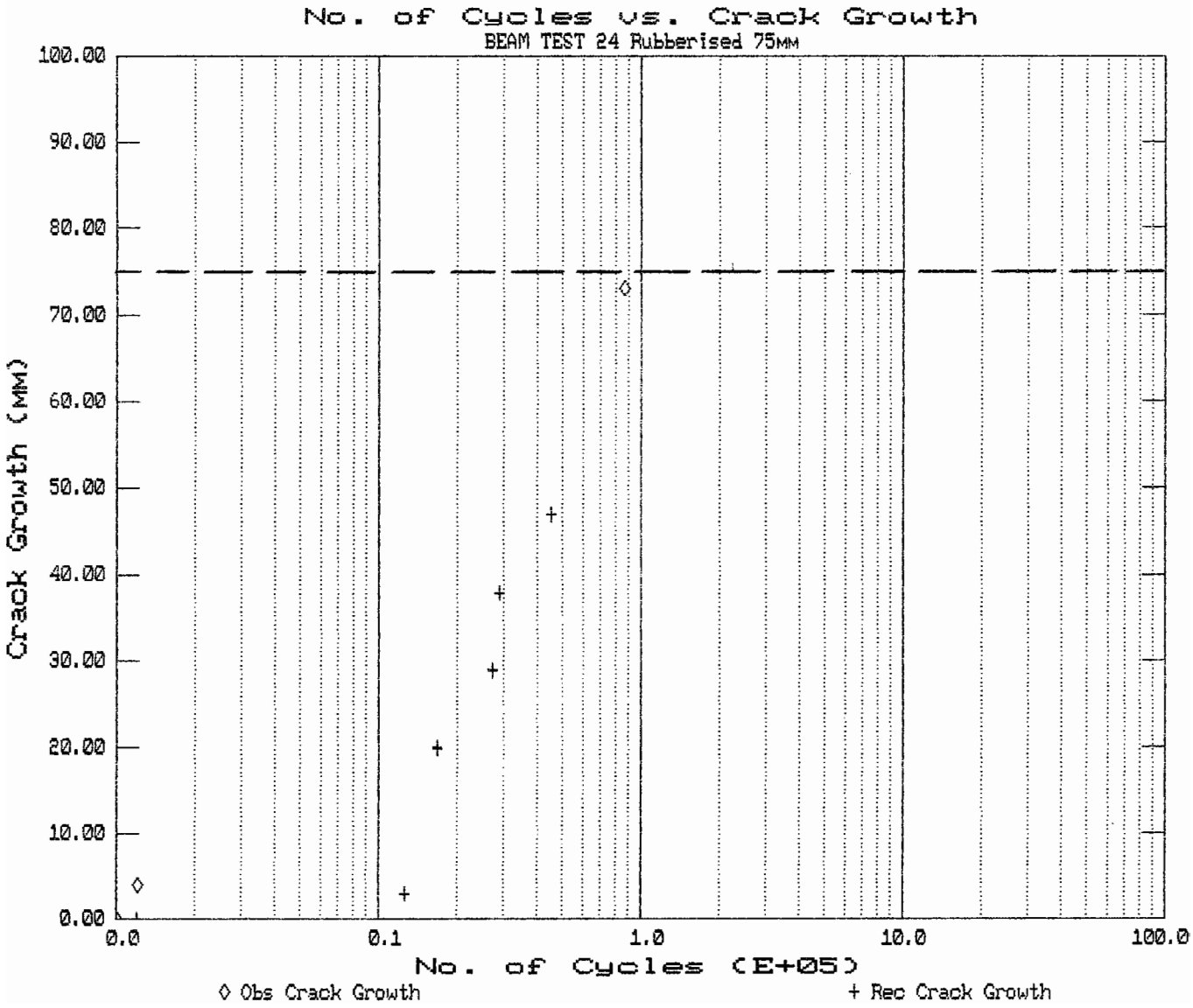
No. of Cycles vs. Crack Growth
BEAM TEST 24 Rubberised 75MM
100.00
90.00
80.00
70.00
60.00
50.00
40.00
30.00
20.00
10.00
0.00
Crack Growth (MM)
0.0
0.1
1.0
10.0
100.0
No. of Cycles (E+05)
◊ Obs Crack Growth
+ Rec Crack Growth

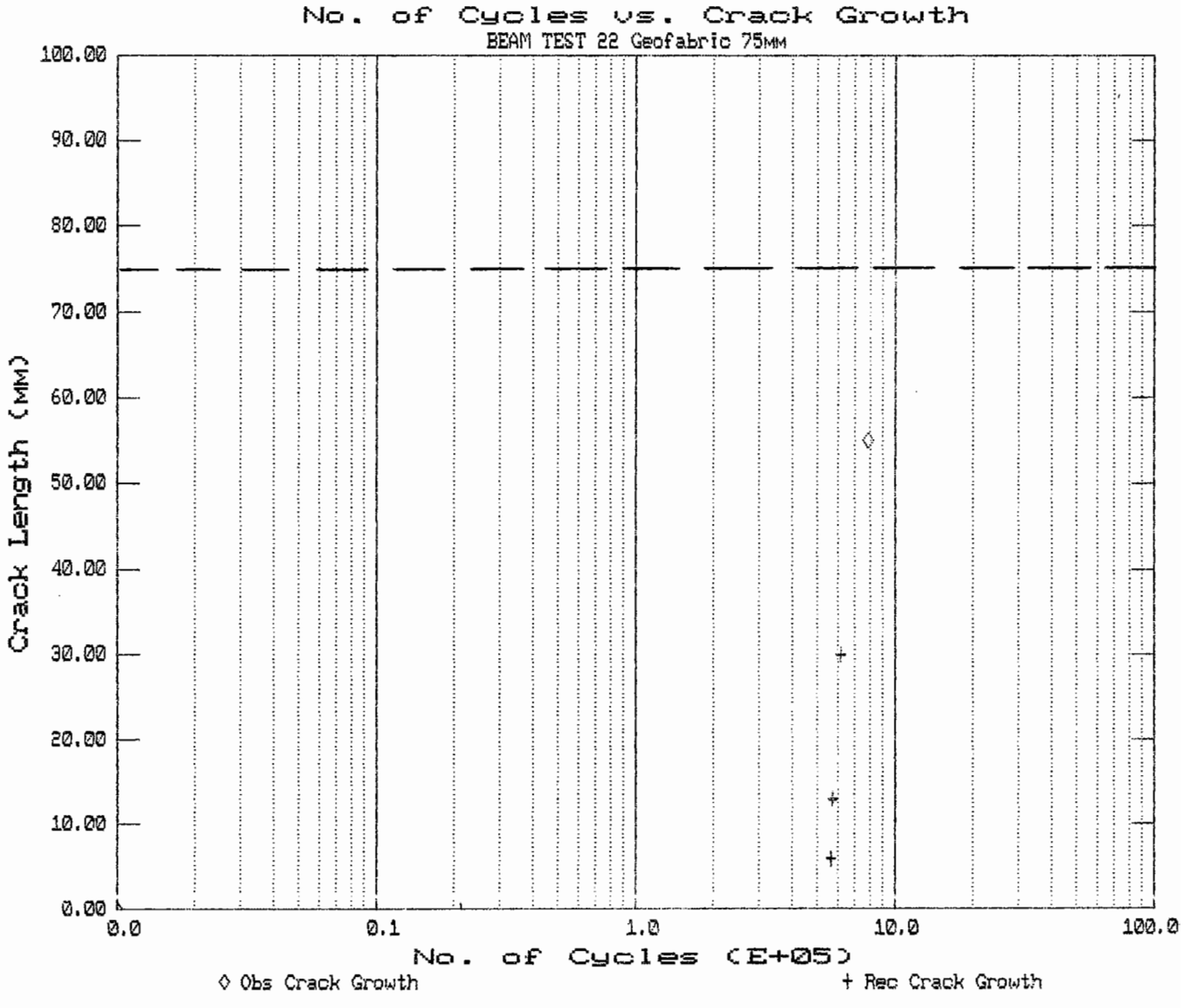
No. of Cycles vs. Crack Growth
BEAM TEST 22 Geofabric 75mm
Crack Length (mm)
100.00
90.00
80.00
70.00
60.00
50.00
40.00
30.00
20.00
10.00
0.00
0.0
0.1
1.0
10.0
100.0
No. of Cycles (E+05)
◊ Obs Crack Growth
+ Rec Crack Growth

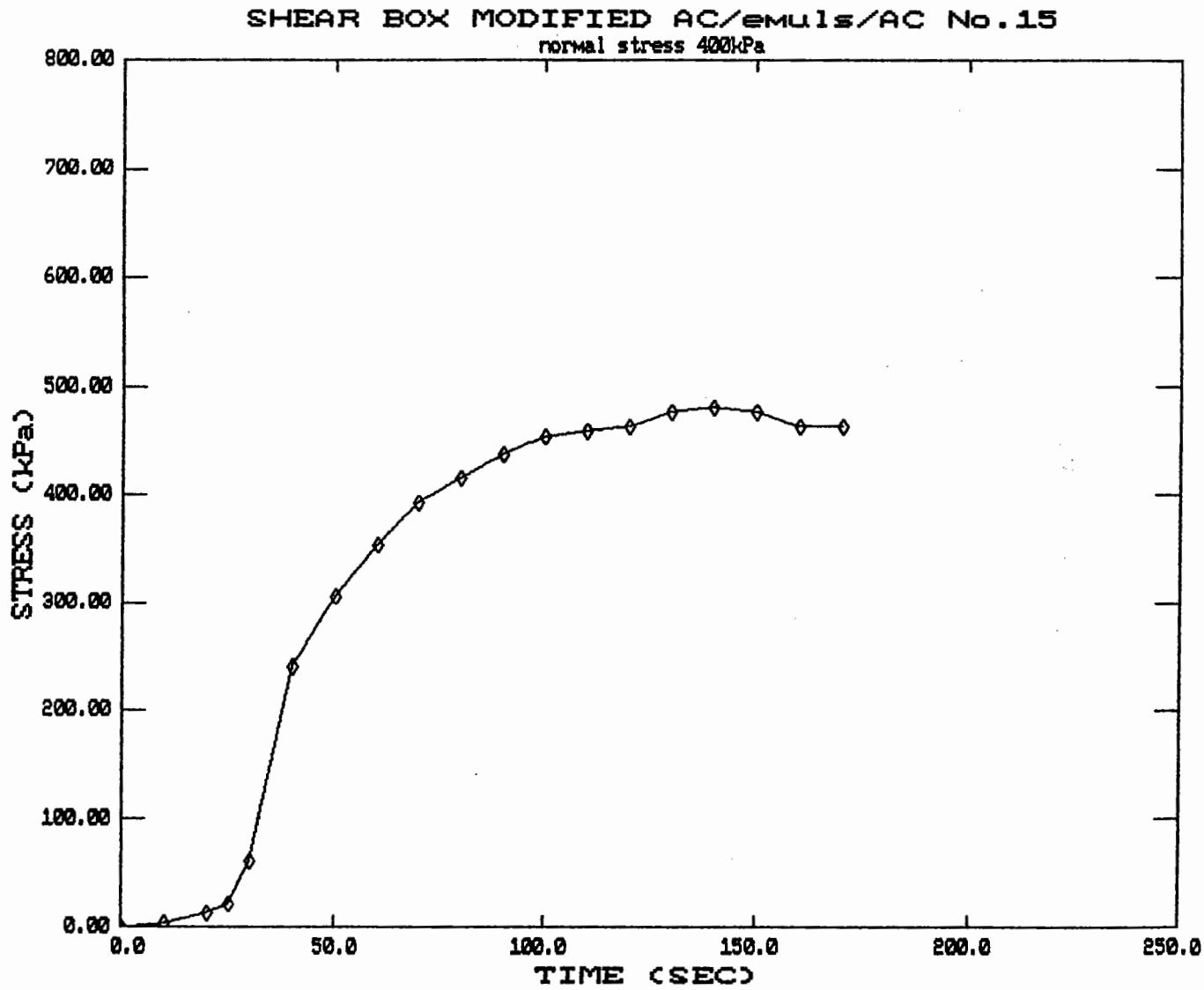
SHEAR BOX MODIFIED AC/emuls/AC No.15
normal stress 400kPa
800.00
700.00
600.00
500.00
400.00
300.00
200.00
100.00
0.00
STRESS (kPa)
0.0
50.0
100.0
150.0
200.0
250.0
TIME (SEC)

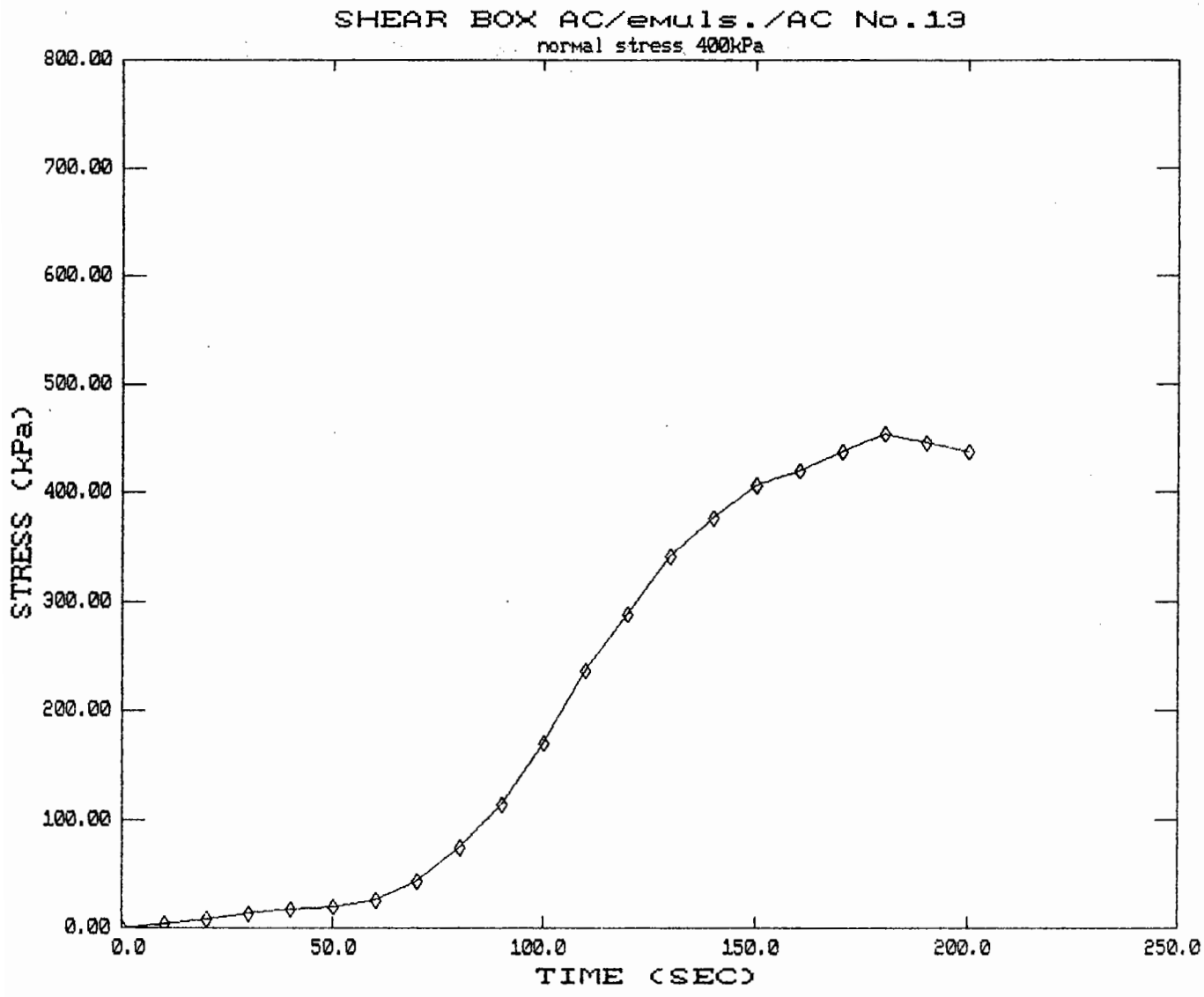
SHEAR BOX AC/emuls./AC No.13
normal stress 400kPa
STRESS (kPa)
800.00
700.00
600.00
500.00
400.00
300.00
200.00
100.00
0.00
0.0
50.0
100.0
150.0
200.0
250.0
TIME (SEC)

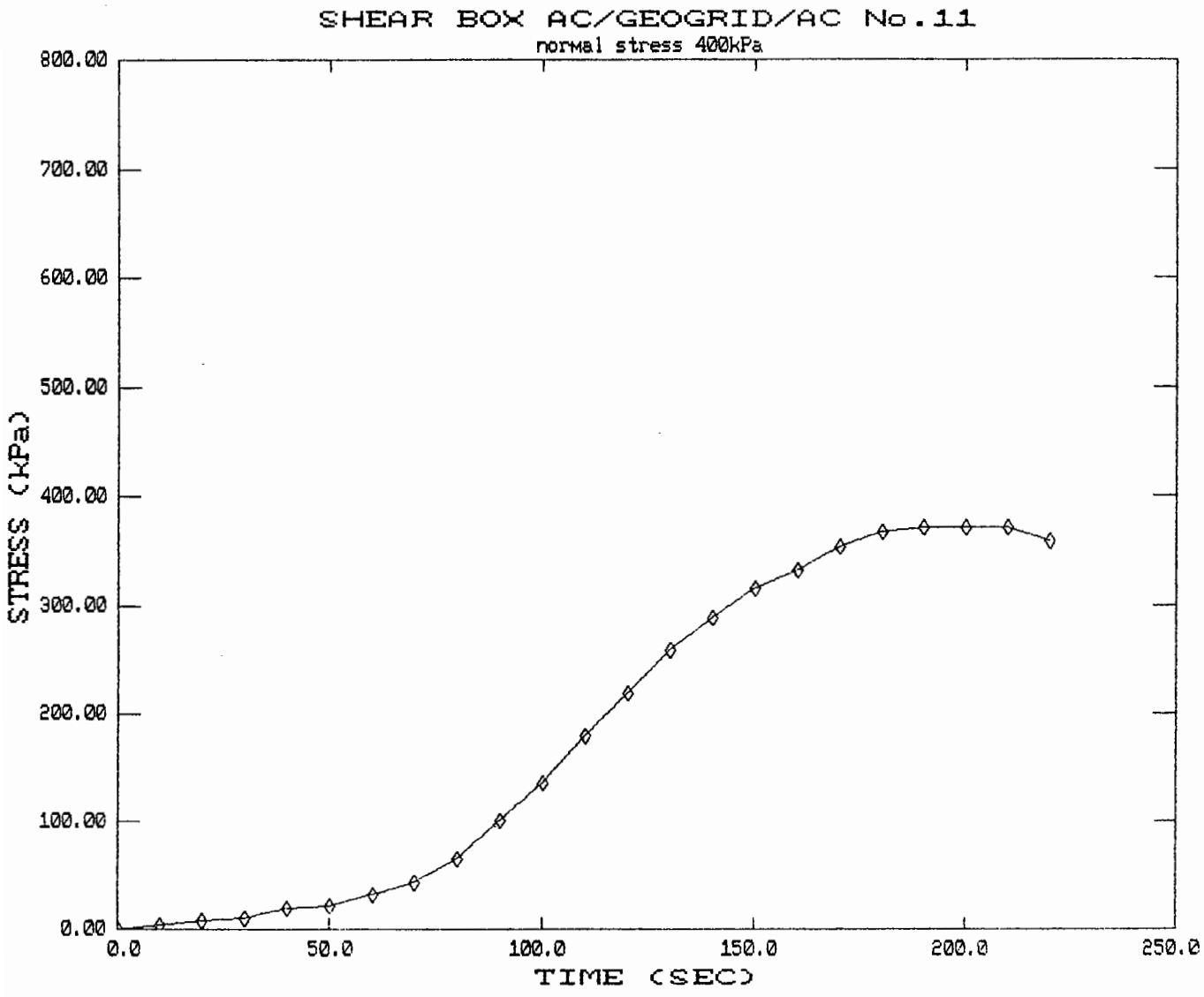
SHEAR BOX AC/GEOGRID/AC No.11
normal stress 400kPa
800.00
700.00
600.00
500.00
400.00
300.00
200.00
100.00
0.00
STRESS (kPa)
0.0
50.0
100.0
150.0
200.0
250.0
TIME (SEC)

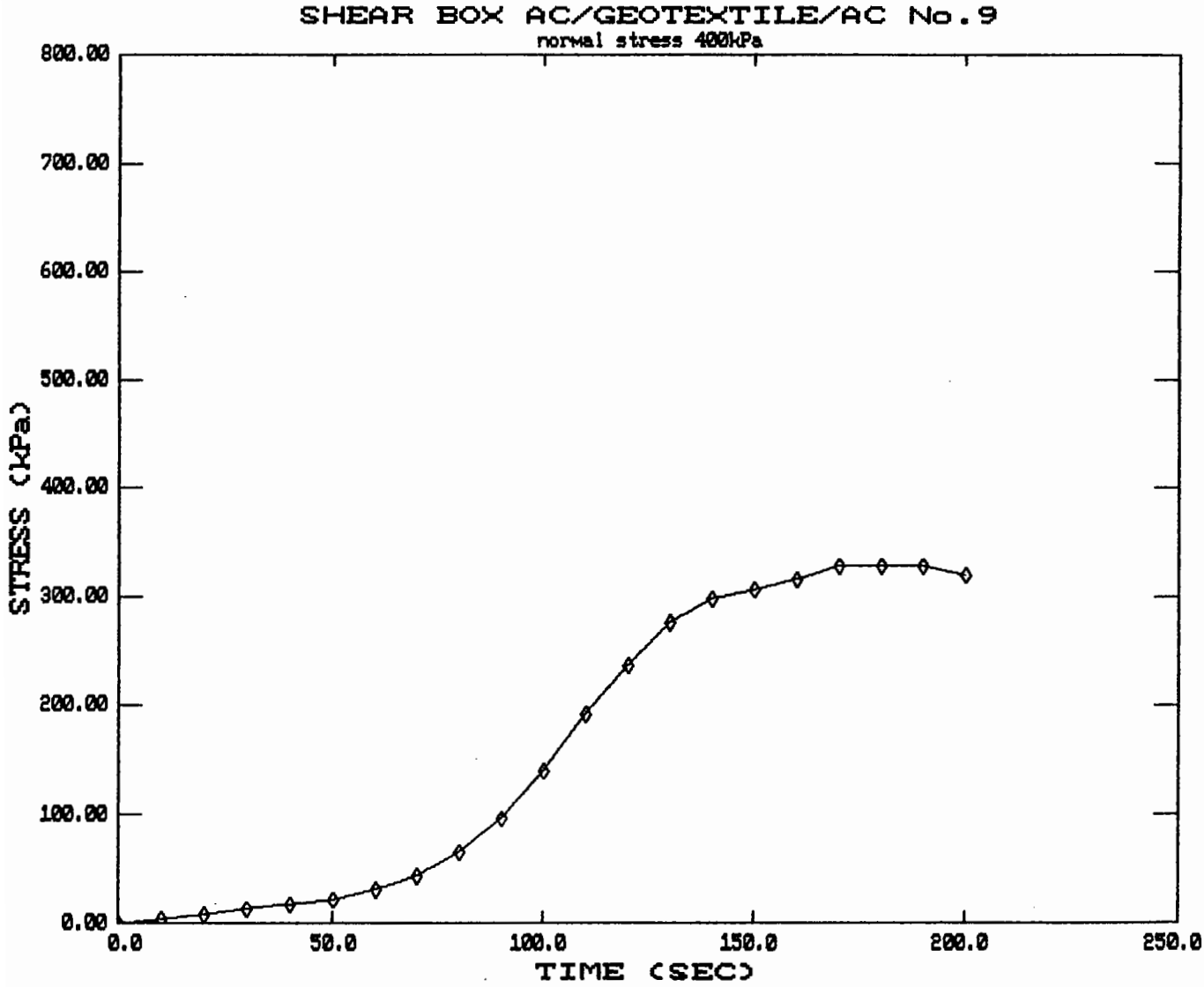
SHEAR BOX AC/GEOTEXTILE/AC No.9
normal stress 400kPa
800.00
700.00
600.00
500.00
400.00
300.00
200.00
100.00
0.00
STRESS (kPa)
0.0
50.0
100.0
150.0
200.0
250.0
TIME (SEC)

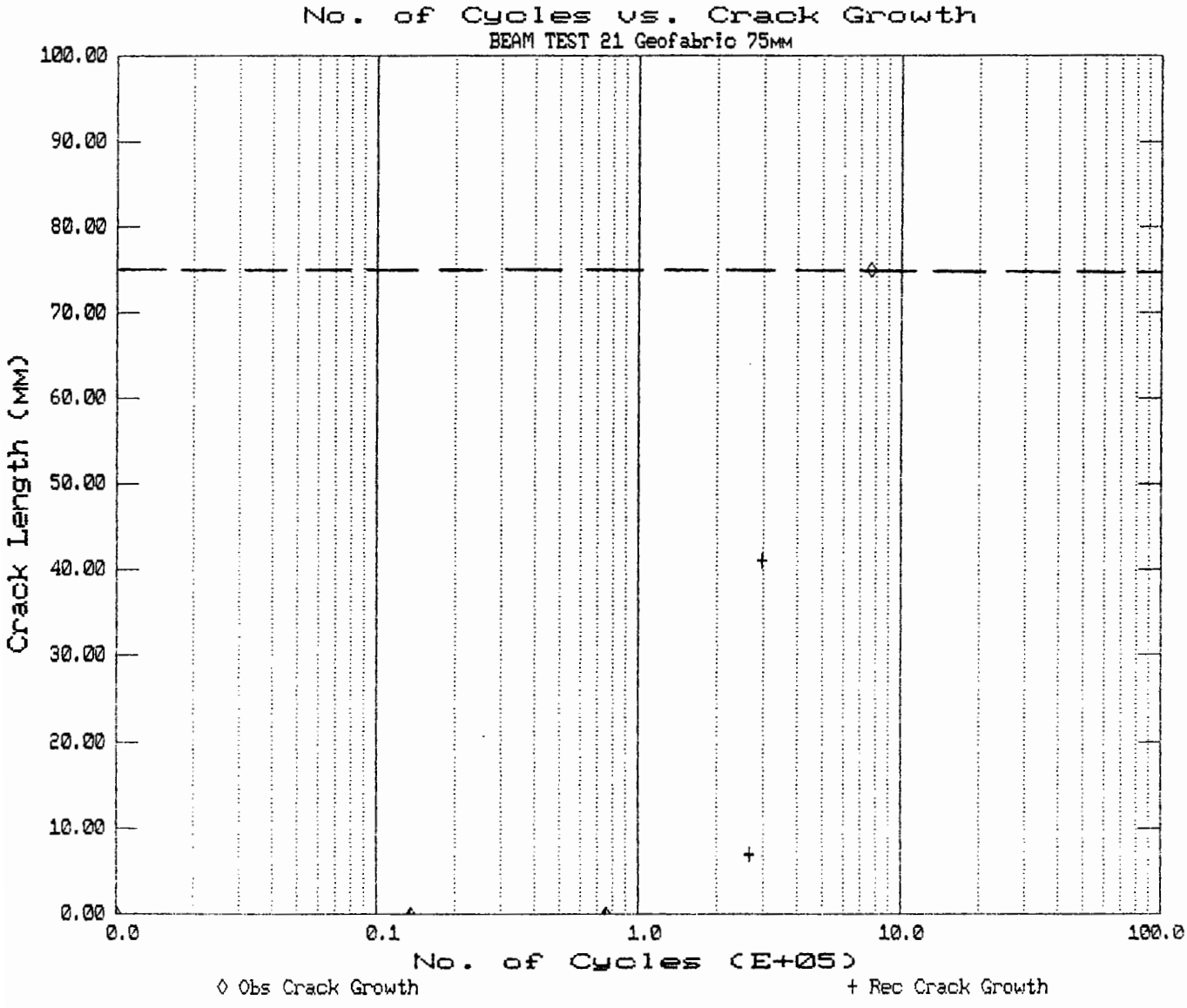
No. of Cycles vs. Crack Growth
BEAM TEST 21 Geofabric 75mm
Crack Length (mm)
100.00
90.00
80.00
70.00
60.00
50.00
40.00
30.00
20.00
10.00
0.00
0.0
0.1
1.0
10.0
100.0
No. of Cycles (E+05)
◊ Obs Crack Growth
+ Rec Crack Growth

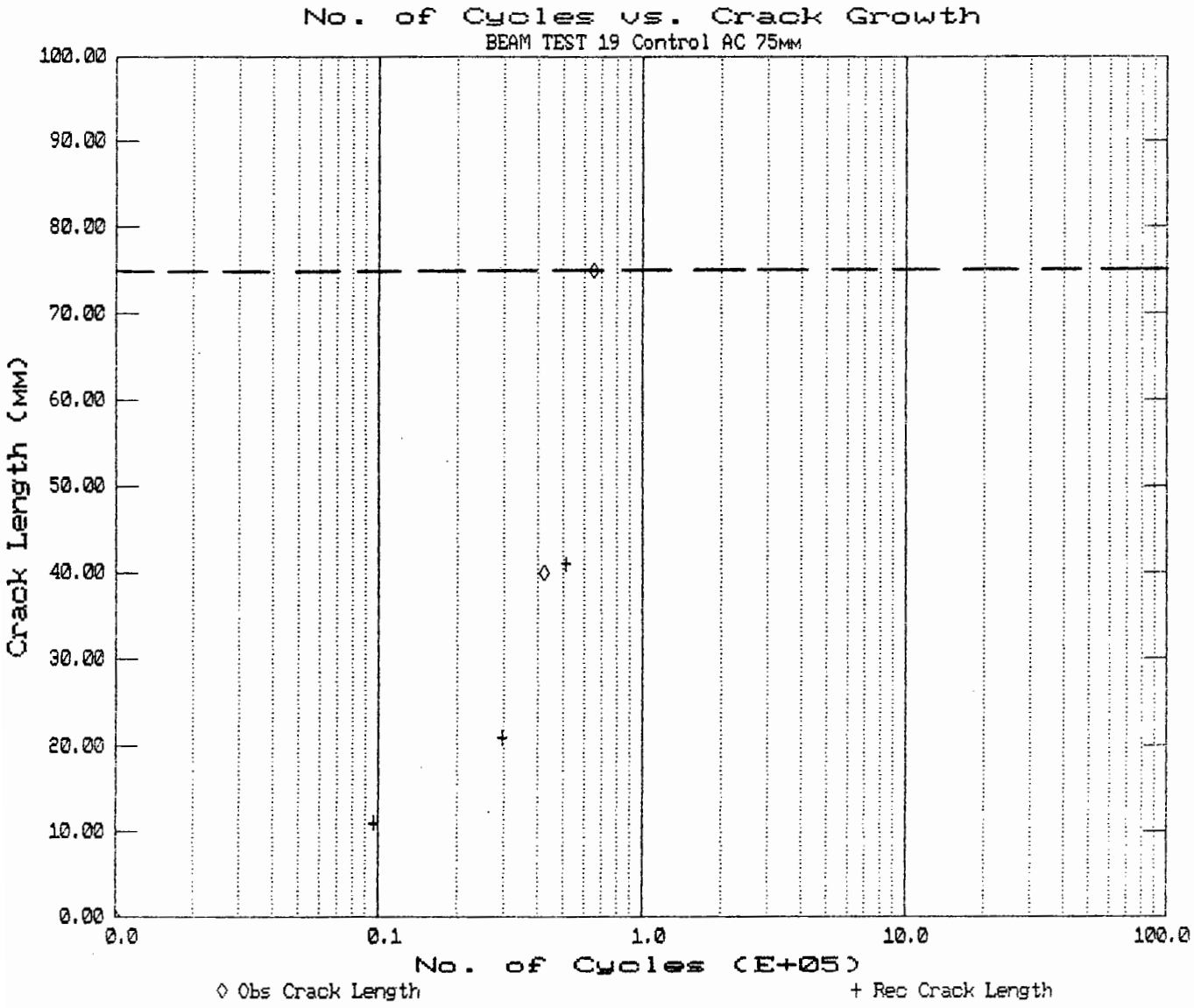
No. of Cycles vs. Crack Growth
BEAM TEST 19 Control AC 75MM
100.00
90.00
80.00
70.00
60.00
50.00
40.00
30.00
20.00
10.00
0.00
Crack Length (MM)
0.0
0.1
1.0
10.0
100.0
No. of Cycles (E+05)
◊ Obs Crack Length
+ Rec Crack Length

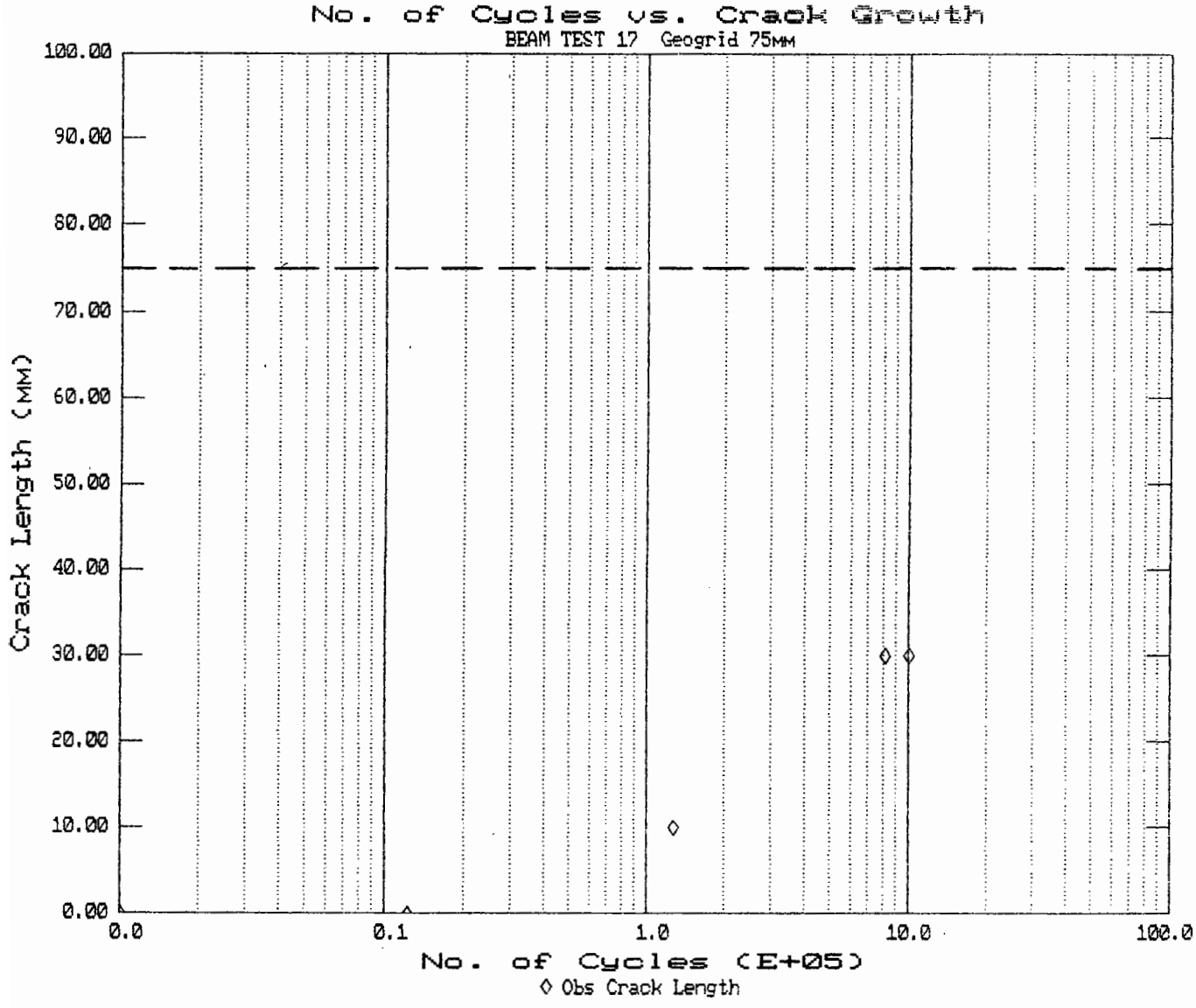
No. of Cycles vs. Crack Growth
BEAM TEST 17 Geogrid 75MM
100.00
90.00
80.00
70.00
60.00
50.00
40.00
30.00
20.00
10.00
0.00
Crack Length (MM)
0.0
0.1
1.0
10.0
100.0
No. of Cycles (E+05)
◊ Obs Crack Length

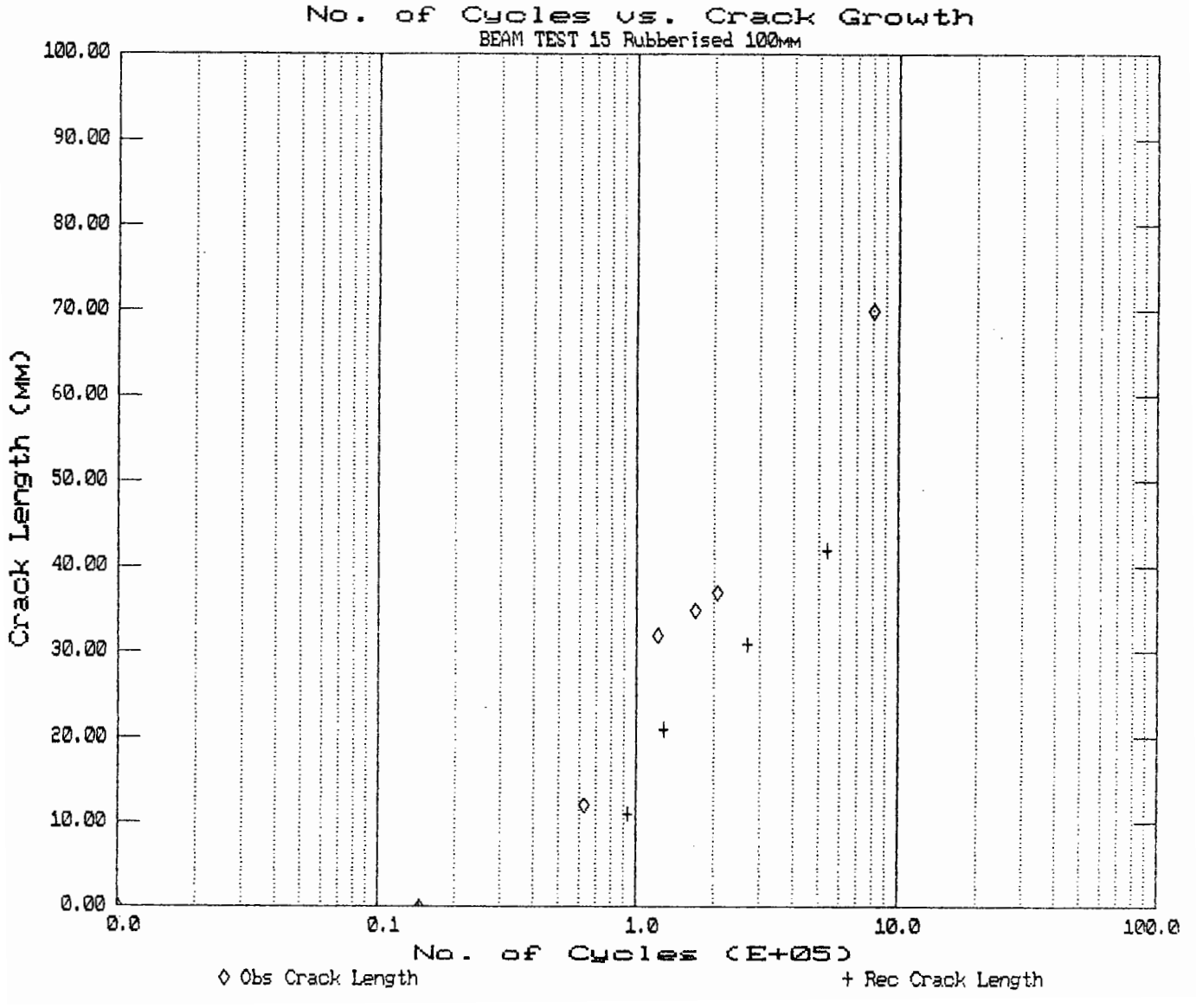
No. of Cycles vs. Crack Growth
BEAM TEST 15 Rubberised 100mm
Crack Length (mm)
100.00
90.00
80.00
70.00
60.00
50.00
40.00
30.00
20.00
10.00
0.00
0.0
0.1
1.0
10.0
100.0
No. of Cycles (E+05)
◊ Obs Crack Length
+ Rec Crack Length

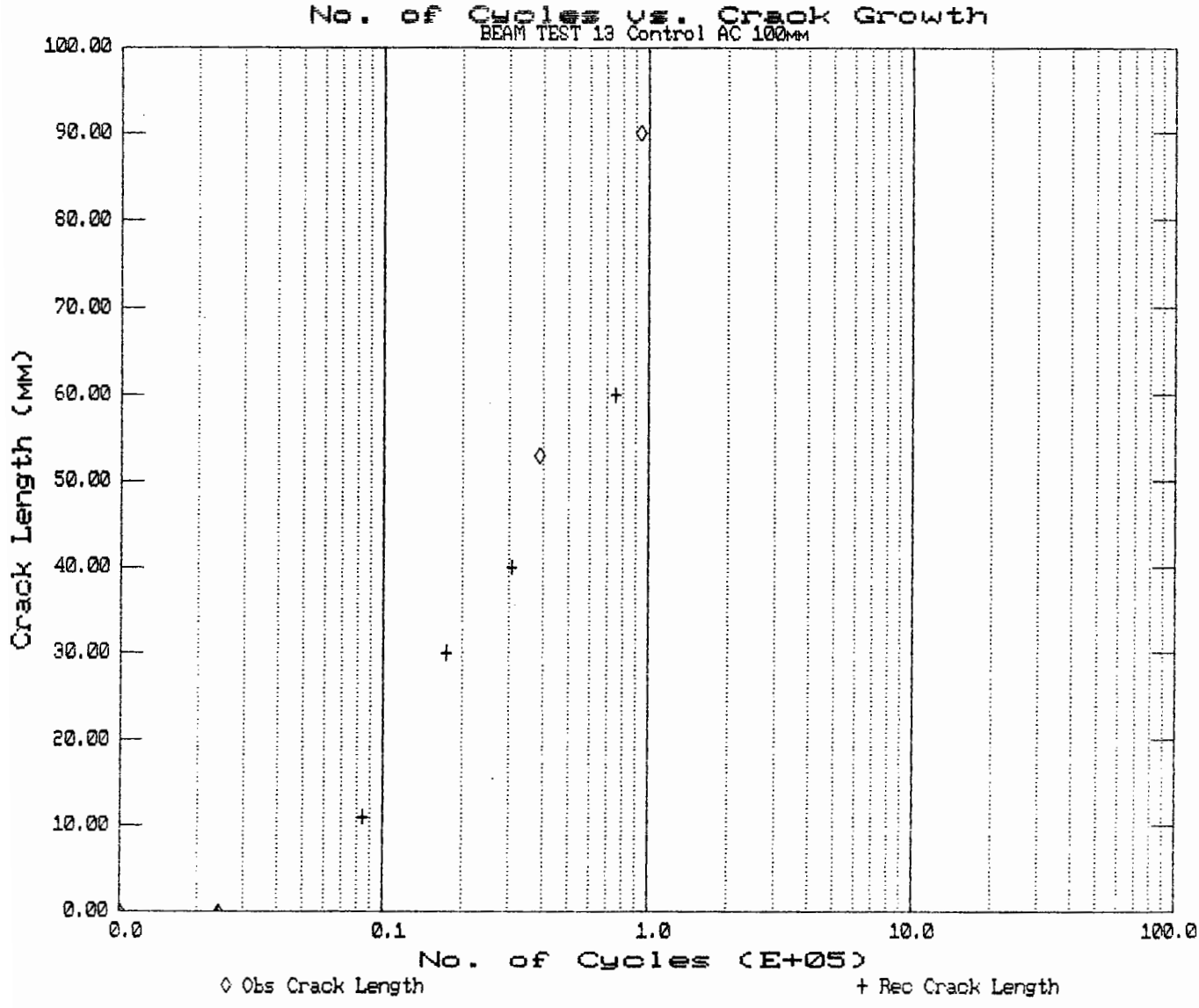
No. of Cycles vs. Crack Growth
BEAM TEST 13 Control AC 100mm
Crack Length (mm)
100.00
90.00
80.00
70.00
60.00
50.00
40.00
30.00
20.00
10.00
0.00
0.0
0.1
1.0
10.0
100.0
No. of Cycles (E+05)
◊ Obs Crack Length
+ Rec Crack Length

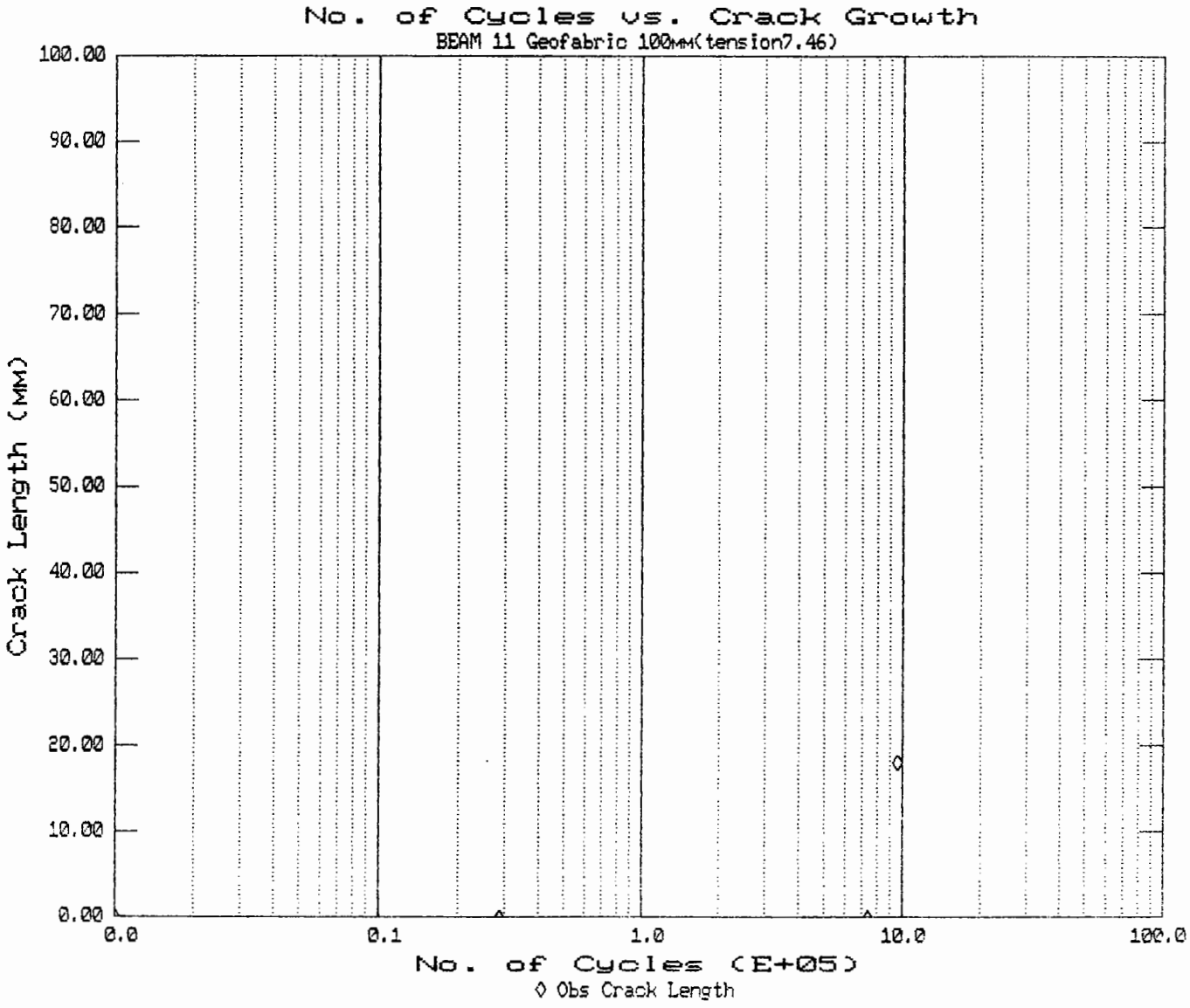
No. of Cycles vs. Crack Growth
BEAM 11 Geofabric 100mm(tension7.46)
Crack Length (mm)
100.00
90.00
80.00
70.00
60.00
50.00
40.00
30.00
20.00
10.00
0.00
0.0
0.1
1.0
10.0
100.0
No. of Cycles (E+05)
◊ Obs Crack Length

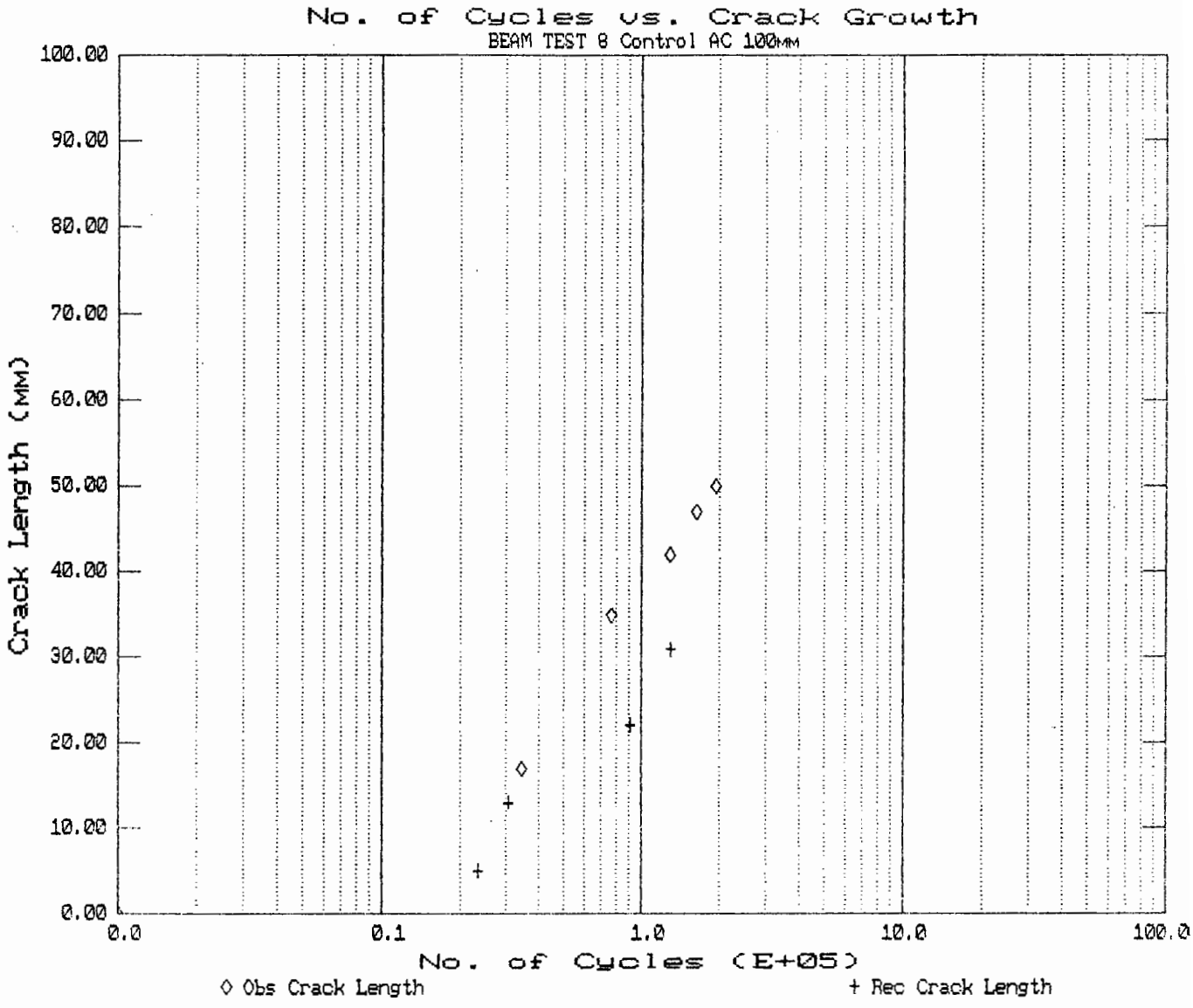
No. of Cycles vs. Crack Growth
BEAM TEST 8 Control AC 100MM
Crack Length (MM)
100.00
90.00
80.00
70.00
60.00
50.00
40.00
30.00
20.00
10.00
0.00
0.0
0.1
1.0
10.0
100.0
No. of Cycles (E+05)
◊ Obs Crack Length
+ Rec Crack Length

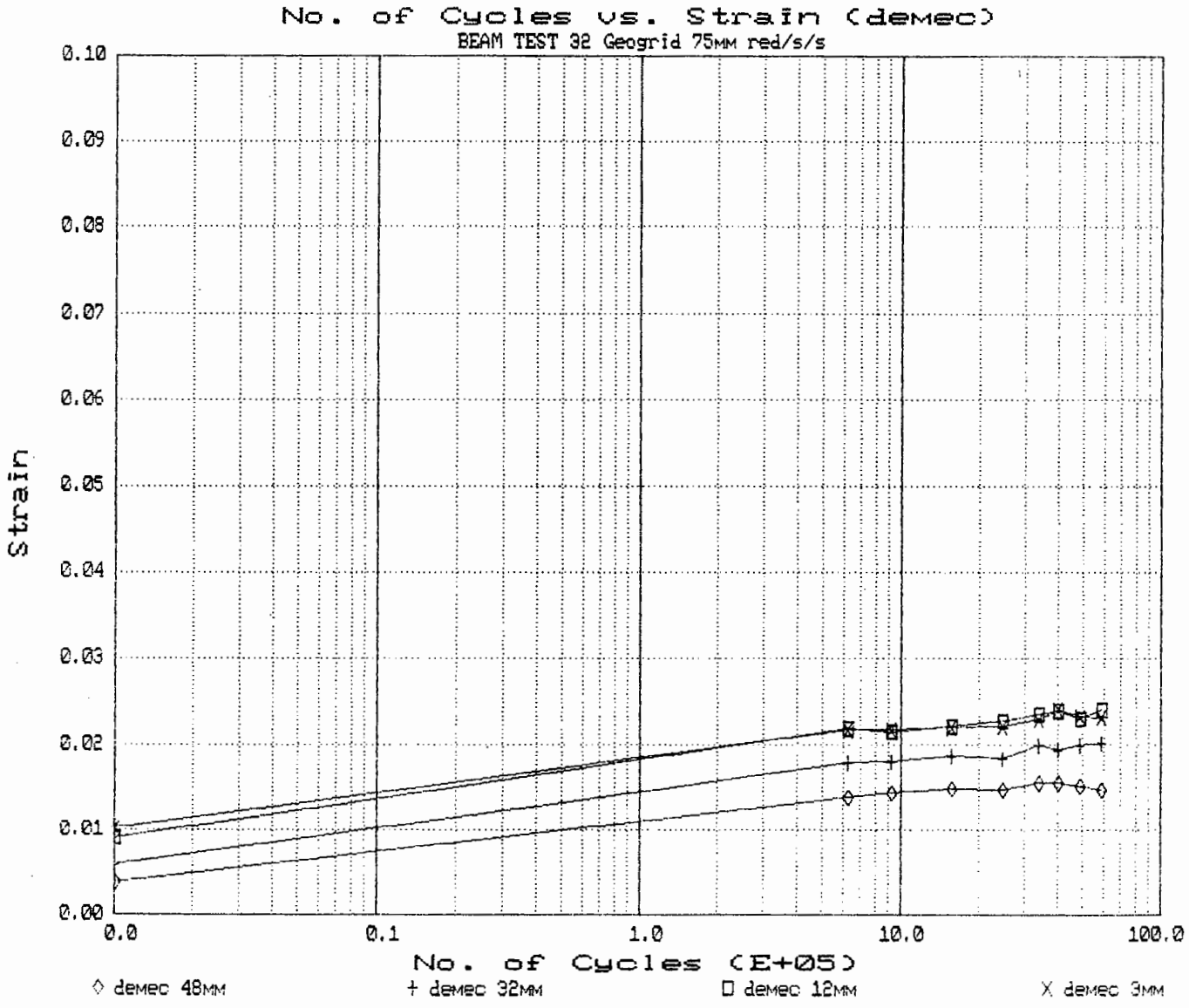
No. of Cycles vs. Strain (demec)
BEAM TEST 32 Geogrid 75mm red/s/s
Strain
0.10
0.09
0.08
0.07
0.06
0.05
0.04
0.03
0.02
0.01
0.00
0.0
0.1
1.0
10.0
100.0
No. of Cycles (E+05)
◊ demec 48mm
+ demec 32mm
□ demec 12mm
X demec 3mm

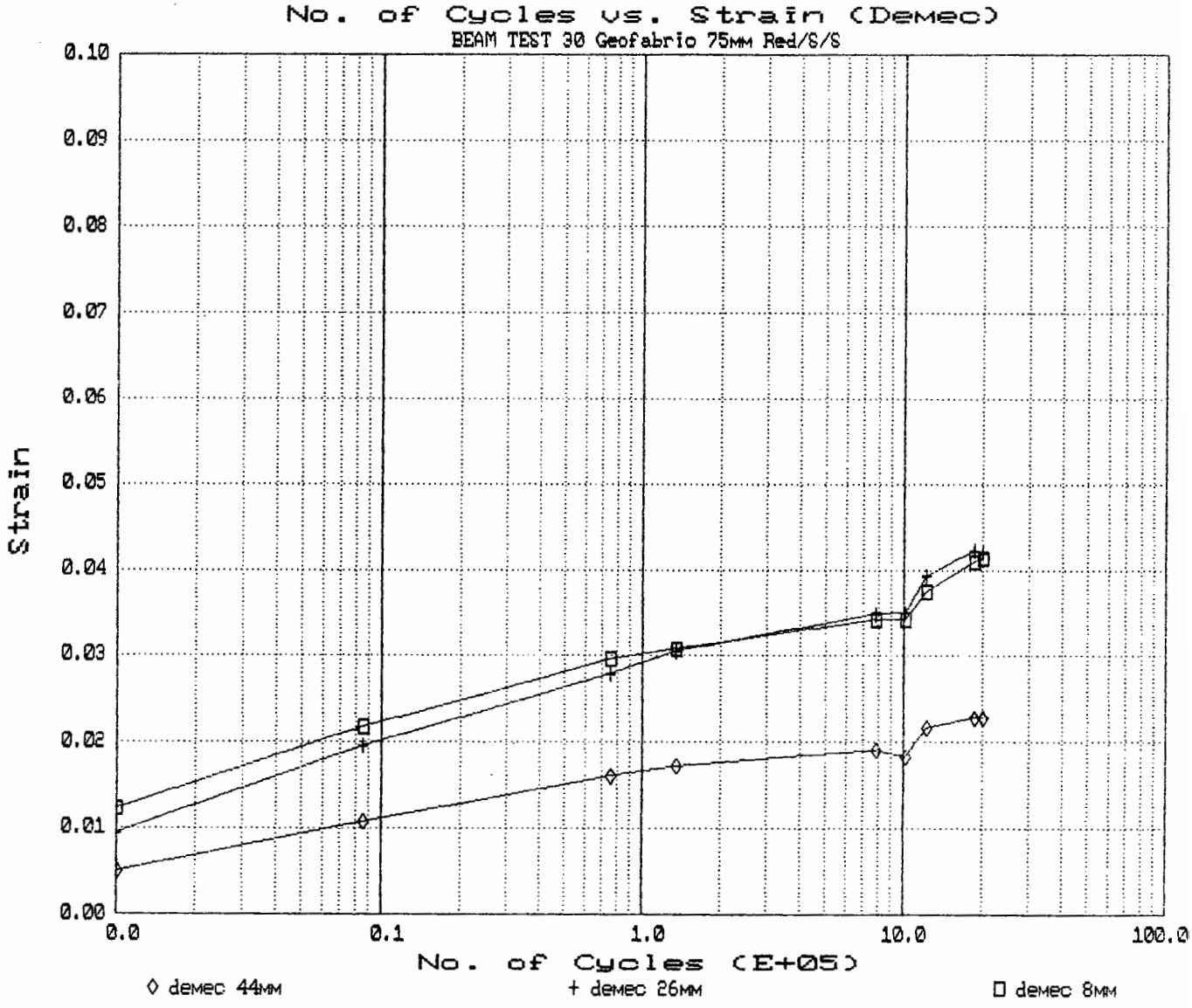
No. of Cycles vs. Strain (Demec)
BEAM TEST 30 Geofabric 75mm Red/S/S
Strain
0.10
0.09
0.08
0.07
0.06
0.05
0.04
0.03
0.02
0.01
0.00
0.0
0.1
1.0
10.0
100.0
No. of Cycles (E+05)
◊ demec 44mm
+ demec 26mm
□ demec 8mm

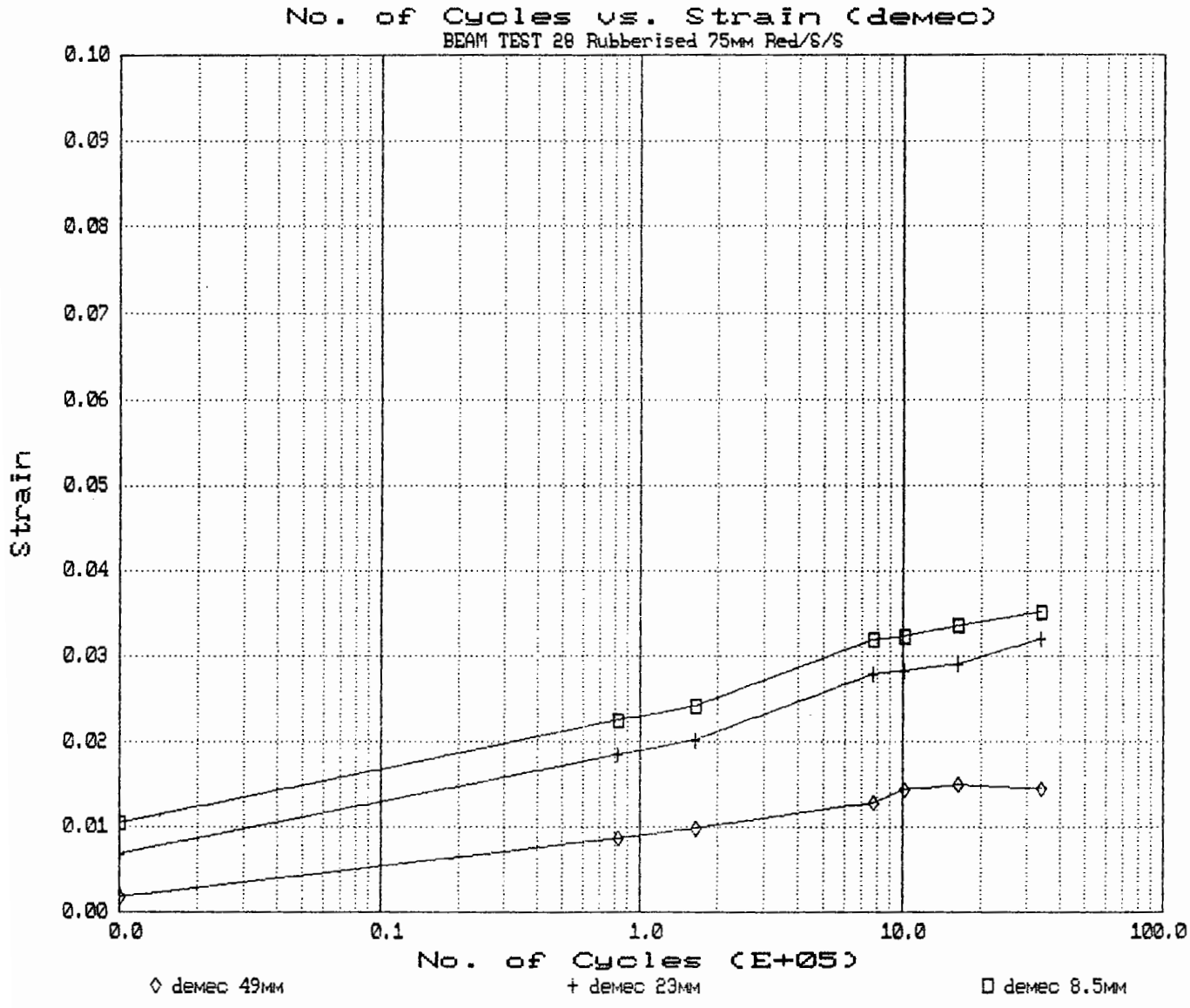
No. of Cycles vs. Strain (demec)
BEAM TEST 28 Rubberised 75mm Red/S/S
Strain
0.10
0.09
0.08
0.07
0.06
0.05
0.04
0.03
0.02
0.01
0.00
0.0
0.1
1.0
10.0
100.0
No. of Cycles (E+05)
◊ demec 49mm
+ demec 23mm
□ demec 8.5mm

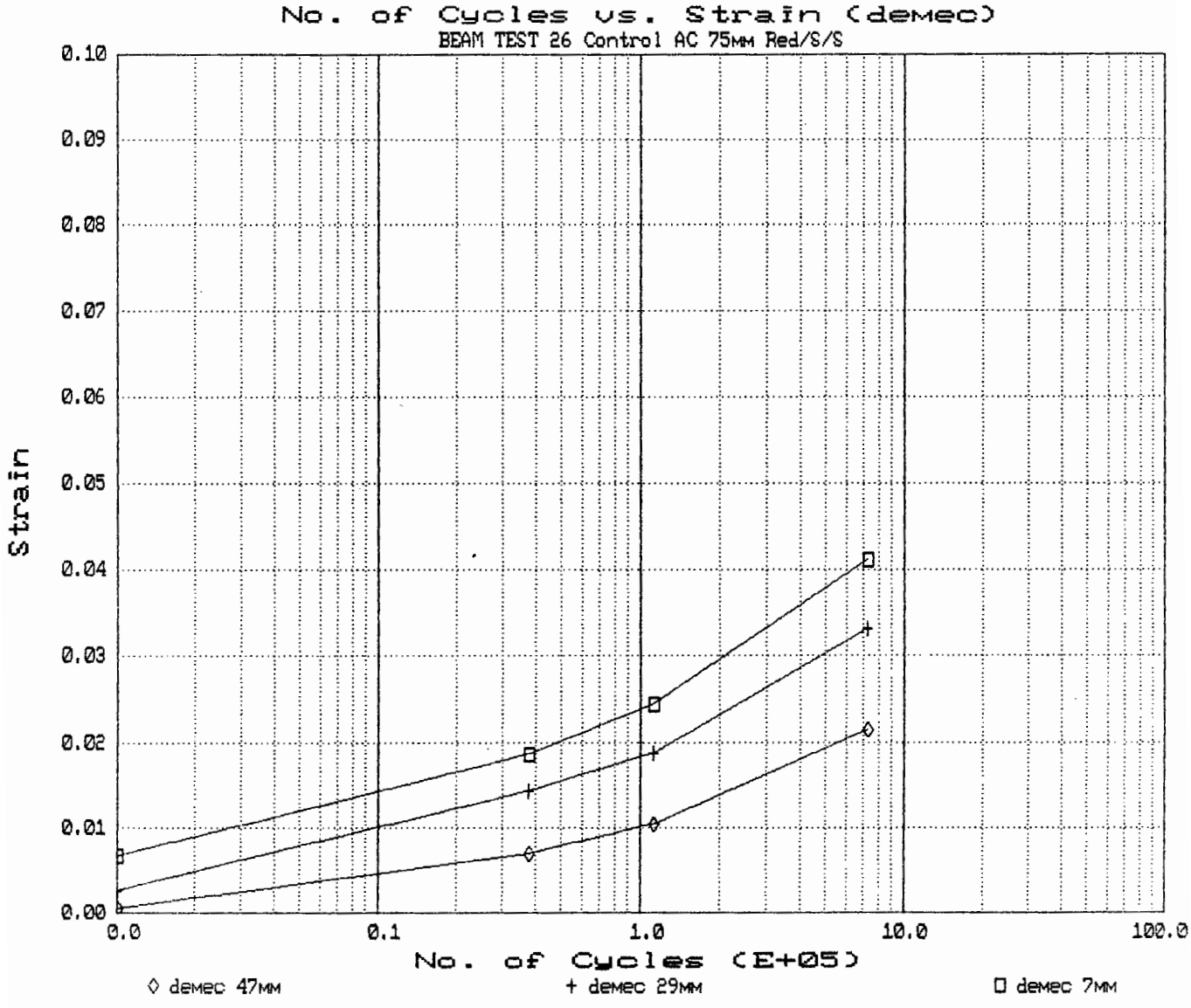
No. of Cycles vs. Strain (demec)
BEAM TEST 26 Control AC 75мм Red/S/S
Strain
0.10
0.09
0.08
0.07
0.06
0.05
0.04
0.03
0.02
0.01
0.00
0.0
0.1
1.0
10.0
100.0
No. of Cycles (E+05)
◊ demec 47мм
+ demec 29мм
□ demec 7мм

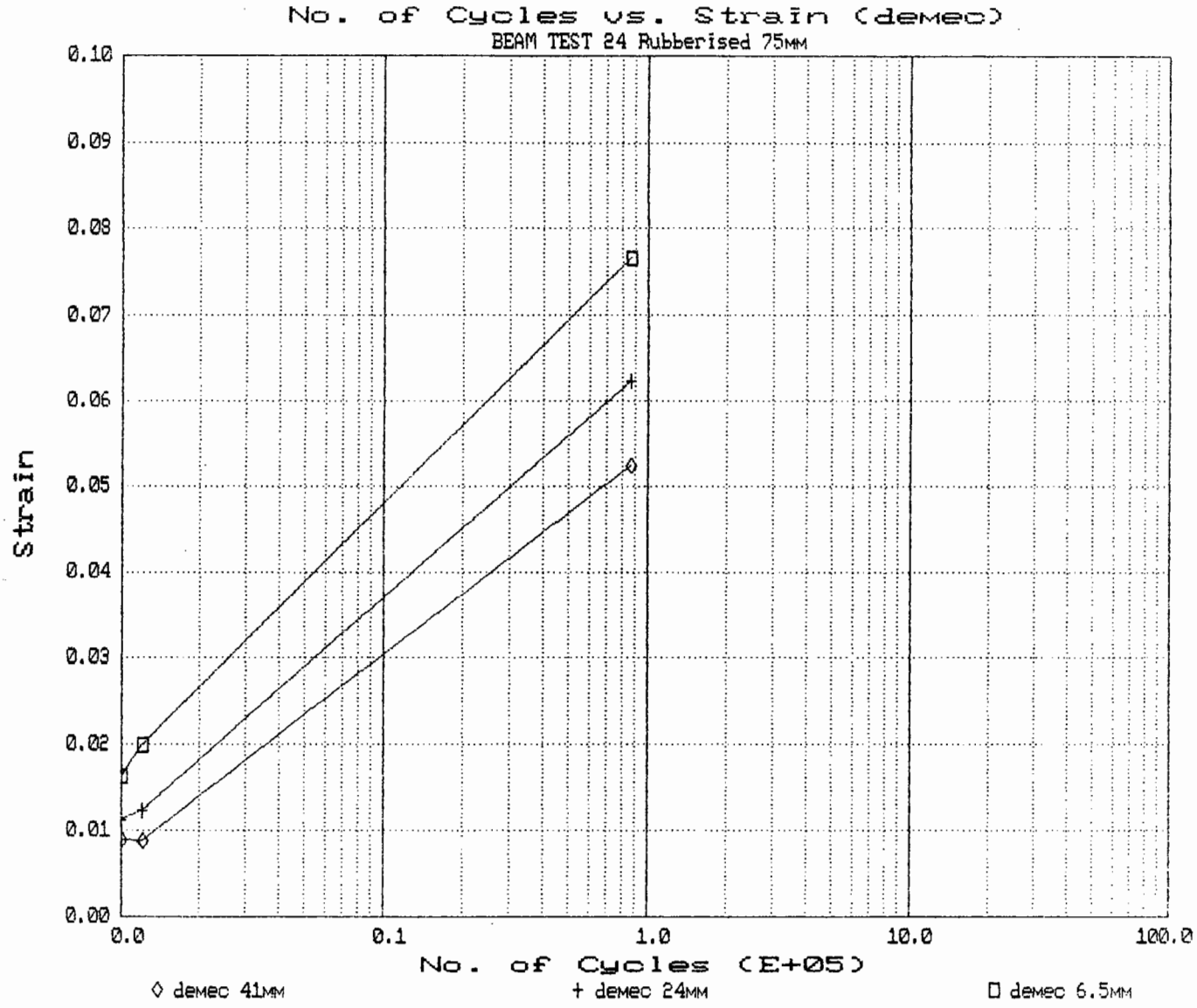
No. of Cycles vs. Strain (demec)
BEAM TEST 24 Rubberised 75mm
Strain
0.10
0.09
0.08
0.07
0.06
0.05
0.04
0.03
0.02
0.01
0.00
0.0
0.1
1.0
10.0
100.0
No. of Cycles (E+05)
◊ demec 41mm
+ demec 24mm
□ demec 6.5mm

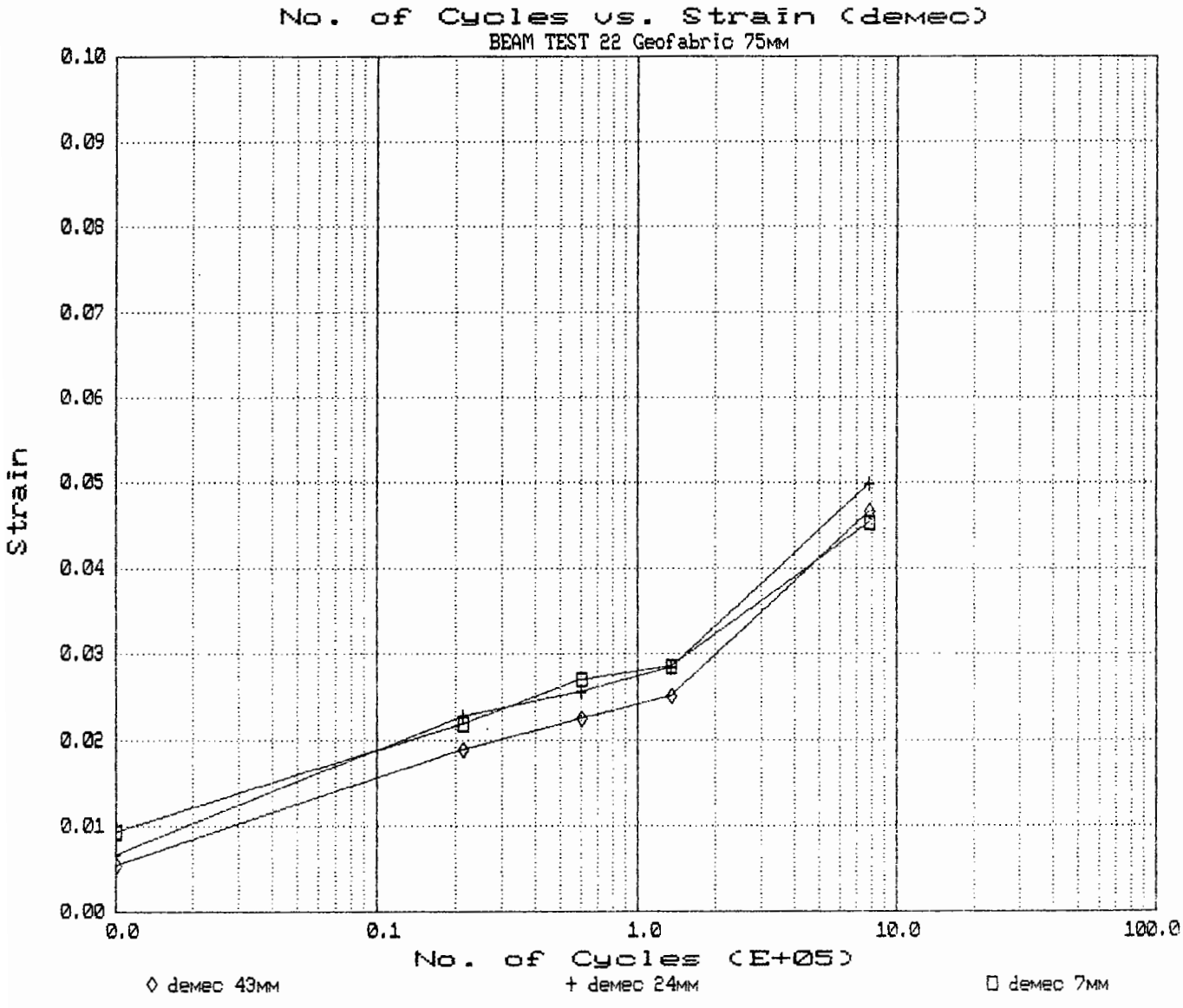
No. of Cycles vs. Strain (demec)
BEAM TEST 22 Geofabric 75mm
Strain
0.10
0.09
0.08
0.07
0.06
0.05
0.04
0.03
0.02
0.01
0.00
0.0
0.1
1.0
10.0
100.0
No. of Cycles (E+05)
◊ demec 43mm
+ demec 24mm
□ demec 7mm

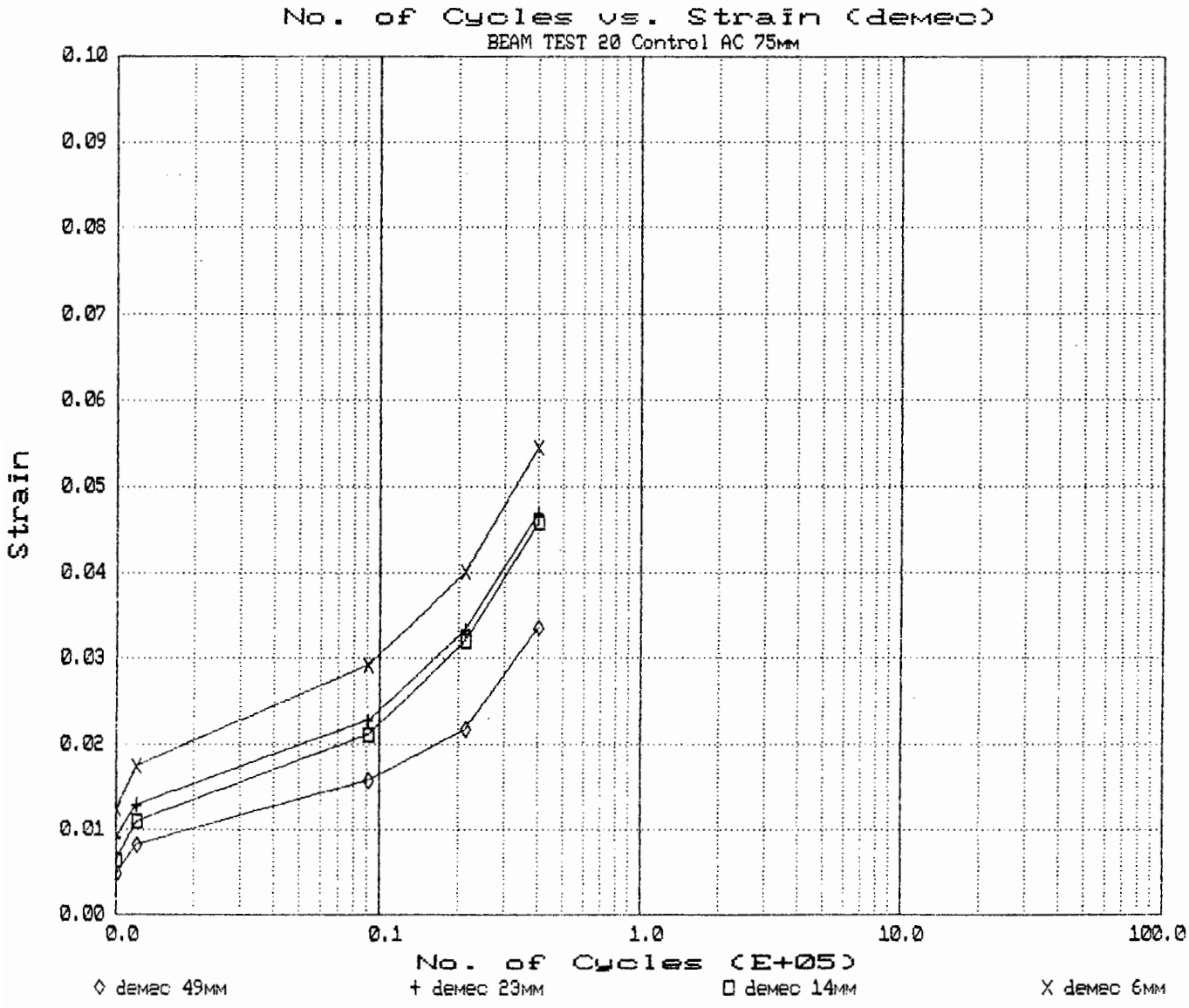
No. of Cycles vs. Strain (demec)
BEAM TEST 20 Control AC 75mm
Strain
0.10
0.09
0.08
0.07
0.06
0.05
0.04
0.03
0.02
0.01
0.00
0.0
0.1
1.0
10.0
100.0
No. of Cycles (E+05)
◊ demec 49mm
+ demec 23mm
□ demec 14mm
X demec 6mm

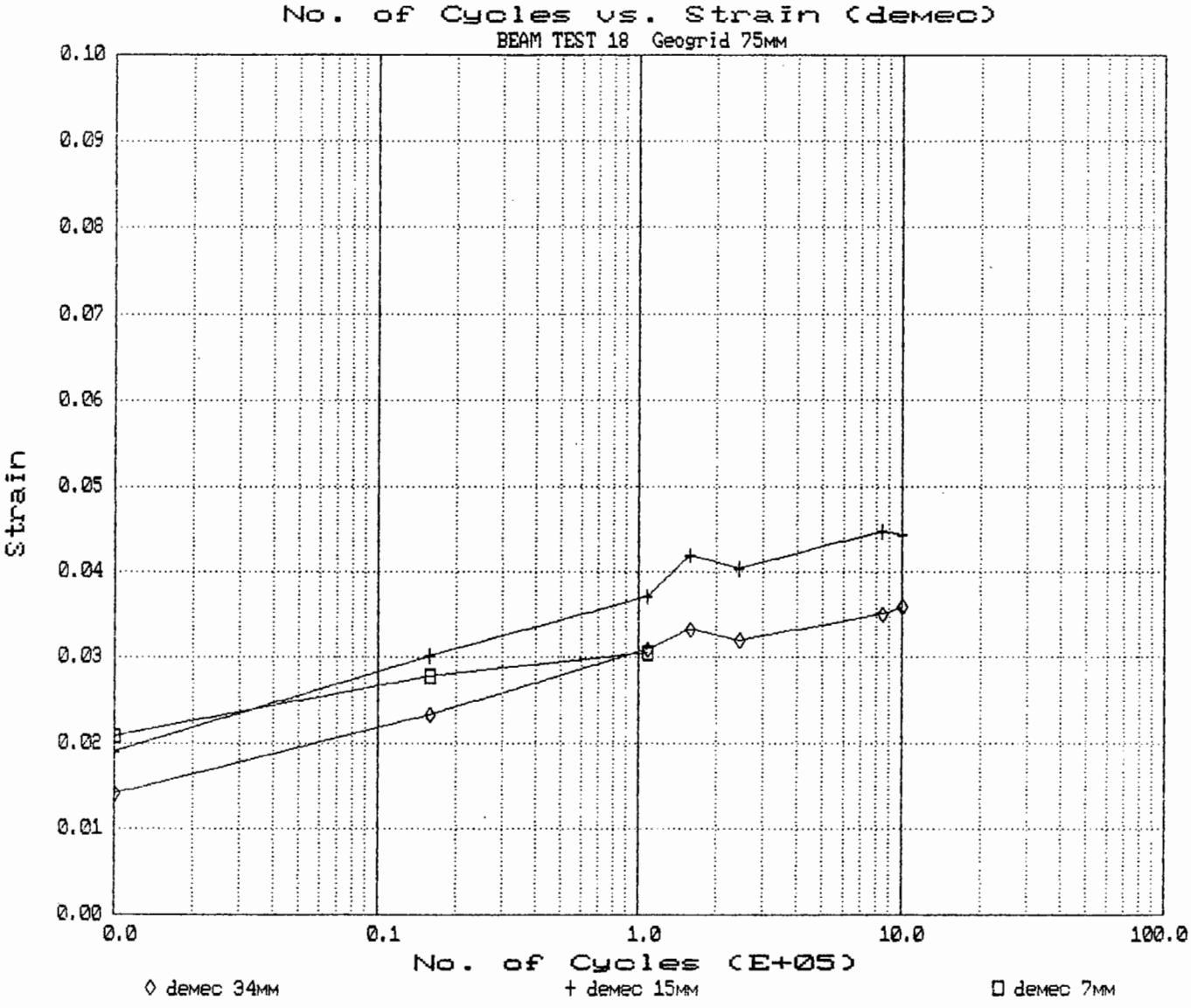
No. of Cycles vs. Strain (demec)
BEAM TEST 18 Geogrid 75mm
Strain
0.10
0.09
0.08
0.07
0.06
0.05
0.04
0.03
0.02
0.01
0.00
0.0
0.1
1.0
10.0
100.0
No. of Cycles (E+05)
◊ demec 34mm
+ demec 15mm
□ demec 7mm

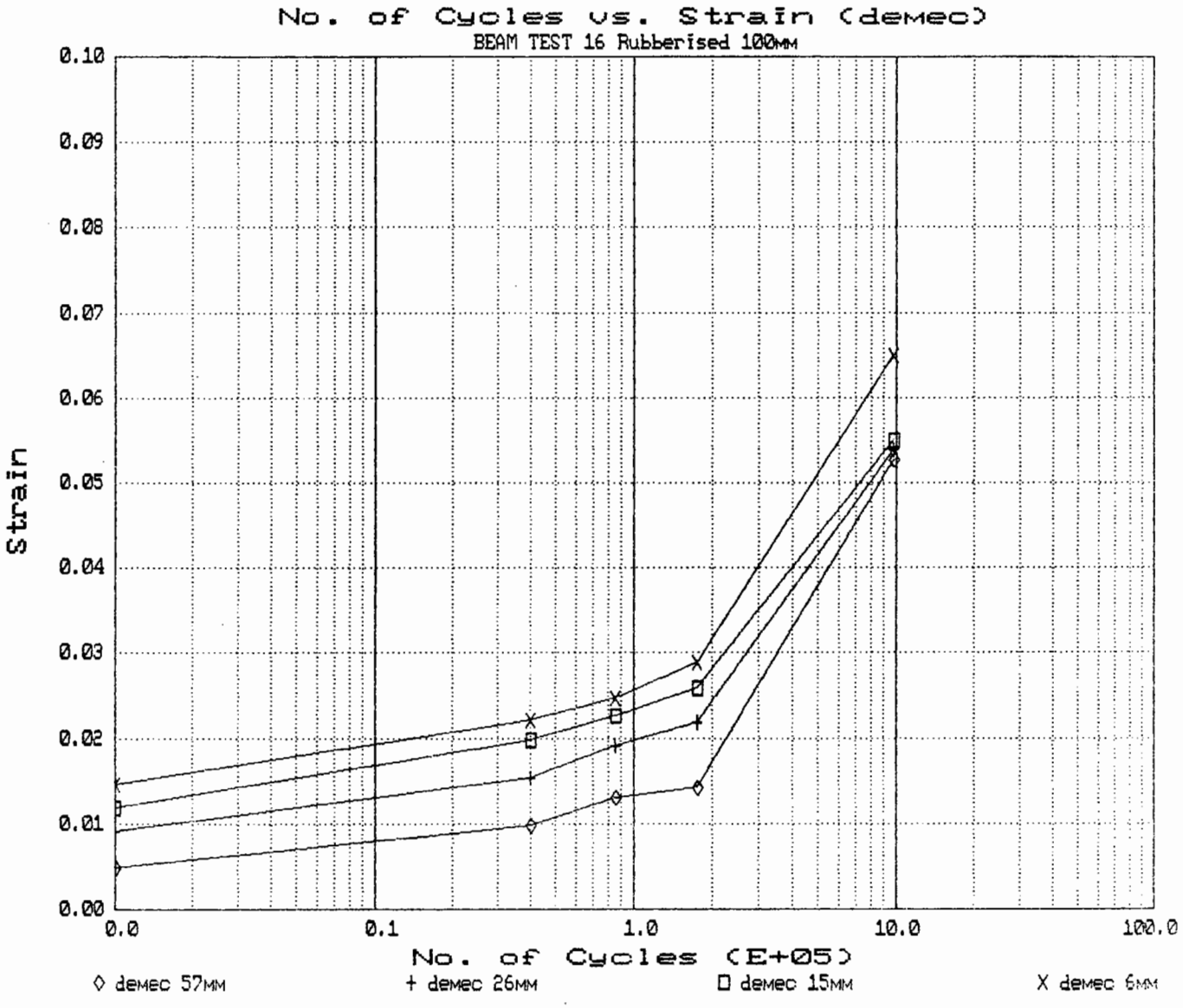
No. of Cycles vs. Strain (demec)
BEAM TEST 16 Rubberised 100mm
Strain
0.10
0.09
0.08
0.07
0.06
0.05
0.04
0.03
0.02
0.01
0.00
0.0
0.1
1.0
10.0
100.0
No. of Cycles (E+05)
◊ demec 57mm
+ demec 26mm
□ demec 15mm
X demec 6mm

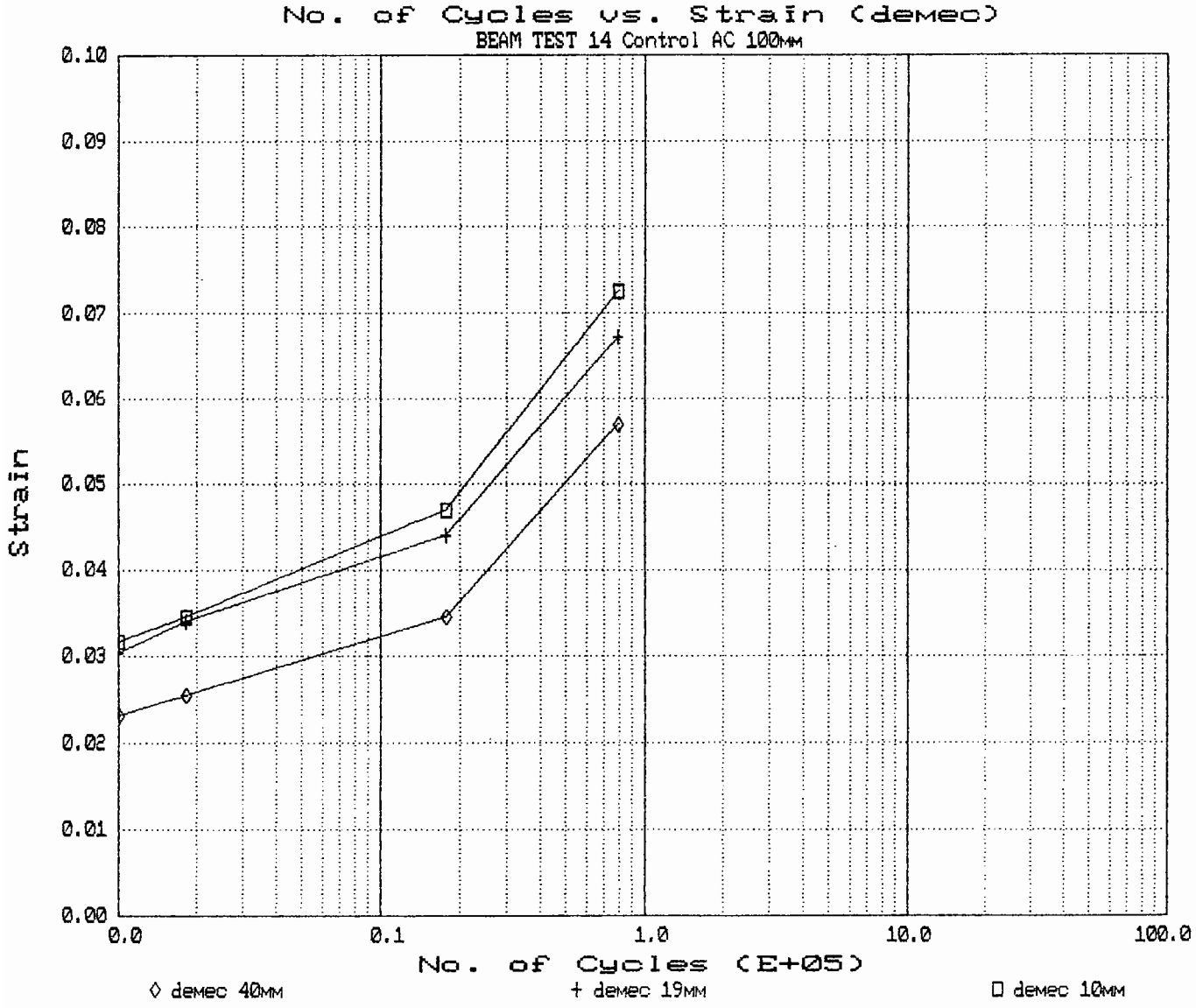
No. of Cycles vs. Strain (demec)
BEAM TEST 14 Control AC 100mm
Strain
0.10
0.09
0.08
0.07
0.06
0.05
0.04
0.03
0.02
0.01
0.00
0.0
0.1
1.0
10.0
100.0
No. of Cycles (E+05)
◊ demec 40mm
+ demec 19mm
□ demec 10mm

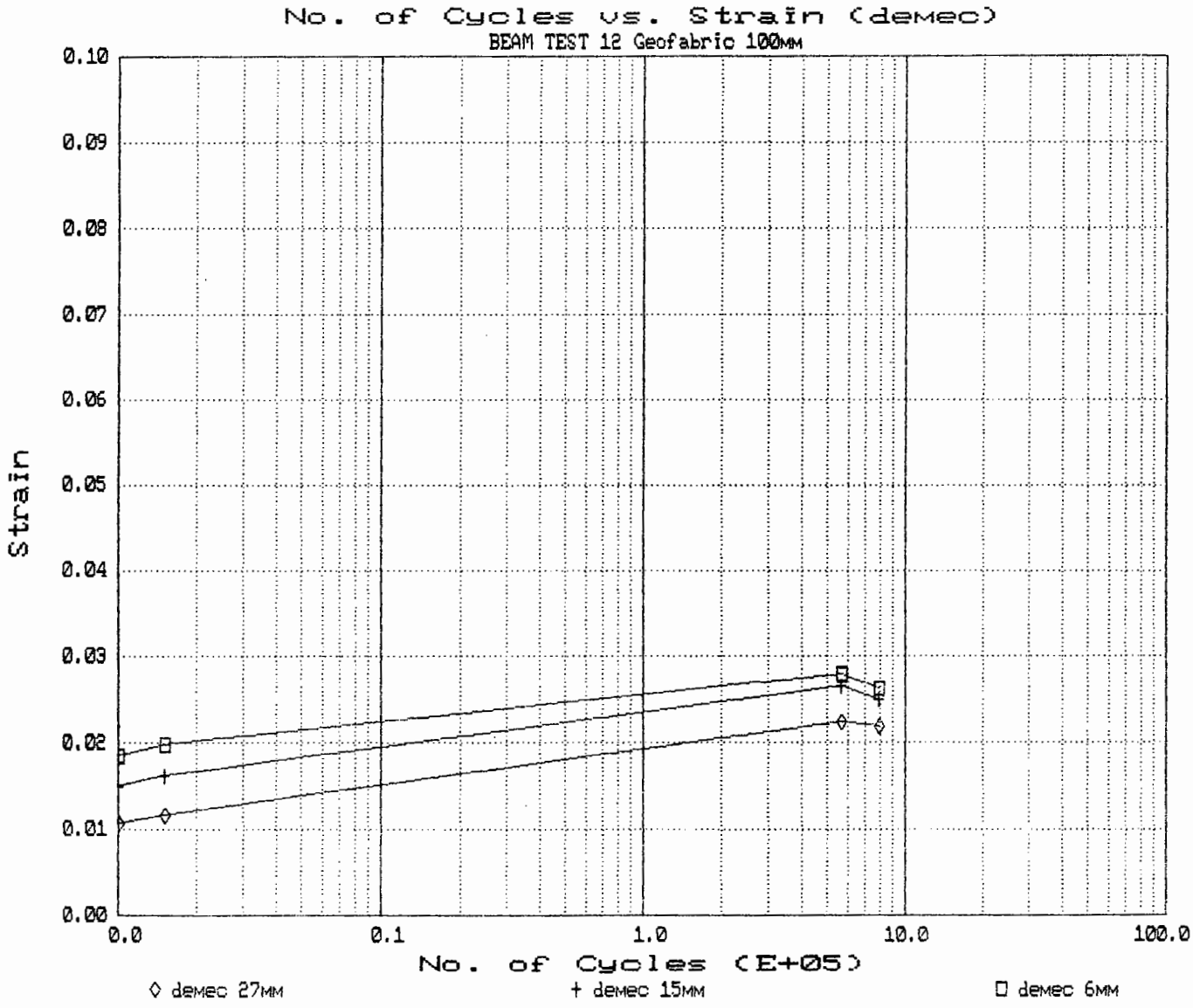
No. of Cycles vs. Strain (demec)
BEAM TEST 12 Geofabric 100мм
Strain
0.10
0.09
0.08
0.07
0.06
0.05
0.04
0.03
0.02
0.01
0.00
0.0
0.1
1.0
10.0
100.0
No. of Cycles (E+05)
◊ demec 27мм
+ demec 15мм
□ demec 6мм

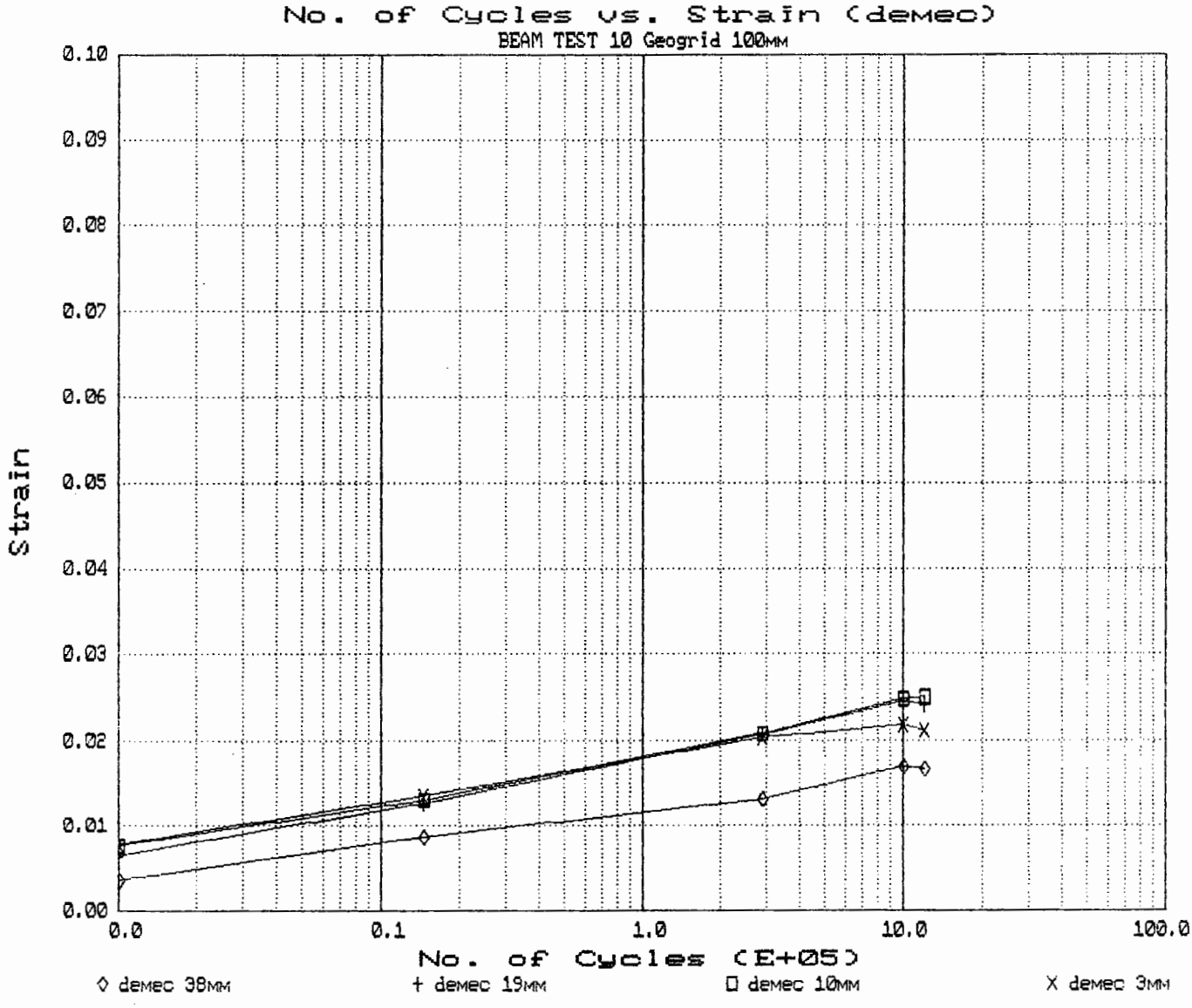
No. of Cycles vs. Strain (demec)
BEAM TEST 10 Geogrid 100mm
Strain
0.10
0.09
0.08
0.07
0.06
0.05
0.04
0.03
0.02
0.01
0.00
0.0
0.1
1.0
10.0
100.0
No. of Cycles (E+05)
◊ demec 38mm
+ demec 19mm
□ demec 10mm
X demec 3mm

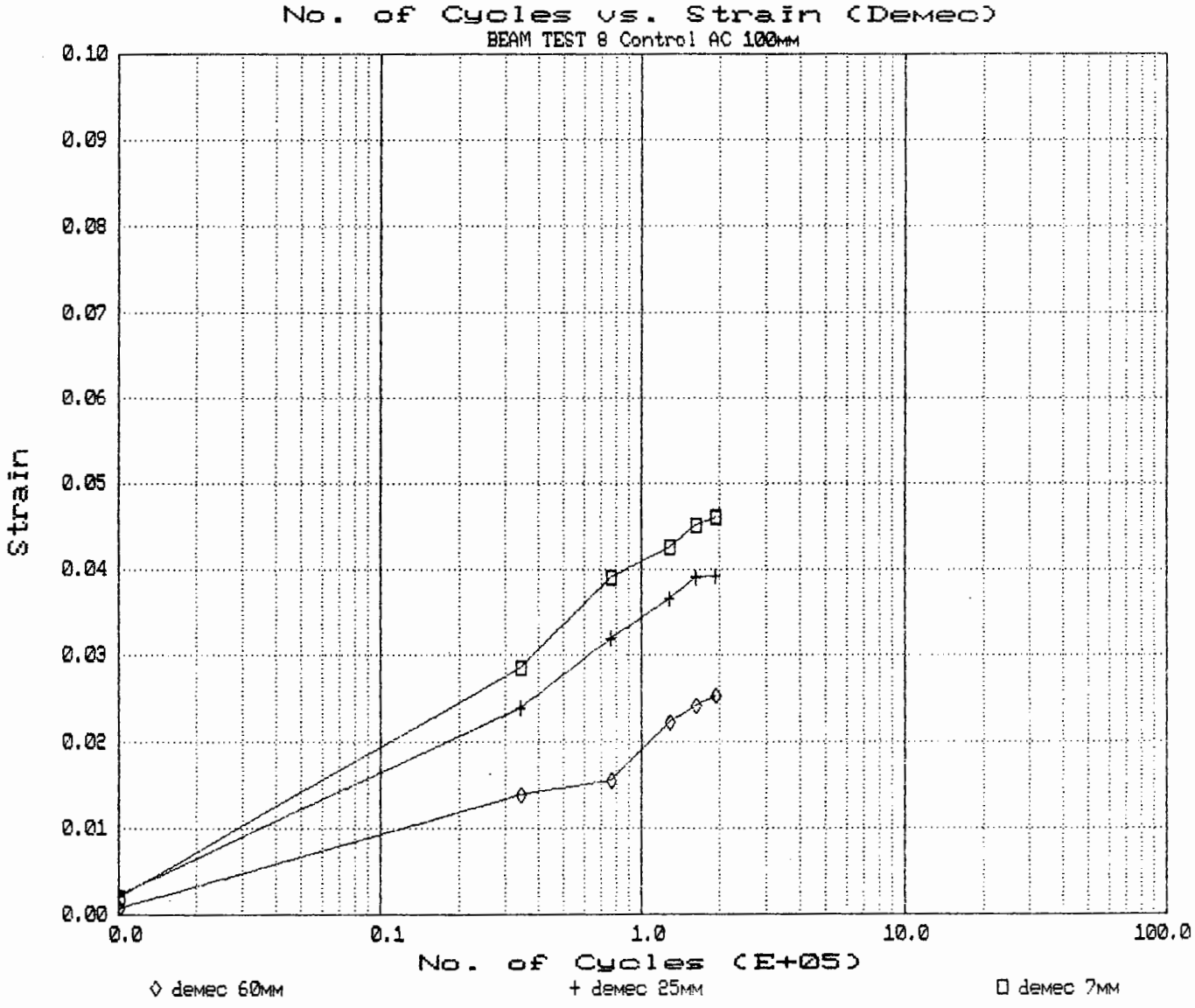
No. of Cycles vs. Strain (Demec)
BEAM TEST 8 Control AC 100mm
Strain
0.10
0.09
0.08
0.07
0.06
0.05
0.04
0.03
0.02
0.01
0.00
0.0
0.1
1.0
10.0
100.0
No. of Cycles (E+05)
◊ demec 60mm
+ demec 25mm
□ demec 7mm